
Phenomenological Applications of Light Cone Sum Rules

A thesis submitted in partial fulfillment of
the requirements for the degree of

Doctor of Philosophy

by

Anshika Bansal

(Roll No. 17330007)

Under the supervision of

Dr. Namit Mahajan

Professor

Theoretical Physics

Physical Research Laboratory, Ahmedabad, India.



DEPARTMENT OF PHYSICS

INDIAN INSTITUTE OF TECHNOLOGY GANDHINAGAR

2022

to
my family

DECLARATION

I declare that this written submission represents my ideas in my own words and where others' ideas or words have been included, I have adequately cited and referenced the original sources. I also declare that I have adhered to all principles of academic honesty and integrity and have not misrepresented or fabricated or falsified any idea/data/fact/source in my submission. I understand that any violation of the above will be cause for disciplinary action by the Institute and can also evoke penal action from the sources which have thus not been properly cited or from whom proper permission has not been taken when needed.

(Name: Anshika Bansal)

(Roll No: 17330007)

CERTIFICATE

It is certified that the work contained in the thesis titled “**Phenomenological Applications of Light Cone Sum Rules**” by **Anshika Bansal** (Roll no: 17330007), has been carried out under my supervision and that this work has not been submitted elsewhere for degree.

I have read this dissertation and in my opinion, it is fully adequate in scope and quality as a dissertation for the degree of Doctor of Philosophy.

Prof. Namit Mahajan
(**Thesis Supervisor**)

Professor

Theoretical Physics Division

Physical Research Laboratory

Navarangpura, Ahmedabad, India

Acknowledgements

Firstly, I would like to convey my most sincere gratitude to my supervisor, Prof. Namit Mahajan for his constant support, patience, motivation, and advises, during the last five years, which has helped me evolve as an independent researcher.

Besides my supervisor, I thank the rest of my Doctoral Studies Committee (DSC) members: Prof. Subhendra Mohanty, Prof. Hiranmaya Mishra, and Dr. Aweek Sarkar for the useful suggestions and comments during the half-yearly meetings which helped me not only get a better understanding of the subject but also helped me become a better presenter. I also wish to thank other members of the PRL theory division, Prof. Srubabati Goswami, Prof. Dilip Angom, Prof. Jitesh Bhutt, Prof. Partha Konar, Prof. Navinder Singh, Dr. Ketan Patel, and Dr. Satyajeet Seth for their lectures during the course work and their comments and discussion during the division seminars. I am also thankful to Dr. Arvind Singh who showed confidence in me and gave me the opportunity to TA the statistics course for the 2019 batch. This experience helped me to learn how to teach and handle a class which will be very helpful in my future career. I also show my gratitude to all the members of the PRL academic committee for monitoring my progress yearly and providing useful suggestions.

I am also very grateful to Prof. Debajyoti Choudhury for making my initial journey to theoretical physics beautiful by giving very insightful lectures on quantum field theory during my master's and motivating me to pursue a career in research. Also, I am very thankful to Prof. T.R. Seshadri for his motivation and suggestions throughout my Ph.D. tenure. I show my sincere gratitude to the SERB school organizers and the lecturers for giving me the opportunity to attend the mains school twice and helping me to get an overall broad knowledge of the different areas and helping me make new friends.

I am also grateful to my senior, Dr. Bhavesh Chauhan for his constant advises and motivation. He always remained there for me as a mentor in my good and bad times which helped me stay focused. I also thank my colleague, collaborator, and friend Mr. Dayanand Mishra for countless fruitful discussions and ideas that have helped me grow personally as well as professionally. I also thank Dr. Bharti Kindra, Dr. Balbeer Singh, and Dr. Akanksha Bhardwaj for fruitful discussions which enhanced my knowledge and understanding of

the subject. I also acknowledge him for proofreading this thesis along with Miss Kavita Kumari and Mr. Biswajit Mondal. I am also thankful to my other friends, Mr. Madhusudhan P. and Mr. Vishal Singh Ngairangbam for the intellectual talks we had which helped me look at things from a different perspective during my rough times during this Ph.D. tenure. This helped me stay motivated and focused, and most importantly positive in life which has helped me grow as a person with more maturity and confidence.

I am deeply thankful to my friends, Miss Shanwlee Show Mondal, Mr. Biswajit Mondal, Dr. Sandeep Rout, Mr. Abhay Kumar, Mr. Goldy Ahuja, Miss Tanya Sharma, and Mr. Vardaan Mongia for letting me share their office spaces during thesis writing. It helped me a lot to concentrate and complete my thesis on time. I am also very grateful to Miss Shivani Baliyan and Dr. Harish for taking very good care of me while I was sick and making me feel like home far away from home. I convey my regards to all other friends and acquaintances in PRL for the good and bad times spent together and for helping me when needed.

Last but not least I am very thankful to my family for always being supportive and letting me pursue my dreams.

(Anshika Bansal)

Abstract

Within the Standard Model (SM) of particle physics, the strong interactions are dictated by the gauge theory called quantum chromodynamics (QCD). QCD is a theory of quarks and gluons, which carry a gauge charge called color. Gluons are the mediators of strong interactions between colored particles, very much like the photon for electromagnetic interactions between electrically charged particles. However, unlike photons, the gluons themselves carry color charge due to the non-abelian nature of QCD. This leads to self-interactions of gluons, and hence to many exciting phenomena in QCD like *asymptotic freedom*, *color confinement*, etc. The quarks and gluons form colorless bound states like *mesons* (the bound state of a quark and anti-quark) and *baryons* (the bound state of three quarks), collectively called *hadrons*, at small energies because of the phenomenon of color confinement. As a result, we only detect colorless hadrons at the detectors.

According to the scattering theory, experimental observables like decay width, scattering cross-sections, etc., can be calculated theoretically by calculating the matrix elements of quark-gluon operators between the initial and final hadron states called the *Hadronic Matrix Elements (HMEs)*. However, the difficulty arises as these hadrons are bound states i.e. are non-perturbative in nature, and hence, the perturbative QCD can not provide a complete solution to these HMEs. Consequently, these HMEs contain the non-perturbative effects in the form of hadronic quantities like form factors, decay constants, etc.

These hadronic quantities are very essential inputs for any prediction within or beyond the SM. Therefore, calculating these quantities is very crucial. There exist several methods like chiral perturbation theory (χPT), lattice QCD (LQCD), QCD sum rules (QCDSRs), etc., to handle these objects. However, none can give precise results with the current techniques and computational skills, and different methods are found to typically work well in different regimes. Therefore, estimations of these quantities, involved in the processes of interest, using different methods is very important to get reliable theoretical estimates for the experimental observables.

In this thesis, we have discussed the applications of the method of *Light Cone Sum Rules (LCSR)*, the QCDSRs on the light cone, to various processes within and beyond the SM, focusing on the calculation of the *Form Factors (FFs)* involved. LCSR is a QCD based method. It uses the analytic properties of the correlation functions, the matrix elements of the quark and gluon operators taken between the vacuum and the hadronic state, and the framework of *Operator Product Expansion (OPE)* to compute these FFs. Along with these properties, it uses *Quark-Hadron duality* which allows one to calculate the correlation functions at large Euclidean momentum transfers which can then be analytically continued to the desired kinematical regime. As stated above, every available non-perturbative method has limitations and domain of applicability, and so does the method of LCSR.

To explore the applications of LCSR and gain better understanding of its limitations, we considered several processes within and beyond the SM involving light as well as heavy quark hadrons. The considered processes are the radiative tau decay (involving a light meson called pion), the proton decay to a positron and a photon (involving a light baryon called proton), the baryon number violating decay of D-meson to an anti-proton and a positron, and the radiative decay of D^* -meson (both involving heavy quark D-meson). In all these cases, the method of LCSR is found to provide reasonable estimates for the form factors involved. All of these are the first applications of LCSR to such processes. Moreover, for the considered cases involving proton and D-mesons, we discussed the first theoretical estimates of the FFs involved which are of great phenomenological importance as they can be very helpful in constraining the Beyond SM (BSM) models, and probing the structure of the hadrons. The results can be further improved with the inclusion of higher-order effects which may also bring some new elements. This method also has the potential to be applied to several other situations like non-leptonic decay modes where systematic calculations still show some discrepancies.

Keywords: Strong interactions, Hadronic Matrix Elements, Form Factors, Light Cone Sum Rules, Baryon number violation, Proton decay.

List of Publications

Publications included in thesis

1. **Anshika Bansal** and Namit Mahajan, "Phenomenology of $\tau^- \rightarrow \pi^- \nu_\tau \gamma$ using light cone sum rules", *Phys. Rev. D* 103 (2021) 5, 056017 [arXiv:2010.00549]
2. **Anshika Bansal** and Namit Mahajan, "Light Cone Sum rules and Form Factors for $p \rightarrow e^+ \gamma$ ", *JHEP* 06 (2022) 161 [arXiv:2204.03448]
3. **Anshika Bansal**, " $D^0 \rightarrow \bar{p} e^+$ Form Factors in LCSR", [arXiv: 2205.13564] [under review]
4. **Anshika Bansal** and Namit Mahajan, " $D^* \rightarrow D \gamma$: Probing the inner structure of charm mesons" [under preparation].

Other publications (not included in the thesis):

1. **Anshika Bansal**, Namit Mahajan and Dayanand Mishra, " $\frac{|V_{ub}|}{|V_{cb}|}$ and quest for new physics", *JHEP* 02 (2022) 130 [arXiv:2112.00363]

Conference proceedings

1. **Anshika Bansal** and Namit Mahajan, "LCSR application to radiative tau decay", *PoS, LHCP2021*, 193.
2. **Anshika Bansal** and Namit Mahajan, " $p \rightarrow e^+ \gamma$ in LCSR framework", *PoS, LHCP2022, XXX*, (to be published as a poster contribution in LHCP 2022.)

List of Figures

1.1	The fundamental particles in the Standard Model of particle physics.	8
1.2	The running of strong coupling with energy scale from various experimental observations along with the theoretical prediction [35].	14
1.3	Feynman diagrams showing $\pi^- \rightarrow \mu^- \bar{\nu}_\mu$ (a) in the SM with W^- exchange and (b) in the EFT theory where W-boson is integrated out.	24
2.1	The Feynman diagram showing the process $e^+e^- \rightarrow e^+e^-$ with a quark loop due to quantum fluctuations.	29
2.2	Flowchart chart showing important tools to derive sum rules along with their importance and function.	30
2.3	Showing the analytic structure of the 2-point correlation function in the upper graph and the spectral density function in the lower graph as a function of q^2 for free theory(left panel) and interacting theory (right panel).	34
2.4	Showing the integration contour, C for the dispersion representation of the 2-point correlation function $\Gamma(q^2)$.	36
2.5	A representative graph of a typical correlation function of two currents between the initial and the final state containing pion and vacuum.	50
3.1	Feynman diagrams showing different contributions to radiative tau decay ($\tau^- \rightarrow \pi^- \nu_\tau \gamma$). (a) and (b) represents the IB contribution, (c) represents the SD contribution, and (d) represents the contact term.	67

- 3.2 Feynman diagram which contributes to the light-cone expansion of the hadronic matrix element for radiative tau decay up to twist-2. The internal line connecting the two currents can be either the up-quark or the down quark. The encircled pion represents that the pion distribution amplitude will enter the LCSR computation. 74
- 3.3 The dependence of structure dependent parameter (SDP), $F_A^{(\pi)}(0)$ and $F_V^{(\pi)}(0)$ on the Borel parameter M (in GeV units) is shown in Blue, Magenta and Green, respectively. In this plot, form factors have been multiplied by im_π to make them dimensionless in and take care of the extra $-i$ in the FFs as noted in the Footnote1. 82
- 3.4 The total Structure Dependent Contribution (blue) to the photon spectrum is shown along with the individual contributions from the vector (magenta), axial vector (green) and the interference (red) of the two are also shown for the two distribution amplitudes. Solid lines are for asymptotic distribution amplitude while dashed ones are for Chernyak-Zitnisky distribution amplitude. 83
- 3.5 The dependence of the IB (solid) contribution on the minimum energy threshold of the photon is shown here. Along with that, the same dependence for total decay width including form factors using asymptotic (dashed) and CZ (dotted) pion distribution amplitude is also shown. 84
- 3.6 (a): The Structure Dependent contribution (blue) to the invariant mass spectrum of $\pi-\gamma$ system is shown here for asymptotic (solid) and Chernyak-Zhitnisky (dashed) pion distribution amplitudes. The contribution from the vector (magenta), axial vector (green) and the interference (red) of the two is also shown. (b): Zoomed in version of (a). 84

- 3.7 The SD contribution (blue) considering (a) Γ_ρ and Γ_{a_1} to be constant and (b) the t dependence of Γ_ρ and Γ_{a_1} is shown here for asymptotic (solid) and Chernyak-Zhitnisky (dashed) pion distribution amplitudes. The contribution from the vector (magenta), axial vector (green) and the interference (red) of the two is also shown. 85
- 3.8 The invariant mass spectrum of $\pi - \gamma$ system for radiative tau decay is shown here considering (a) asymptotic and (b) CZ pion distribution amplitude. The contributions from the IB (magenta), SD (green) and the interference (red) of the two is also shown. The shaded region shows the uncertainties. 85
- 4.1 Feynman diagrams which contribute to the light-cone expansion of the hadronic matrix element for proton decay to positron and a photon up to two particle twist-2 and twist-3 contributions. The vertex on the left represents the proton interpolations current while the vertex on the right represents the dim-6 BNV operator. The encircled photon represents that the photon distribution amplitudes are entering the LCSR computation. (a) represents the the usual non-condensate contribution while (b) and (c) represent the condensates contributions as discussed in the text. 100
- 4.2 The physical FF, $A_{LL}(s_0, P_e^2)$ is calculated from the combination of F_{LL}^{TP} and F_{LL}^{KPP} employing photon DAs. Left panel: $A_{LL}^{TP+KPP}(s_0, P_e^2)$ vs P_e^2 is shown for three values of $s_0 = (1.4 \text{ GeV})^2$ (violate dotted), $s_0 = (1.44 \text{ GeV})^2$ (red solid) and $s_0 = (1.5 \text{ GeV})^2$ (blue dashed) at the Borel Mass, $M^2 = 2 \text{ GeV}^2$. Right Panel: $A_{LL}^{TP+KPP}(s_0, P_e^2)$ vs M is shown for three values of $P_e^2 = 0.5 \text{ GeV}^2$ (red solid), $P_e^2 = 1 \text{ GeV}^2$ (red dashed) and $P_e^2 = 2 \text{ GeV}^2$ (red dotted) at the continuum threshold, $s_0 = (1.44 \text{ GeV})^2$ 108
- 4.3 Same as Fig(4.2) but now with the combinations of F_{LL}^T and F_{LL}^{KPP} . 108

- 4.4 The physical FF, $A_{LR}(s_0, P_e^2)$ is calculated from the combination of F_{LR}^{TP} , F_{LR}^{PK} and F_{LR}^{PP} employing photon DAs. Left panel: $A_{LR}^{TP+PK+PP}(s_0, P_e^2)$ vs P_e^2 is shown for three values of $s_0 = (1.4 \text{ GeV})^2$ (violate dotted), $s_0 = (1.44 \text{ GeV})^2$ (red solid) and $s_0 = (1.5 \text{ GeV})^2$ (blue dashed) at the Borel Mass, $M^2 = 2 \text{ GeV}^2$. Right Panel: $A_{LR}^{TP+PK+PP}(s_0, P_e^2)$ vs M is shown for three values of $P_e^2 = 0.5 \text{ GeV}^2$ (red solid), $P_e^2 = 1 \text{ GeV}^2$ (red dashed) and $P_e^2 = 2 \text{ GeV}^2$ (red dotted) at the continuum threshold, $s_0 = (1.44 \text{ GeV})^2$ 109
- 4.5 Same as Fig(4.4) but now with the combinations of F_{LR}^{TP} , F_{LR}^{PK} and F_{LR}^P 109
- 4.6 Same as Fig(4.4) but now with the combinations of F_{LR}^{TP} , F_{LR}^{KPP} and F_{LR}^{PP} 110
- 4.7 Same as Fig(4.4) but now with the combinations of F_{LR}^{TP} , F_{LR}^{KPP} and F_{LR}^P 110
- 4.8 The physical FF, $A_{LR}^{TP+KPP}(s_0, P_e^2)$ (left pannel) and $A_{LR}^{TP+KPP+PP}(s_0, P_e^2)$ (right panel) vs P_e^2 are shown at $s_0 = (1.44 \text{ GeV})^2$ and $M^2 = 2 \text{ GeV}^2$ along with the uncertainties associated with the parameters involved in photon DAs. The bands represents the uncertainties. 111
- 4.9 Feynman diagram which contributes to the light-cone expansion to proton decay to positron and photon in case-2 up to twist-3. The vertex on the left represents the electromagnetic current while the vertex on the right represents the dim-6 BNV operator. The encircled proton represents that the proton distribution amplitude will enter the LCSR computation. 111

- 4.10 The physical FF, $A_{LL}(s_0, K^2)$ is calculated from the combination of F_{LL}^1 , F_{LL}^4 and F_{LL}^5 employing proton DAs. Left panel: $A_{LL}^{1+4+5}(s_0, K^2)$ vs K^2 is shown for three values of $s_0 = (1.4 \text{ GeV})^2$ (violate dotted), $s_0 = (1.44 \text{ GeV})^2$ (red solid) and $s_0 = (1.5 \text{ GeV})^2$ (blue dashed) at the Borel Mass, $M^2 = 2 \text{ GeV}^2$. Right Panel: $A_{LL}^{1+4+5}(s_0, K^2)$ vs M is shown for three values of $K^2 = 0.5 \text{ GeV}^2$ (red solid), $K^2 = 1 \text{ GeV}^2$ (red dashed) and $K^2 = 2 \text{ GeV}^2$ (red dotted) at the continuum threshold, $s_0 = (1.44 \text{ GeV})^2$ 117
- 4.11 The physical FF, $A_{LR}(s_0, K^2)$ is calculated from the combination of F_{LR}^1 , F_{LR}^4 and F_{LR}^5 employing proton DAs. Left panel: $A_{LR}^{1+4+5}(s_0, K^2)$ vs K^2 is shown for three values of $s_0 = (1.4 \text{ GeV})^2$ (violate dotted), $s_0 = (1.44 \text{ GeV})^2$ (red solid) and $s_0 = (1.5 \text{ GeV})^2$ (blue dashed) at the Borel Mass, $M^2 = 2 \text{ GeV}^2$. Right Panel: $A_{LR}^{1+4+5}(s_0, K^2)$ vs M is shown for three values of $K^2 = 0.5 \text{ GeV}^2$ (red solid), $K^2 = 1 \text{ GeV}^2$ (red dashed) and $K^2 = 2 \text{ GeV}^2$ (red dotted) at the continuum threshold, $s_0 = (1.44 \text{ GeV})^2$ 118
- 4.12 The physical FF, $A_{LL}^{1+4+5}(s_0, K^2)$ (left panel) and $A_{LR}^{1+4+5}(s_0, K^2)$ (right panel) vs K^2 are shown at $s_0 = (1.44 \text{ GeV})^2$ and $M^2 = 2 \text{ GeV}^2$ along with the uncertainties associated with the parameters involved in proton DAs. The bands represents the uncertainties. 118
- 5.1 Feynman diagrams contributing to the light-cone expansion of the correlation function for $D^0 \rightarrow \bar{p}e^+$ decay to the leading order. The encircled D represents that the distribution amplitudes for D-meson enters the LCSR computation. The vertex on the left represents the proton interpolation current while the vertex on the right represents the dim-6 BNV operators. (a) represents the usual non-condensate contribution while (b) represents the considered contribution coming from the condensates. 128

- 5.2 The FFs, $F_{LL}^{A,n}$ with $A \in \{S, V, T\}$ and $n \in \{0, 1\}$ are extracted from different combinations of $F_{LL}^{A,r}$ with $r \in \{S, V, P, VP\}$ using the proton interpolation current χ_{IO} . Left panel: We plot $F_{LL}^{A,n}$ vs P_e^2 for $s_0 = (1.4 \text{ GeV})^2$ (dashed), $s_0 = (1.44 \text{ GeV})^2$ (solid) and $s_0 = (1.5 \text{ GeV})^2$ (dotted) with $M = 2\text{GeV}$. Right panel: We plot $F_{LL}^{A,n}$ vs M^2 for $P_e^2 = 0.1 \text{ GeV}^2$ (dashed), $P_e^2 = 0.5 \text{ GeV}^2$ (solid) and $P_e^2 = 1 \text{ GeV}^2$ (dotted) with $s_0 = (1.44\text{GeV})^2$ 135
- 5.3 Same as Fig.(1) for $F_{LR}^{A,n}$ extracted from $F_{LR}^{A,r}$ 136
- 5.4 Same as Fig.(1) but for interpolation current, χ_{LA} 137
- 5.5 Same as Fig.(3) for $F_{LR}^{A,n}$ extracted from $F_{LR}^{A,r}$ 138
- 5.6 The representative graphs showing the variation of errors with P_e^2 for some $F_{\Gamma\Gamma'}^{A,r}$ functions calculated using the proton interpolation current, χ_{IO} . The shaded regions represents the error band and the central line gives the calculated values of the $F_{\Gamma\Gamma'}^{A,r}$ functions . 140
- 5.7 The representative graphs showing the variation of errors with P_e^2 for some $F_{\Gamma\Gamma'}^{A,r}$ functions calculated using the proton interpolation current, χ_{LA} . The shaded regions represents the error band and the central line gives the calculated values of the $F_{\Gamma\Gamma'}^{A,r}$ functions . 141
- 5.8 Feynman diagram contributing to the light-cone expansion of the correlation function for $D_q^* \rightarrow D_q \gamma$ up to leading order. The encircled D_q represents that the distribution amplitudes for D_q -meson enters the LCSR computation. The encircled vertex on the left represents the D_q^* interpolation current while the vertex on the right represents the electromagnetic current. 143
- 5.9 Plots showing the variation of g_{D^+} as a function of w_0 : (a) for different values of M^2 and fixed $s_0 = 6.5 \text{ GeV}^2$, and (b) for different values of s_0 and fixed $M^2 = 6 \text{ GeV}^2$. The Magenta line represents the expected value of g_{D^+} using the experimental data as tabulated in Table-5.3. The point at which the theoretical and experimental graphs are cutting each other is our expected value of w_0 146

List of Tables

1.1	The field representation of the SM particles under the SM gauge group \mathcal{G}_{SM} . The first and second entry in the bracket represents field representation under $SU(3)_c$ and $SU(2)_L$, respectively. The subscript gives the hypercharge Y	9
1.2	The list of mesons and their quark contents along with their masses, decay widths and the spin-parity taken from [35].	17
1.3	The list of baryons and their valence quark contents along with their masses, decay widths and the spin-parity taken from [35].	17
3.1	Tabulating the values obtained for different contribution of the normalised decay width (normalised to the non-radiative decay width i.e. $\bar{\Gamma} = \Gamma(\tau \rightarrow \pi\nu_\tau\gamma)/\Gamma(\tau \rightarrow \pi\nu_\tau)$) using the asymptotic DA (ϕ_π^{asym}) and the CZ DA (ϕ_π^{CZ}) of the pion.	86
5.1	Tabulation of all the 12 independent FFs at $P_e^2 = 0.5 \text{ GeV}^2$ for $s_0 = (1.44 \text{ GeV})^2$ and $M = 2 \text{ GeV}$ calculated using the proton interpolation current χ_{IO} . The errors are associated with the errors in the parameters used for the numerical analysis.	139
5.2	Tabulation of all the 12 independent FFs at $P_e^2 = 0.5 \text{ GeV}^2$ for $s_0 = (1.44 \text{ GeV})^2$ and $M = 2 \text{ GeV}$ calculated using the proton interpolation current χ_{LA} . The errors are associated with the errors in the parameters used for the numerical analysis.	139

5.3	Tabulating the values of the branching ratios for $D_q^* \rightarrow D_q \gamma$ ($q = u, d, s$) decay and the total decay width of the D_q^* -mesons [35], along with the experimental estimation of the $D_q^* D_q \gamma$ coupling, g_{D_q} defined in Eqn.(5.46).	145
6.1	Tabulating the branching ratios for the radiative and non-radiative decay modes of kaon to muon and electron (values taken from [35]).	154
B.1	Tabulating the invariant functions and the gamma matrix structures that appear in the general decomposition of the matrix element of the non-local three quark operator which helps us define the nucleon DAs.	172
B.2	The twist classification of nucleon DAs.	173
D.1	The numerical values of various parameters used in the numerical analysis performed for the form factor and decay width calculations for radiative tau decay.	180
D.2	The numerical values of various parameters used during the numerical analysis of both the cases considered in Chapter-4 for determination of the form factors involved in radiative proton decay.	181
D.3	The numerical values of the parameters used during numerical analysis for the form factors involved in $D^0 \rightarrow \bar{p}e^+$ and $D^* D \gamma$ coupling discussed in Chapter-5	181

Contents

Abstract	iii
List of Publications	v
List of Figures	vii
List of Tables	xiii
1 Introduction	5
1.1 The Standard Model of Particle Physics	6
1.2 Quantum ChromoDynamics and Hadrons	12
1.3 Hadronic Matrix Elements and the Form Factors	16
1.4 Methods to calculate the hadronic form factors	19
1.5 Effective Field Theories	22
1.6 Organisation of thesis	25
2 Light Cone Sum Rules in a Nutshell	27
2.1 SVZ Sum Rules	28
2.1.1 Understanding SVZ sum rules and its tools	29
2.1.1.1 Kallen-Lehmann representation	32
2.1.2 SVZ sum rules in quantum mechanics	43
2.1.2.1 An example: Harmonic Oscillator in an external electric field	44
2.1.3 Limitations of SVZ sum Rules	47
2.2 Theory of hard exclusive processes	48
2.2.1 Light cone dominance and OPE	50

2.2.1.1	Light cone dominance	51
2.2.1.2	Light Cone OPE	53
2.2.2	Light Cone Distribution amplitudes and the Conformal Symmetry	56
2.2.2.1	Conformal group and its collinear subgroup	58
2.3	Light Cone Sum Rules (LCSR)	61
3	LCSR in radiative tau decay	65
3.1	Introduction	66
3.2	Amplitude Computation	69
3.3	Form Factors in LCSR framework	74
3.4	Numerical results	80
3.5	Discussion and Conclusions	85
4	Exploring LCSR application to proton decay	89
4.1	Introduction	90
4.2	Amplitude Computation	92
4.3	Form Factors in the LCSR framework	95
4.3.1	Case-1: Using proton interpolation and photon DAs	95
4.3.1.1	Proton interpolation current	95
4.3.1.2	Numerical Analysis	107
4.3.2	Case-2: Using photon interpolation and proton DAs	110
4.3.2.1	Numerical Analysis	116
4.4	Discussion and Conclusions	117
5	The heavy meson system and LCSR	121
5.1	Introduction	122
5.2	Amplitude parameterization	123
5.3	Form Factors in LCSR	125
5.3.1	Case-1: $P_\Gamma = P'_\Gamma = P_L$	129
5.3.2	Case-2: $P_\Gamma = P_L$ and $P'_\Gamma = P_R$	131
5.4	Results	133
5.5	$D^*D\gamma$: Probing the inner structure of the charm mesons	141

5.6	Conclusions and Discussion	147
6	Summary and Future Work	151
6.1	Summary	151
6.2	Future Works	154
A	Important definitions, identities and integrals	157
A.1	Important definitions	157
A.2	Important identities	159
A.3	Important integrals	162
B	Light cone propagator and distribution amplitudes	165
B.1	Light cone propagator	165
B.2	Light cone distribution amplitudes (DAs)	167
B.2.1	Light-Meson DAs	167
B.2.2	Photon DAs	169
B.2.3	Nucleon DAs	171
B.2.4	Heavy meson DAs	174
C	Kinematics for radiative tau decay	175
C.1	Kinematics and decay width	175
C.2	t -dependence of decay width of intermediate vector mesons	178
D	Numerical values of various parameters	179

Chapter 1

Introduction

For decades, the fundamental goal of studying particle and astroparticle physics has been to understand the origin and structure of the Universe from smallest to largest scales. According to the present mass-energy budget of the Universe, we understand only 5% of the Universe, while rest of 95% is a complete mystery. This 5% is made up of elementary particles which have four fundamental interactions: electromagnetic (EM), weak, strong, and gravitational. The Standard Model (SM) of particle physics (to be discussed in detail in Section-1.1) describes the first three fundamental interactions while the gravitational interaction is not part of the SM. It has obtained great success in explaining various observed phenomena. However, it fails to explain phenomena like the matter-anti-matter asymmetry of the Universe [1], [2], the masses of neutrinos [3], [4], the dark matter, and dark energy [5], [6], and also several deviations from the SM predictions like in B-meson decays [7], [8], the anomalous magnetic moment of the muon [9], [10], etc. (see [11] for more details). All of these suggest towards physics Beyond the SM (BSM). The signatures for BSM can be seen either through direct searches or indirect evidences. Collider experiments, like the Large Hadron Collider (LHC), have looked for direct signatures but have had no success so far. The other possibility to probe BSM physics is by looking at the indirect effects of quantum fluctuations at low energies due to microphysics at higher energies. Low energy probes like rare decays of leptons and hadrons, and related observables, provide access to look for these indirect searches (with the help of

Effective Field Theories (EFTs) (see Section-1.5)) by studying the rare decays, asymmetries, and CP-violating effects [12]. These studies require precise theoretical predictions.

However, to make theoretical predictions on any observable involving strong interactions at low energies, the inputs on the non-perturbative hadronic quantities like form factors (FFs), decay constants, etc., are required. Although, calculating these quantities is a complicated and cumbersome task due to color confinement, a property of strong interactions (to be discussed in Section-1.2). Except for a few observables, which can be defined such that they are free from these hadronic quantities, like lepton flavor universality (LFU) ratios (R_K, R_{K^*}) [13], [14], these hadronic quantities are required everywhere, whether it is a precision calculation of flavor observables or decay width calculations of processes within or beyond the SM. Thus they are crucial inputs for making any prediction within or beyond the SM.

This thesis will discuss the complications and available possible methods (with the main focus on the method of Light Cone Sum Rules (LCSR)) to compute these hadronic parameters theoretically, especially the form factors, within the context of SM and BSM interactions. Let us now review the SM of particle physics, and the theory of strong interaction including the nitty-grities and involved challenges along with possible solutions.

1.1 The Standard Model of Particle Physics

The Glashow-Weinberg-Salam model [15]–[17], popularly known as the Standard Model (SM) of particle physics, dictates the fundamental interactions (EM, weak and strong but not gravitational) between the elementary particles. The development of the SM was gradual and was driven by many theoretical and experimental results. Within the SM, the elementary particles are classified as fermions, gauge bosons, and the Higgs boson. The fermions are further classified as quarks and leptons. They are of six types (or flavors) and are organized in three generations or families in order of increasing masses¹. The six flavors of

¹Why there are three generations is still an open question.

quarks are: up (u), down (d), strange (s), charm (c), bottom or beauty (b), and top or truth (t). The six flavour of leptons are: electron (e), muon (μ), tau (τ), and their corresponding neutrinos (ν_e, ν_μ, ν_τ). The fundamental interactions between these particles are mediated by the gauge bosons of the gauge group of the SM i.e. $\mathcal{G}_{SM} = SU(3)_c \otimes SU(2)_L \otimes U(1)_Y$. Here, $SU(3)_c$ is a non-abelian gauge group and dictates the theory of strong interactions, known as Quantum ChromoDynamics (QCD). $SU(2)_L$ and $U(1)_Y$ are the gauge groups associated with the weak isospin and the weak hypercharge, respectively. Collectively, the gauge group $SU(2) \otimes U(1)_Y$ provides the ElectroWeak (EW) theory, a combined framework to explain the weak and the electromagnetic interactions. It breaks spontaneously to $U(1)_Q$ due to Spontaneous Symmetry Breaking (SSB) when the Higgs scalar field acquires a non-zero Vacuum Expectation Value (VEV). $U(1)_Q$ is the group of electric charge transformations. The electric charge Q is related to the weak hypercharge, Y and the third component of the weak isospin, T_3 via the Gell-Mann-Nishijima formula [18], [19] given by

$$Q = T_3 + \frac{Y}{2}. \quad (1.1)$$

The gauge bosons which mediate the EM, weak and strong interactions are named as the photon (γ), the W^\pm and Z^0 , and the gluons g , respectively. The last piece of the SM is the Higgs boson which is responsible for mass generation of all the particles in the SM [20]–[25] and was finally discovered in 2012 [26], [27]. The fundamental particles along with their basic properties are shown in Fig.(1.1). Though, the Higgs provides mass to all the particles, the mechanism for the mass generation of fermions and gauge bosons is different. The gauge bosons acquire mass due to SSB, while the fermions acquire mass due to the Yukawa interactions between the fermions and the Higgs boson. The neutrinos, photon and gluons still remain mass-less within the SM.

The most general Lagrangian for the SM consistent with \mathcal{G}_{SM} and the condition of renormalizability is given by

$$\mathcal{L}_{SM} = \mathcal{L}_{\text{kinetic}} + \mathcal{L}_{\text{interaction}} + \mathcal{L}_{\text{Higgs}} + \mathcal{L}_{\text{Yukawa}} \quad (1.2)$$

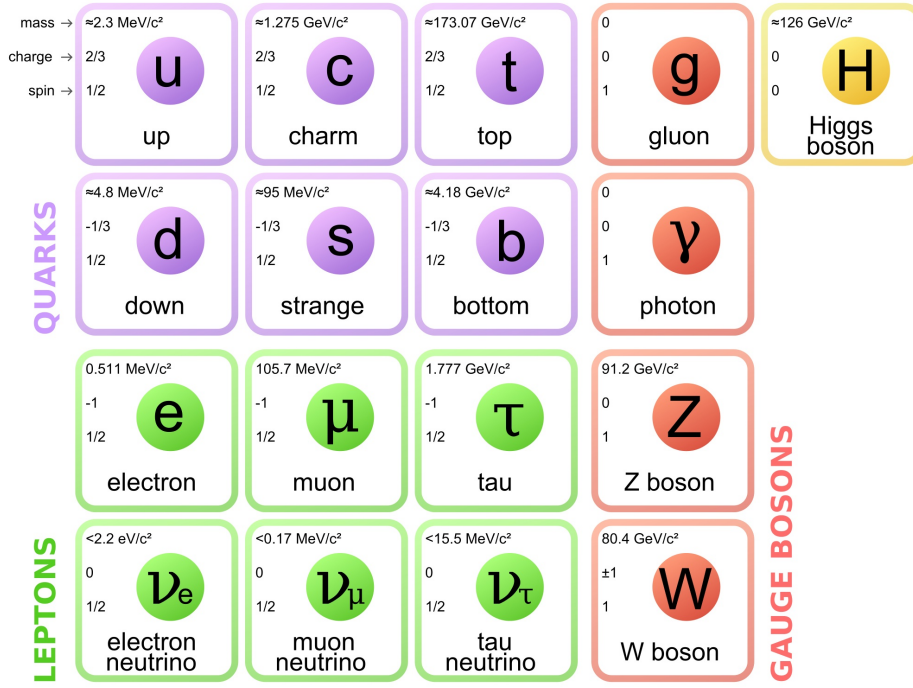


Figure 1.1: The fundamental particles in the Standard Model of particle physics. (Source: <https://www.quantumdiaries.org>).

where, $\mathcal{L}_{\text{kinetic}}$, $\mathcal{L}_{\text{interaction}}$, $\mathcal{L}_{\text{Yukawa}}$, and $\mathcal{L}_{\text{Higgs}}$ are various kinetic and interaction terms of elementary particles and we will now discuss them one by one.

$\mathcal{L}_{\text{kinetic}}$ and $\mathcal{L}_{\text{interaction}}$ are the kinetic and interaction terms for fermions and gauge bosons. The explicit form of these terms is

$$\mathcal{L}_{\text{kinetic}} + \mathcal{L}_{\text{interaction}} = i \sum_{\psi} \bar{\psi} \not{D} \psi - \frac{1}{4} B_{\mu\nu} B^{\mu\nu} - \frac{1}{2} \text{Tr} \{ \mathbf{W}_{\mu\nu} \mathbf{W}^{\mu\nu} \} - \frac{1}{2} \text{Tr} \{ \mathbf{G}_{\mu\nu} \mathbf{G}^{\mu\nu} \}, \quad (1.3)$$

where the summation in the first term runs over all the fermions. $\not{D} = D_{\mu} \gamma^{\mu}$ with D_{μ} being the covariant derivative that acts on the fermions. $B_{\mu\nu}$, $\mathbf{W}_{\mu\nu}$, and $\mathbf{G}_{\mu\nu}$ are the field strength tensors of the gauge fields B_{μ} , W_{μ}^i ($i = \{1, 2, 3\}$), and G_{μ}^a ($a = \{1, \dots, 8\}$) corresponding to $U(1)_Y$, $SU(2)_L$, and $SU(3)_C$ gauge groups, respectively. The explicit expressions for these field strength tensors read as

$$\begin{aligned} B_{\mu\nu} &= \partial_{\mu} B_{\nu} - \partial_{\nu} B_{\mu}, \\ \mathbf{W}_{\mu\nu} &= \partial_{\mu} \mathbf{W}_{\nu} - \partial_{\nu} \mathbf{W}_{\mu} + ig_2 [\mathbf{W}_{\mu}, \mathbf{W}_{\nu}], \\ \mathbf{G}_{\mu\nu} &= \partial_{\mu} \mathbf{G}_{\nu} - \partial_{\nu} \mathbf{G}_{\mu} + ig_s [\mathbf{G}_{\mu}, \mathbf{G}_{\nu}] \end{aligned} \quad (1.4)$$

where $\mathbf{W}_\mu = W_\mu^i \frac{\sigma_i}{2}$ and $\mathbf{G}_\mu = G_\mu^a \frac{\lambda_a}{2}$ with σ_i and λ_a being the Pauli and Gell-Mann matrices, respectively (collected in Appendix-A). We have also used Einstein's summation convention over the repeated indices. The gauge group of SM treats the left- and right-chiral fields differently. As a result, the covariant derivative D_μ acts differently on different fields. To understand that, let us first have a look at the representation of different particles under the SM gauge group. These representations are provided in Table-2.4. The left-handed fermions transform as

field	Q_L^i	u_R^i	d_R^i	E_L^i	e_R^i	γ	g	W^\pm, z^0	H
repr.	$(\mathbf{3}, \mathbf{2})_{\frac{1}{3}}$	$(\mathbf{3}, \mathbf{1})_{\frac{4}{3}}$	$(\mathbf{3}, \mathbf{1})_{-\frac{2}{3}}$	$(\mathbf{1}, \mathbf{2})_{-1}$	$(\mathbf{1}, \mathbf{1})_{-2}$	$(\mathbf{1}, \mathbf{1})_0$	$(\mathbf{8}, \mathbf{1})_0$	$(\mathbf{1}, \mathbf{3})_0$	$(\mathbf{1}, \mathbf{2})_1$

Table 1.1: The field representation of the SM particles under the SM gauge group \mathcal{G}_{SM} . The first and second entry in the bracket represents field representation under $SU(3)_c$ and $SU(2)_L$, respectively. The subscript gives the hypercharge Y .

a doublet under $SU(2)_L$ while the right-handed fermions transform as a singlet. Furthermore, the quarks and leptons are $SU(3)_C$ triplet and singlet, respectively. Consequently, the covariant derivatives for different fields are given as

$$\begin{aligned}
D_\mu Q_L &= (\partial_\mu - iY g_1 B_\mu - ig_2 \mathbf{W}_\mu - ig_s \mathbf{G}_\mu) Q_L, \\
D_\mu q_R &= (\partial_\mu - iY g_1 B_\mu - ig_s \mathbf{G}_\mu) q_R, \\
D_\mu E_L &= (\partial_\mu - iY g_1 B_\mu - ig_2 \mathbf{W}_\mu) E_L, \\
D_\mu e_R &= (\partial_\mu - iY g_1 B_\mu) e_R,
\end{aligned} \tag{1.5}$$

where Q_L and E_L are the left-handed quark and lepton doublets, respectively. $q_R \in \{u_R, d_R\}$ and e_R are the right-handed quark and lepton singlets. These can be explicitly written as

$$\begin{aligned}
Q_L^i &\equiv \begin{pmatrix} u_L^i \\ d_L^i \end{pmatrix} \equiv \left(\begin{pmatrix} u_L \\ d_L \end{pmatrix}, \begin{pmatrix} c_L \\ s_L \end{pmatrix}, \begin{pmatrix} t_L \\ b_L \end{pmatrix} \right), \\
E_L^i &\equiv \begin{pmatrix} \nu_L^i \\ e_L^i \end{pmatrix} \equiv \left(\begin{pmatrix} \nu_{e,L} \\ e_L \end{pmatrix}, \begin{pmatrix} \nu_{\mu,L} \\ \mu_L \end{pmatrix}, \begin{pmatrix} \nu_{\tau,L} \\ \tau_L \end{pmatrix} \right), \text{ and}
\end{aligned}$$

$$u_R^i \equiv \begin{pmatrix} u_R & c_R & t_R \end{pmatrix}, \quad d_R^i \equiv \begin{pmatrix} d_R & s_R & b_R \end{pmatrix}, \quad e_R^i \equiv \begin{pmatrix} e_R & \mu_R & \tau_R \end{pmatrix}.$$

The right-handed neutrinos are absent, leaving neutrinos massless in the SM. g_1 and g_2 are the electroweak couplings constants and are related to the electron charge, e by the relation

$$e = \frac{g_1 g_2}{\sqrt{g_1^2 + g_2^2}}. \quad (1.6)$$

The coupling constant for the strong interactions is represented as g_s . Moreover, one commonly uses α_{em} and α_s to represent the coupling strengths for the electromagnetic and strong interactions, respectively, and are defined as

$$\alpha_{em} = \frac{e^2}{4\pi}, \quad \text{and} \quad \alpha_s = \frac{g_s^2}{4\pi}, \quad (1.7)$$

respectively. α_{em} is popularly known as the fine structure constant and its value at low energy is $\sim \frac{1}{137}$ ².

The second last term of the SM Lagrangian is $\mathcal{L}_{\text{Higgs}}$. It includes the kinetic and self interaction terms for the Higgs field and is given by

$$\mathcal{L}_{\text{Higgs}} = (D_\mu H)^\dagger (D_\mu H) - \frac{m_H^2}{2v^2} (H^\dagger H - v^2)^2 \quad (1.8)$$

where m_H is the mass of the Higgs and v is the VEV. The Higgs field also transforms as a doublet under $SU(2)_L$ and hence the covariant derivative for the Higgs field is

$$D_\mu H = (\partial_\mu - iY_e g_1 B_\mu - ig_2 \mathbf{W}_\mu) H. \quad (1.9)$$

Finally, $\mathcal{L}_{\text{Yukawa}}$ is the Yukawa interaction term and is given by

$$\mathcal{L}_{\text{Yukawa}} = -Y_e \bar{E}_L H e_R - Y_d \bar{Q}_L H d_R - Y_u \bar{Q}_L \tilde{H} u_R + h.c., \quad (1.10)$$

where $\tilde{H} = i\sigma_2 H^\dagger$, and Y_e , Y_d , and Y_u are the Yukawa coupling constants.

Eqn.(1.10) is written in the flavor basis. In this basis, there are no mixing terms for the quarks of different generations. However, for practical applications, it is

²These coupling strengths vary with energy as a result of renormalisation (see Section-1.2 for more details).

convenient to write them in the mass basis i.e. the basis in which the matrix of the Yukawa couplings is diagonal. This can be done by performing a bi-unitary rotation of the quark fields given by

$$u_L \rightarrow U_u u_L, \quad d_L \rightarrow U_d d_L. \quad (1.11)$$

where U_L and U_d are the unitary matrices. These rotations affect the quark couplings with W^\pm bosons. The modified interaction Lagrangian for quark interaction with the W-bosons reads as

$$W_\mu^+ \bar{u}_L \gamma^\mu d_L + W_\mu^- \bar{d}_L \gamma^\mu u_L \rightarrow W_\mu^+ u_L^i \gamma^\mu (V_{CKM})^{ij} d_L^j + W_\mu^- \bar{d}_L^i \gamma^\mu (V_{CKM}^\dagger)^{ij} u_L^j. \quad (1.12)$$

Here, V_{CKM} is a unitary matrix that results in the mixing of different generation quarks and is known as the Cabibbo-Kobayashi-Maskawa (CKM) matrix [28], [29]. It is given by

$$U_u^\dagger U_d \equiv V_{CKM} = \begin{pmatrix} V_{ud} & V_{us} & V_{ub} \\ V_{cd} & V_{cs} & V_{cb} \\ V_{td} & V_{ts} & V_{tb} \end{pmatrix} \quad (1.13)$$

and has 4 independent parameters: 3 rotation angles and 1 complex phase. The complex phase in the CKM matrix is the only source of CP violation in the SM³. Consequently, the SM has eighteen free parameters which include the masses of the fermions except for neutrinos which are mass-less in the SM, the coupling constants, the angles and phase of the CKM matrix, and the mass and the VEV of Higgs.

After this brief introduction to the SM of particle physics, let us understand the theory of strong interactions in some detail. This thesis is focused on the challenges involved in calculating processes involving strong interactions at low energies.

³CP violation in the SM is not sufficient to explain the matter anti-matter asymmetry of the Universe.

1.2 Quantum ChromoDynamics and Hadrons

Quantum ChromoDynamics (QCD) is the theory of strong interactions described by the $SU(3)_c$ local non-abelian gauge group⁴. The fundamental degrees of freedom in QCD are the quarks and gluons. The quarks are the matter particles while the gluons are the mass-less gauge bosons that act as the mediator of strong interactions between quarks. QCD is very similar to the well-studied Quantum ElectroDynamics (QED), the theory which explains the interaction of photons with the charged particles. Like the electric charge in QED, QCD also has a charge called *color*. Though there are various similarities between QED and QCD, the major difference arises due to the non-abelian nature of QCD. It results in the self-interaction of gluons as they also carry the color charge while photons are charge neutral and hence do not interact among themselves. Because of these self-interactions of gluons, QCD becomes very complicated and leads to the interesting phenomenon of *color confinement*. It is the property of strong interactions which results in the formation of colorless bound states of quarks and gluons, known as *hadrons*, at low energies or equivalently at large distances. This property of strong interactions arises as a consequence of renormalization. To understand it, let us look at the QCD Lagrangian

$$\mathcal{L}_{\text{QCD}} = -\frac{1}{4}(\mathbf{G}_{\mu\nu})^2 + \sum_k \bar{\psi}_k^j (i\not{D} - m)_{ij} \psi_k^i + \mathcal{L}_{\text{gauge}} + \mathcal{L}_{\text{ghost}} \quad (1.14)$$

where $\mathbf{G}_{\mu\nu}$ is the gluon field strength tensor defined in Eqn.(1.4), and the covariant derivative D_μ here is

$$D_\mu = \partial_\mu - ig_s \mathbf{G}_\mu \quad (1.15)$$

with $\mathbf{G}_\mu = G_\mu^a \frac{\lambda_a}{2}$ ($a = \{1 \dots 8\}$). The sum over k runs over all flavors of quarks and $\{i, j\}$ represents the color indices for quarks.

The first term represents the kinetic and self-interaction terms for gluons while the second term represents the kinetic and interaction terms for quarks with gluons. The third, and the fourth terms are the gauge fixing and the ghost terms, respectively and are required to consistently quantize QCD and also to get rid

⁴A group is called non-abelian if the generators of the group do not commute.

of the redundant/unphysical degrees of freedom (d.o.f.) in the theory (for detail look at [30],[31]).

According to the perturbation theory, the scattering amplitude for a process can be calculated order by order in α_s including all the possible Feynman diagrams⁵ for the process at each order. At the leading order ($\mathcal{O}(\alpha_s^0)$), one does not encounter any problem. However, one encounters divergences in the intermediate steps while computing the higher orders quantum corrections (like $\mathcal{O}(\alpha_s)$) i.e. the loop diagrams. In field theoretical language, the divergences which arise due to integration over the large (ultra high) momentum of the particle running in the loop, which can take any value of the momentum from zero to infinity, are called the *UV divergences*⁶. Moreover, the real cross-section should be finite which demands for a procedure to take care of these infinities. According to this procedure, these infinities are first regularised, and the parameters are then redefined via renormalization. Consequently, the physical parameters like coupling constants, fermion masses, etc. are found to be scale-dependent and thus run with the scale. The physical parameters are the renormalized counterparts of the bare parameters which are written in the Lagrangian (Eqn.(1.14)). Measuring, say, the coupling at one scale, i.e. in a specific experiment, then allows one to know the value at a different scale relevant for different experiments. The dependence of the coupling strength $\alpha_s(= \frac{g_s^2}{4\pi})$ on the energy scale Q is shown in Fig.(1.2). Mathematically, it can be written as (upto 1-loop corrections)

$$\alpha_s(Q) = \frac{2\pi}{\beta_0} \frac{1}{\ln\left(\frac{Q}{\Lambda_{QCD}}\right)} \quad (1.16)$$

where $\beta_0 = 11 - \frac{2n_f}{3}$ is known as the beta function at 1-loop with n_f being the number of active flavors of quarks, and $\Lambda_{QCD} \sim 200\text{MeV}$ provides the Landau pole for QCD. Furthermore, in contrast to QED, the coupling strength for QCD decreases with an increase in energy, and this is referred to as *asymptotic freedom*. Consequently, at high energies $\alpha_s \ll 1$ and hence the quarks and gluons behave

⁵The graphical representations to show the flow and interactions of the particles.

⁶The divergences which arise when the loop momentum goes to zero are called InfraRed (IR) divergences.

almost like free particles, and the perturbation theory is applicable at those energy scales. However, at low energies ($Q \leq 1\text{GeV}$) α_s becomes large and QCD becomes non-perturbative, leading to the phenomenon of color confinement. It leads to the formation of hadrons at low energies or equivalently large distances (for details on the subject, see eg. [31]–[34]).

The hadrons are the colorless bound states of quarks and gluons. These states

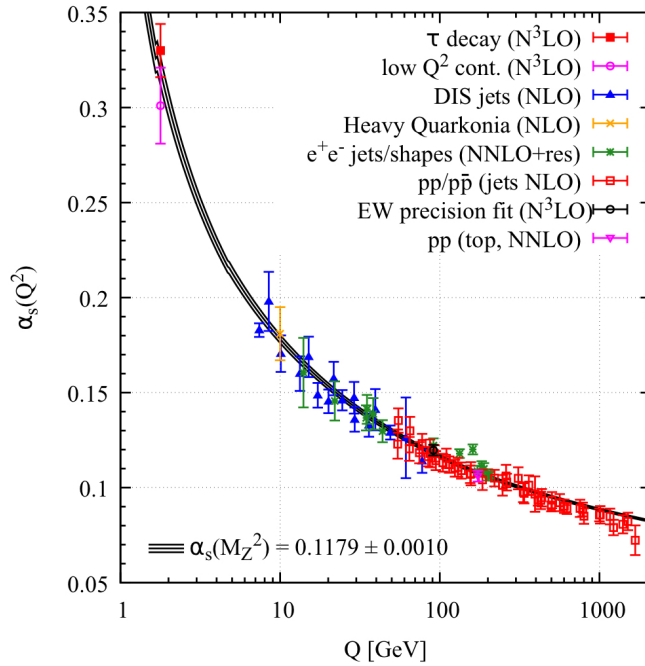


Figure 1.2: The running of strong coupling with energy scale from various experimental observations along with the theoretical prediction [35].

have a characteristic energy scale of $\mathcal{O}(\Lambda_{QCD})$. They are of mainly two types: *mesons*, the bound states of a quark and anti-quark, and *baryons* (*anti-baryons*), the bound states of three quarks (anti-quarks) which can be written as

$$\begin{aligned}
 |\text{Meson}\rangle &= \frac{1}{\sqrt{N_c}} |q_1^i \bar{q}_{2i}\rangle \\
 |\text{Baryon}\rangle &= \frac{1}{\sqrt{2N_c}} \epsilon_{ijk} |q_1^i q_2^j q_3^k\rangle, \quad |\text{Anti-baryon}\rangle = \frac{1}{\sqrt{2N_c}} \epsilon_{ijk} |\bar{q}_1^i \bar{q}_2^j \bar{q}_3^k\rangle \quad (1.17)
 \end{aligned}$$

where, $N_c = 3$, is the number of colors, $\{i, j, k\}$ are the color indices, and the Einstein summation convention over the repeated indices is used. As the quark-gluon interactions are flavor universal, any combination of $\{q_1, q_2, q_3\} \in \{u, d, s, c, b\}$ is

possible⁷. Experimentally, mesons with all the flavor combinations are observed while for the case of baryons with two or three heavy quarks are yet to be discovered⁸. The exotic states like tetraquark and pentaquarks are also possible and have been observed. We will not discuss them further, for more details look at [36] and references therein.

The states defined in Eqn.(1.17) are called the valence states with a minimal number of constituent quarks and anti-quarks, collectively called the valence quarks. These states can have an infinite number of virtual quarks, anti-quarks, and gluons called the sea quarks such that the state remains color neutral. The hadrons are the bound states defined as a superposition of all such states with n number of sea quarks, anti-quarks, and gluons. It can be understood with the help of the example of the bound state of a hydrogen atom (an example taken from [37]). According to non-relativistic quantum mechanics, this state is made up of a valence proton and a valence electron. However, in the field theoretical description, there will be quantum corrections due to the emission of virtual photons and electron-positron pairs. Hence, the hydrogen atom is not just a state given by a bound state of valence electron and proton but is a sum of infinite set of states consisting of one and more virtual photons and electron-positron pairs such that they carry the same quantum number as the hydrogen atom. Hence, one can write a hydrogen state as a superposition of states as

$$|\text{Hydrogen}\rangle = |e^- p\rangle \oplus |e^- p\gamma^*\rangle \oplus |e^- pe^+e^-\rangle + \dots \quad (1.18)$$

In QED, these virtual states do not have large effects and the effect of these states can be seen only in subtle effects like the Lamb shift. However, in QCD the states involving extra quarks, anti-quarks, and gluons are very important. The coupling strength α_s is large and the average energy of these virtual particles is $\sim \mathcal{O}(\Lambda_{QCD})$, i.e of the order of the hadronic scale.

At colliders, one detects only these color-neutral bound states and no free colored quarks. To have a theoretical estimate of the experimentally observed quantities

⁷The top quark, t decays before it can hadronize and does not form bound states like other quarks.

⁸With the exception of a couple of doubly charmed baryons.

like decay widths or scattering cross-sections, etc., one is required to use the scattering theory. According to the scattering theory, the probability amplitude of any process involving the decay or scattering of particles is determined by the matrix element of the relevant operator(s) in the interaction Lagrangian between the initial, i and the final, f state.

$$\mathcal{A}(i \rightarrow f) \sim \langle f | \hat{\mathcal{O}} | i \rangle \quad (1.19)$$

In QCD, interactions are governed by operators, $\hat{\mathcal{O}}$, made up of quarks and gluons. However, due to the color confinement, the initial and the final states are the hadrons or the QCD vacuum⁹, collectively known as hadronic states. Consequently, only perturbative QCD can not provide a theoretical estimate of physical observables and an input regarding the non-perturbative effects arising due to confinement must be included inevitably when strong interactions are involved in any process. The matrix elements of the quark-gluon operators between the initial and the final hadronic states (like the one in Eqn.(1.19)) are known as the *Hadronic Matrix Elements (HMEs)*. These are non-perturbative in nature. Before moving ahead with the details of these HMEs and how to calculate them, we collect all mesons and baryons used throughout this thesis along with their properties in Table-1.2 and Table-1.3. These lists are not even close to the complete list. The full list of mesons and baryons can be found in [35].

1.3 Hadronic Matrix Elements and the Form Factors

Hadron Matrix Elements (HMEs) are defined as the matrix elements of the quark and gluon operators between the initial and the final hadronic states.

⁹QCD vacuum is not an empty state. It is rather filled with fluctuating quarks and gluons such that the total number of quarks and gluons present in the vacuum must satisfy the quantum numbers of the vacuum, i.e. it must be color neutral, have zero electroweak charges, and must have the spin parity, $J^P = 0^+$ with non-zero average densities (see [37] to learn more about QCD vacuum).

Meson	Valence quark	Mass (MeV)	Full Width (MeV)	Mean life (s)	J^P
π^0	$\frac{u\bar{u}-d\bar{d}}{\sqrt{2}}$	(134.9768 ± 0.0005)	-	$(8.52 \pm 0.18) \times 10^{-17}$	0^-
π^+	$u\bar{d}$	(139.57039 ± 0.00018)	-	$(2.6033 \pm 0.0005) \times 10^{-8}$	0^-
$\rho(770)$	$\frac{u\bar{u}-d\bar{d}}{\sqrt{2}}$	(775.26 ± 0.25)	149.1 ± 0.8	-	1^-
$\omega(782)$	$\frac{u\bar{u}+d\bar{d}}{\sqrt{2}}$	(782.65 ± 0.12)	(8.49 ± 0.08)	-	1^-
$a_1(1260)$	$\frac{u\bar{u}-d\bar{d}}{\sqrt{2}}$	(1230 ± 40)	250 to 600	-	1^+
K^+	$u\bar{s}$	(493.677 ± 0.016)	-	$(1.2380 \pm 0.0020) \times 10^{-8}$	0^-
D^0	$c\bar{u}$	(1864.83 ± 0.005)	-	$(410.1 \pm 1.5) \times 10^{-15}$	0^-
D^+	$c\bar{d}$	(1869.65 ± 0.05)	-	$(1040 \pm 7) \times 10^{-15}$	0^-
D_s^+	$c\bar{s}$	(1968.34 ± 0.07)	-	$(504 \pm 4) \times 10^{-15}$	0^-
$D^{*0}(2007)$	$c\bar{u}$	(2006.85 ± 0.05)	< 2.1	-	1^-
$D^{*+}(2010)$	$c\bar{d}$	(2010.26 ± 0.05)	(0.0834 ± 0.0018)	-	1^-
D_s^{*+}	$c\bar{s}$	(2112.2 ± 0.4)	< 1.9	-	$??$

Table 1.2: The list of mesons and their quark contents along with their masses, decay widths and the spin-parity taken from [35].

Baryon	Valence quark	Mass (MeV)	Full Width (MeV)	Mean life	J^P
p	uud	$(938.272081 \pm 0.000006)$	-	$> 2.1 \times 10^{29}$ years	$\frac{1}{2}^+$
n	udd	$(939.565413 \pm 0.000006)$	880.2 ± 1.0	-	$\frac{1}{2}^+$
Λ	uds	(1115.683 ± 0.006)	-	$(2.632 \pm 0.02) \times 10^{-10}$ s	$\frac{1}{2}^+$
Λ_b	udb	(5619.60 ± 0.17)	-	$(1.470 \pm 0.010) \times 10^{-12}$ s	$\frac{1}{2}^+$

Table 1.3: The list of baryons and their valence quark contents along with their masses, decay widths and the spin-parity taken from [35].

Theoretically, their study is extremely complicated and tedious. This is because of the fact that the quarks and gluons inside hadrons interact at the energies of the order of Λ_{QCD} at which QCD becomes non-perturbative, and can no longer be treated as a perturbation theory. To compute these HMEs, one parameterizes them in terms of the non-perturbative objects called the *form factors* (*FFs*). These FFs are the essential theoretical inputs required to make any theoretical prediction within or beyond the SM. In general, the scattering matrix elements (or amplitudes) are analytic and unitary and are parameterized in terms of these FFs. Consequently, the FFs follow the principles of analyticity and unitarity.

The term form factor was first encountered in atomic physics while studying the scattering of an electron from an atom. In atomic physics the quantum mechanical initial and final states can be properly described in terms

of wave functions, while the mechanism of hadron formation can neither be described by a potential nor by perturbation theory. Consequently, wave function description is not possible for hadrons which makes the calculation of hadron FFs in QCD very challenging. We will discuss the available approximate methods to handle this difficulty in the next Section. Despite these huge differences between the atomic and hadronic systems, there are various similarities between the FFs involved in atomic and hadronic problems. Let us understand the basic properties of FFs using an atomic physics example where calculating them is easier.

Consider the elastic scattering of an electron from an atom (see [37] for a detailed discussion involving a general case)

$$e^{-}(\vec{k}) + A_0 \rightarrow e^{-}(\vec{k}') + A_0 \quad (1.20)$$

where \vec{k} and \vec{k}' are the three momentum of the incoming and the outgoing electron, respectively. A_0 represent the ground state of the atom. The amplitude for this process reads as

$$\mathcal{M}_{00} = \langle \vec{k}'; 0 | \hat{V} | \vec{k}; 0 \rangle = -\frac{4\pi Ze^2}{|\vec{q}|^2} + \frac{4\pi e^2}{|\vec{q}|^2} F(\vec{q}) \quad (1.21)$$

where Z is the atomic number, $\vec{q} = \vec{k}' - \vec{k}$ is the momentum transfer, and \hat{V} is the operator corresponding to the Coulomb potential given by (neglecting the atomic recoil)

$$V(\{\vec{x}_i\}, \vec{y}) = -\frac{Ze^2}{|\vec{y}|} + \sum_{i=1}^Z \frac{e^2}{|\vec{y} - \vec{x}_i|}. \quad (1.22)$$

Here, \vec{x}_i are the positions of electrons in the atom with respect to the atomic nucleus, and \vec{y} is the position of the scattered electron. The function $F(\vec{q})$ in Eqn.(1.21) is called the form factor and is defined as

$$F(\vec{q}) = \langle 0 | \left(\sum_i e^{i\vec{q} \cdot \vec{X}_i} \right) | 0 \rangle = \int d\vec{x} e^{i\vec{q} \cdot \vec{x}} \rho(\vec{x}). \quad (1.23)$$

where \vec{X} is the position operator with eigenvalues x_i , $\rho(\vec{x}) = |\psi_0(\vec{x})|^2$ is the average charge density of electrons in the atom in the ground state. In the limit

$\vec{q} \rightarrow 0$, $F(\vec{q})_{\vec{q} \rightarrow 0} = Ze$ i.e., the total charge of the electrons in the atom.

The FF reproduces the symmetry of the charge density in the momentum space i.e. $F(\vec{q}) = F(q^2)$ with $q \equiv |\vec{q}|$. Hence, the form factors can be used to understand the charge distribution inside the atom. In the spherical coordinates such that \vec{q} is parallel to z-axis, the form factor after angular integration turns out to be

$$F(q^2) = \frac{4\pi}{q} \int_0^\infty dr r \rho(r) \sin(qr) \quad (1.24)$$

where $r = \sqrt{|\vec{x}|^2}$. Hence, the FFs are spherically symmetric. Furthermore, $F(q^2)$ is a real-valued function of q^2 and at large q values, they are dominated by small distances ($r \sim 1/q$) as the integrand has a highly oscillatory function $\sin(qr)$ which is suppressed for large r values

The hadronic FFs have a similar physical interpretation. They capture the effect of the dynamics of strong interactions and can be very helpful in understanding the structure of hadrons. They typically depend on how the momentum of the hadron is distributed among different constituent quarks and gluons. These are the functions of the transferred four-momentum squared to preserve the Lorentz invariance of the theory. Furthermore, short-distance dominance of the form factors at large momentum transfer is valid for the case of hadron FFs as well. Moreover, the electric charge of the hadron can be calculated by calculating the electromagnetic form factor at zero momentum transfer. Let us now look at the various possible methods to calculate these FFs.

1.4 Methods to calculate the hadronic form factors

There are several non-perturbative methods to calculate these hadronic form factors like the constituent quark model [38], the MIT bag model [39], the Chiral perturbation theory (χPT) [40]–[43], the Lattice QCD (LQCD) [44]–[46], and the QCD sum rules (QCDSRs) [47]–[49], etc. Out of all the available non-perturbative methods, only LQCD and QCDSRs are QCD based, while others are some sort of an effective theory (EFT)/model.

Now, let us briefly review three of the most commonly used methods to calculate the hadron form factors:

1. **Chiral perturbation theory:** Along with the obvious symmetries of the Lagrangian like Lorentz invariance, gauge invariance etc., the QCD Lagrangian is found to have chiral symmetry in the limit of massless quarks, known as the chiral limit. As the quark masses are very small compared to the typical hadronic scale, $m_u, m_d, m_s \ll \Lambda_{QCD}$, QCD can be considered to have the chiral limit, and the quark masses can be treated as perturbations. In this chiral limit, the chiral symmetry $(SU(3)_L \times SU(3)_R)$ of QCD Lagrangian is spontaneously broken into $SU(3)_{L+R}$ resulting in eight pseudoscalar mesons which can be identified as the corresponding Goldstone bosons. These Goldstones have derivative couplings, and hence typical amplitude goes as $\frac{E^2}{\Lambda^2}$, where Λ is related to the breaking scale, F such that $\Lambda \sim 4\pi F$. Consequently, one can write an effective theory, known as *chiral perturbation theory* (χPT) to describe the QCD interactions in terms of the low mass mesons (eg. π, K, η, \dots). These low mass mesons are the (pseudo)-Goldstone bosons of spontaneous chiral symmetry breaking such that the Lagrangian is invariant under the chiral symmetry group, and the light quark mass terms act as the explicit breaking terms and transform linearly under this group. See [40]–[43] for detailed reviews.

2. **Lattice QCD:** Unlike the above discussed χPT , lattice QCD (LQCD) is a QCD formulation on a discretized Euclidean space-time grid. It has the same degrees of freedom as in QCD i.e. quarks and gluons, with no new parameters and hence retains the fundamental characteristics of QCD. LQCD solves QCD numerically by using computer simulations analogous to the ones used for statistical mechanics systems. The discretized space-time provides a non-perturbative regularisation scheme. Hence, we do not encounter any UV divergences as the finite lattice spacing, a , provides an UV cutoff given by π/a . For $a \rightarrow 0$, these computations provide the continuum limit. The numerical simulations in LQCD are non-perturbative implementations of the Feynman path integral approach of Quantum Field

Theory (QFT). Here, the calculations of the field theoretical observables proceed exactly the same way one would have done analytically given the ability to do such calculations. Hence, LQCD simulations allow us to calculate HMEs numerically using the fundamental principles of QCD with no extra assumptions. See for example [44]–[46] for detailed reviews.

3. **QCD sum rules:** It is another method that is based on the fundamentals of QCD. This method allows calculating the HMEs using the analytic properties of the correlation function of the interpolating quark currents of the hadrons taken at large virtualities (momentum squared, $|Q^2| \rightarrow \infty$). The correlation functions are the matrix elements of the time ordered product of these interpolating currents taken between vacuum or the on-shell states. These correlation functions are of dual nature. On one side, they can be written as the sum over the hadronic states using dispersion relations. These dispersion relations include contributions from the lowest energy hadron state and the continuum and heavier states. The contribution from the continuum and heavier hadronic states can be written in terms of the spectral densities which are not known and can be approximated by using the *quark hadron duality*. It approximates the perturbatively computed amplitudes in QCD (under certain assumptions and in specific energy regime) to the amplitudes calculated considering hadrons as the fundamental particles. On the other side, the correlation functions can be treated in the framework of Operator Product Expansion (OPE). OPE enables one to separate the short and long-distance quark-gluon interactions such that the former can be calculated using perturbative QCD (pQCD) and the latter can be parameterized in terms of vacuum condensates or distribution amplitudes (DAs). One can then match the two and perform Borel transformation as a final step to reduce the uncertainties due to approximations of quark hadron duality and to get rid of the divergences in the dispersion relations. Finally, one obtains the sum rule which helps in calculating the hadronic quantities like FFs.

The QCDSRs are of two types: the SVZ sum rules (SVZ SRs) and the

Light Cone Sum Rules (LCSR). LCSR is a hybrid of the SVZ SRs and the theory of hard exclusive processes. We will discuss more about it in Chapter-2.

None of the above mentioned methods can give a precise estimation of the hadronic FFs with the presently available computational and technical tools. Every method has its advantages and limitations over the other. As a result of it, none of these methods can be preferred over the other at present and it is essential to have estimates from different methods. However, with the advances in computational facilities, LQCD is expected to surpass all other methods. LCSR on the other hand is faster and complimentary to LQCD, as in many cases, LCSR and LQCD results are found to be more reliable in different energy regimes such that the combined analysis of the two gives a fairly good estimate of the hadronic object in the full Q^2 region [37], [50]. Taking a step ahead in this direction, we considered various processes within the SM and BSM scenarios where the application of LCSR was not explored, and compute the involved form factors. Before moving to the detailed description of the method of LCSR, let us review the basics of the effective field theories (EFTs).

1.5 Effective Field Theories

The basic idea of an EFT is that only a few d.o.f. will be relevant and dynamical at a given energy scale, while all other d.o.f. will be integrated out¹⁰. The effects of the integrated out d.o.f. are encoded in the coefficients of the local operators known as the *Wilson coefficients (WCs)*. These coefficients can be calculated by the so-called matching of the effective theory to the full theory. As both the theories should give equal results in the infra-red (IR) region, one matches the result of the two theories at some IR scale and gets the values of the WCs. They can be considered as the coupling strength of the corresponding operators as they do not depend on the initial and final states involved in the process. Let us

¹⁰The origin of this terminology lies in the path integral formalism of field theory. By integrating out the particular fields/particles, one means that they are no longer dynamical degrees of freedom. They can no longer appear as the initial and final state particles and can only contribute virtually.

now try to gain a better understanding of EFTs.

We know very well that to explain a phenomenon at the macroscopic scale, one does not require complete knowledge of the theory which explains the phenomena at the microscopic scale (QCD). For example to construct a bridge, one does not require the theory of quarks and gluon. It only requires a knowledge of Newton's laws, elasticity, fluid dynamics, etc. Even for a condensed matter system which consists of only charged electrons and ions, and photons, QED can be considered an effective field theory built out of the SM by integrating out all the heavier particles like W and Z bosons, heavier leptons and quarks, and writing interactions in terms of electrons, protons, ions, and photons. To explain such a system one does not need knowledge of strong or weak interactions.

Furthermore, let us consider an example of the simplest EFT, the Fermi theory for the weak interaction of four fermions, for the pion decay ($\pi^- \rightarrow \mu^- \nu_\mu$). In the full theory i.e., the SM, we know that the mediator for weak interactions between the quarks and leptons is the W and Z bosons. The weak current via which one explains the interactions mediated by W-boson reads as

$$j_W^\mu = V_{ij} (\bar{u}_i \gamma^\mu P_L d_j) + (\bar{\nu}_\ell \gamma^\mu P_L \ell). \quad (1.25)$$

where $\{i, j\}$ represent the flavors of the up and down-type quarks, and ℓ and ν_ℓ represent the different flavors of the leptons and their neutrinos. V_{ij} is the CKM matrix defined in Eqn.(1.13). In the full theory i.e., SM, the Feynman diagram for pion decay is shown in Fig.(1.3(a)) resulting in the tree-level amplitude for this process to be

$$\mathcal{A} = \left(\frac{-ig_2}{\sqrt{2}} \right)^2 V_{ud} (\bar{u} \gamma^\mu P_L d) \left(\frac{-i \left(g_{\mu\nu} - \frac{p_\mu p_\nu}{m_W^2} \right)}{p^2 - M_w^2} \right) (\bar{\mu} \gamma^\nu P_L \nu_\mu) \quad (1.26)$$

where, g_2 is the coupling constant of the weak interactions, and p is the momentum carried by $W - boson$. If $p^2 \ll m_W^2$ i.e., the momentum transferred square is small, the propagator can be Taylor expanded in powers of $\frac{p}{m_W}$. Then, the

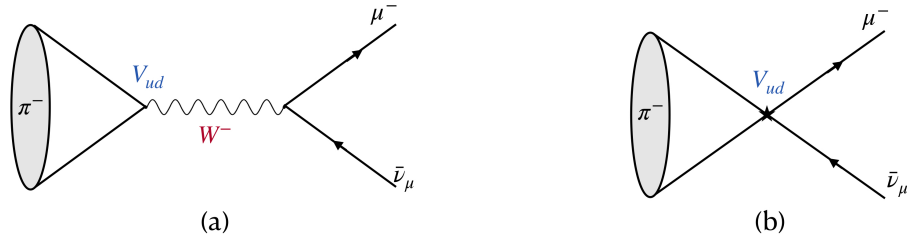


Figure 1.3: Feynman diagrams showing $\pi^- \rightarrow \mu^- \bar{\nu}_\mu$ (a) in the SM with W^- exchange and (b) in the EFT theory where W-boson is integrated out.

amplitude in Eqn.(1.26) becomes

$$\mathcal{A} = \frac{i}{m_W^2} \left(\frac{-ig_2}{\sqrt{2}} \right)^2 V_{ud} (\bar{u}\gamma^\mu P_L d) (\bar{\mu}\gamma_\mu P_L \nu_\mu) + \mathcal{O}\left(\frac{p^2}{m_W^4}\right). \quad (1.27)$$

Consequently, the effective Lagrangian for the π -decay in the four Fermi theory reads as

$$\begin{aligned} \mathcal{L}_{\text{eff}} &= -\frac{4G_F}{\sqrt{2}} V_{ud} (\bar{u}\gamma^\mu P_L d) (\bar{\mu}\gamma_\mu P_L \nu_\mu) \\ &= -\frac{4G_F}{\sqrt{2}} V_{ud} C(\mu) \mathcal{O}(\mu) \end{aligned} \quad (1.28)$$

where G_F is the Fermi's constant and is related to g_2 by

$$\frac{G_F}{\sqrt{2}} \equiv \frac{g_2^2}{8m_W^2}. \quad (1.29)$$

The W-boson is no longer a dynamical degree of freedom and has been integrated out. Its effect has been captured in the the Wilson coefficient, $C(\mu)$ which is simply unity in the present case, and $\mathcal{O}(\mu)$ represents the effective four fermion operator. Here, μ represents the scale dependence of the WC and operator and must cancel in the final result. However, in practical calculations it does not cancel due to truncation of the infinite series to certain order. The Feynman diagram for the pion decay using the effective Lagrangian, \mathcal{L}_{eff} , is a vertex diagram as shown in Fig.(1.3(b)). For more details on EFTs look at [51]. We will see a more general form of effective Lagrangian in Chapter-4 and 5 while dealing with BSM processes including the Baryon Number Violating (BNV) decays.

1.6 Organisation of thesis

We have organised the thesis as follows: In Chapter-2, we have discussed the method of LCSR in details. We discuss all the tools and techniques required to derive these sum rules. In Chapter-3, we discuss the application of LCSR to the light meson system by considering the radiative tau decay ($\tau^- \rightarrow \pi^- \nu_\tau \gamma$). In Chapter-4, we explored LCSR application to the baryonic system like proton by considering proton decay to a photon and a positron. The form factors involved in this case can be calculated in two ways, firstly, by using the proton interpolation current and the photon distribution amplitudes, and secondly, by using the photon interpolation current and the proton distribution amplitude. We discuss both these cases one by one in this chapter. In Chapter-5, we further explored the application of LCSR to the heavy meson system by considering a BNV decay of D^0 -meson i.e., $D^0 \rightarrow \bar{p} e^+$. The form factors involved are calculated by interpolating the proton state with the most general interpolation current. In this chapter we have also discussed how the experimental information on decay widths of radiative decays of D^* -mesons can be used to probe the structure of the D-meson. Finally, in Chapter-6, we conclude our findings and provide the future directions. Moreover, this thesis consists of four Appendices. In Appendix-A, we collect all the useful identities, integrals and definitions. In Appendix-B, we discuss the particle propagator near the light cone. Furthermore, in this Appendix, we collect the definitions and forms of the light cone DAs used throughout this thesis. The Appendix-C covers the kinematics involved in the decay width calculation of the radiative tau decay. Finally in Appendix-D, we collect the numerical values of all the parameters used in this thesis.

Chapter 2

Light Cone Sum Rules in a Nutshell

As already discussed in Chapter-1, the hadronic quantities like FFs are very essential theoretical inputs to calculate any process within or beyond the SM. Light Cone Sum Rules (LCSR) is one of the most effective method to calculate these hadronic quantities in terms of universal non-perturbative quantities known as *distribution amplitudes (DAs)* (discussed briefly in Section-1.4). It is a QCD-based method and has been employed successfully to determine various non-perturbative quantities like decay constants and form factors. Though these sum rules successfully calculate the hadronic quantities of interest, they have limited accuracy in many cases. It is mainly because of two reasons. Firstly, the uncertainties arising due to approximations in the Operator Product Expansion (OPE), and secondly, the uncertainties due to approximations involved in using quark hadron duality (We will discuss them in detail in Section-2.1.1). Despite that, it has an ensured place in the toolkit of QCD practitioners because of its relative ease compared to other methods like lattice QCD.

As already stated in Section-1.4, LCSR is a hybrid of the SVZ SRs and the theory of hard exclusive processes. Therefore, before moving to the details of LCSR, let us first understand SVZ SRs and the theory of hard exclusive processes. Thereafter, we will see how a marriage of the two leads to the beautiful technique of LCSR to compute these hadronic quantities.

2.1 SVZ Sum Rules

SVZ sum rules were first derived by Shifman, Vainshtein, and Zakharov (SVZ) in 1979 [48] and were named after them. It is a QCD-based semi-phenomenological method that helps one to determine the characteristics of the low-lying hadrons. To derive these sum rules one needs a suitable correlation function where the initial and final state hadrons of the HME are interpolated with the interpolation currents written in terms of quarks and gluons. The interpolation currents are such that they have the same quantum numbers as the hadrons of interest. Such correlation functions have dual nature and hence can be written using two representations.

According to the first representation, it can be written using the short-distance OPE at $q^2 \rightarrow -\infty$ i.e., large negative momentum transferred square. The OPE allows one to separate the short and the long-distance physics contributions. The short-distance contribution can be calculated using pQCD while the long-distance contribution can be encoded in the universal non-perturbative objects called *vacuum condensates*¹. We will discuss more about OPE in Section-2.1.1. On the other hand, the second representation can be written directly in terms of physical hadronic states in the form of a dispersion relation using unitarity and analyticity of the correlation function. All the physical hadronic states with the proper quantum numbers contribute to the dispersion relation. The dispersive integrals in the dispersion relation are unknown. In practical applications, the unknown non-perturbative hadronic quantities are related or equal to the residue of the lowest state contribution (as will be explained in detail in Section-2.1.1). However, the contributions from the higher and the continuum states can be approximated in terms of the perturbatively calculated correlation function using *quark-hadron duality* (see Section-2.1.1). The sum rule can then be written by matching the two representations. As a final step one performs *Borel transformation* (to be discussed in Section-2.1.1) in order to remove the divergences from dispersion relations. It also reduces the systematic uncertainty

¹The vacuum condensates are the vacuum expectation values of the quark-gluon local operators that are zero by definition in perturbation theory. They are ordered according to their canonical mass dimension.

due to quark-hadron duality by suppressing the contributions coming from the higher states and the continuum. The final sum rule can then be used to extract the hadronic quantity of interest. However, there are limitations to the usage of SVZ sum rules which we will discuss in Section-2.1.3. Thereafter, we will discuss how LCSR help us to deal with these limitations.

Let us now understand SVZ SRs and the tools mentioned above in better detail using a simple field theoretical example.

2.1.1 Understanding SVZ sum rules and its tools

Consider an example of a simple correlation function, say $e^+e^- \rightarrow e^+e^-$ scattering with quantum fluctuations due to quarks as shown in Fig.(2.1) [52]. It is a correlation function of the quark currents with no initial or final state hadrons such that the quarks can propagate only at short distances. It can be written as

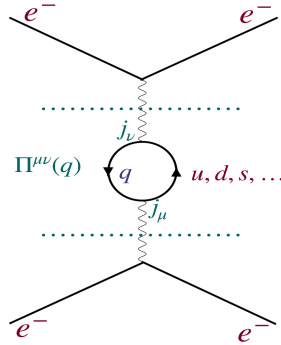


Figure 2.1: The Feynman diagram showing the process $e^+e^- \rightarrow e^+e^-$ with a quark loop due to quantum fluctuations.

$$\Pi_{\mu\nu}(q) = i \int d^4x e^{iq \cdot x} \langle 0 | T \{ j_\mu(x) j_\nu(0) \} | 0 \rangle = (q_\mu q_\nu - q^2 g_{\mu\nu}) \Pi(q^2) \quad (2.1)$$

where q is the momentum that is flowing inside the loop, $j_\mu = \sum_q Q_q \bar{q} \gamma_\mu q$ is the electromagnetic current for quarks, q with the sum running over all flavors. $\Pi(q^2)$ is the scalar function that encodes all the information of the effect of strong interactions, and the Lorentz structure on the right-hand side (r.h.s.) of Eqn.(2.1) is dictated by current conservation i.e. $\partial_\mu j^\mu = 0$. It is important to note that $\Pi(q^2)$ is an analytic function of q^2 and is defined for all the values of

q^2 . Now our task is to derive a sum rule for $\Pi(q^2)$. For that, let us first gain a better understanding of the tools required to derive these sum rules. There are four main tools, namely

1. Short-distance OPE,
2. Dispersion relation,
3. Quark hadron duality, and
4. Borel transformations.

A schematic flowchart of these tools along with their importance and function in the derivation of the sum rules is shown in Fig.(2.2). Let us discuss them one

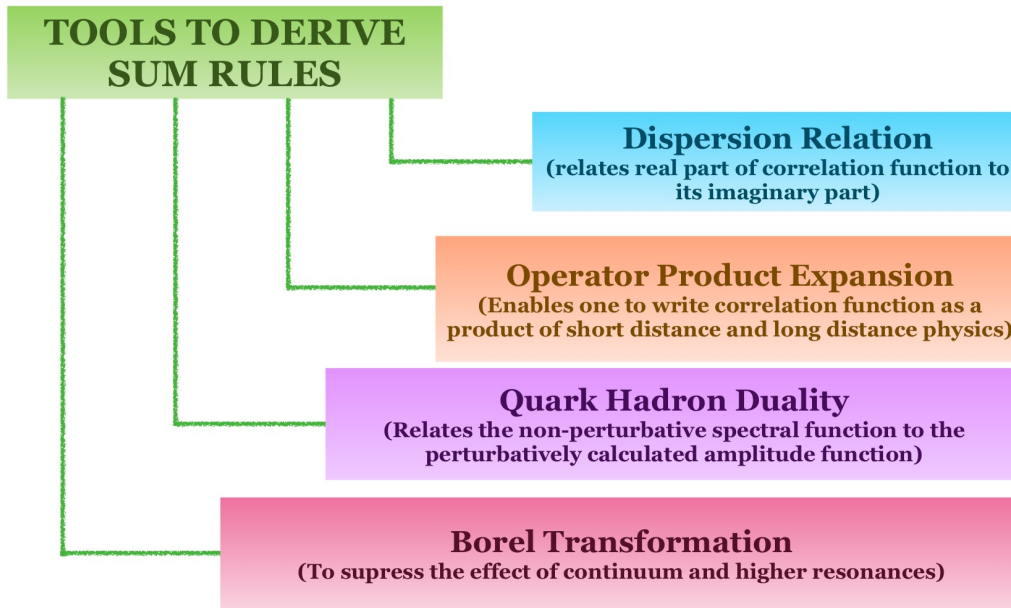


Figure 2.2: Flowchart chart showing important tools to derive sum rules along with their importance and function.

by one and understand their importance for deriving a sum rule for $\Pi(q^2)$.

1. **Short-distance Operator Product Expansion:** Operator product expansion (OPE) provides a systematic method to calculate $\Pi(Q^2)$ with $Q^2 = -q^2$ in the deep Euclidean region ($Q^2 \gg \Lambda_{QCD}$). It was introduced in particle physics by Wilson [53]. According to it, one can consistently separate the long-distance (i.e. the distance $\geq \mu^{-1}$) and the short-distance

(i.e. the distance $\leq \mu^{-1}$) contributions, where, μ is some normalization point which separates the two regions. This separation is possible because of internal reasons, like the exchange of heavy W -boson, c, b - quarks, etc. The observable quantities do not depend on the value of μ and hence one can choose μ according to the convenience. Mathematically, the statement of OPE reads as

$$\Pi^{pert}(q^2) = \sum_d C_d(q^2, \mu) \langle 0|O_d|0\rangle(\mu). \quad (2.2)$$

Here, $C_d(q^2, \mu)$ are known as the Wilson coefficients (WCs) and $\langle 0|O_d|0\rangle(\mu)$ represents the vacuum expectation of the local operators, O_d , of different dimension, d , both evaluated at μ . The sum over d implies a sum over all the Lorentz and gauge invariant local operators of different dimensions built from the quark and gluon fields. WCs capture the short distance (high energy) effects and can be calculated in perturbation theory using pQCD. However, the vacuum expectations of the local operators capture the long-distance (low energy) effects and hence are non-perturbative in nature. The lowest (zero) dimension operator is the unit operator, $\mathbb{1}$. The higher dimensional operators capture the information of QCD vacuum fields in the form of vacuum condensates of quarks and gluons such as $\langle \bar{q}q \rangle$, $\langle G_{\mu\nu}^2 \rangle$, etc. These vacuum condensates are the universal non-perturbative quantities and hence can be estimated using the experimental data on the well-studied modes.

$\Pi(q^2)$ in deep Euclidean region is dominated by the physics at short distances i.e., $x_\mu \rightarrow 0$ (see [52] for a physical argument for short-distance dominance). According to the short distance OPE, the it gets the main contribution from the lowest dimension operator and the contribution of the higher dimension operators decreases as we go to higher and higher dimension operators. This OPE dictates the first representation of $\Pi(q^2)$ as discussed above. However, in Section-2.1.3, we will see how this short-distance OPE becomes a problem while computing the three-point correlation functions. Later, in Section-2.2.1.2, we will see how an OPE at light-

like distances ($x^2 \rightarrow 0$) rescues the situation. Before that let us move to the second representation of $\Pi(q^2)$, written directly in terms of the hadronic states.

2. **Dispersion Relation:** It helps us in writing $\Pi(q^2)$ directly in terms of the physically observed hadronic states. Its origin lies in classical electrodynamics in the form of Kramers-Kronig dispersion relations [54], [55]. It relates the real part of an amplitude to its imaginary part which is usually better accessible to us.

The dispersion relation and the Wilson's OPE were considered to be two successful approaches to explain the theory of strong interactions outside field theories. However, lately both became a part of QFT. As already discussed, Wilson's OPE uses the expansion of products to explain strong interactions. On the other hand, the dispersion relation uses the analyticity and unitarity properties of the correlation function. It will become more clear as we move forward.

Before discussing the dispersion relation corresponding to $\Pi(q^2)$, let us discuss a simple example of a two-point correlator of scalar theory in order to get a better understanding of the importance and physics behind the dispersion relations. The dispersion relation corresponding to two point correlator is known as the Kallen-Lehmann (KL) spectral representation.

2.1.1.1 Kallen-Lehmann representation

KL representation helps us to determine the analytic structure i.e., the singularities like the poles, branch cuts, etc., of the 2-point correlation function. It shows that the dispersion relations can be derived from the first principle in QFT and captures the analytic structure of the correlation function.

To understand it, let us consider the Fourier transform of the 2-point correlator of the scalar field, ϕ given by (we follow [56] for the discussion below).

$$\Gamma(q^2) = i \int d^4x e^{iq \cdot x} \langle 0 | T \{ \phi(x) \phi^\dagger(0) \} | 0 \rangle \quad (2.3)$$

where T represents the time ordering. For a free theory, this correlator is nothing but the propagator for the field ϕ . However, for an interacting case, it is a non-trivial object given by

$$\Gamma(q^2) = \begin{cases} \frac{1}{m^2 - q^2 - i\epsilon} = -\Delta_F(q^2, m^2), & \text{free} \\ \frac{Z(\lambda)}{m^2 - q^2 - i\epsilon} + f(\lambda, q^2), & \text{interacting} \end{cases} \quad (2.4)$$

where λ is the coupling constant of the theory, and $-\Delta_F(q^2, m^2)$ represents the propagator of the field ϕ with mass m . The function $Z(\lambda)$ is the field renormalization factor, and the function $f(\lambda, q^2)$ is the function of interest. Its properties will be the main focus of our discussion further. In the limit of free theory, i.e. $\lambda \rightarrow 0$, both these functions must satisfy the following conditions

$$Z(\lambda) \rightarrow 1, \quad f(\lambda, q^2) \rightarrow 0, \quad \text{for } (\lambda \rightarrow 0). \quad (2.5)$$

The free theory case in Eqn.(2.4) suggests that the analytic properties of the correlation function are determined by the mass spectrum (as shown in Fig.(2.3)).

Focusing now on the interacting case, let us consider only the positive frequency distribution for computational simplicity. In that case

$$\langle 0 | \phi(x) \phi^\dagger(0) | 0 \rangle = \begin{cases} \Delta_+(x^2, m^2) = \int \frac{d^4q}{(2\pi)^3} e^{-iq \cdot x} \delta^+(q^2 - m^2), & \text{free} \\ (*), & \text{interacting} \end{cases} \quad (2.6)$$

where, $\delta^+(q^2 - m^2) = \delta(q^2 - m^2)\theta(q_0)$ which ensures the positive energies and the on-shell condition. $(*)$ is the object which determines the spectral representation. Using the unitarity condition, one can insert a complete set of states i.e. $\mathbb{1} = \sum_n |n\rangle\langle n|$ which results in

$$(*) = \sum_n \langle 0 | \phi(x) | n(q_n) \rangle \langle n(q_n) | \phi^\dagger(0) | 0 \rangle. \quad (2.7)$$

Here, $|n\rangle$ represents a complete set of single-particle states as well as all multi-particle states. Furthermore, using the property of the trans-

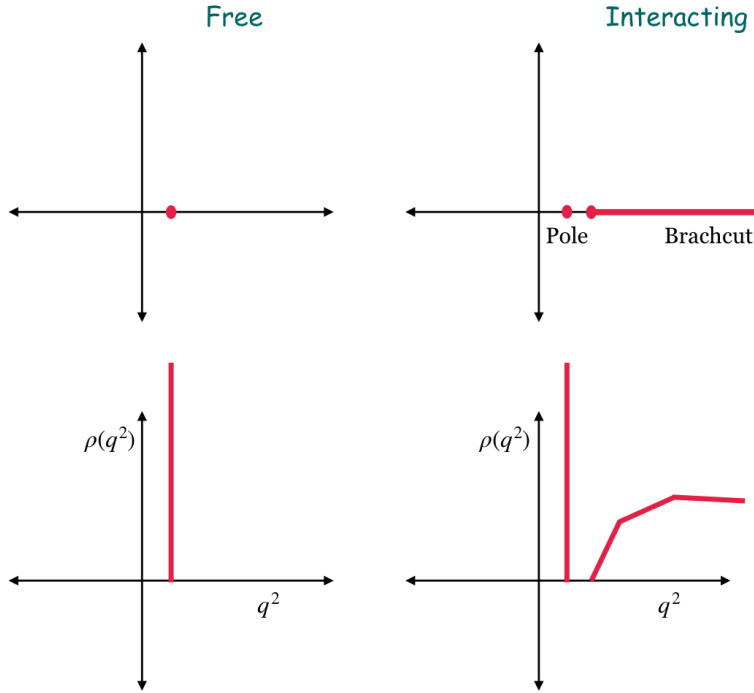


Figure 2.3: Showing the analytic structure of the 2-point correlation function in the upper graph and the spectral density function in the lower graph as a function of q^2 for free theory(left panel) and interacting theory (right panel).

lation invariance of the scalar theory along with the property that $1 = \frac{1}{(2\pi)^4} \int d^4q e^{-iq \cdot x} \int d^4x e^{iq \cdot x}$, and further interchanging \sum_n and $\int d^4x$ ², one gets

$$\begin{aligned}
 (*) &= \int d^4q e^{-iq \cdot x} |\langle 0 | \phi(0) | n(q_n) \rangle|^2 \equiv \sum_n \delta(q - q_n) |f_n|^2 \\
 &= (2\pi)^{-3} \rho(q^2) \theta(q_0) \quad (2.8)
 \end{aligned}$$

where, $|f_n|^2 = |\langle 0 | \phi(0) | n(q_n) \rangle|^2$ and $\rho(q^2)$ is the spectral density function which is positive definite as a consequence of unitarity. $(2\pi)^{-3}$ is a factor inserted for convenience and $\theta(q_0)$ ensures positive energies. The condition of positive energies comes from the same condition on the energies of the external particles as in Eqn.(2.6). Moreover, using the property of the delta function i.e.

$$\int d^4q F(q^2) = \int d^4q \int ds \delta(s - q^2) F(s),$$

²These interchanges are not always possible. They are ill-defined when there are UV divergences involved. Look at [56] for more details.

where $F(q^2)$ is some arbitrary function of q^2 , and exchanging $\int ds$ and $\int d^4q$, one gets

$$(*) = \int_0^\infty ds \rho(s) \Delta_+(x^2, s). \quad (2.9)$$

This is a spectral representation that can be generalized to the negative frequencies as well and finally results in the Kallen-Lehmann (KL) spectral representation given by

$$\Gamma(q^2) = \int_0^\infty \rho(s) (-\Delta_F(s, q^2)) = \int_0^\infty ds \frac{\rho(s)}{s - q^2 - i\epsilon}. \quad (2.10)$$

where $\epsilon \rightarrow 0^+$. This representation tells us that the analytic structure of the correlation function has a one-to-one correspondence with the mass spectrum of the theory. It was found independently by Kallen [57] and Lehmann [58]. The analytic structure of the integrand on the r.h.s. of Eqn.(2.10) is such that it has poles corresponding to the single-particle states and a branch cut corresponding to the multi-particle states (as shown in Fig.(2.3)). The spectral density on the r.h.s in Eqn.(2.10) can then be related to the imaginary part of the correlator $\Gamma(q^2)$ using Cauchy's integral formula which states that

$$\begin{aligned} \Gamma(q^2) &= \frac{1}{2\pi i} \oint_C dz \frac{\Gamma(z)}{z - q^2} \\ &= \frac{1}{2\pi i} \oint_{|z|=R} dz \frac{\Gamma(z)}{z - q^2} + \frac{1}{2\pi i} \int_0^R dz \frac{\Gamma(z + i\epsilon) - \Gamma(z - i\epsilon)}{z - q^2}. \end{aligned} \quad (2.11)$$

where C is the contour as shown in Fig.(2.4), R is the radius of the circle of the contour, C which can go up to infinity. Hence, the first term on r.h.s. will vanish. However, the second term which gives the discontinuity along the branch cut and can be written in terms of an integral over the imaginary part of $\Gamma(q^2)$ using the Schwartz reflection principle which states that

$$\Gamma(z + i\epsilon) - \Gamma(z - i\epsilon) = \text{disc}(\Gamma(z)) = 2i\text{Im}\Gamma(z) \text{ at } z > t_{min} \quad (2.12)$$

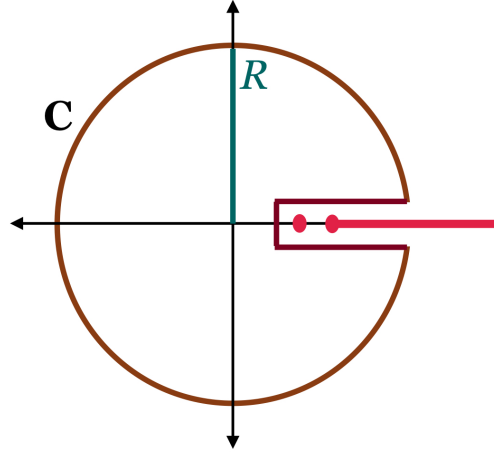


Figure 2.4: Showing the integration contour, C for the dispersion representation of the 2-point correlation function $\Gamma(q^2)$.

where $t_{min} = m^2$ is defined such that $\Gamma(z)$ is real for $z < t_{min}$.

For practical applications, it is useful to separate out the lowest state contribution. As a result of Cauchy's integral theorem, one can write

$$\Gamma(q^2) = \frac{|f_0|^2}{m^2 - q^2 - i\epsilon} + \frac{1}{\pi} \int_{s_0^h}^{\infty} dz \frac{\text{Im}\Gamma(z)}{z - q^2 - i\epsilon} \quad (2.13)$$

where f_0 is the residue of the lowest state and s_0^h is the continuum threshold (equal to $4m^2$ in many cases). f_0 is the non-perturbative object that one usually intends to extract using the method of sum rules.

On equating Eqn.(2.10) and Eqn.(2.13), one can write,

$$\rho(s) = |f_0|^2 \delta(m^2 - s) + \frac{1}{\pi} \text{Im}\Gamma(s) \theta(s - s_0^h). \quad (2.14)$$

Now, after understanding the KL representation, let us go back to the dispersion relation corresponding to our considered correlation function given in Eqn.(2.1).

At $q^2 > 0$, the long-distance effects become important which leads to the materialization of the quark-anti-quark pair generated by the current j_μ into neutral vector bosons as well as the heavier states along with the continuum to preserve the spin-parity of the current. Consequently, on inserting a complete set of states with $J^P = 1^-$, like we did while deriving

the KL representation, the

$$2 \operatorname{Im}\Pi_{\mu\nu}(q) = \sum_n \int d\tau_n (2\pi)^4 \delta^{(4)}(q - p_n) \langle 0 | j_\mu | n \rangle \langle n | j_\nu | 0 \rangle. \quad (2.15)$$

This is nothing but the unitarity relation or the Optical theorem. The sum runs over all the possible hadronic states, $|n\rangle$ with $J^P = 1^-$ i.e., the complete set of neutral vector mesons and the multi-particle continuum with $J^P = 1^-$, $d\tau_n$ represents the phase space volume of these states. Furthermore, the correlation function can be further written as

$$\frac{1}{\pi} \operatorname{Im}\Pi(q^2) = f_V^2 \delta(q^2 - m_V^2) + \rho^h(q^2) \theta(q^2 - s_0^h) \quad (2.16)$$

where we have separated the contribution coming from the lowest energy state and lumped the continuum and the heavier state contributions into the spectral density $\rho^h(q^2)$. m_V and f_V are the mass and the residue of the lowest vector meson state, respectively. The contribution coming from the continuum and the heavier states are more complicated and we represent it with the spectral density, $\rho^h(q^2)$ (for more details look at [52]). Consequently, the dispersion relation for $\Pi(q^2)$, using the Cauchy's integral formula, can be written as

$$\Pi^{had}(q^2) = \frac{f_V^2}{(m_V^2 - q^2)} + \frac{1}{\pi} \int_{s_0^h}^{\infty} ds \frac{\operatorname{Im}(\Pi^{had}(s))}{(s - q^2)}. \quad (2.17)$$

where '*had*' is the superscripts represents that this is the representation of $\Pi(q^2)$ written directly in terms of hadronic states.

In practical applications, the non-perturbative hadronic quantities are related to f_V . Hence, the problem of computing the hadronic object reduces to the computation of the residue of the lowest state contribution to the dispersion relation³. The contribution coming from the heavier and the

³These dispersion relations can, in general, have divergences. It is because of the fact that in general, the correlation function may have ultraviolet (UV) divergences like in the case of the correlation function in Eqn.(2.1). As a result of these UV divergences, the imaginary part of the correlation function does not vanish at asymptotic boundaries and thus, the dispersion integrals are divergent (see [52] for more details). Such divergences can be taken care of by performing Borel transformations or equivalently by subtracting the first few terms of the

continuum states can be approximated using the quark hadron duality and are further suppressed using the Borel transformation for better stability of the sum rule. We will discuss them below.

3. **Quark Hadron Duality:** As the name suggests, it bridges the gap between the theoretical predictions based on the perturbative calculations involved in QCD in terms of quarks and gluons and the experimentally observable quantities written directly in terms of hadronic states in the form of the dispersion relation. This idea was formulated when Poggio, Quinn, and Weinberg suggested that at high energies some inclusive hadronic cross sections coincide approximately with the cross sections calculated in QCD and are appropriately averaged over a certain energy range.

The spectral densities in Eqn.(2.16) are unknown. If one had successfully developed a method to calculate these spectral densities exactly then a duality approximation would have not been required as that will provide a complete solution to the theory of strong interactions. However, that is not the case in practical calculations. Moreover, these spectral densities can be approximated using the statement of *local quark hadron duality* according to which

$$\text{Im}(\Pi^{\text{cont}}(s)) \rightarrow \text{Im}(\Pi^{\text{pert}}(s)) \text{ at } s \rightarrow \infty. \quad (2.18)$$

where $\text{Im}(\Pi^{\text{cont}}(s))$ is the contribution to $\Pi^{\text{had}}(s)$ coming from the heavy states and the continuum. The validity of this assumption relies on the fact that partonic representation can be approximated to the hadronic representation at high energies as QCD is a valid theory for strong interactions in that regime.

Furthermore, in the deep Euclidean region i.e. $q^2 \rightarrow -\infty$, all the condensate contributions are negligible which leads to the validity of $\Pi(q^2) \rightarrow \Pi^{\text{pert}}(q^2)$. This along with the statement of local quark hadron duality leads to

$$\frac{1}{\pi} \int_{s_0^h}^{\infty} ds \frac{\text{Im}\Pi(s)}{(s - q^2)} \simeq \frac{1}{\pi} \int_{4m^2}^{\infty} ds \frac{\text{Im}\Pi^{\text{pert}}(s)}{(s - q^2)} \quad (2.19)$$

Taylor series expansion of the correlation function at $q^2 = 0$).

at $q^2 \rightarrow -\infty$. This is the statement of *global quark hadron duality*.

Now combining Eqn.(2.18) and Eqn.(2.19), one can postulate that at sufficiently large $Q^2 = -q^2$, we have

$$\frac{1}{\pi} \int_{s_0^h}^{\infty} ds \frac{\text{Im}\Pi(s)}{(s - q^2)} \simeq \frac{1}{\pi} \int_{s_0}^{\infty} ds \frac{\text{Im}\Pi^{pert}(s)}{(s - q^2)} \quad (2.20)$$

where s_0 is the continuum threshold, not necessarily equal to s_0^h . It is an independent parameter in the sum rule calculations and its value depends on the particle spectrum of the correlation function. Typically, its value is roughly approximated to the value of the resonance next to the ground state resonance that can enter in the correlation function: $s_0 \sim (m_M + \Delta)^2$ where $\Delta \sim \mathcal{O}(\Lambda_{QCD})$. The final value of s_0 is fixed by demanding stability of the final hadronic quantity against a variation in the value of s_0 ⁴. This introduces the first source of systematic uncertainties in the sum rule calculations. The statement of *semi-local quark-hadron duality* in Eqn.(2.20) is what one practically uses in the sum rule calculations (for more detail one can look at [37], [59]).

Apart from this, there are two other forms of uncertainties coming from here. First is the natural uncertainty arising due to the truncation of the infinite series in $\alpha_s(Q^2)$ as well as the condensates. The computational difficulties increase with every order in α_s which makes it nearly impossible to sum up this infinite series. Similarly, for a series in condensates, it is not possible to sum up the complete series. Consequently, both these series are required to be truncated up to some finite terms. Second, are the deviations from the duality, known as the duality violations. These are the major sources of systematic uncertainties in the sum rule calculations. Removing

⁴The choice of s_0 close to the next resonance can be loosely understood in the following way; our objective is to approximate the contribution coming from the heavier (or continuum) states with the contribution obtained from the QCD calculations. As this approximation has better validity in the large energy limit therefore, setting s_0 too small will lead to larger uncertainties. On the other hand, if we take its value to be very large then we will end up missing out on the contribution coming from the states between the ground state and the value of s_0 which will again lead to large uncertainties in the result. Therefore, one looks for the stable window of s_0 in the vicinity of the next resonance to optimise the uncertainties and pick a value from this stable window.

these uncertainties is one of the major challenges for the QCD practitioners as even lattice calculations can not shed light on them. This is because of the fact that duality violation can not be separated from Minkowskian kinematic and lattice is a Euclidean approach to QCD. Therefore, to understand these violations we need analytical solutions. There are various models like an instanton-based model, resonance-based model, etc, which can describe these duality violations but at present a complete solution is still lacking (see for example [60], [61] and references therein). Though a proper analytical method to compute these violations does not exist, the uncertainties due to these violations can be reduced by suppressing the contribution of the higher state and the continuum which were approximated using these dualities. This can be done by performing Borel transformations.

4. **Borel Transformation:** To understand the power of Borel transform [62], let us first consider a simple example. Consider a function $A(x)$ given by

$$A(x) = \sum_{k=0}^{\infty} A_k x^{k+1} \quad (2.21)$$

The Borel transform of this function is defined as (with M being the parameter called Borel mass)

$$B(M) = \sum_{k=0}^{\infty} \left(\frac{A_k}{k!} \right) M^k \quad (2.22)$$

One sees that higher coefficients are factorially suppressed. Further, if A_K has a factorial divergence like $k!$ then $B(M)$ will be an analytic function in the neighborhood of origin. Moreover, if the function $A(x)$ itself is a good analytic function then the following equality holds

$$A(x) = \int_0^{\infty} dM \text{Exp} \left(\frac{-M}{x} \right) B(M) \quad (2.23)$$

This allows to recover the original series. The inverse relation also holds if $B(M)$ is such that it can be analytically continued on the positive real

axis up to infinity. The function in Eqn.(2.22) (provided that the integral converges) is the Borel sum of the asymptotic expansion in Eqn.(2.21).

In practical calculations, the above is then achieved by the mathematical operation given by the operator [49]

$$\mathcal{B}_{M^2} = \lim_{\substack{-q^2, n \rightarrow \infty \\ -q^2/n = M^2}} \frac{(-q^2)^{(n+1)}}{n!} \left(\frac{d}{dq^2} \right)^n. \quad (2.24)$$

In a typical sum rule calculation, the most commonly encountered function of q^2 is

$$f(q^2) = \frac{1}{(m^2 - q^2)^k} \quad (2.25)$$

where k is some integer providing the power of the denominator. The Borel transformation of this function is given by

$$\hat{\mathcal{B}}_{M^2} f(q^2) \equiv \hat{\mathcal{B}}_{M^2} \frac{1}{(m^2 - q^2)^k} = \frac{1}{(k-1)!} \frac{e^{-m^2/M^2}}{(M^2)^k}. \quad (2.26)$$

It is easy to convince oneself that for $m^2 > M^2$, the term on the r.h.s. of Eqn.(2.26) gets an exponential suppression. Consequently, on performing a Borel transformation (on say Eqn.(2.17)) and choosing $M^2 < s_0^h$, the continuum contribution can get an exponential suppression. Also, it provides a factorial suppression to the power-corrections and hence reduces the impact of higher dimensional condensate terms of the OPE.

The Borel transformations of $(q^2)^k$ vanishes i.e., $\hat{\mathcal{B}}(q^2)^k = 0$. It results in killing off any subtraction terms that appear in the form of polynomial in q^2 which may appear as a consequence of the divergences in the dispersion relation. Consequently, Borel transformation helps us in improving the accuracy and stability of the sum rule. The Borel mass is another independent parameter in the sum rules calculations. As stated above it must be lesser than or close to the continuum threshold such that the heavier and continuum states' contributions can be suppressed properly. It is determined by demanding a very small variation of the final hadronic parameter against its variation. For M , one usually tries to find a region where the

graph of the derived hadronic quantity vs the Borel mass shows a plateau. This region is known as the *Borel window*. The sum rule is considered to be reliable if the contribution coming from the continuum and higher resonances is small, the dependence on the Borel parameter is weak and there are no unnatural numerical cancellations in the result. After performing Borel transform of Eqn.(2.17), one gets,

$$\Pi^{had}(M^2) = f_V^2 e^{-m_V^2/M^2} + \frac{1}{\pi} \int_{s_0^h}^{\infty} ds \operatorname{Im}(\Pi^{had}(s)) e^{-s/M^2}, \quad (2.27)$$

where M is the Borel mass.

Finally, on approximating the second term of Eqn.(2.27) using the statement of semi-local quark hadron duality given in Eqn.(2.20) and equating the two representations obtained using OPE and dispersion relation, one get the final sum rule for f_V as

$$f_V^2 e^{-m_V^2/M^2} + \frac{1}{\pi} \int_{s_0}^{\infty} ds \operatorname{Im}\Pi^{(pert)}(s) e^{-s/M^2} = \sum_d \mathcal{C}_d(M^2, \mu) \langle 0|O_d|0\rangle(\mu) \quad (2.28)$$

where s_0 is the continuum threshold, $\mathcal{C}_d(M^2, \mu)$ are the Borel transformed perturbatively calculated WCs and $\langle 0|O_d|0\rangle$ are the non-perturbative objects which can be written in terms of the vacuum condensates.

f_V turns out to be a function of the universal non-perturbative quantities called vacuum condensates, the independent parameters introduced by the sum rule calculations s_0 and M , and the perturbatively calculable short-distance coefficients. One saturates the sum rule with the lowest energy resonance i.e. the ground state and the contribution from the higher resonances and the continuum are suppressed. The μ dependence of the vacuum condensates, introduced by OPE, is supposed to be canceled by the μ dependence of the perturbatively calculated coefficients. However, as the infinite expansion is truncated to some finite terms, the μ dependence does not disappear completely and leads to another source of theoretical uncertainty in the sum rule calculations. The application of SVZ sum rules is not limited to QFT. It can be seen in quantum mechanics as well. Let us see a quantum mechanical example to develop a better understanding.

2.1.2 SVZ sum rules in quantum mechanics

In this section, we will try to understand the power of SVZ sum rules with the help of a simple quantum mechanical example of the harmonic oscillator by determining its ground state energy (following [63]). In quantum mechanics, the Green function of the time-dependent Schrödinger equation is given by,

$$G(x_2, t_2; x_1, t_1) = \sum_{k=0}^{\infty} \psi_k(x_2) \psi_k^*(x_1) \exp[-iE_k(t_2 - t_1)] \quad (2.29)$$

where ψ_k represents the wave function of a quantum state with energy E_k , and the sum over k runs over all the possible quantum states. The Euclidean Green function $M(\tau)$ can be obtained from the Green function given in Eqn.(2.29) by analytically continuing the time t to the imaginary time $\tau = it$, also known as the Euclidean time, such that

$$M(\tau) \equiv G(0, -i\tau; 0, 0) \quad (2.30)$$

This Euclidean Green function, $M(\tau)$ here plays an equivalent role of the Borel transformed correlation function in field theory and hence is the object of interest here.

From Eqn.(2.29) and Eqn.(2.30), $M(\tau)$ can be written as a sum of the ground state contribution and the contribution coming from the excited states as

$$M(\tau) = |\psi_0(0)|^2 \exp(-E_0\tau) + M_c(\tau) \quad (2.31)$$

where $M_c(\tau)$ represents the contribution coming from the excited states given by

$$M_c(\tau) = \sum_{k=1}^{\infty} |\psi_k(0)|^2 \exp(-E_k\tau). \quad (2.32)$$

One can calculate the ground state parameters E_0 and $|\psi_0|^2$ unambiguously if ground state contribution dominates $M(\tau)$. It is possible for large Euclidean time, $\tau > \tau_c$ for which the continuum contribution experiences an exponential damping.

According to the Born series, $M(\tau)$ can be calculated perturbatively in the Euclidean region. Let us call it $M_{pert}(\tau)$ which usually contains the first few terms of the truncated Born series of $M(\tau)$. Therefore, $M_{pert}(\tau)$ can approximate $M(\tau)$ accurately only for sufficiently small Euclidean times such that ($\tau < \tau_B$) where τ_B is some upper limit for the validity of truncation of the Born series.

Consequently, $M(\tau)$ and $M_{pert}(\tau)$ are like two sides of the same coin and are valid for different regions of the value of τ . The sum rule can be obtained by equating the two sides such that a fiducial region exists where this equality holds. Such a condition is possible for $\tau_c < \tau < \tau_B$. For such a region, the ground state energy E_0 can be calculated approximately as

$$E_0 = -\frac{d}{d\tau} \ln [M_{pert}(\tau) - M_c(\tau)] \quad (2.33)$$

Finding such a region for realistic situations is not obvious. However, there are several systems where such a fiducial region is found to exist and it has been found that this procedure does provide a reasonably reliable estimate of the ground state. A harmonic oscillator (HO) in an external electric field is an example of one such system. Let us see the power of SVZ sum rules by calculating the ground state energy of a HO in an external electric field.

2.1.2.1 An example: Harmonic Oscillator in an external electric field

The Hamiltonian for a one-dimensional harmonic oscillator (HO) placed in a constant external electric field, E is given by

$$H = -\frac{1}{2m} \frac{d^2}{dx^2} + \frac{1}{2} m \omega^2 x^2 - eEx. \quad (2.34)$$

where ω is the frequency of oscillation and m is the mass of the particle. This is an exactly solvable system with the eigenvalues, E_k and eigenfunctions, ψ_k given by

$$E_k = \left(k + \frac{1}{2} - \epsilon \right) \omega \quad (2.35)$$

with $\epsilon \equiv \frac{(\epsilon E)^2}{2m\omega^3}$ and $k = 0, 1, 2, \dots$, and

$$\psi_k(x) = \phi_k(x - x_0) \quad (2.36)$$

with $x_0 \equiv \frac{\epsilon E}{m\omega^2}$ and $\phi_k(x)$ being the eigenfunctions in the absence of external electric field. Let us now try to find the ground state energy E_0 using the method of SVZ sum rules. As a starting point, we need Euclidean Green's function for this system which reads as

$$\begin{aligned} M(\tau) &= \text{Exp}(\epsilon\omega\tau) \sum_{k=0}^{\infty} \phi_k(-x_0)\phi_k^*(-x_0) \exp\left[-\left(k + \frac{1}{2}\right)\omega\tau\right] \\ &= \exp(\epsilon\omega\tau) G_{\text{HO}}(-x_0, -i\tau; -x_0, 0). \end{aligned} \quad (2.37)$$

Here, G_{HO} is the Green function for the harmonic oscillator in the absence of the electric field given by

$$G_{\text{HO}}(x_2, t_2; x_1, t_1) = \left(\frac{m\omega}{2\pi i \sin(\omega T)}\right)^{1/2} \exp\left\{i\frac{m\omega}{2\sin(\omega T)} [(x_1^2 + x_2^2) \cos(\omega T) - 2x_1x_2]\right\} \quad (2.38)$$

with $T = t_2 - t_1$. Therefore,

$$M(\tau) = \left(\frac{m\omega}{2\pi \sinh(\omega\tau)}\right)^{1/2} \exp\left[\epsilon\omega\tau \left(1 - \frac{\tanh(\frac{\omega\tau}{2})}{(\frac{\omega\tau}{2})}\right)\right] \quad (2.39)$$

This is the exact form of the Euclidean Green function for the harmonic oscillator in an external electric field. Moreover, in order to stay close to the field-theoretic case where one can sum up only a finite number of terms of an infinite series, let us take only a few terms of the Born series with the perturbative potential given by

$$V(x) = \frac{1}{2}m\omega^2x^2 - eEx \quad (2.40)$$

Considering only the first few terms of the Born series, the perturbative form of the Euclidean Green function reads as,

$$M_{\text{pert}}(\tau) = M_0(\tau) \left[1 - \frac{(\omega\tau)^2}{12} + \frac{(\omega\tau)^2}{12} + \epsilon\frac{(\omega\tau)^3}{12} + \frac{(\omega\tau)^4}{160}\right]. \quad (2.41)$$

which obviously coincides with the expansion of Eqn.(2.39) in powers of ϵ and $(\omega\tau)$. Here, $M_0(\tau)$ corresponds to a one dimensional free particle Euclidean Green function and is given by

$$M_0(\tau) = \left(\frac{m}{2\pi\tau} \right)^{1/2} \quad (2.42)$$

Therefore, the lowest order correction to the $M(\tau)$ due to the presence of the external electric field reads as

$$\delta M_{\text{pert}}(\tau) = M_0(\tau) \frac{(\omega\tau)^3}{12} \epsilon \quad (2.43)$$

Our next goal is to approximate the contribution coming from the excited states, $M_c(\tau)$ in Eqn.(2.31). This can be done using the free motion approximation, according to which the Euclidean Green function for a free particle can be written as (see for details)

$$M_0(\tau) = \int_0^\infty dE \rho_0(E) \exp(-E\tau) \quad (2.44)$$

where $\rho_0(E) = \frac{1}{\pi} \left(\frac{m}{2E} \right)^{1/2}$. Consequently, one can assume that the excited state contribution can be approximated as

$$M_c(\tau) \approx M_c^{(0)}(\tau; E_c) = \int_{E_c}^\infty dE \rho_0(E) \exp(-E\tau) \quad (2.45)$$

where all the interaction effects have been captured in the free parameter E_c known as the continuum threshold here. This parameter has to be determined simultaneously with the ground state parameters (as we will see below).

Furthermore, as discussed above, the important criteria to derive the sum rule is to find the fiducial region (τ_c, τ_B) where the method of sum rules is valid. In order to find this region, following, we demand that the contribution coming from the excited states should not exceed 30% of the contribution of the ground state and the corrections due to the truncated terms of the Born series must be smaller than 30% of the free particle Green function. The first condition sets the lower boundary of the fiducial region i.e. τ_c while the second condition sets the upper

boundary i.e. τ_B . The ground state energy can be calculated using Eqn.(2.41) and Eqn.(2.45) in Eqn.(2.33) if $\tau_c < \tau_B$. In [63], it has been reported that the fiducial region exists which follows the above-mentioned criteria for $\epsilon \leq 0.05$. The continuum threshold E_c can be tuned such that the ground state energy, E_0 , calculated using Eqn.(2.33), is approximately constant with a variation in τ in the fiducial region $\tau_c < \tau < \tau_B$. Finally, one takes this value of E_0 to be the approximate ground state energy for the system. The uncertainties in the determination of the ground state energy of the HO without an external electric field and the shift in the energy due to the presence of the external electric field are at most 20% (see [63] for details).

Though the SVZ sum rules are found to give reasonable estimates for the physical quantities of interest, there are certain limitations of these sum rules which we will discuss next.

2.1.3 Limitations of SVZ sum Rules

The SVZ sum rules face problems while computing the three-point correlation functions. We mention the major limitations in brief here. For details, one can look at [52], [64]. While computing SVZ sum rules for a three-point sum rule

- Short-distance OPE (short-distance expansion in terms of condensates) upsets power counting in large Q^2 . The sum rule for the form factor looks like,

$$F(Q^2) \sim \# \frac{1}{Q^2} + \#(Q^2)^0 + \#Q^2 + \dots$$

- Practical calculations often suffer from contributions that are not suppressed even after Borel transformations. These can be taken care of by using double dispersion relation and then performing Borel transformation in both the variables. However, this brings other caveats (see for example [64] for details).

These limitations of the SVZ sum rules related to the three-point sum rules can be taken care of by marrying SVZ sum rules to the theory of hard exclusive processes (to be discussed in brief in the next Section). By doing so one now

has an OPE near the light cone ($x^2 \rightarrow 0$) instead of short distance ($x_\mu \rightarrow 0$). This leads to a partial summation of the infinite series of the local operators. It is an expansion in the new parameter called twist and no longer an expansion in the canonical mass dimensions. We will discuss more about light cone OPE in Section-2.2.1.2. Before going into details of the light cone OPE let us discuss the theory of hard exclusive processes.

2.2 Theory of hard exclusive processes

As discussed in Section-1.2, the strong interactions are perturbative at large energies (short distances) and non-perturbative at small energies (long distances) because of the property of the asymptotic freedom and color confinement. We have also discussed that because of the property of confinement, we observe only colorless hadrons at experiments and not the colored quarks and gluons, and thus, one can not get rid of the non-perturbative effects even if probed with high enough energy. Consequently, it is necessary to have an information about the constituents of hadron when large momenta are transferred to these extended objects. The exclusive processes where the momentum transferred is large can test both the detailed structure as well as the internal dynamics of the hadronic wave-function at short distances. There are two possible configurations by which the momentum can be transferred among the constituents of the hadron called partons. First, where one of the partons carries all the momentum. In this case, the large momentum can be transferred to this fast moving parton which finally recombines with the soft cloud of virtual quarks, anti-quarks and gluons. Second, where we pick up a Fock state with minimum number of constituents (for example a quark and an anti-quark for a meson and three quarks for a baryon (as given in Eqn.(1.17))) separated by small transverse distances and a hard gluon is exchanged in this configuration. Both the configurations are possible, however, it is not known which configuration is more favourable. It can be studied only case by case (see [64]–[66] for more details). In the first configuration, the transverse distances are not restricted which makes this mechanism difficult to study. One can write a factorisation formula that helps in writing a hadronic

matrix element as a convolution of a hard scattering kernel and the light cone distribution amplitudes of the hadrons in the asymptotic limit ($Q^2 \sim \frac{1}{x^2} \rightarrow \infty$, where x denotes the transverse separation between the partons) or equivalently near the light cone. Mathematically, this factorization formula can be written as

$$\langle f | \hat{\mathcal{O}}(x, 0) | i \rangle_{x^2 \rightarrow 0} \sim \int_0^1 du \int_0^1 dv \phi_f(v, \bar{v}) \otimes T_H(u, v) \otimes \phi_i(u, \bar{u}) \quad (2.46)$$

where $|f\rangle$ and $|i\rangle$ are the outgoing and incoming meson states, $\hat{\mathcal{O}}(x, 0)$ is a bilocal quark-gluon operator with x being the transverse separation between the partons. $u, \bar{u} = 1 - u$, and $v, \bar{v} = 1 - v$ are the momentum fractions carried by the quark and the anti-quark in the initial and the final state meson, respectively. T_H is the hard scattering kernel and can be computed using perturbative QCD. ϕ_i and ϕ_f are the light cone distribution amplitudes for the initial and the final state mesons. These DAs are the universal non-perturbative objects that are useful in gaining insight about the structure of the hadron (we will discuss more about them in Section-2.2.2). Consequently, one can extract information about the dynamics of the strong interaction and the structure of the hadron using the smallest configuration of a hadron given that it had been probed with a very high energy probe. For such a scenario the dynamics is dominated by the contributions near the light cone. We will discuss more about light cone dominance in the next section by considering a specific example of $e^+e^- \rightarrow \pi^0 e^+e^-$ scattering. Before moving to the next section, let us convince ourselves that a description in minimum number of constituents is valid. This idea was originated while studying the asymptotic behavior of the form factors. It was found that the asymptotic behavior of these hadronic quantities depends mainly on the number of constituents, the interaction Lagrangian, the value of spin, and angular momentum of the hadron. A dimensional counting rule was proposed which predicts the asymptotic behaviour of these form factors, $F(q^2)$, as a function of the minimum number of constituents given by

$$F(q^2) \sim \frac{\text{const}}{(q^2)^{n-1}} \quad (2.47)$$

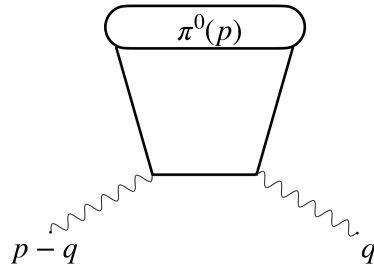


Figure 2.5: A representative graph of a typical correlation function of two currents between the initial and the final state containing pion and vacuum.

where 'const' is some constant factor and n is the minimum number of constituents, i.e. $n = 2$ for mesons and $n = 3$ for baryons (see [65] for more details). This rule was found to agree well with the experimental data on the form factors of pion and nucleons as well as various large angle scattering cross-sections. Therefore, the description of hadrons in terms of minimum number of constituents gains its validity. Let us now understand the light cone dominance for such a description and how it leads to a new type of operator product expansion near light cone called as light cone OPE.

2.2.1 Light cone dominance and OPE

To understand the light cone dominance and light cone operator product expansion, let us consider the example of a process where two currents fuse into a meson for example $e^+e^- \rightarrow \pi^0 e^+e^-$ scattering [52]. Here, two virtual photons with momentum say q and $p-q$ are fusing into the neutral pion with momentum p , i.e.

$$\gamma^*(q)\gamma^*(p-q) \rightarrow \pi^0(p). \quad (2.48)$$

where $q = p_1 - p_2$ and $p - q = p_3 - p_4$ with $p_1, p_2, p_3,$ and p_4 being the four momenta of the incoming and outgoing electron and positron, respectively (see Fig.(2.5)). The hadronic matrix element that captures the strong interaction dynamics for this process can be written as

$$F_{\mu\nu}(p, q) = i \int d^4x e^{-iq \cdot x} \langle \pi^0(p) | T \{ j_\mu^{em}(x) j_\nu^{em}(0) \} | 0 \rangle \quad (2.49)$$

The important observation about this matrix element is that if $Q^2(= -q^2)$ and $|(p - q)^2|$ are large, then this matrix element is dominated by the dynamics near the light cone instead of the short distance dynamics like we had for $\Pi_{\mu\nu}$ defined in Eqn.(2.1). Let us now convince ourselves about this statement of light cone dominance.

2.2.1.1 Light cone dominance

To proceed with, let us consider an invariant variable ν defined as

$$\nu = p \cdot q = \frac{(q^2 - (p - q)^2)}{2}. \quad (2.50)$$

Therefore, for $Q^2 \gg \Lambda_{QCD}^2$ and $|(p - q)^2| \gg \Lambda_{QCD}^2$, $|\nu|$ will also be large i.e.,

$$|\nu| \sim |(p - q)^2| \sim Q^2 \gg \Lambda_{QCD}^2. \quad (2.51)$$

It is important to note that the above condition holds true even for non vanishing momentum of pion. Moreover, for convenience, let us define a ratio ξ such that

$$\xi = 2\nu/Q^2 \quad (2.52)$$

is finite ~ 1 in the region defined by Eqn.(2.51).

Now, to find the dominant region for the matrix element defined in Eqn.(2.49), the argument of the exponential in the integrand ($q \cdot x$) must follow

$$q \cdot x \leq \mathcal{O}(1) \quad (2.53)$$

in order to avoid large oscillations, which from the Riemann-Lebesque theorem will otherwise strongly suppress the integrand.

Let us now consider a reference frame where the three-momentum of pion ($|\vec{p}| \sim \mu$) is non-vanishing but small compared to the virtuality of photon i.e. $\mu^2 \ll Q^2, \nu$. As the mass of pion is also small, this implies that the zeroth component of the pion four momentum will also be of the order of μ i.e. $|p_0| \sim \mu$. Also, let us consider that in this frame, there is only one non-vanishing component for

the four momentum q and p such that we can write

$$q^\mu = (q_0, 0, 0, q_3), \quad p^\mu \sim (\mu, 0, 0, -\mu). \quad (2.54)$$

Therefore, in such a frame, using Eqn.(2.50) and Eqn.(2.52), we can write

$$p \cdot q = p_0 q_0 - p_3 q_3 \implies (q_0 + q_3) \sim \frac{Q^2 \xi}{2\mu} \quad (2.55)$$

which can be further solved using $Q^2 = q_3^2 - q_0^2$. It finally results into

$$q_0 \sim \frac{Q^2 \xi}{4\mu} - \frac{\mu}{\xi}, \quad \text{and} \quad q_3 \sim \frac{Q^2 \xi}{4\mu} + \frac{\mu}{\xi}. \quad (2.56)$$

Using this, the argument of the exponential in the integrand of Eqn.(2.49) will become

$$q \cdot x = q_0 x_0 - q_3 x_3 \simeq \frac{Q^2 \xi}{4\mu} (x_0 - x_3) - \frac{\mu}{\xi} (x_0 + x_3). \quad (2.57)$$

Consequently, in order to satisfy the condition of dominance given in Eqn.(2.53), we demand

$$(x_0 - x_3) \leq \frac{4\mu}{Q^2 \xi}, \quad \text{and} \quad (x_0 + x_3) \leq \frac{\xi}{\mu}. \quad (2.58)$$

The multiplication of these inequalities results into

$$x_0^2 - x_3^2 \leq \frac{4}{Q^2} < \frac{4}{Q^2} + x_1^2 + x_2^2 \implies x^2 \leq \frac{4}{Q^2} \quad (2.59)$$

As a result, at $Q^2 \gg \Lambda_{QCD}^2$ i.e. at asymptotic Q^2 , the matrix element given in Eqn.(2.49) will be dominated by the region given by $x^2 \rightarrow 0$ i.e. near the light cone. It is important to note here that the condition in Eqn.(2.59) is a Lorentz invariant object and hence does not depend on the reference frame one considers. Consequently, the condition of light cone dominance is true in general for any matrix element of the form given in Eqn.(2.49). Moreover, as this condition is true even for large components of the position four vector, x^μ , the short distance dominance is not valid in general for matrix elements of the form given in Eqn.(2.49). Now, after convincing ourselves about the light-cone dominance of this matrix element, let us now see how the operator product

expansion changes near the light cone.

2.2.1.2 Light Cone OPE

In Section-2.1.1, we have discussed the OPE at short distance ($x_\mu \rightarrow 0$), according to which a product of currents/operators at different space-time points can be written as an expansion of the product of perturbatively calculable Wilson coefficients and the universal non-perturbative quantities called vacuum condensates of increasing canonical dimension, d (see Eqn.(2.2)). In this section, we will discuss the operator product expansion near the light cone ($x^2 \rightarrow 0$) and will see how such an expansion partially sum over the local operators of different dimensions and resolves the problem of power counting as discussed in Section-2.1.3. Let us again consider the matrix element given in Eqn.(2.49). According to the light cone OPE [37], [67], the product of currents involved in this matrix element can be written as

$$T \{j_\mu^{em}(x)j_\nu^{em}(0)\} |_{x^2 \rightarrow 0} = \sum_t [C_t(x^2)\mathcal{O}_t(x, 0)]. \quad (2.60)$$

Here, $\mathcal{O}_t(x, 0)$ are the bilocal operators of quarks, gluons and anti-quarks which encode the low energy dynamics while $C_t(x^2)$ are the coefficient functions which can be calculated using pQCD. It is an infinite expansion in the so called *twist*, t , which is defined as the difference of canonical dimension and the spin. We will discuss more about it below. At zeroth order in α_s , the coefficient function for the minimum twist, $C_{t_{min}}(x^2)$, is nothing but the free-quark propagator itself. For practical applications, this infinite series can be truncated to a finite number of terms. When one substitutes Eqn.(2.60) in Eqn.(2.49), the higher order terms turn out to be inversely proportional to the powers of Q^2 which is large and thus truncation to a finite number of terms is a reasonable approximation. Consequently, there are two major differences between the short distance OPE and the light cone OPE. First is that the former includes local operators while the latter includes bilocal operators. Secondly, the former is an expansion in canonical dimension while the latter is an expansion in twist.

To get a better understanding, let us compute the product of currents given

in Eqn.(2.60) in more detail. Using the light cone propagator (discussed in Appendix-B) and the identities collected in Appendix-A, one obtains

$$T \{j_\mu^{em}(x)j_\nu^{em}(0)\} |_{x^2 \rightarrow 0} = -\frac{\epsilon_{\mu\nu\alpha\beta}x^\alpha}{12\pi^2(x^2)^2} [(\bar{u}(x)\gamma^\beta\gamma_5 u(0) - \bar{d}(x)\gamma^\beta\gamma_5 d(0)) + (\bar{u}(0)\gamma^\beta\gamma_5 u(x) - \bar{d}(0)\gamma^\beta\gamma_5 d(x))] + \dots \quad (2.61)$$

This is already starting to have a form of an OPE. The coefficient outside the square bracket on the r.h.s is the perturbatively calculated coefficient function and the operators inside the square bracket are the bi-local operators. Ellipses represents the higher order terms. The matrix element can be calculated by substituting it in Eqn.(2.49). The leading order result for the matrix element will read as

$$F_{\mu\nu}(p, q) = -i\frac{\epsilon_{\mu\nu\alpha\beta}}{12\pi^2} \int d^4x e^{-iq.x} \frac{x^\alpha}{(x^2)^2} \langle [\pi^0(p) | (\bar{u}(x)\gamma^\beta\gamma_5 u(0) - \bar{d}(x)\gamma^\beta\gamma_5 d(0)) + (\bar{u}(0)\gamma^\beta\gamma_5 u(x) - \bar{d}(0)\gamma^\beta\gamma_5 d(x)) | 0] \rangle_{x^2 \rightarrow 0}. \quad (2.62)$$

The r.h.s. of this equation involves a new hadronic matrix elements of bilocal quark-anti-quark operators sandwiched between the π^0 state and the vacuum state. To understand more about these bilocal operators, let us consider one of these operators and expand it at around $x = 0$ in terms of a power series of local operators such that

$$\bar{u}(x)\gamma^\beta\gamma_5 u(0) = \sum_{r=0}^{\infty} \frac{1}{r!} \bar{u}(0) \left(\overleftarrow{D}.x \right)^r \gamma^\beta\gamma_5 d(0) \quad (2.63)$$

where \overleftarrow{D} represents that the covariant derivative which appears due to gauge invariance is operating on the left u-quark. In the fixed point gauge i.e. $x_\mu G^\mu = 0$, the covariant derivative can be replaced by an ordinary derivative. This then is an infinite series in the local operators with increasing dimension. As the bilocal matrix element in Eqn.(2.62) depends only on the four momentum of pion i.e. p_μ , the matrix element of the infinite series in Eqn.(2.63) between the pion and

the vacuum state can be decomposed as

$$\begin{aligned}
& \langle \pi^0(p) | \bar{u}(x) \gamma^\beta \gamma_5 d(0) | 0 \rangle \\
&= \sum_{r=0}^{\infty} \frac{1}{r!} x_{\mu_1} x_{\mu_2} \dots x_{\mu_r} [(-i)^{r+1} p^\beta p^{\mu_1} p^{\mu_2} \dots p^{\mu_r} \mathcal{M}_r^d \\
&- (-i)^{r+1} g^{\mu_1 \mu_2} p^\beta p^{\mu_3} \dots p^{\mu_r} \mathcal{M}_r^{d+2} + \{\dots\}] \tag{2.64}
\end{aligned}$$

where $\{\dots\}$ represents more terms with two or more number of metric tensor, $g^{\mu_i \mu_j}$ with $(i, j = 1, \dots, r)$. By construction, $\mathcal{M}_0^{d+2} = \mathcal{M}_1^{d+2} = 0$. This expansion is totally symmetric in μ_1, μ_2, \dots and \mathcal{M}_r^d and \mathcal{M}_r^{d+1} are the invariant coefficients (the matrix elements of the local operators) which differ in dimension by two units. These coefficients are non-perturbative in nature. For example, for $r=0$,

$$\langle \pi^0(p) | \bar{u}(0) \gamma^\beta \gamma_5 u(0) | 0 \rangle = -i p^\beta \mathcal{M}_0^d \tag{2.65}$$

which implies that \mathcal{M}_0^d has a direct relation with the pion decay constant, f_π given by

$$\mathcal{M}_0^d = \frac{f_\pi}{\sqrt{2}}. \tag{2.66}$$

The infinite series of these invariant coefficients can not be truncated to some finite order. However, there is a different hierarchy on the r.h.s. of Eqn.(2.64). After performing the integral over x (see [37] for more details), one finds out that the second term on the r.h.s of Eqn.(2.64) has an extra factor of $1/Q^2$ compared to the first term and the other factors in the numerator are of $\mathcal{O}(1)$. Hence, the local operators of different dimensions are having same power of $1/Q^2$. However, a closer look at Eqn.(2.64) reveals that the local operators in the first and second term have different twist. The lowest twist which enters the above expansion is 2 as the dimension of the operator is 3 and Lorentz spin is 1. Consequently, one can say that the light cone OPE is an expansion in twist rather than the expansion in canonical dimension and it sums an infinite set of local operators of the same twist. In the next section, we will see how these matrix elements of the bilocal operators can be written in terms of the so called light cone distribution amplitudes (DAs) of increasing twist which have a direct physical significance.

We will also see how these invariant coefficients \mathcal{M}_r are related to these DAs. Furthermore, we will have a better understanding of twist by discussing the application of conformal symmetry in QCD.

2.2.2 Light Cone Distribution amplitudes and the Conformal Symmetry

As discussed in Section-2.2, when large momentum is transferred to the hadronic system, the hadronic state can be considered to be dominated by its valence configuration given in Eqn.(1.17). Therefore, near the light cone, a hadronic state, for example $|M(p)\rangle$ for a meson, M , with momentum p can be written as

$$|M(p)\rangle = \int_0^1 du \phi_M(u) |q_1(up)\bar{q}_2(\bar{u}p)|M\rangle \quad (2.67)$$

where, q_1 and \bar{q}_2 represents the quark and the anti-quark, respectively. u is the fraction of the meson momentum carried by the quark and $\bar{u} = 1-u$ is the fraction carried by the anti-quark. $\phi_M(u)$ is the *light cone distribution amplitude (DA)* for meson, M . Using Eqn.(2.67), the matrix element of the bilocal operator⁵ in Eqn.(2.62) can be parameterized, at the leading order near the light cone, as

$$\langle \pi^0(p) | \bar{u}(x) \gamma_\mu \gamma_5 u(0) | 0 \rangle_{x^2=0} = -ip_\mu \frac{f_\pi}{\sqrt{2}} \int_0^1 du e^{iup \cdot x} \phi_\pi(u, \mu) \quad (2.70)$$

where $\phi_\pi(u, \mu)$ is the twist-2 DA of pion. This DA is normalised to unity such that

$$\int_0^1 du \phi_\pi(u, \mu) = 1 \quad (2.71)$$

⁵For the gauge invariance of these operators, a path ordered Wilson line given by

$$[x, y] = P \exp \left[ig_s \int_0^1 dt (x-y)_\mu \mathbf{G}^\mu(tx + (1-t)y) \right] \quad (2.68)$$

is present between the quark and the anti-quark where $\mathbf{G}_\mu = G_\mu^a T^a$ with G_μ^a being the gluon field. However, for convenience, we work in the fixed point gauge, also called the Fock-Schwinger gauge, given by

$$x^\mu G_\mu^a(x) = 0. \quad (2.69)$$

In this gauge the Wilson line goes to unity. Therefore, we do not write it explicitly, however, it is present unless otherwise stated.

The explicit form for $\phi_\pi(u, \mu)$ is presented in Eqn.(2.81). The invariant coefficient \mathcal{M}_r of twist-2 local operators in Eqn.(2.64) is therefore directly related to the moments of the pion distribution amplitude given by

$$M_r = -i \frac{f_\pi}{\sqrt{2}} \int_0^1 du u^r \phi_\pi(u, \mu). \quad (2.72)$$

Thus, the distribution amplitude $\phi_\pi(u)$ multiplied by the pion decay constant f_π is the universal non-perturbative quantity that enters the light cone OPE and encode the dynamics of strong interactions at long distances. These distribution amplitudes (including the higher twist DAs) play a very essential role in the QCD description of the hard exclusive processes as discussed in Section-2.2. They play a similar role as parton distribution functions play for the case of deep inelastic collisions. In the computation of light cone sum rules, they are the universal non-perturbative quantities very much like the vacuum condensates in the calculation of the SVZ sum rules.

Distribution amplitudes are the dimensionless functions of the collinear momentum fractions carried by the constituents of the hadron, at zero transverse separation. They are defined as the probability amplitudes to find constituents carrying a particular fraction of the hadron momentum. For example, the two-particle DAs of a meson are defined as the probability amplitude to find the quark q_1 and anti-quark q_2 with momentum fractions u and \bar{u} , respectively of the collinear momentum of the energetic meson, M . Similarly, for three-particle DAs, the momentum fractions (α_1 , α_2 , and α_3) will be carried by the quark, anti-quark and gluon. These three-particle DAs arises due to higher order terms in the light-cone propagator (discussed in Appendix-B).

Along with these lowest twist DAs, higher twist DAs are present. They appear due to three physical reasons. Firstly, the contribution coming from the so called bad component of the spinor field (will be better understood when we will discuss the application of conformal symmetry below). Secondly, the contribution coming due to the transverse motion of the quark or the anti-quark present in the leading twist configuration. Thirdly, the contributions coming due to the presence of higher Fock states including extra gluons and/or quark-anti-quark pairs.

For the case of mesons, one can use the QCD equations of motion to write the effect of bad components in terms of the higher Fock states. Consequently, for the case of mesons, the higher twist effects are suppressed compared to the leading twist effects. Thus, considering only leading twist effects may be a reasonable approximation for the meson case. However, for the case of baryons, the QCD equations of motion are insufficient to write the bad components contribution in terms of higher Fock states. As a result, the higher twist effects might turn out to be important for the case of baryons and are dominated by the contribution coming from the bad components of the three-quark state of a baryon. To gain more insight of the physics captured by these DAs, let us discuss the case of light mesons explicitly. For more details one is suggested to look at [68] and references therein.

For the case of light mesons, these distributions can be determined by using the property of conformal symmetry of QCD which is valid in the mass-less limit at tree level. These DAs are defined by the coefficients of the conformal expansion, an expansion in terms of conformal spin which physically corresponds to a separation between the transverse and the longitudinal d.o.f. similar to the partial wave expansion in spherical harmonics in quantum mechanics. We will discuss conformal symmetry and conformal expansion below. Before that let us understand how this separation of d.o.f. helps us. The transverse degrees can be simply integrated out and leads to a dependence on the renormalization scale, μ , which can be described by renormalization group equations. However, the longitudinal d.o.f. correspond to the longitudinal momentum fractions which can be understood using the collinear sub-group given by $SL(2, \mathbf{R})$ (see below).

2.2.2.1 Conformal group and its collinear subgroup

The conformal transformation is defined as the scaling of metric such that the Minkowskian interval, $ds^2 = g_{\mu\nu}(x)dx^\mu dx^\nu$ remains constant i.e.

$$g'_{\mu\nu}(x') = \omega(x)g_{\mu\nu}(x) \quad (2.73)$$

such that $ds'^2 = g'_{\mu\nu}(x')dx'^{\mu}dx'^{\nu} = ds^2$. Consequently, the conformal symmetry preserves the angles so that the light-cone remains invariant. There are fifteen generators of the conformal symmetry in 4 dimensions including four translations, P_{μ} , six Lorentz rotations, $M_{\mu\nu}$, one dilatation, D , and 4 special conformal transformations, K_{μ} , which form the conformal group. The usual Poincare group is a subset of the conformal group (for more details about the conformal symmetry and group, see for eg. [69]). For a particle which propagates near the light cone, the full conformal group reduces to its collinear subgroup, $SL(2, \mathbb{R})$ group with 4 generators P_+ , M_{-+} , D and K_- where we have used the notation of light cone coordinates given in Appendix-A.

For practical convenience, one defines the linear combinations of these generators given by

$$\begin{aligned} L_+ &= L_1 + iL_2 = -iP_+, & L_- &= L_1 - iL_2 = (i/2)K_-, \\ L_0 &= (i/2)(D + M_{-+}), & E &= (i/2)(D - M_{-+}). \end{aligned} \quad (2.74)$$

The twist is defined by the commutator of the generator E with the field $\phi(x) \rightarrow \phi(\alpha n)$ which lives on the light ray, i.e.

$$[E, \phi(\alpha)] = \frac{1}{2}(\ell - s)\phi(\alpha). \quad (2.75)$$

where, s is the eigen value of the spin operator Σ_{+-} such that

$$\Sigma_{+-}\phi(\alpha) = s\phi(\alpha), \quad (2.76)$$

and ℓ is the scaling dimension which is not necessarily equal to the canonical dimension for a QFT. The difference between the two is known as the anomalous dimension. However, for a classical theory i.e. field theory at tree level, the anomalous dimension is zero and the scaling dimension coincides with the canonical dimension. The twist $t = \ell - s$ defined in Eqn.(2.75) is known as the conformal twist i.e. dimension minus the spin projection on the plus axis. It is different from the geometric twist which is defined as the dimension minus the spin and corresponds to the full conformal group.

Now let us consider a general bilocal operator which one encounters in QCD applications to hard exclusive processes

$$\mathcal{O}_\mu(\alpha_1, \alpha_2) = \bar{\psi}(\alpha_1)\Gamma_\mu\psi(\alpha_2) \quad (2.77)$$

such that $\psi(x) = \psi(\alpha n) \equiv \psi(\alpha)$ represents a the quark as a light-ray and Γ represents a string of γ -matrices with Lorentz spin-1. This operator results into an infinite series of local operators of quark and anti-quark fields, and the covariant derivative. The quark field ψ has different spin projections which can be identified using the spin projection operators given by

$$\Pi_+ = \frac{1}{2}\gamma_-\gamma_+, \quad \Pi_- = \frac{1}{2}\gamma_+\gamma_-, \quad \Pi_+ + \Pi_- = 1 \quad (2.78)$$

Therefore the plus (good) and the minus (bad) components of the quark field are

$$\psi_+ = \Pi_+\psi, \quad \psi_- = \Pi_-\psi, \quad \psi = \psi_+ + \psi_-, \quad (2.79)$$

This quantization of the quark field is same as the light-cone quantization. To find the conformal operators of these fields let us first realise that the ψ_+ and ψ_- has spin $+1/2$ and $-1/2$, respectively which implies that the twist for ψ_+ and ψ_- components of the quark field are different as the canonical dimension for both the components is $3/2$. Explicitly, the twist for ψ_+ and ψ_- components are 1 and 2, respectively. Therefore, the operator \mathcal{O}_μ with different components of the quark field has different properties under conformal transformations. The operator \mathcal{O}_μ has a twist-2, twist-3 and twist-4 component given by

$$\begin{aligned} \text{twist-2 : } \quad \mathcal{O}_+ &= \bar{\psi}_+\gamma_+\psi_+ \equiv \mathcal{O}^{1,1}, \\ \text{twist-3 : } \quad \mathcal{O}_\perp &= \bar{\psi}_+\gamma_\perp\psi_- + \bar{\psi}_-\gamma_\perp\psi_+ \equiv \mathcal{O}^{1,1/2} + \mathcal{Q}^{1/2,1}, \\ \text{twist-4 : } \quad \mathcal{O}_- &= \bar{\psi}_-\gamma_-\psi_- \equiv \mathcal{O}^{1/2,1/2}, \end{aligned} \quad (2.80)$$

Here, the superscript represent the conformal spins of the quark and anti-quark entering the operator. These conformal local operators of different twists can be written in terms of Gegenbauer polynomials (see [68] for details), and result into

the final form of DAs in terms of these polynomials. For example, the twist-2 distribution amplitude of pion is written as

$$\phi_\pi(u, \mu) = 6u\bar{u} \left[1 + \sum_{n=2,4,\dots} a_n(\mu) C_n^{3/2}(u - \bar{u}) \right]. \quad (2.81)$$

Here, $C_n^{3/2}$ are the Gegenbauer polynomials and a_n are the multiplicatively renormalizable coefficient defined as,

$$a_n(\mu) = a_n(\mu_0) \left(\frac{\alpha_s(\mu)}{\alpha_s(\mu_0)} \right)^{\gamma_n/\beta_0} \quad (2.82)$$

with $\alpha_s = \frac{g_s^2}{4\pi}$ (g_s is the strong coupling constant), β_0 is the leading QCD β -function and

$$\gamma_n = \frac{4}{3} \left[-3 - \frac{2}{(n+1)(n+2)} + 4 \left(\sum_{k=1}^{(n+1)} \frac{1}{k} \right) \right]. \quad (2.83)$$

The other distribution amplitudes of light mesons like pion are collected in Appendix-B along with the distribution amplitudes of heavy mesons, baryons and photons used throughout this thesis. For details on how to determine these distribution amplitude we suggest the reader to look at [70]–[72] and references therein.

2.3 Light Cone Sum Rules (LCSR)

After having understood the physics of SVZ sum rules (SVZ SRs) ((see Section-2.1)) and the theory of hard exclusive processes (see Section-2.2), we are now ready to understand the method of light cone sum rules (LCSR). It was developed as a hybrid of the SVZ SRs and the theory of hard exclusive processes in order to deal with the limitations of the SVZ sum rules as discussed in Section-2.1.3 (see [37], [52], [64] and references therein for details).

The basic idea here is to expand the products of the currents near the light cone ($x^2 \rightarrow 0$) instead of short distances ($x^\mu \rightarrow 0$) as the correlation functions are dominated by the light cone separations (as discussed in Section-2.2.1.1). Due to

light cone dominance, the perturbative calculation provides an operator product expansion near the light cone. The light cone OPE is an expansion in *twist* (as discussed in Section-2.2.1.2) instead of the canonical dimension [67]. This expansion helps in partially summing over the local operators and hence one can avoid some of the irregularities of the OPE truncation in the three-point sum rules. The method of LCSR has proved to be superior to SVZ SRs in calculating FFs involved in various hadronic transitions as one can now include both the hard and the soft (end-point) contributions.

Apart from the difference in OPE, there is another major difference between SVZ SRs and LCSR. In the case of SVZ SRs, one typically calculates the correlation functions for the vacuum to vacuum transitions while in LCSR, the correlation functions are taken to be the matrix elements of the time-ordered product of quark and gluon currents taken between vacuum and an on-shell state (like mesons, baryons or photon). As a result of this, the light cone distribution amplitudes (LCDAs) enter in the LCSR calculations as the basic non-perturbative objects. These LCDAs are the universal objects and can be defined by the matrix element of the quark operators of different twists between the vacuum and the on-shell state. The conformal symmetry of QCD dictates the form of these LCDAs for the case of light quark hadrons and have a better physical interpretation (as discussed in Section-2.2.2). The rest of the tools are common in SVZ SRs and LCSR. One can use the same procedure to derive the final sum rule as discussed in Section-2.1.1 for SVZ SRs.

To summarize, the non-perturbative hadronic quantities like form factors can be derived using the method of light cone sum rules by writing the correlation function of interest as an operator product expansion near the light cone and equating it with the representation obtained directly in terms of hadronic states in the form of dispersion relation. To approximate the unknown spectral densities which enter in the dispersion relation, one uses the statement of quark-hadron duality which relates these unknown spectral densities to the perturbatively calculated spectral densities. As a final step, one performs Borel transformation to get rid of the divergences in the dispersion relation and to reduce the systematic uncertainties arising due to the duality approximations. Borel transformations

improves the stability and reliability of the sum rules. The duality approximations and the Borel transformation brings two independent parameters in the final results. These parameters can be fixed by checking the stability of the sum rules against their variation. Remainder of the thesis is devoted to the applications of LCSR to the physical processes involving different hadrons within and beyond the SM of particle physics.

Chapter 3

LCSR in radiative tau decay: An application to light meson system

After collecting and understanding all the tools and machinery required to derive light cone sum rules in Chapter-2, we now move ahead to see its application for various physical processes. As a first application, we consider one meson radiative decay of tau, i.e. $\tau^- \rightarrow \pi^- \nu_\tau \gamma$. This process includes a light meson, pion. The non-radiative decay of tau to pion and tau neutrino is found to have a branching ratio of $(10.82 \pm 0.05)\%$ [73]. However, the radiative mode has not been detected experimentally yet. Theoretically it is expected to have a branching ratio of $\mathcal{O}(10^{-3})$ which is not very small and should be measurable in near future. Therefore, it is an important mode to study. In this chapter, we discuss this radiative tau decay in full detail. It includes two time-like form factors (FFs): the axial-vector and the vector FFs, which can be very useful in understanding the structure of pion. We first calculate these FFs in the framework of LCSR. Later, using the LCSR predictions for these FFs, we provide an estimate for the structure dependent parameter (SDP) for pion. SDP is defined as the ratio of the axial to the vector form factor at zero momentum transfer. It helps in determining the structure of pion. Furthermore, we provide estimates for the invariant mass spectrum of the $\pi - \gamma$ system along with the normalised decay width contribution coming from different contributions (see below). This chapter is based on [74].

3.1 Introduction

τ being the heaviest lepton with mass, $m_\tau = 1776.86 \pm 0.12 \text{ MeV}$ [73] has numerous decay channels (see for example [75]–[79] for different aspects of τ lepton physics.). Because of its large mass, it is the only lepton that can decay into hadrons. As discussed in Chapter-1, the electroweak part of the SM is reasonably well understood while one is still lacking in developing a proper methodology to understand the strong interactions. The study of hadronic decays of τ helps us in developing a better understanding of the dynamics of strong interaction involved in the hadronization of QCD currents by providing a cleaner environment.

In particular, we will discuss the one meson radiative tau decay, i.e. $\tau^- \rightarrow \pi^- \nu_\tau \gamma$, in this chapter. Experimentally, the branching ratio of the non-radiative one meson decay of tau, i.e. $\tau^- \rightarrow \pi^- \nu_\tau$ is found to be $(10.82 \pm 0.05)\%$ [73]. Therefore, one expects the branching ratio for radiative mode to be $\mathcal{O}(10^{-3})$. One can understand it by writing the branching ratio of the radiative mode as a product of branching ratios of $\tau \rightarrow \rho \nu_\tau$ and $\rho \rightarrow \pi \gamma$. Using the values of these branching ratios from [73], one gets an estimate $\sim 10^{-3}$ for the radiative mode, which is about 10^{-2} of the non-radiative branching ratio. However, the branching ratio of this mode is not very small, it has never been observed experimentally and a detailed study of this mode becomes important.

The total decay amplitude of this process can be written as a sum of two contributions [80]–[84] namely internal bremsstrahlung (IB) and the structure dependent (SD) contributions. They can be defined as:

- **Internal Bremsstrahlung (IB):** The contribution that comes from the emission of photon from either the incoming or the outgoing particles, considering them to be point-like. This contribution can be calculated trivially with the use of scalar QED for the point-like charged pion and using spinor QED for the case of photon emission from tau. Diagrammatically, this is shown in (a) and (b) of Fig.(3.1).
- **Structure Dependent (SD):** This contribution is governed by the dynamics of strong interactions and includes non-trivial parts. The pion can

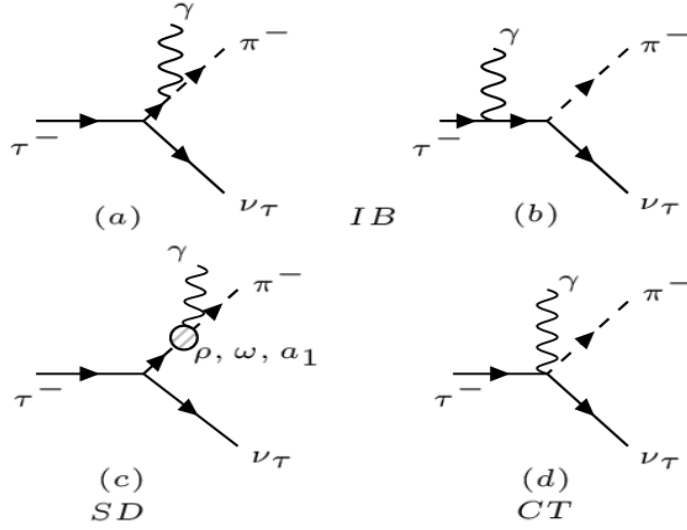


Figure 3.1: Feynman diagrams showing different contributions to radiative tau decay ($\tau^- \rightarrow \pi^- \nu_\tau \gamma$). (a) and (b) represents the IB contribution, (c) represents the SD contribution, and (d) represents the contact term.

no longer be treated as a point-like particle and its partonic structure will play a role. This contribution appears as a result of the hadronization of the intermediate quark currents γ^μ and $\gamma^\mu \gamma_5$ with $J^P = 1^-$ and $J^P = 1^+$, respectively ((c) of Fig.(3.1)). Consequently, it depends on the long distance dynamics. It can be parameterized in terms of two form factors namely the vector FF ($F_V^{(\pi)}$) and the axial-vector FF ($F_A^{(\pi)}$) as a result of the Lorentz and the gauge symmetry. These form factors are the non-perturbative objects that encode the information of the dynamics of strong interactions involved in the hadronization of the intermediate quark currents. Therefore, their evaluation requires a non-perturbative treatment such as, Light Cone Sum Rules (LCSR), Chiral Perturbation Theory χ PT or Lattice QCD. This contribution also includes a so called *Contact Term* (*CT*). This term emerges as a consequence of gauge invariance. It can be graphically represented as in (d) of Fig.(3.1).

We will see the explicit form of these contributions in Section-3.2 where they will be calculated and discussed in detail. Moreover, we will see that the IB contribution consists of two terms. One of them is independent of m_τ while the other turns out to be proportional to m_τ . Later we will see that the CT contributions turns out to be equal and opposite to the m_τ independent term of

the IB contributions and hence gets cancelled in the total amplitude.

Before moving to the actual calculations involved, let us review some important features of the one meson radiative decay of tau. The amplitude for this process is related to that of the radiative pion decay via crossing symmetry with one major difference that comes at the level of kinematics. The square of the momentum transferred between the pion-photon and leptonic system in the case of radiative tau decay can take values up to m_τ^2 . While, for the radiative pion decay, the maximum value it can take is m_π^2 which is almost negligible. Furthermore, the FFs involved in the case of radiative pion decay are space-like. However, for the case of radiative tau decay, they are time-like as both the pion and the photon are in the final state. Consequently, the study of these form factors becomes complicated as the light flavoured mesons (ρ , ω , a_1) can now be created on-shell and give resonant structures in the pion-photon invariant mass spectrum.

Therefore, in order to understand this process, the first important task is to calculate these time-like FFs. These form factors are helpful in probing the structure of the pion as the ratio of these FFs at zero momentum transferred square, known as the *structure dependent parameter (SDP)*. Mathematically, it can be written as

$$\gamma = \frac{F_A^{(\pi)}(0)}{F_V^{(\pi)}(0)}. \quad (3.1)$$

As these form factors at zero momentum transferred square are same for the radiative pion decay and the radiative tau decay, one can get an experimental estimate of γ using the experimental determination of these FFs using the radiative pion decay. The numerical values of $F_A^{(\pi)}(0)$ and $F_V^{(\pi)}(0)$ from such a determination are (0.0119 ± 0.0001) and (0.0254 ± 0.0017) , respectively [73]. Consequently, the value of γ turns out to be equal to (0.4685 ± 0.0353) . A consistent study of the radiative decay of tau into a pion and a tau neutrino helps us in developing a consistent way to determine this parameter theoretically. Apart from probing the structure of the pion, this decay mode is also useful in understanding the light-by-light hadronic contribution to the muon anomalous magnetic moment, $(g - 2)_\mu$ [85]. Furthermore, in [86], the authors have discussed how this decay mode can provide means for the mass generation of the tau neutrino.

In the past, these gauge invariant time-like form factors involved in the radiative tau decay have been parametrized using Breit-Wigner type resonances [87], light front quark model [83] and resonance χ PT [84], etc. Majorly, the differences in the literature stem from the vastly different approaches adopted to determine or estimate these FFs. It affects the predictions for the rate and spectrum, as well as the extraction of γ , including the sign. It can be better understood by taking an example. Consider the case where the resonances are included via Breit-Wigner method. The relative phase between the different contributions has always been a suspecting issue in such a case. The main aim of this chapter is to provide a consistent determination of these form factors using the method of LCSR.

In the rest of the chapter, we will first discuss the different contributions to the amplitude (as mentioned above) in detail and then discuss the calculation of the form factors involved using the method of light cone sum rules. Thereafter, we will present the results obtained for the structure dependent parameter, decay width and the invariant mass spectrum. Finally, we will summarize the results along with its future endeavours.

3.2 Amplitude Computation

Photon, being the charge carrier of the electromagnetic interactions, can be emitted from any of the charged particles involved in the process. Therefore, in the present case, it can be emitted either from the pion or the tau-lepton as the tau-neutrino is charge neutral (see Fig.(3.1)). Moreover, as discussed above, pion is a composite object with an internal structure comprising of a quark-anti-quark pair as valance constituents along with the sea quarks and gluons. This internal structure also contributes to the process and gives rise to two non-perturbative form factors.

As already discussed, the amplitude of the process $\tau^- \rightarrow \pi^- \nu_\tau \gamma$ includes various contributions: Internal Bremsstrahlung (IB), Structure Dependent (SD) and Contact term (CT). IB contribution comes from the emission of the photon from tau and pion (considering pion to be the point object). SD contribution comes from the emission of photon from the internal structure of the pion. The contact

term in an interesting effective contribution and has its origin in the gauge invariance of a QED amplitude [88]. This amplitude can be written as (employing the low energy four-Fermi effective Hamiltonian obtained by integrating out the heavy W-boson as discussed in Section-1.5),

$$\mathcal{A}(\tau^-(p_1) \rightarrow \pi^-(p_2)\nu_\tau(p_3)\gamma(k)) = \frac{G_F}{\sqrt{2}}V_{ud} \langle \pi^-\nu_\tau\gamma | (\bar{\nu}_\tau\Gamma^\mu\tau)(\bar{d}\Gamma_\mu u) | \tau^- \rangle \quad (3.2)$$

where $\Gamma^\mu = \gamma^\mu(1 - \gamma_5)$, G_F is the Fermi's constant as defined in Eqn.(1.29), and V_{ud} is the CKM element (see Eqn.(1.13)).

The amplitude in Eqn.(3.2) can be factorised into two parts as

$$\begin{aligned} \mathcal{A}(\tau^-(p_1) \rightarrow \pi^-(p_2)\nu_\tau(p_3)\gamma(k)) \\ = \frac{G_F}{\sqrt{2}}V_{ud} [\langle \pi^-\gamma | (\bar{d}\Gamma_\mu u) | 0 \rangle \langle \nu_\tau | (\bar{\nu}_\tau\Gamma^\mu\tau) | \tau^- \rangle + \langle \nu_\tau\gamma | (\bar{\nu}_\tau\Gamma^\mu\tau) | \tau^- \rangle \langle \pi^- | (\bar{d}\Gamma_\mu u) | 0 \rangle] \end{aligned} \quad (3.3)$$

where the first term of the right hand side dictates the photon emission from the final state pion (including the contribution coming from its internal structure) and the second term dictates the photon emission from the initial state tau lepton. This factorization of the amplitude holds for energetic photons and at the leading order in $\frac{1}{m_\tau}$ and α_{em} .

Furthermore, using the matrix element of the pion defined as

$$\langle \pi^-(p_2) | (\bar{d}\gamma^\mu(1 - \gamma_5)u) | 0 \rangle = if_\pi p_2^\mu \quad (3.4)$$

where f_π is the pion decay constant, and interpolating the photon state with the electromagnetic current, j_{em}^α , the amplitude in Eqn.(3.3) can further be written as

$$\begin{aligned} \mathcal{A}(\tau^- \rightarrow \pi^-\nu_\tau\gamma) = \frac{G_F}{\sqrt{2}}V_{ud} \left[-ie\epsilon_\alpha^*(\bar{u}_\nu\Gamma_\mu u_\tau) \int d^4x e^{ikx} \langle \pi^- | T\{j_{em}^\alpha(x)\bar{d}\Gamma^\mu u(0)\} | 0 \rangle \right. \\ \left. - ef_\pi p_{2\mu}\epsilon_\alpha^* \int d^4x e^{ikx} \langle \nu_\tau | T\{j_{em}^\alpha(x)\bar{\nu}_\tau\Gamma^\mu\tau(0)\} | \tau^- \rangle \right] \end{aligned} \quad (3.5)$$

where, ϵ_α is the polarisation vector for the photon. $j_{em}^\alpha(x) = Q_\psi \bar{\psi}(x) \gamma^\alpha \psi(x) = -\bar{\tau} \gamma^\alpha \tau + Q_u \bar{u} \gamma^\alpha u + Q_d \bar{d} \gamma^\alpha d$. Q_u and Q_d are the electromagnetic charges of u and d quarks, respectively in units of e .

The second term on the r.h.s. of Eqn.(3.5) is the trivial one and can be calculated using the Feynman rules of QED. The final form of this term turns out to be

$$\begin{aligned} \langle \nu_\tau \gamma | \bar{\nu}_\tau \Gamma^\mu \tau | \tau^- \rangle \langle \pi^- | \bar{d} \Gamma_\mu u | 0 \rangle &= -i e f_\pi \bar{u}_\nu(p_3) \not{\epsilon}^* (1 - \gamma_5) u_\tau(p_1) \\ &+ \frac{i e f_\pi m_\tau}{2 p_1 \cdot k} \{ \bar{u}_\nu(p_3) [(2 \epsilon^* \cdot p_1) - \not{k} \not{\epsilon}^*] (1 + \gamma_5) u_\tau(p_1) \}. \end{aligned} \quad (3.6)$$

However, the first term is non-trivial and is more interesting as it encodes the dynamics of strong interactions. To compute this term, let us first define a hadronic matrix element given by

$$T^{\alpha\mu}(p_2, k) = i \int d^4 x e^{ikx} \langle \pi^- | T \{ j_{em}^\alpha(x) \bar{d} \Gamma^\mu u(0) \} | 0 \rangle. \quad (3.7)$$

Moreover, the application of the Ward identity, which comes as a consequence of the conservation of electromagnetic current, results into

$$k_\alpha T^{\alpha\mu}(p_2, k) = \langle \pi^- | \bar{d}(0) \Gamma^\mu u(0) | 0 \rangle = i f_\pi p_2^\mu \quad (3.8)$$

in the momentum space. Here, we have used the commutator of the electromagnetic charge operator and the electroweak current of the pion, which is given by

$$[j_{em}^0(x), \bar{d} \Gamma^\mu u(0)] = -Q_u \delta^3(x) \bar{d}(0) \Gamma^\mu u(x) + Q_d \delta^3(x) \bar{d}(x) \Gamma^\mu u(0). \quad (3.9)$$

Besides, the hadronic matrix element defined in Eqn.(3.7) can also be written in terms of the momentum of the pion (p_2) and the photon (k) by using the general covariant decomposition as

$$T^{\alpha\mu}(p_2, k) = A g^{\alpha\mu} + B p^{2\alpha} p^{2\mu} + C p^{2\alpha} k^\mu + D k^\alpha p^{2\mu} + E k^\alpha k^\mu + i F_V^{(\pi)} \epsilon^{\alpha\mu\beta\nu} p_{2\beta} k_\nu \quad (3.10)$$

where $A, B, C, D, E, F_V^{(\pi)}$ are the gauge invariant scalar functions of $(p_2 + k)^2$. $\epsilon^{\alpha\mu\beta\nu}$ is the totally anti-symmetric tensor known as the Levi-civita tensor. On contracting Eqn.(3.10) with k_α , one obtains

$$k_\alpha T^{\alpha\mu}(p_2, k) = Ak^\mu + B(p_2.k)p_2^\mu + C(p_2.k)k^\mu. \quad (3.11)$$

We can now compare Eqn.(3.8) and Eqn.(3.11) and get

$$C = \frac{-A}{(p_2.k)}, \quad \text{and} \quad B = \frac{if_\pi}{(p_2.k)}. \quad (3.12)$$

Using these conditions on the scalar functions C and B , the hadronic matrix element in Eqn.(3.10) can be written as

$$T^{\alpha\mu}(p_2, k) = F_A^{(\pi)} [g^{\alpha\mu}(P.k) - P^\alpha k^\mu] + iF_V^{(\pi)} \epsilon^{\alpha\mu\beta\nu} P_\beta k_\nu - if_\pi g^{\alpha\mu} + if_\pi \frac{P^\alpha P^\mu}{P.k} \quad (3.13)$$

where $F_A^{(\pi)} = \frac{A+if_\pi}{P.k}$ and $P = p_1 - p_3 = p_2 + k$ implies $p_2.k = P.k$. Consequently, the first term of Eq.(3.5) reads as

$$\begin{aligned} & \langle \pi^- \gamma | \bar{d} \Gamma_\mu u | 0 \rangle \langle \nu_\tau | \bar{\nu}_\tau \Gamma^\mu \tau | \tau^- \rangle \\ &= ie\epsilon^{*\alpha} [\bar{u}_\nu \Gamma^\mu u_\tau] \left[iF_A^{(\pi)} \{g_{\alpha\mu}(P.k) - P_\alpha k_\mu\} - F_V^{(\pi)} \epsilon_{\alpha\mu\beta\nu} P^\beta k^\nu \right] \\ &+ ie\epsilon^{*\mu} f_\pi \bar{u}_\nu \Gamma_\mu u_\tau - ief_\pi \frac{\epsilon^*.P}{P.k} \bar{u}_\nu \not{P} (1 - \gamma_5) u_\tau. \end{aligned} \quad (3.14)$$

Here, the first term on the r.h.s., written in terms of the gauge invariant scalar functions $F_A^{(\pi)}$ and $F_V^{(\pi)}$, determines the SD contribution as discussed above. The second terms is the so called contact term which appeared purely as a consequence of gauge invariance. The last term provides the IB contribution coming from the emission of photon from the pion treated as a point particle.

As a result, the final form for the amplitude of the radiative tau decay can then

be written by using Eqn.(3.6) and Eqn.(3.14) in Eqn.(3.5) as

$$\begin{aligned}
\mathcal{A}(\tau^-(p_1) \rightarrow \pi^-(p_2)\nu_\tau(p_3)\gamma(k)) & \\
&= \frac{G_F}{\sqrt{2}}V_{ud} \left[ie\epsilon^{*\alpha}(\bar{u}_\nu\Gamma^\mu u_\tau) \left\{ iF_A^{(\pi)} [g_{\alpha\mu}(P.k) - P_\mu k_\alpha] - F_V^{(\pi)} \epsilon_{\alpha\mu\beta\nu} P^\beta k^\nu \right\} \right. \\
&\quad \left. + ief_\pi m_\tau \bar{u}_\nu \left\{ \frac{\epsilon^* \cdot p_1}{p_1 \cdot k} - \frac{\not{k}\not{\epsilon}^*}{2p_1 \cdot k} - \frac{\epsilon^* \cdot p_2}{p_2 \cdot k} \right\} (1 + \gamma_5) u_\tau \right]. \quad (3.15)
\end{aligned}$$

In the final amplitude, the contribution coming from the contact terms gets cancelled against the m_τ independent contribution of photon emission from τ (see Eqn.(3.6)) and Eqn.(3.14). For further simplification, we write the amplitude as a sum of different contributions as

$$\mathcal{A}(\tau^- \rightarrow \pi^- \nu_\tau \gamma) = \mathcal{A}_{IB} + \mathcal{A}_V + \mathcal{A}_A = \mathcal{A}_{IB} + \mathcal{A}_{SD} \quad (3.16)$$

where \mathcal{A}_{IB} depicts the internal bremsstrahlung contribution. \mathcal{A}_V and \mathcal{A}_A represents the contribution coming from the vector and the axial-vector form factor terms. They collectively provides the structure dependent contribution, \mathcal{A}_{SD} . The explicit forms of these contributions are

$$\mathcal{A}_{IB} = \frac{G_F}{\sqrt{2}}V_{ud} \left[ief_\pi m_\tau \bar{u}_\nu \left\{ \frac{\epsilon^* \cdot p_1}{p_1 \cdot k} - \frac{\not{k}\not{\epsilon}^*}{2p_1 \cdot k} - \frac{\epsilon^* \cdot p_2}{p_2 \cdot k} \right\} (1 + \gamma_5) u_\tau \right], \quad (3.17)$$

$$\mathcal{A}_V = -\frac{G_F}{\sqrt{2}}V_{ud} \left[ie\epsilon^{*\alpha}(\bar{u}_\nu\Gamma^\mu u_\tau) \left(F_V^{(\pi)} \epsilon_{\alpha\mu\beta\nu} P^\beta k^\nu \right) \right], \text{ and} \quad (3.18)$$

$$\mathcal{A}_A = \frac{G_F}{\sqrt{2}}V_{ud} \left[ie\epsilon^{*\alpha}(\bar{u}_\nu\Gamma^\mu u_\tau) \left(iF_A^{(\pi)} [g_{\alpha\mu}(P.k) - P_\mu k_\alpha] \right) \right]. \quad (3.19)$$

The form factors, $F_A^{(\pi)}$ and $F_V^{(\pi)}$, are the unknown non-perturbative quantities. Therefore, in order to make any prediction for the decay width for this process, we first need the information on these FFs. In the next section, we will see how one can get estimates for these form factors using the method of light cone sum rules.

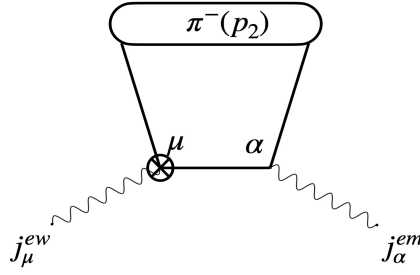


Figure 3.2: Feynman diagram which contributes to the light-cone expansion of the hadronic matrix element for radiative tau decay up to twist-2. The internal line connecting the two currents can be either the up-quark or the down quark. The encircled pion represents that the pion distribution amplitude will enter the LCSR computation.

3.3 Form Factors in LCSR framework

As discussed in Chapter-2, the starting point to derive the sum rules is to determine the relevant hadronic matrix element for the process. In the present case, that matrix element is given by Eqn.(3.7) (see Fig. (3.2)) as

$$T^{\alpha\mu}(p_2, k) = i \int d^4x e^{ikx} \langle \pi^- | T \{ Q_u \bar{u} \gamma^\alpha u(x) \bar{d} \Gamma^\mu u(0) + Q_d \bar{d} \gamma^\alpha d(x) \bar{d} \Gamma^\mu u(0) \} | 0 \rangle \quad (3.20)$$

where Q_u (Q_d) is the charge of up (down) quark in units of e . Furthermore, this matrix element can be written using two representations. First using OPE near the light cone, and the second using dispersion relation directly in terms of hadronic states. Then, in order to derive the sum rules, we equate the matrix element obtained using both these representations (see Chapter-2 for details).

To derive the first representation, the matrix element in Eqn.(3.20) can be simplified using the light-cone propagator given in Appendix-B, and using the definition of the light cone distribution amplitude (DA) of the pion given by

$$\langle \pi^0(p) | \bar{u}(y) \gamma_\mu \gamma_5 u(x) | 0 \rangle_{x^2=0} = -i f_\pi p_\mu \int_0^1 du e^{i(up_2 \cdot y + \bar{u}p \cdot x)} \phi(u, \mu) \quad (3.21)$$

where $\bar{u} = 1 - u$ and $\phi(u, \mu)$ is leading twist-2 DA of the pion (details can be found in Appendix-B). The matrix element in Eqn.(3.20) then becomes

$$T^{\alpha\mu}(p_2, k) = if_\pi \int d^4x \frac{e^{ikx}}{2\pi^2 x^4} \int_0^1 du \phi(u, \mu) \left[i\epsilon^{\mu\beta\alpha\rho} x_\beta p_{2\rho} (Q_u e^{i\bar{u}p_2x} + Q_d e^{iup_2x}) \right. \\ \left. + (x^\mu p_2^\alpha - g^{\mu\alpha}(x.p_2) + x^\alpha p_2^\mu) (Q_u e^{i\bar{u}p_2x} - Q_d e^{iup_2x}) \right]. \quad (3.22)$$

Here, we considered only the two particle contribution of the light cone propagator. The higher order terms involving one or more gluons are neglected (see Appendix-B for details). Now, on performing the integration over x and using the fact that $\phi(u, \mu)$ is symmetric under the exchange of u and \bar{u} , we find the first representation for the matrix element $T^{\alpha\mu}$ in terms of light cone distribution amplitudes as

$$T^{\alpha\mu}(P, k) = if_\pi \int_0^1 du \frac{\phi(u, \mu)}{P^2 \bar{u} + k^2 u} \left[i\epsilon^{\mu\beta\alpha\rho} \frac{P_\rho k_\beta}{3} + 2\bar{u} \{P^\alpha P^\mu - (P.k)g^{\mu\alpha}\} \right. \\ \left. - \{g^{\mu\alpha}(P.k) - P^\alpha k^\mu\} (1 - 2\bar{u}) \right]. \quad (3.23)$$

Comparing this QCD representation of $T^{\alpha\mu}(P, k)$ with the general decomposition in terms of FFs given in Eqn.(3.13), we obtain the forms of vector and axial-vector FFs in QCD as

$$F_V^{QCD}(t) = \frac{if_\pi}{3} \int_0^1 du \frac{\phi(u, \mu)}{t\bar{u} + k^2 u}, \quad \text{and} \quad (3.24)$$

$$F_A^{QCD}(t) = -if_\pi \int_0^1 du \phi(u, \mu) \left(\frac{1 - 2\bar{u}}{t\bar{u} + k^2 u} \right), \quad (3.25)$$

respectively with $t = P^2 = (p_2 + k)^2$ is the invariant mass square of the $\pi - \gamma$ system.

Now, after having the first representation, we move towards the second representation using dispersion relation in terms of the hadronic states. In order to derive the dispersion relation, let us insert a complete set of states $|n\rangle$ in the matrix element in Eqn.(3.20) to get

$$\langle \pi^- | T \{ j_{em}^\alpha(x) j_{ew}^\mu(0) \} | 0 \rangle = \langle \pi^- | j_{em}^\alpha(x) | n \rangle \langle n | j_{ew}^\mu(0) | 0 \rangle \quad (3.26)$$

where, $|n\rangle = |\rho\rangle + |\omega\rangle + |a_1\rangle + \text{higher resonances} + \text{continuum}$, such that it satisfies the quantum numbers of the matrix element. The sum rules will be saturated by the contributions coming from lowest energy states i.e., ρ, ω, a_1 -mesons¹. Therefore, we will focus on the contributions coming from these states.

- **ρ and ω -meson** contribution: The contribution from the ρ -meson contribution will come from

$$\langle \pi^-(p_2) | j_{em}^\alpha(x) | \rho(p_2 + k) \rangle \langle \rho(p_2 + k) | j_{ew}^\mu(0) | 0 \rangle. \quad (3.27)$$

This can be simplified by using the matrix element of the electroweak current between a vacuum and the ρ -meson given by

$$\langle \rho(p_2 + k) | \bar{d}\Gamma_\mu u | 0 \rangle = -im_\rho f_\rho \epsilon_\mu^{(\rho)*}, \quad \text{and} \quad (3.28)$$

the matrix element of the electromagnetic current between the pion and the ρ -meson state given by

$$\langle \pi^-(p_2) | j_{em}^\alpha(x) | \rho(p_2 + k) \rangle = \epsilon^{\alpha\lambda\beta\nu} \epsilon_\lambda^{(\rho)} p_{2\beta} k_\nu F_{\rho\pi}(k^2). \quad (3.29)$$

Here, m_ρ and f_ρ represents the mass and decay constant of ρ -meson, respectively. $\epsilon_\mu^{(\rho)}$ represents the polarization vector for the ρ -meson, and $F_{\rho\pi}(k^2)$ is a scalar function of k^2 which carries the information of the transition of ρ -meson into a pion via the electromagnetic current.

Using the above mentioned definitions along with the sum over polarizations of vector meson given by

$$\epsilon_\lambda^{(V)} \epsilon_\nu^{(V)*} = -g_{\lambda\nu} + \frac{(p_2 + k)_\lambda (p_2 + k)_\nu}{m_V^2} \quad (3.30)$$

where $g_{\lambda\nu}$ is the metric tensor and $V = \rho$ for the present case, the contri-

¹At the present level of accuracy, the contribution of the higher resonances is roughly 20% of these resonances because of the Borel suppression.

bution coming from Eqn.(3.27) can be written as

$$\langle \pi^-(p_2) | j_{em}^\alpha(x) | \rho(p_2 + k) \rangle \langle \rho(p_2 + k) | j_{ew}^\mu(0) | 0 \rangle = im_\rho f_\rho \epsilon^{\alpha\lambda\beta\nu} g_\lambda^\mu p_{2\beta} k_\nu F_{\rho\pi}(k^2). \quad (3.31)$$

This is the ρ -meson contribution to the dispersion relation. The contribution of ω -meson is almost equal to the ρ -meson contribution where we have neglected the very small difference between the masses of the two mesons. Therefore, in order to incorporate the contribution coming from the ω -meson, we will simply multiply the ρ -meson contribution by two in the dispersion relation.

- **a_1 -meson contribution:** The contribution from a_1 -meson will come from

$$\langle \pi^-(p_2) | j_{em}^\alpha(x) | a_1(p_2 + k) \rangle \langle a_1(p_2 + k) | j_{ew}^\mu(0) | 0 \rangle, \quad (3.32)$$

Similar to the case of ρ - and ω -meson contribution, it can be simplified by using the matrix element of the electroweak current between a vacuum and the a_1 -meson similar to Eqn.(3.28), and the matrix element of electromagnetic current between the pion and the a_1 -meson state given by

$$\langle \pi^-(p_2) | j_{em}^\mu(x) | a_1(p_2 + k) \rangle = [(2p_2 - k) \cdot k g^{\mu\lambda} - (2p_2 - k)^\mu k^\lambda] \epsilon_\lambda^{(a_1)*} G_{a_1\pi}(k^2). \quad (3.33)$$

Here, $\epsilon_\lambda^{(a_1)*}$ is the polarization vector for a_1 -meson, and $G_{a_1\pi}(k^2)$ is a scalar function of k^2 which carries the information of the transition of a_1 -meson into a pion. Using these definitions along with the polarization sum given in Eqn.(3.30), the contribution of the a_1 -meson to the dispersion relation turns out to be

$$\begin{aligned} & \langle \pi^-(p_2) | j_{em}^\alpha(x) | a_1(p_2 + k) \rangle \langle a_1(p_2 + k) | j_{ew}^\mu(0) | 0 \rangle \\ & = im_{a_1} f_{a_1} [2p_2 \cdot k g^{\alpha\mu} - 2p_2^\alpha k^\mu] G_{a_1\pi}(k^2) \end{aligned} \quad (3.34)$$

where m_{a_1} and f_{a_1} are the mass and the decay constant of the a_1 -meson,

respectively.

Using the contribution coming from the ρ , ω , and a_1 -mesons, the dispersion relation for $T^{\alpha\mu}$ defined in Eqn.(3.20) turns out to be (see Section-2.1.1 for details)

$$T^{\alpha\mu}(p_2, k) = \frac{2im_\rho f_\rho \epsilon^{\alpha\lambda\beta\nu} g_\lambda^\mu p_{2\beta} k_\nu F_{\rho\pi}(k^2)}{m_\rho^2 - (p_2 + k)^2 - im_\rho \Gamma_\rho} + \frac{im_{a_1} f_{a_1} [2p_2 \cdot k g^{\alpha\mu} - 2p_2^\alpha k^\mu] G_{a_1\pi}(k^2)}{m_{a_1}^2 - (p_2 + k)^2 - im_{a_1} \Gamma_{a_1}} + \frac{1}{\pi} \int_{s_0^h}^{\infty} ds \frac{\text{Im}\{T^{\alpha\mu}(s, k)\}}{s - k^2 - i\epsilon} \quad (3.35)$$

where s_0^h is the threshold of the lowest continuum state, and Γ_ρ and Γ_{a_1} are the decay widths of ρ and a_1 mesons, respectively. The last term on the r.h.s. of this equation represents the contribution coming from the heavier states and the continuum.

Now, we are ready to write the sum rules for the form factors $F_V^{(\pi)}$ and $F_A^{(\pi)}$. The sum rule for $F_V^{(\pi)}$ can be written by taking the form of $F_V^{(\pi)}(t)$ from Eqn.(3.35) and equating it with the form obtained in Eq.(3.24), i.e.

$$\frac{2m_\rho f_\rho F_{\rho\pi}(k^2)}{m_\rho^2 - t - im_\rho \Gamma_\rho} + \frac{1}{\pi} \int_{s_0^h}^{\infty} ds \frac{\text{Im}\{F_V(s)\}}{s - t - i\epsilon} = \frac{if_\pi}{3} \int_0^1 du \frac{\phi(u, \mu)}{t\bar{u} + k^2 u}. \quad (3.36)$$

Now, using the duality approximation (as explained in Section-2.1.1), we can approximate the heavier state and continuum contribution to the perturbatively calculated form such that

$$\frac{1}{\pi} \int_{s_0^h}^{\infty} ds \frac{\text{Im}\{F_V(s, k)\}}{s - t - i\epsilon} \simeq \frac{1}{\pi} \int_{s_0}^{\infty} ds \frac{\text{Im}\{F_V^{QCD}(s, k)\}}{s - t - i\epsilon} \quad (3.37)$$

where s_0 is the continuum threshold, a free parameter in sum rules calculation and $\text{Im}\{F_V^{QCD}(s, k)\}$ is the imaginary part of $F_V^{QCD}(s, k)$ which can be calculated from Eqn.(3.24) using Eqn.(A.13) such that

$$\frac{1}{\pi} \text{Im}\{F_V^{QCD}(t)\} = \frac{if_\pi}{3} \int_0^1 du \phi(u, \mu) \delta(t\bar{u} + k^2 u). \quad (3.38)$$

Using Eqn.(3.37) and Eqn.(3.38) in Eqn.(3.36), the sum rule for $F_V^{(\pi)}(t)$ simplifies to

$$\frac{2m_\rho f_\rho F_{\rho\pi}(k^2)}{m_\rho^2 - t} = \frac{if_\pi}{3} \int_0^{u_0} du \frac{\phi(u)}{t\bar{u} + k^2 u}. \quad (3.39)$$

$u_0 = \frac{s_0}{k^2 + s_0} = 1$ (as $k^2 = 0$).

Similarly, the sum rule for $F_A^{(\pi)}(t)$ turns out to be

$$\frac{2im_{a_1}f_{a_1}G_{a_1\pi}(k^2)}{m_{a_1}^2 - t} = -if_\pi \int_0^{u_0} \phi(u) \left(\frac{1 - 2\bar{u}}{t\bar{u} + k^2u} \right) \quad (3.40)$$

using the duality approximation and the imaginary part of $F_A^{QCD}(s, k)$ (see Eqn.(3.25)) given by

$$\frac{1}{\pi} \text{Im}\{F_A^{QCD}(t)\} = -if_\pi \int_0^1 du \phi(u, \mu) (1 - 2\bar{u}) \delta(t\bar{u} + k^2u). \quad (3.41)$$

Finally after performing Borel transformation on these sum rules and substituting them back in Eqn.(3.35), we get the final analytical forms for $F_V^{(\pi)}$ and $F_A^{(\pi)}$ as²

$$F_V^{(\pi)}(t) = -i \frac{f_\pi}{3(m_\rho^2 - t - im_\rho\Gamma_\rho)} \int_0^1 du \frac{\phi(u)}{\bar{u}} e^{\frac{m_\rho^2}{M^2}}, \quad \text{and} \quad (3.42)$$

$$F_A^{(\pi)}(t) = -i \frac{f_\pi}{m_{a_1}^2 - t - im_{a_1}\Gamma_{a_1}} \int_0^1 \frac{\phi(u)}{\bar{u}} (1 - 2\bar{u}) e^{\frac{m_{a_1}^2}{M^2}}, \quad (3.43)$$

respectively. M is the Borel parameter here and the on-shell condition for photon (i.e. $k^2 = 0$) has been used. Also, the pion is considered to be mass-less, i.e. $m_\pi^2 = 0$ approximation is used.

Furthermore, it is interesting to note that the vector form factor at zero momentum transferred ($t = 0$) can be related to the anomaly term (or Wess-Zumino-Witten term) in $\pi\gamma\gamma$ vertex given by $\frac{1}{(4\pi^2 f_\pi)}$. Using the KSFR-II relation ([89], [90]), according to which $m_\rho^2 = 2g_{\rho\pi\pi}^2 f_\pi^2$ along with the assumptions that the ρ -coupling $g_{\rho\pi\pi}$ is universal i.e. $g_{\rho\pi\pi} = g_{\rho NN} = g_{\rho\gamma} = g = 2\pi\sqrt{3/N_c}$, and the pion electromagnetic form factor is dominated by ρ meson contribution, one finds that a correct form emerges from $F_V^{(\pi)}(0)$ up to an overall factor of $e^{\frac{m_\rho^2}{M^2}}$ which must tend to unity. As we will see in the next section, the choice of Borel mass, M which provides a stable window for the form factors, trivially yields unity for this factor within a few percent.

Moreover, before moving to the numerical results, it may be worthwhile to pon-

²It is important to note here that these form factors have dimension of inverse mass and there is an extra factor of $-i$ coming because of the way initial amplitude is defined: $\mathcal{A}(\tau^- \rightarrow \pi^- \nu_\tau \gamma)$ instead of $i\mathcal{A}(\tau^- \rightarrow \pi^- \nu_\tau \gamma)$ as is often done.

der over possible duality violations. These violations arise due to the use of perturbatively evaluated spectral functions, which are given by the imaginary parts of the form factors (see Section-2.1.1), over the entire kinematical range. The perturbative effects occur at $\frac{1}{Q}$ where Q is the hard scale which is $\sim m_\tau$ for the present case of radiative tau decay, while, the time scale over which the partons come together to form final hadrons is $\mathcal{O}\left(\frac{Q}{\Lambda_{QCD}^2}\right)$. Therefore, the use of perturbatively evaluated spectral densities is not a correct approximation and brings uncertainties. As discussed in Chapter-2, it is rather difficult to exactly quantify the magnitude of such violations. However, having an estimation is rather important as otherwise they may lead to large uncertainties in the final results. To have an educated guess for these duality violations, one possible way is to use an instanton model. In this model the light quark amplitudes are suppressed. A rough calculation yields a quantity of the form $\text{Exp}[-Q\rho]/Q^n$, where ρ denotes the mean instanton size, in the Euclidean domain. This Euclidean form can be analytically continued to the Minkowski space which would have an oscillating factor multiplied by negative powers of the energy released in the hard process $\sim \mathcal{O}(m_\tau)$. An alternate method to calculate these duality violation can be by considering a comb of hadronic resonances that would contribute to the process and carry out the algebra. Both these methods bring similar conclusions that the violations are $\sim 10\%$ [59] (also see [91], [92] for detailed analyses for inclusive tau decays). This is typically the amount of duality violations that one expect in this case as well. However, a more detailed calculation is required to reveal the exact amount of such violations for the case of radiative tau decay. Such calculations are out of the scope of this thesis. Now, after having a possible estimate for the uncertainties due to duality violations, let us now move to the numerical results for various physical quantities like structure dependent parameter, decay width, etc., using the form factors evaluated above.

3.4 Numerical results

The analytic expressions for the vector and axial-vector form factors calculated using LCSR can be read from Eq.(3.42) and Eq.(3.43), respectively. Asymptot-

ically, both of these has $\frac{1}{t}$ dependence on the invariant mass squared (t of the $\pi - \gamma$ system) as expected from perturbative QCD in the asymptotic regime. For performing numerical analysis using these form factors we need the explicit form of the distribution amplitude ($\phi_\pi(u, \mu)$) of pion. For the present work, we consider two forms namely the asymptotic form (where $\mu \rightarrow \infty$) and Chernyak-Zhitnisky (CZ) form (where C_2 term is considered) of the pion DA provided in Eqn.(2.81). The explicit expressions for these forms are

$$\phi_\pi^{asym}(u, \mu) = 6u\bar{u}, \text{ and} \quad (3.44)$$

$$\phi_\pi^{CZ}(u, \mu) = 6u\bar{u} \left[1 + \frac{3a_2(\mu)}{2} \{5(u - \bar{u})^2 - 1\} \right] \quad (3.45)$$

where, $a_2(\mu)$ is defined in Eqn.(B.13) with $n = 2$, and μ being the renormalization scale.

The structure dependent parameter defined in Eq.(3.1), which provides the information about the structure of pion (see Section-3.1), is also calculated using both these forms for pion distribution amplitudes. The values of the various parameters used for the numerical computation are collected in Appendix-D. The form factors depend on the value of the Borel parameter, M , and hence also the structure dependent parameter, γ . Fig.(3.3) shows the variation of $F_A^{(\pi)}(0)$, $F_V^{(\pi)}(0)$ and SDP (γ) with the variation in the value of M . The variation of the observables with M dictates the model dependence here. As can be seen from the plot, all the observables are quite stable in the chosen Borel window. The value of γ for $M = 3.35$ GeV is 0.469 (using CZ distribution amplitude) which matches well, including the sign, with the experimental value of γ obtained from the radiative pion decay.

Further, we calculate all the contributions to the decay width for the radiative tau decay using $M = 3.35$ GeV and the FFs given in Eq.(3.42) and Eq.(3.43). The differential decay rate for the radiative tau decay is given by,

$$d\Gamma(\tau^- \rightarrow \pi^- \nu_\tau \gamma) = \frac{1}{512\pi^5} E_\tau \delta^{(4)}(k + p_2 + p_3 - p_1) \overline{|\mathcal{A}|^2} \frac{d^3k d^3p_2 d^3p_3}{E_\gamma E_\pi E_\nu} \quad (3.46)$$

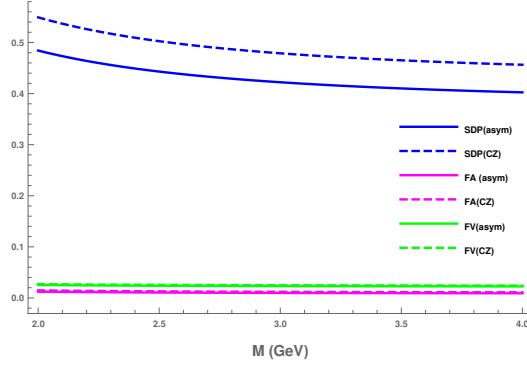


Figure 3.3: The dependence of structure dependent parameter (SDP), $F_A^{(\pi)}(0)$ and $F_V^{(\pi)}(0)$ on the Borel parameter M (in GeV units) is shown in Blue, Magenta and Green, respectively. In this plot, form factors have been multiplied by im_π to make them dimensionless in and take care of the extra $-i$ in the FFs as noted in the Footnote1.

where, $E_\tau, E_\pi, E_\gamma, E_\nu$ are the energies of tau-lepton, pion, photon and neutrino, respectively. $|\overline{\mathcal{A}}|^2$ is the spin averaged square of the amplitude which has been calculated in Section-3.2.

In terms of the functions used in Eq.(3.16),

$$|\overline{\mathcal{A}}|^2 = |\overline{\mathcal{A}_{IB}}|^2 + |\overline{\mathcal{A}_{SD}}|^2 + 2\mathcal{R}e\{\overline{\mathcal{A}_{IB}^* \mathcal{A}_{SD}}\} \quad (3.47)$$

where, $|\overline{\mathcal{A}_{SD}}|^2 = |\overline{\mathcal{A}_A}|^2 + |\overline{\mathcal{A}_V}|^2 + 2\mathcal{R}e\{\overline{\mathcal{A}_A^* \mathcal{A}_V}\}$.

The kinematical details to compute the decay rate can be found in Appendix-C.

The structure dependent contribution to the photon spectrum is shown in Fig.(3.4) using both forms of pion distribution amplitudes. The IB contribution suffers from infrared divergences which can be taken care of by putting a threshold on the photon energy. Fig.(3.5) shows the threshold energy dependence of the IB contribution as well as the full decay width of the radiative tau decay. The SD contribution is free from any kind of divergences.

$F_A^{(\pi)}(t)$ gets contribution from a_1 meson while $F_V^{(\pi)}(t)$ from ρ (and ω) meson. Fig.(3.6) shows the SD contribution to the invariant mass spectrum of $\pi - \gamma$ system. The higher and sharper peak corresponds to the contribution coming from the vector mesons while the shorter and broader peak corresponds to the axial vector contribution. The vector contribution to the total decay width dominates over the axial-vector contribution.

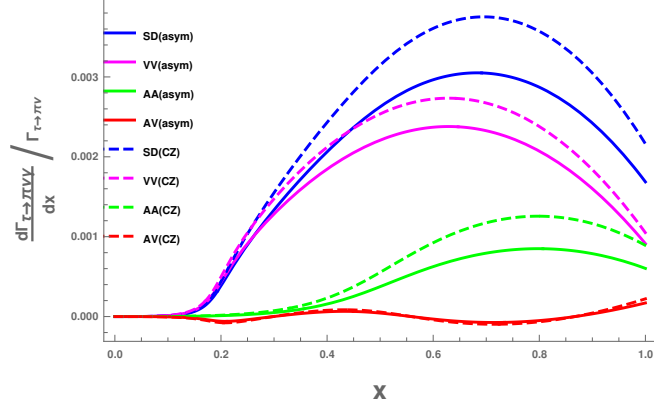


Figure 3.4: The total Structure Dependent Contribution (blue) to the photon spectrum is shown along with the individual contributions from the vector (magenta), axial vector (green) and the interference (red) of the two are also shown for the two distribution amplitudes. Solid lines are for asymptotic distribution amplitude while dashed ones are for Chernyak-Zitnisky distribution amplitude.

As ρ and a_1 -mesons are not very narrow, the effect of t dependence of the widths is also studied using the prescription provided in [93]. The t dependence of Γ_ρ does not have significant effect as it is not that wide while the effect of Γ_{a_1} is clearly visible as one can see from Fig.(3.7). The explicit forms of t dependence of the decay widths are provided in Eqn.(C.14) and Eqn.(C.15). We have also computed the effect of decay width of a_1 -meson Γ_{a_1} , as it has huge uncertainty, and found that the decay width of radiative tau decay decreases with an increase in Γ_{a_1} . The results reported here are calculated using $\Gamma_{a_1} = 425$ MeV.

Fig.(3.8) represents all the contributions to the invariant mass spectrum of the $\pi - \gamma$ system. The IB contribution dominates at the low photon energy for which we have used the minimum energy threshold of 50 MeV.

After integrating over the full phase space and applying an energy threshold of 50 MeV for the IB contribution, we get the numerical results for different contributions to the decay width (normalised to the non-radiative decay width Eq.(C.9) i.e. $\bar{\Gamma} = \Gamma(\tau \rightarrow \pi\nu_\tau\gamma)/\Gamma(\tau \rightarrow \pi\nu_\tau)$) as tabulated in Table-3.1.

Since we consider radiative rate normalised to the non-radiative one, the uncertainty in IB contribution is negligible compared to the SD contribution which dominates the error budget. Therefore, no uncertainty is shown for the IB part. The final uncertainties are about 10%. From the above it is evident that there is a dependence on the form of the distribution amplitude chosen to

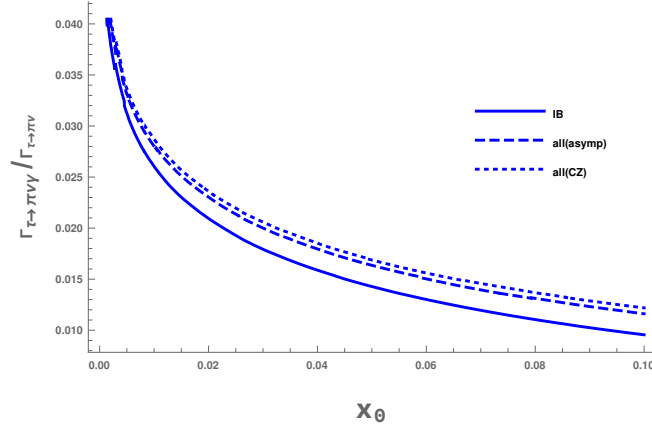


Figure 3.5: The dependence of the IB (solid) contribution on the minimum energy threshold of the photon is shown here. Along with that, the same dependence for total decay width including form factors using asymptotic (dashed) and CZ (dotted) pion distribution amplitude is also shown.

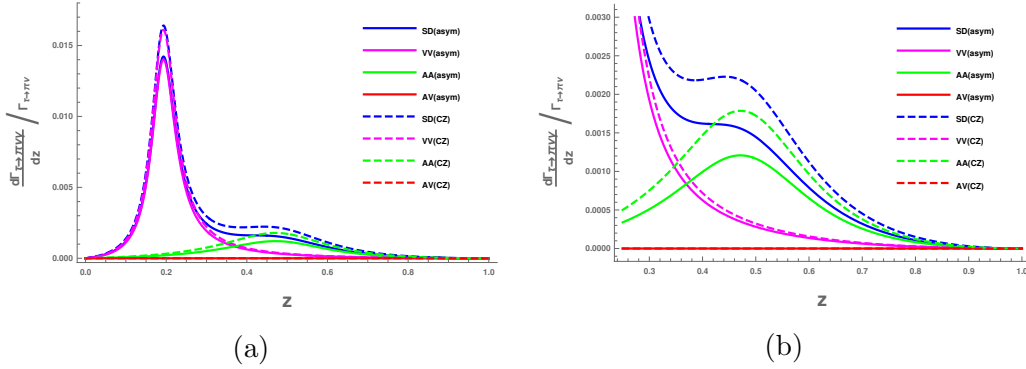


Figure 3.6: (a): The Structure Dependent contribution (blue) to the invariant mass spectrum of $\pi-\gamma$ system is shown here for asymptotic (solid) and Chernyak-Zhitnisky (dashed) pion distribution amplitudes. The contribution from the vector (magenta), axial vector (green) and the interference (red) of the two is also shown. (b): Zoomed in version of (a).

evaluate these form factors. However, the difference is not too large, which is reassuring.

Having obtained detailed predictions for the pion in the final state, it is also instructive to have an estimate of the decay width for the kaon in the final state. Again, normalising to the appropriate non-radiative width, and employing the asymptotic distribution amplitude (keeping the Borel parameter, $M = 3.35$ GeV), we get

$$\bar{\Gamma}^K = \Gamma(\tau \rightarrow K\nu\gamma)/\Gamma(\tau \rightarrow K\nu) \sim 8 \times 10^{-3} \quad (3.48)$$

This (appropriately normalised) rate is roughly half of that for the pion.

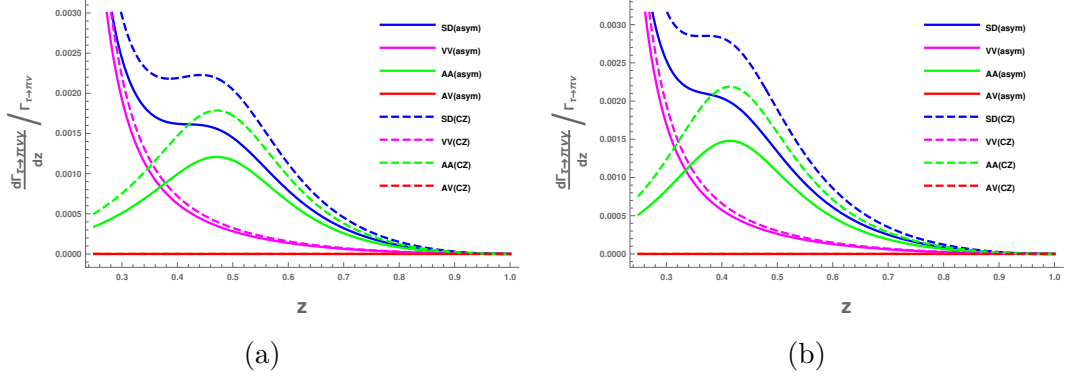


Figure 3.7: The SD contribution (blue) considering (a) Γ_ρ and Γ_{a_1} to be constant and (b) the t dependence of Γ_ρ and Γ_{a_1} is shown here for asymptotic (solid) and Chernyak-Zhitnisky (dashed) pion distribution amplitudes. The contribution from the vector (magenta), axial vector (green) and the interference (red) of the two is also shown.

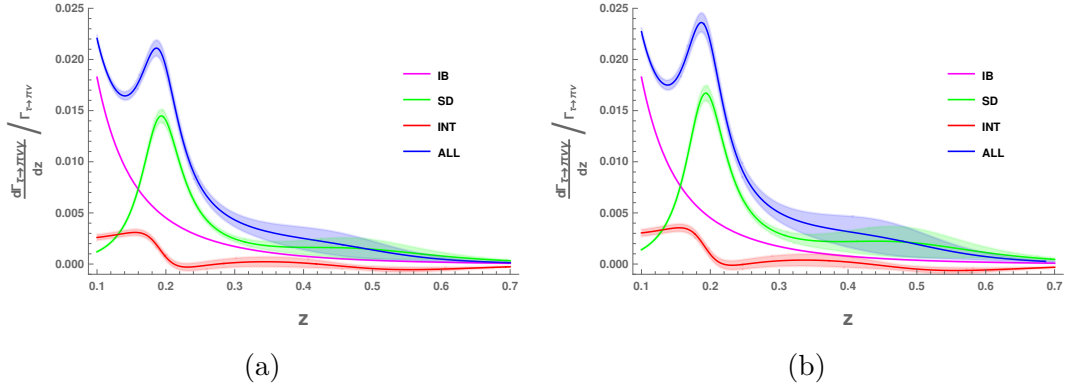


Figure 3.8: The invariant mass spectrum of $\pi - \gamma$ system for radiative tau decay is shown here considering (a) asymptotic and (b) CZ pion distribution amplitude. The contributions from the IB (magenta), SD (green) and the interference (red) of the two is also shown. The shaded region shows the uncertainties.

3.5 Discussion and Conclusions

In this chapter, we have provided detailed predictions for the rate and photon spectrum for the process $\tau^- \rightarrow \pi^- \nu_\tau \gamma$. Employing Ward identity from the beginning, the amplitude was written so as to include the contact term which is necessitated by gauge invariance. The decay involves two time like FFs. These have been calculated in the present work employing the Light Cone Sum Rules, to twist-2 accuracy. The FFs, which automatically via the dispersion relations, encode the contributions from the vector and axial-vector mesons, have the right asymptotic behaviour expected from perturbative QCD. The ratio of the axial-vector to vector form factor at zero momentum transfer defines the pion structure

Contribution	Value using ϕ_π^{asym}	Value using ϕ_π^{CZ}
$\bar{\Gamma}_{IB}$	1.36×10^{-2}	1.36×10^{-2}
$\bar{\Gamma}_{VV}$	$(1.47 \pm 0.06) \times 10^{-3}$	$(1.47 \pm 0.06) \times 10^{-3}$
$\bar{\Gamma}_{AA}$	$(3.97 \pm 2.45) \times 10^{-4}$	$(5.91 \pm 3.62) \times 10^{-4}$
$\bar{\Gamma}_{AV}$	~ 0	~ 0
$\bar{\Gamma}_{SD}$	$(1.87 \pm 0.30) \times 10^{-3}$	$(2.29 \pm 0.43) \times 10^{-3}$
$\bar{\Gamma}_{int}$	$(3.82 \pm 2.14) \times 10^{-4}$	$(4.90 \pm 2.60) \times 10^{-4}$
$\bar{\Gamma}_{all}$	$(1.56 \pm 0.04) \times 10^{-2}$	$(1.61 \pm 0.06) \times 10^{-2}$

Table 3.1: Tabulating the values obtained for different contribution of the normalised decay width (normalised to the non-radiative decay width i.e. $\bar{\Gamma} = \Gamma(\tau \rightarrow \pi\nu_\tau\gamma)/\Gamma(\tau \rightarrow \pi\nu_\tau)$) using the asymptotic DA (ϕ_π^{asym}) and the CZ DA (ϕ_π^{CZ}) of the pion.

dependent parameter, γ . Our evaluation of this parameter, along with the sign, matches very well with the experimental value obtained from $\pi \rightarrow \ell\nu\gamma$, where the relevant pion-photon FFs, unlike the present case, are space like. The obtained values for the normalised rate and the photon spectrum are similar to those obtained in [84] using Resonance χ PT. This provides a cross-check on the theoretical predictions employing a totally different method for computing the non-perturbative quantities. We have also provided an estimate for the appropriately normalised rate with kaon in the final state instead of a pion. This normalised rate is approximately half of that for the pion. The present study employed distribution amplitudes to twist-2 accuracy. The uncertainties reported here are the uncertainties associated with the uncertainties of the various parameters used. There will be further uncertainties associated with quark hadron duality approximation, and higher twist and high order contributions. The pion is considered to be massless here. The effect of such an assumption is less than 1% on the values of the FFs. The uncertainties associated with quark hadron duality violation, like in inclusive tau decays are expected to be at 10% level, and can be calculated in a particular model to parametrise the spectral density.

Precise calculations of these duality violations is indeed an important missing piece but is out of the scope of present work. It would be interesting to consider both higher twist contributions as well as contributions that are higher order in α_s . These can have a significant impact on the phenomenology of radiative one meson tau decays.

Chapter 4

Exploring LCSR application to proton decay

After discussing the application of LCSR to the light meson system in the previous chapter, we now move to the case of a light baryon system like proton. Proton is the lightest baryon with mass $m_p = 0.938$ GeV [35]. To explain the matter-anti-matter asymmetry of the Universe, Sakharov proposed three conditions in 1967 [94]. One of these conditions is the requirement of Baryon Number Violation (BNV). Within the SM of particle physics, baryon number is a conserved quantity. Therefore, the matter-antimatter asymmetry can not be explained within the SM and hence BSM physics is required. In the BSM scenarios where BNV is possible, proton is allowed to decay (see below). Consequently, proton decay is one of the most important signatures for BSM physics.

In this chapter, we will discuss the decay of proton to a positron and a photon, i.e. $p \rightarrow e^+\gamma$. As we will see, this process involves two independent physical form factors. We discuss these FFs in the framework of light cone sum rules. Within this framework, there exist two possibilities to calculate these FFs. First, by considering the correlation function by interpolating the proton state and using the photon distribution amplitudes. Second, where the correlation function is obtained by interpolation of the photon state with the electromagnetic current and the proton DAs are used. In this chapter, we will discuss both these approaches to calculate these FFs one by one and will discuss the numerical results

in both the scenarios. This chapter is based on the study presented in [95].

4.1 Introduction

As discussed in Chapter-1, the SM of particle physics is the most successful model which explains the electromagnetic, weak, and strong interactions among the fundamental particles, but, fails in explaining various phenomena. The matter-antimatter asymmetry of the Universe is one such phenomena and motivates us towards the study beyond the SM. As, in 1967, Sakharov proposed three conditions to explain this matter-antimatter asymmetry which are: 1) the baryon number violation, 2) the violation of C and CP symmetries, where C represents the charge and P represents the parity, and 3) Out of thermal equilibrium [94]. The baryon number is a conserved quantity within the SM as a consequence of the accidental symmetry of the SM. However, baryon number violation is well motivated at the perturbative level in the theories of grand unification (GUTs), SuperSymmetry (SUSY), various models of baryogenesis, model building in string theory and in the extra dimension theories, etc. (see for example [96]–[106] and references therein).

Therefore, in order to probe these BSM models, BNV processes can play a very important role. Proton decay is one such process. The proton being the lightest baryon is a stable particle in the SM. However, these BSM scenarios motivate the decay of proton which makes this decay one of the very crucial tests for these BSM scenarios and also an important window to understand the nature of matter unification. Any signature of it will be a clear indication towards physics beyond the SM as it is forbidden in the SM.

In GUTs, quarks and leptons fall in the common multiplets. Therefore, in such theories, proton decay is possible even at the tree level via the exchange of super-heavy gauge bosons or scalar and/or vector leptoquarks. By integrating out these heavy particles, one can then write effective baryon and lepton number violating operators of dim-6 such that they are consistent with the SM gauge symmetry. Instead of baryon (B) or lepton (L) number conservation, these operators are found to conserve (B-L). As a result, proton always decay into an antilep-

ton (or antineutrino) (see [107]–[110] for reviews on proton decays). In several GUT models, the most favourable channel for the decay of proton is found to be $p \rightarrow e^+\pi^0$. To compute the decay width for this process, or any process involving hadron, one requires an input on the non-perturbative FFs (as discussed in Section-1.3). The FFs involved in this decay have been studied using various models of QCD, such as relativistic quark model, QCD sum rules, effective chiral theory, lattice QCD, [111]–[117]. In a very recent study [118], these FFs are studied using the method of LCSR.

There are various experiments like Kolar Gold Field [119], NUSEX [120], SOUDAN [121], Kamiokande [122], etc., which have been designed detect proton decay. Presently, the largest proton water Cherenkov detector, known as the Super-Kamiokande detector is the most sensitive detector for proton decay searches. It puts the most stringent lower bounds on the partial life time for the proton decays, $p \rightarrow e^+\pi^0$ given by $\tau_p > 10^{34}$ years [123]. With the advances in experimental techniques, it becomes important to consider other decay channels including the radiative decay modes. The present lower bound for the radiative proton decay modes $p \rightarrow e^+\gamma$ and $p \rightarrow \mu^+\gamma$ are $\tau_p > 6.7 \times 10^{32}$ years and $\tau_p > 4.8 \times 10^{32}$ years, respectively [35]. Theoretically, these modes are expected to be suppressed by α_{em} . In [124], $p \rightarrow e^+\gamma$ was studied within SU(5) GUT set up. It was pointed out there that this might be an experimentally more feasible channel as there will be less nuclear absorption. The form factors involved in this process were evaluated with a simple harmonic oscillator potential as a model for binding the quarks inside the proton. In [125], it was studied in the framework of bag model and the conclusions were made that this decay mode is not feasible at experiments due to small decay rate. However, the experimental facilities are advancing over the time (see [126] for a review of different experiments and expected sensitivities expected at future experiments). Thus, a reanalysis of this mode becomes important, including a fresh attempt at evaluation of the form factors in a consistent way.

In the Water-Cherenkov experiments, such as Super-Kamiokande, the decay products of the proton are measured approximately at rest which makes the relevant energy scale for the process to be the proton mass (see [127] for a review

on Super-Kamiokande). At these energy scales, a perturbative description for the hadronic transitions is not possible in QCD because of color confinement and an alternative non-perturbative way is required to get an estimate of the HMEs which can help us in probing the baryon-number violating physics with the help of experimental data (as discussed in Chapter-2). Therefore, in this chapter, we will discuss the use of LCSR to study $p \rightarrow e^+\gamma$.

The rest of the chapter will discuss the computation of the form factors involved in this process using LCSR framework. We will first discuss the amplitude of this process using dim-6 effective operators and see how this amplitude can be written in terms of two independent form factors. Then we will discuss two different possibilities to compute these FFs using LCSR. Later, we will provide numerical analysis for the FFs obtained using both the possibilities. Finally, we will conclude our findings with a naive comparison between the results obtained using the two possibilities.

4.2 Amplitude Computation

As already discussed, proton decay is a baryon number violating process and hence is forbidden in the SM. However, it is possible to write higher dimensional baryon number violating effective operators that allow the decay of proton. In a BSM scenario, like GUTs, proton decay is possible even at tree level. This process proceeds via an exchange of heavy gauge bosons or leptoquarks. To write the effective operators, one can then integrate out these heavy particles (as discussed in Section-1.5). The Lagrangian corresponding to the dim-6 baryon number violating effective operators which preserves the gauge symmetry of the SM can be written as [128]–[131]

$$\mathcal{L}_B^{(6)} = \sum_{\Gamma, \Gamma'} c_{\Gamma\Gamma'} \mathcal{O}_{\Gamma\Gamma'} = \sum_{\Gamma, \Gamma'} c_{\Gamma\Gamma'} \epsilon^{abc} (\bar{d}_a^c P_\Gamma u_b) (\bar{e}^c P_{\Gamma'} u_c) \quad (4.1)$$

where $\{\Gamma, \Gamma'\} \in \{L, R\}$ are the chirality projection operators. $c_{\Gamma\Gamma'}$ are the Wilson coefficients. The superscript c denotes charge conjugation such that $\bar{d}^c = -d^T C^{-1}$ with $C = i\gamma^2\gamma^0$ being the charge conjugation operator and T in

the superscript denotes the transpose. The indices a, b, c represent the color indices. This effective Lagrangian is written in terms of the physical states of the quarks and leptons at the relevant scale which means that all the flavour mixing and perturbative renormalization group (RG) effects, along with the short distance information, are collectively lumped in the WCs $c_{\Gamma'}$. As this chapter is mainly focused on the evaluation of the form factors involved which are defined below, the exact details of these effects are not of particular relevance here. Thus, we do not discuss about them further. These dependencies must be straightforwardly expressed in a concrete model which allows proton decay.

Having the interaction Lagrangian in hand (Eqn.(4.1)), the transition amplitude for the radiative proton decay $p \rightarrow e^+ + \gamma$ can be written as the matrix element given by

$$\begin{aligned} \mathcal{A}(p(p_p) \rightarrow e^+(p_e)\gamma(k)) &= \sum_{\Gamma'} c_{\Gamma'} \langle e^+(p_e)\gamma(k) | \mathcal{O}_{\Gamma'} | p(p_p) \rangle \\ &= \sum_{\Gamma'} c_{\Gamma'} \langle e^+(p_e)\gamma(k) | \epsilon^{abc} (\bar{d}_a^c P_{\Gamma} u_b) (\bar{e}^c P_{\Gamma'} u_c) | p(p_p) \rangle \end{aligned} \quad (4.2)$$

with all the flavor effects being absorbed in the WCs, $c_{\Gamma'}$ (as discussed above). The condition that this transition amplitude must be gauge invariant, allows us to parameterize it as

$$\mathcal{A}(p(p_p) \rightarrow e^+(p_e)\gamma(k)) = \sum_{\Gamma'} c_{\Gamma'} \bar{v}_e^c P_{\Gamma'} \left\{ \epsilon_{\alpha^*} A_{\Gamma'} \frac{i\sigma^{\alpha\beta} k_{\beta}}{m_p} \right\} u_p(p_p). \quad (4.3)$$

where $A_{\Gamma'}$ are the four non-perturbative gauge invariant physical form factors involved in the process. Furthermore, due to parity conservation in QCD, these physical FFs get related among themselves as

$$A_{LL} = -A_{RR} \quad A_{LR} = -A_{RL}, \quad (4.4)$$

resulting in only two independent form factors. For the present discussion, let us choose them to be A_{LL} and A_{LR} . Therefore, in order to have a prediction about the branching ratio, the knowledge of these FFs is the only hurdle. All

other factors in the amplitude given in Eqn.(4.3) are known once we choose a particular model which leads to proton decay. We focus on the computation of these FFs here.

As both proton and positron are charged, the photon can be emitted from either of them. The computation of photon emission from positron is trivial. We do not explicitly show it here as it does not contribute to the dipole transition depicted above. However, the photon emission from proton is non-trivial and contributes to the form factors. The photon can now be emitted from either of the u-quarks or the d-quark and thus, can be helpful in understanding the dynamics of strong interaction inside the proton. The transition matrix element for the photon emission from proton can be factorised into the leptonic and hadronic parts as

$$\langle e^+(p_e)\gamma(k) | \mathcal{O}_{\Gamma\Gamma'} | p(p_p) \rangle = \bar{v}_e^c(p_e) H_{\Gamma\Gamma'}(p_P, p_e) u_p(p_p). \quad (4.5)$$

where $H_{\Gamma\Gamma'}(p_P, p_e) u_p(p_p)$ is the hadronic matrix element (HME) of interest and is given by

$$H_{\Gamma\Gamma'}(p_P, p_e) u_p(p_p) = \langle \gamma(k) | \epsilon^{abc} (d_a^T C P_\Gamma u_b) (P_{\Gamma'} u_c) | p(p_p) \rangle. \quad (4.6)$$

This HME can be most generally parameterized in terms of six invariant scalar functions $F_{\Gamma\Gamma'}^n$, with $n = 1, \dots, 6$ (see [132]) as

$$\begin{aligned} H_{\Gamma\Gamma'}(p_P, p_e) u_p(p_p) = P_{\Gamma'} \epsilon_\mu^* \left[F_{\Gamma\Gamma'}^1 \frac{\not{k} p_p^\mu}{m_p^2} + F_{\Gamma\Gamma'}^2 \frac{\not{k} k^\mu}{m_p^2} + F_{\Gamma\Gamma'}^3 \gamma^\mu + i F_{\Gamma\Gamma'}^4 \frac{\sigma^{\mu\nu} k_\nu}{m_p} \right. \\ \left. + F_{\Gamma\Gamma'}^5 \frac{p_p^\mu}{m_p} + F_{\Gamma\Gamma'}^6 \frac{k^\mu}{m_p} \right] u_p(p_p) \end{aligned} \quad (4.7)$$

where $\sigma^{\mu\nu} = \frac{i}{2}[\gamma^\mu, \gamma^\nu]$. Neglecting the mass of positron, the physical form factors ($A_{\Gamma\Gamma'}$) can then be related to these invariant scalar functions, $F_{\Gamma\Gamma'}^n$, as

$$A_{\Gamma\Gamma'} = \frac{F_{\Gamma\Gamma'}^1}{2} + F_{\Gamma\Gamma'}^4 + \frac{F_{\Gamma\Gamma'}^5}{2}. \quad (4.8)$$

Let us now discuss how to get these form factors using the method of LCSR.

4.3 Form Factors in the LCSR framework

As discussed in Chapter-2, in order to calculate form factor in LCSR framework, we need a correlation function of quark-gluon operators between a vacuum and a hadronic state as a starting object. In the present case, such a correlation function can be obtained from the HME given in Eq.(4.6) by interpolating either the proton or the photon state. Consequently, there are two possibilities to calculate the form factors, $A_{\Gamma\Gamma'}$ defined in Eqn.(4.8) within the framework of LCSR:

1. Interpolating the proton state with proton interpolation current and using the distribution amplitudes (DAs) of photon.
2. Interpolating the photon state with the electromagnetic current and using the distribution amplitudes (DAs) for proton.

Hereafter, in this chapter, we will discuss both these scenarios one by one with the aim that we can finally make some comparison between the outcomes of the two which can be helpful in getting a deeper understanding of the underlying non-perturbative dynamics due to strong interaction.

4.3.1 Case-1: Using proton interpolation and photon DAs

To find the relevant correlation function in this case, first of all we need an interpolation current for proton state. Such an interpolation current is not uniquely defined. Therefore, it is interesting to discuss a little about the interpolation current for proton before jumping to the calculation of the form factors.

4.3.1.1 Proton interpolation current

While writing an interpolation current, two things are required to be kept in mind. First, the interpolation current must have the quark-constituent of the state. Second, it must satisfy all the quantum numbers of the state. There are two operators which can satisfy both these criteria for a proton [133], [134].

These operators are

$$\chi_1(x) = \epsilon^{lmn} (u_l^T(x) C \gamma_5 d_m(x)) u_n(x), \quad \chi_2(x) = \epsilon^{lmn} (u_l^T(x) C d_m(x)) \gamma_5 u_n(x) \quad (4.9)$$

where, $\{l, m, n\}$ represents the color indices, the superscript T represents the transpose and C is the charge conjugation matrix. Both these operators can be used to excite a ground state proton from the vacuum.

Moreover, a linear combination of both these operators will also excite a ground state proton from the vacuum. Therefore, in general, the proton interpolation current can be written as

$$\chi_t(x) = \chi_1(x) + t\chi_2(x) \quad (4.10)$$

where, t is a general parameter and can take any value from the set of real numbers. It is defined such that

$$\langle 0 | \chi_t(0) | p(p_p) \rangle = m_p \lambda_p^t u_p(p_p) \quad (4.11)$$

where m_p is the mass of proton, λ_p^t is the interaction strength of this interpolation current with the proton state, and $u_p(p_p)$ represents the spinor for the proton state having momentum p_p .

In literature, the most commonly used linear combinations are

$$\chi_{LA}(x) = \chi_1(x), \text{ and} \quad (4.12)$$

$$\chi_{IO}(x) = 2(\chi_2(x) - \chi_1(x)). \quad (4.13)$$

The former can be obtained from Eqn.(4.10) by simply putting $t = 0$ and is the most commonly used form for proton interpolation in lattice QCD calculations $\langle 0 | \chi_{LA} | p(p_p) \rangle = m_p \lambda_{p2} u_p(p_p)$. The latter can be obtained as $\chi_{IO}(x) = -2\chi_t(x)$ with $t = -1$. Using the Fierz transformation (discussed in Appendix-A), it can

be rewritten as

$$\chi_{IO}(x) = \epsilon^{lmn} (u^{Tl}(x) C \gamma_\mu u^m(x)) \gamma_5 \gamma^\mu d^n(x) \quad (4.14)$$

This is popularly known as the Ioffe current [133]. It is defined such that

$$\langle 0 | \chi_{IO}(0) | p(p_p) \rangle = m_p \lambda_p u_p(p_p), \quad (4.15)$$

where λ_p is the interaction strength of the Ioffe current with the proton state. In literature, this current is found to provide the maximum stability against the Borel mass, the parameter introduced in LCSR computations [70].

There is another linear combination which has been found to be used in sum rule calculations given by

$$\begin{aligned} \chi'(x) &= 2(\chi_2 + \chi_1) \\ &= \frac{1}{2} \epsilon^{abc} (u^{Ta}(x) C \sigma_{\mu\nu} u^b(x)) \sigma^{\mu\nu} \gamma_5 d^c(x) \end{aligned} \quad (4.16)$$

such that,

$$\langle 0 | \chi_A(0) | p(p_p) \rangle = m_p \lambda'_p u_p(p_p) \quad (4.17)$$

It can be obtained from the general form in Eqn.(4.10) by putting $t=1$ and multiplying the r.h.s. by a factor of 2.

Now, after having an understanding of the proton interpolation current, we move back to our discussion on the form factor calculation using LCSR. For the further discussion we will use the Ioffe current given in Eqn.(4.14) for proton interpolation and will call it simply $\chi(x)$ instead of χ_{IO} for notational simplicity. The correlation function which is obtained after interpolating the proton state in Eqn.(4.6) using Ioffe current reads as

$$\Pi_{\Gamma\Gamma'}(p_p, p_e) = i \int d^4x e^{ip_e \cdot x} \langle \gamma(k) | T \{ Q_{\Gamma\Gamma'}(x) \bar{\chi}(0) \} | 0 \rangle \quad (4.18)$$

where $\bar{\chi}(0) \equiv \chi^\dagger(0) \gamma^0$, $Q_{\Gamma\Gamma'}(x) = \epsilon^{abc} (d_a^T C P_\Gamma u_b) (P_{\Gamma'} u_c)$ and T denotes the time

ordering.

By inserting a complete set of intermediate hadronic states with the same quantum number as the proton and isolating the pole contribution coming from the ground state proton, one gets a hadronic parameterization for this correlation function as

$$\begin{aligned}
\Pi_{\Gamma\Gamma'}^{had}(p_p, p_e) &= -\frac{m_p \lambda_p}{p_p^2 - m_p^2} H_{\Gamma\Gamma'}(p_e, p_p) (\not{p}_p + m_p) + \dots \\
&= \epsilon_\mu^* P_{\Gamma'} \left[\Pi_{\Gamma\Gamma'}^{had,PK} \frac{\not{k} p_p^\mu}{m_p^2} + \Pi_{\Gamma\Gamma'}^{had,KK} \frac{\not{k} k^\mu}{m_p^2} + \Pi_{\Gamma\Gamma'}^{had,V} \gamma^\mu + \Pi_{\Gamma\Gamma'}^{had,T} \frac{i\sigma^{\mu\nu} k_\nu}{m_p} \right. \\
&\quad + \Pi_{\Gamma\Gamma'}^{had,P} \frac{p_p^\mu}{m_p} + \Pi_{\Gamma\Gamma'}^{had,K} \frac{k^\mu}{m_p} + \Pi_{\Gamma\Gamma'}^{had,KPP} \frac{\not{k} p_p^\mu \not{p}_p}{m_p^3} + \Pi_{\Gamma\Gamma'}^{had,KKP} \frac{k^\mu \not{k} \not{p}_p}{m_p^3} \\
&\quad \left. + \Pi_{\Gamma\Gamma'}^{had,VP} \frac{\gamma^\mu \not{p}_p}{m_p} + \Pi_{\Gamma\Gamma'}^{had,TP} \frac{i\sigma^{\mu\nu} k_\nu \not{p}_p}{m_p^2} + \Pi_{\Gamma\Gamma'}^{had,PP} \frac{\not{p}_p p_p^\mu}{m_p^2} + \Pi_{\Gamma\Gamma'}^{had,KP} \frac{k^\mu \not{p}_p}{m_p^2} \right]
\end{aligned} \tag{4.19}$$

where ellipses represent the heavier states i.e. excited states and continuum, contributions. The twelve invariant scalar functions, $\Pi_{\Gamma\Gamma'}^{had,r}$ with $r = \{PK, KK, V, T, P, K, KPP, KKP, VP, TP, PP, KP\}$, will be used to derive the physical FFs A_{LL} and A_{LR} by deriving sum rules for them (see below).

As a first step to write sum rules for these scalar function, we parameterize them in terms of spectral densities using the dispersion relation given by

$$\Pi_{\Gamma\Gamma'}^{had,r}(p_p^2, P_e^2) = \int_0^\infty ds \frac{\rho_{\Gamma\Gamma'}^{had,r}(s, P_e^2)}{s - p_p^2}. \tag{4.20}$$

where $P_e^2 = -p_e^2$, and $\rho_{\Gamma\Gamma'}^{had,r}(s, P_e^2)$ are the spectral densities and are related to the imaginary part of these scalar functions as

$$\rho_{\Gamma\Gamma'}^{had,r}(s, P_e^2) = \frac{1}{\pi} \text{Im} \Pi_{\Gamma\Gamma'}^{had,r}(s + i\epsilon, P_e^2). \tag{4.21}$$

These spectral densities can be written by separating the pole contribution and the heavy states contributions as

$$\rho_{\Gamma\Gamma'}^{had,r}(s, P_e^2) = \lambda_p m_p^2 \delta(s - m_p^2) F_{\Gamma\Gamma'}^r(s, P_e^2) + \rho_{\Gamma\Gamma'}^{heavy,r}(s, P_e^2) \tag{4.22}$$

where $F_{\Gamma\Gamma'}^r(s, P_e^2)$ are the residues of the ground state contributions. These can be related to $F_{\Gamma\Gamma'}^n(s, P_e^2)$ (Eqn.(4.7)) for $s = m_p^2$ i.e proton being on-shell, the condition ensured by the delta function. These relations reads as,

$$\begin{aligned}
F_{\Gamma\Gamma'}^{PK}(s, P_e^2) &= F_{\Gamma\Gamma'}^{KPP}(s, P_e^2) = F_{\Gamma\Gamma'}^1(s, P_e^2), \\
F_{\Gamma\Gamma'}^{KK}(s, P_e^2) &= F_{\Gamma\Gamma'}^{KKP}(s, P_e^2) = F_{\Gamma\Gamma'}^2(s, P_e^2), \\
F_{\Gamma\Gamma'}^V(s, P_e^2) &= F_{\Gamma\Gamma'}^{VP}(s, P_e^2) = F_{\Gamma\Gamma'}^3(s, P_e^2), \\
F_{\Gamma\Gamma'}^T(s, P_e^2) &= F_{\Gamma\Gamma'}^{TP}(s, P_e^2) = F_{\Gamma\Gamma'}^4(s, P_e^2), \\
F_{\Gamma\Gamma'}^P(s, P_e^2) &= F_{\Gamma\Gamma'}^{PP}(s, P_e^2) = F_{\Gamma\Gamma'}^5(s, P_e^2), \\
F_{\Gamma\Gamma'}^K(s, P_e^2) &= F_{\Gamma\Gamma'}^{KP}(s, P_e^2) = F_{\Gamma\Gamma'}^6(s, P_e^2).
\end{aligned} \tag{4.23}$$

According to the quark-hadron duality, the spectral densities of the heavier states, $\rho_{\Gamma\Gamma'}^{heavy,r}(s, P_e^2)$, can be approximated to the spectral densities computed using QCD (see Section-2.1.1) as

$$\int_{s_0}^{\infty} ds \frac{\rho_{\Gamma\Gamma'}^{heavy,r}(s, P_e^2)}{s - p_p^2} \approx \int_{s_0}^{\infty} ds \frac{\rho_{\Gamma\Gamma'}^{QCD,r}(s, P_e^2)}{s - p_p^2} = \int_{s_0}^{\infty} ds \frac{1}{\pi} \frac{\text{Im}(\Pi_{\Gamma\Gamma'}^{QCD,r}(s, P_e^2))}{s - p_p^2} \tag{4.24}$$

where s_0 is the continuum threshold, a free parameter in sum rule calculation. It is expected to be chosen such that it is well above the ground state proton state but close to the lightest excitation state, which is the Roper resonance with mass of 1.44 GeV for the present case. Therefore, s_0 will be chosen in the vicinity of $(1.44 \text{ GeV})^2$ (see below).

Consequently, according to Eqn.(4.24), in order to compute the contribution of the heavier states, we need the evaluation of the correlation functions $\Pi_{\Gamma\Gamma'}^r(s, P_e^2)$ in QCD. For that we need the time ordered product in Eqn.(4.18) which can be computed by partially contracting the quark fields and by employing the completeness relation given by

$$q(x)\bar{q}(0) = \frac{-1}{4} (\bar{q}(0)\Gamma_A q(x)) \Gamma^A. \tag{4.25}$$

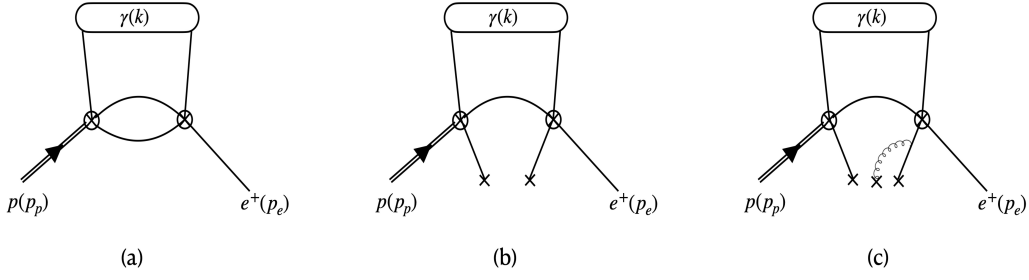


Figure 4.1: Feynman diagrams which contribute to the light-cone expansion of the hadronic matrix element for proton decay to positron and a photon up to two particle twist-2 and twist-3 contributions. The vertex on the left represents the proton interpolations current while the vertex on the right represents the dim-6 BNV operator. The encircled photon represents that the photon distribution amplitudes are entering the LCSR computation. (a) represents the the usual non-condensate contribution while (b) and (c) represent the condensates contributions as discussed in the text.

Here, $q = \{u, d\}$ and Γ_A represents the basis of gamma matrices chosen to be

$$\Gamma_A = \left\{ 1, \gamma_5, \gamma^\rho, i\gamma_\rho\gamma_5, \frac{1}{\sqrt{2}}\sigma^{\rho\sigma} \right\}. \quad (4.26)$$

Using these relations and partially contracting the quark fields, the time ordered product in Eqn.(4.18) simplifies to (see Fig. (4.1))

$$\begin{aligned} T \{Q_{\Gamma\Gamma'}(x)\bar{\chi}(0)\} = & -\frac{1}{2}\epsilon^{lmn}\epsilon^{ijk}P_{\Gamma'} \left[(\bar{u}_l(0)\Gamma_A u_i(x)) \left\{ \Gamma_A \gamma_\mu \tilde{S}_{jm}^{(u)}(x) P_\Gamma S_{nk}^{(d)}(x) \gamma^\mu \gamma_5 \right. \right. \\ & + \left. \left. S_{jm}^{(u)}(x) \gamma_\mu \tilde{\Gamma}_A P_\Gamma S_{nk}^{(d)}(x) \gamma^\mu \gamma_5 \right\} \right. \\ & \left. + (\bar{d}_l(0)\Gamma_A d_i(x)) \left\{ S_{kn}^{(u)}(x) \gamma_\mu \tilde{S}_{jm}^{(u)}(x) P_\Gamma \Gamma_A \gamma^\mu \gamma_5 \right\} \right]. \end{aligned} \quad (4.27)$$

where $S^{ij}(x)$ is the quark propagator at the light like separations, and

$$\tilde{\Gamma}_A = C\Gamma_A^T C^{-1} = \eta_i \Gamma_A \quad (4.28)$$

with

$$\eta_i = \begin{cases} 1, & \Gamma_A = 1, i\gamma_5, \gamma_\mu \gamma_5 \\ -1, & \Gamma_A = \gamma_\mu, \sigma_{\mu\nu} \end{cases}. \quad (4.29)$$

In the massless limit, $S^{ij}(x)$ is given by (see Appendix-B for details)

$$S_{ij}(x) = \frac{i\not{x}}{2\pi^2 x^4} \delta_{ij} - \frac{\langle \bar{q}q \rangle}{12} \delta_{ij} \left(1 + \frac{m_0^2 x^2}{16} \right) + \dots \quad (4.30)$$

where $\langle \bar{q}q \rangle$ represents the quark condensate, and ellipses denote higher terms including one or more gluon exchanges. We will neglect these higher terms for the present discussion. m_0 is a parameter associated with the mixed condensate as

$$\langle \bar{q}g_s G \cdot \sigma q \rangle = m_0^2 \langle \bar{q}q \rangle \quad (4.31)$$

where $G \cdot \sigma = G_{\mu\nu} \sigma^{\mu\nu}$. Substituting Eqn.(4.27) back in Eqn.(4.18) and rearranging the terms, we end up having a matrix element of two or more particle (quarks and gluons) operators between a vacuum and a photon state. These matrix elements can then be written in terms of photon light cone distribution amplitudes (DAs) of varying twist [71]. The present discussion involves only two particle DAs of twist-2 and twist-3. The effects coming from the higher twist DAs (expected to be small) are out of scope of this thesis.

At this point, it is important to note that at twist-2 there exist only one DA for photon labelled as $\phi_\gamma(u)$. It appears in the matrix element of two quark operator with $\Gamma_A = \frac{1}{\sqrt{2}} \sigma^{\rho\sigma}$. Moreover, at twist-3, there are two two-particle DAs labelled as $\psi^v(u)$, and $\psi^a(u)$ and appears for $\Gamma_A = \{\gamma_\rho, i\gamma_\rho \gamma_5\}$. Therefore, in the present discussion, three DAs of photon will contribute namely, $\phi_\gamma(u)$, $\psi^v(u)$, and $\psi^a(u)$ (see Appendix-B for more details about these DAs). On using the definition of these DAs, and summing up all the contributions, the correlation function in Eqn.(4.18) can be finally computed in QCD as

$$\begin{aligned} \Pi_{\Gamma\Gamma'}^{QCD}(p_p, p_e) = \epsilon_\mu^* P_{\Gamma'} \left[\Pi_{\Gamma\Gamma'}^{QCD,PK} \frac{\not{k} p_p^\mu}{m_p^2} + \Pi_{\Gamma\Gamma'}^{QCD,KK} \frac{\not{k} k^\mu}{m_p^2} + \Pi_{\Gamma\Gamma'}^{QCD,V} \gamma^\mu + \Pi_{\Gamma\Gamma'}^{QCD,T} \frac{i\sigma^{\mu\nu} k_\nu}{m_p} \right. \\ + \Pi_{\Gamma\Gamma'}^{QCD,P} \frac{p_p^\mu}{m_p} + \Pi_{\Gamma\Gamma'}^{QCD,K} \frac{k^\mu}{m_p} + \Pi_{\Gamma\Gamma'}^{QCD,KPP} \frac{\not{k} p_p^\mu \not{p}_p}{m_p^3} + \Pi_{\Gamma\Gamma'}^{QCD,KKP} \frac{k^\mu \not{k} \not{p}_p}{m_p^3} \\ \left. + \Pi_{\Gamma\Gamma'}^{QCD,VP} \frac{\gamma^\mu \not{p}_p}{m_p} + \Pi_{\Gamma\Gamma'}^{QCD,TP} \frac{i\sigma^{\mu\nu} k_\nu \not{p}_p}{m_p^2} + \Pi_{\Gamma\Gamma'}^{QCD,PP} \frac{\not{p}_p p_p^\mu}{m_p^2} + \Pi_{\Gamma\Gamma'}^{QCD,KP} \frac{k^\mu \not{p}_p}{m_p^2} \right] \quad (4.32) \end{aligned}$$

where $\Pi_{\Gamma\Gamma'}^{QCD,r}$ with $r = \{PK, KK, V, T, P, K, KPP, KKP, VP, TP, PP, KP\}$, are the QCD analogues of the scalar functions introduced in Eqn.(4.19). The full analytic expressions for these functions in QCD are:

- For $\Gamma = \Gamma' = L$:

$$\Pi_{LL}^{QCD, KK}(p_e, p_p) = -\frac{em_p^2 \langle \bar{q}q \rangle^2 \chi}{6} (Q_u - Q_d) \int_0^1 du \left[\frac{\phi_\gamma(u)}{P^2} \left(1 + \frac{m_0^2}{4P^2} \right) \right] \quad (4.33)$$

$$\Pi_{LL}^{QCD, V}(p_e, p_p) = \frac{e \langle \bar{q}q \rangle^2 \chi}{6} (Q_u - Q_d) \int_0^1 du \left[uk^2 \frac{\phi_\gamma(u)}{P^2} \left(1 + \frac{m_0^2}{4P^2} \right) \right] \quad (4.34)$$

$$\begin{aligned} \Pi_{LL}^{QCD, T}(p_e, p_p) = & -em_p \langle \bar{q}q \rangle \int_0^1 du \left[\frac{3Q_u \chi}{16\pi^2} \phi_\gamma(u) P^2 \ln(-P^2) + \frac{f_{3\gamma}(Q_u - Q_d)}{6} \right. \\ & \times \left\{ \frac{1}{P^2} \left(1 + \frac{m_0^2}{4P^2} \right) \left(u\psi^{(v)}(u) - \frac{\bar{\psi}^{(v)}(u)}{2} \right) \right. \\ & \left. \left. + \frac{\psi^a(u)}{2P^4} \left(1 + \frac{m_0^2}{2P^2} \right) (uk \cdot p_p - p_p^2) \right\} \right] \quad (4.35) \end{aligned}$$

$$\Pi_{LL}^{QCD, P}(p_e, p_p) = \frac{em_p f_{3\gamma} \langle \bar{q}q \rangle}{12} (Q_u - Q_d) \int_0^1 du \frac{uk^2 (2\bar{\psi}^v(u) + \psi^a(u))}{P^4} \left(1 + \frac{m_0^2}{2P^2} \right) \quad (4.36)$$

$$\begin{aligned} \Pi_{LL}^{QCD, K}(p_e, p_p) = & \frac{em_p f_{3\gamma} \langle \bar{q}q \rangle}{6} (Q_u - Q_d) \int_0^1 du \left[\frac{1}{P^2} \left(1 + \frac{m_0^2}{4P^2} \left(u\psi^v(u) + \frac{\bar{\psi}^v(u)}{2} \right) \right) \right. \\ & \left. - (uk^2 \bar{\psi}^v(u) + u(p_p \cdot k) \psi^a(u)) \frac{1}{P^4} \left(1 + \frac{m_0^2}{2P^2} \right) \right] \quad (4.37) \end{aligned}$$

$$\Pi_{LL}^{QCD, KPP}(p_e, p_p) = -\frac{em_p^3 f_{3\gamma} \langle \bar{q}q \rangle}{12} (Q_u - Q_d) \int_0^1 du \frac{2\bar{\psi}^v(u) + \psi^a(u)}{P^4} \left(1 + \frac{m_0^2}{2P^2} \right) \quad (4.38)$$

$$\Pi_{LL}^{QCD,KKP}(p_e, p_p) = \frac{em_p^3 f_{3\gamma} \langle \bar{q}q \rangle}{12} (Q_u - Q_d) \int_0^1 du \frac{u\psi^a(u)}{P^4} \left(1 + \frac{m_0^2}{2P^2} \right) \quad (4.39)$$

$$\begin{aligned} \Pi_{LL}^{QCD,VP}(p_e, p_p) = & -\frac{em_p f_{3\gamma} \langle \bar{q}q \rangle}{6} (Q_u - Q_d) \int_0^1 du \left[\frac{\psi^v(u)}{P^2} \left(1 + \frac{m_0^2}{4P^2} \right) \right. \\ & \left. - (k \cdot p_p - uk^2) \frac{\psi^a(u)}{2P^4} \left(1 + \frac{m_0^2}{2P^2} \right) \right] \end{aligned} \quad (4.40)$$

$$\Pi_{LL}^{QCD,TP}(p_e, p_p) = \frac{em_p^2 \langle \bar{q}q \rangle^2 \chi}{6} (Q_u - Q_d) \int_0^1 du \left[\frac{\phi_\gamma(u)}{P^2} \left(1 + \frac{m_0^2}{4P^2} \right) \right] \quad (4.41)$$

- For $\Gamma = L$ and $\Gamma' = R$:

$$\begin{aligned} \Pi_{LR}^{QCD,PK}(p_e, p_p) = & -em_p^2 \int_0^1 du \left[\frac{\langle \bar{q}q \rangle^2 \chi Q_u \phi_\gamma(u)}{3 P^2} \left(1 + \frac{m_0^2}{4P^2} \right) + \frac{f_{3\gamma}}{16\pi^2} \right. \\ & \times \left\{ \left\{ \frac{1}{3} (2(Q_u + Q_d)u\psi^v(u) + (7Q_u + Q_d)\bar{\psi}^v(u)) \right. \right. \\ & \left. \left. + Q_u\psi^a(u) \right\} \ln(-P^2) + \frac{2(Q_u + Q_d)}{3P^2} u (p_p \cdot k - uk^2) \bar{\psi}^v(u) \right\} \end{aligned} \quad (4.42)$$

$$\begin{aligned} \Pi_{LR}^{QCD,KK}(p_e, p_p) = & \frac{em_p^2 f_{3\gamma}}{24\pi^2} \int_0^1 du u^2 \left[\left\{ (Q_u + Q_d)\psi^v(u) + (4Q_u + Q_d) \frac{\bar{\psi}^v(u)}{u} \right\} \right. \\ & \left. \times \ln(-P^2) + (Q_u + Q_d)(p_p \cdot k - uk^2) \frac{\bar{\psi}^v(u)}{P^2} \right] \end{aligned} \quad (4.43)$$

$$\begin{aligned}
\Pi_{LR}^{QCD,V}(p_e, p_p) = & e \int_0^1 du \left[\frac{\langle \bar{q}q \rangle^2 \chi Q_u (p_p \cdot k) \phi_\gamma(u)}{3 P^2} \left(1 + \frac{m_0^2}{4P^2} \right) \right. \\
& + \frac{f_{3\gamma}}{16\pi^2} \left\{ \frac{1}{3} ((7Q_u + Q_d) \psi^v(u) P^2 - (Q_u + Q_d) \bar{\psi}^v(u) \right. \\
& \left. \left. \times (p_p \cdot k - uk^2) + Q_u \psi^a(u) (p_p \cdot k) \right\} \ln(-P^2) \right] \quad (4.44)
\end{aligned}$$

$$\begin{aligned}
\Pi_{LR}^{QCD,T}(p_e, p_p) = & \frac{em_p \langle \bar{q}q \rangle}{6} \int_0^1 du \left[\frac{Q_d}{8\pi^2} \chi \phi_\gamma(u) (5P^2 + 2u(p_p \cdot k - uk^2)) \ln(-P^2) \right. \\
& \left. + f_{3\gamma} Q_u (p_p^2 - up_p \cdot k) \frac{\psi^a(u)}{P^4} \left(1 + \frac{m_0^2}{2P^2} \right) \right] \quad (4.45)
\end{aligned}$$

$$\begin{aligned}
\Pi_{LR}^{QCD,P}(p_e, p_p) = & \quad (4.46) \\
& \frac{em_p \langle \bar{q}q \rangle}{3} \int_0^1 du \left[\frac{Q_d}{8\pi^2} \chi uk^2 \phi_\gamma(u) \ln(-P^2) - f_{3\gamma} Q_u \left\{ \frac{\psi^v(u)}{P^2} \left(1 + \frac{m_0^2}{4P^2} \right) \right. \right. \\
& \left. \left. + \left(\bar{\psi}^v(u) (k \cdot p_p - uk^2) - \frac{uk^2 \psi^a(u)}{2} \right) \frac{1}{P^4} \left(1 + \frac{m_0^2}{2P^2} \right) \right\} \right] \quad (4.47)
\end{aligned}$$

$$\begin{aligned}
\Pi_{LR}^{QCD,K}(p_e, p_p) = & - \frac{em_p \langle \bar{q}q \rangle}{3} \int_0^1 du \left[\frac{Q_d}{8\pi^2} \chi u (p_p \cdot k) \phi_\gamma(u) \ln(-P^2) \right. \\
& - f_{3\gamma} Q_u \left\{ \left(u \psi^v(u) + \frac{\bar{\psi}^v(u)}{2} \right) \frac{1}{P^2} \left(1 + \frac{m_0^2}{4P^2} \right) \right. \\
& \left. \left. + \left(u (k \cdot p_p - uk^2) \bar{\psi}^v(u) - \frac{u (p_p \cdot k) \psi^a(u)}{2} \right) \frac{1}{P^4} \left(1 + \frac{m_0^2}{2P^2} \right) \right\} \right] \quad (4.48)
\end{aligned}$$

$$\begin{aligned}
\Pi_{LR}^{QCD,KPP}(p_e, p_p) = & - \frac{em_p^3 \langle \bar{q}q \rangle}{6} \int_0^1 du \left[\frac{Q_d}{4\pi^2} \chi \phi_\gamma(u) \ln(-P^2) \right. \\
& \left. + f_{3\gamma} Q_u \frac{\psi^a(u)}{P^4} \left(1 + \frac{m_0^2}{2P^2} \right) \right] \quad (4.49)
\end{aligned}$$

$$\begin{aligned} \Pi_{LR}^{QCD,KKP}(p_e, p_p) = \frac{em_p^3 \langle \bar{q}q \rangle}{6} \int_0^1 du \left[\frac{Q_d}{4\pi^2} \chi u \phi_\gamma(u) \ln(-P^2) \right. \\ \left. + f_{3\gamma} Q_u \frac{u\psi^a(u)}{P^4} \left(1 + \frac{m_0^2}{2P^2} \right) \right] \quad (4.50) \end{aligned}$$

$$\begin{aligned} \Pi_{LR}^{QCD,VP}(p_e, p_p) = \frac{em_p \langle \bar{q}q \rangle}{6} \int_0^1 du (p_p \cdot k - uk^2) \left[\frac{Q_d}{4\pi^2} \chi \phi_\gamma(u) \ln(-P^2) \right. \\ \left. + f_{3\gamma} Q_u \frac{\psi^a(u)}{P^4} \left(1 + \frac{m_0^2}{2P^2} \right) \right] \quad (4.51) \end{aligned}$$

$$\begin{aligned} \Pi_{LR}^{QCD,TP}(p_e, p_p) = em_p^2 \int_0^1 du \left[\frac{\langle \bar{q}q \rangle^2 \chi Q_u \phi_\gamma(u)}{3 P^2} \left(1 + \frac{m_0^2}{4P^2} \right) \right. \\ \left. + \frac{f_{3\gamma} Q_u}{16\pi^2} \psi^a(u) \ln(-P^2) \right] \quad (4.52) \end{aligned}$$

$$\begin{aligned} \Pi_{LR}^{QCD,PP}(p_e, p_p) = \frac{em_p^2 f_{3\gamma}}{24\pi^2} (Q_u + Q_d) \int_0^1 du \left[\psi^v(u) \ln(-P^2) \right. \\ \left. + (p_p \cdot k - uk^2) \frac{\bar{\psi}^v(u)}{P^2} \right] \quad (4.53) \end{aligned}$$

$$\begin{aligned} \Pi_{LR}^{QCD,KP}(p_e, p_p) = -\frac{em_p^2 f_{3\gamma}}{24\pi^2} (Q_u + Q_d) \int_0^1 du \left[(u\psi^v(u) + \bar{\psi}^v(u)) \ln(-P^2) \right. \\ \left. + (p_p \cdot k - uk^2) \frac{u\bar{\psi}^v(u)}{P^2} \right] \quad (4.54) \end{aligned}$$

where $P^2 = (p_p - uk)^2 = (p_e + uk)^2 = \bar{u}p_p^2 - up_e^2 - u\bar{u}k^2$ with u and $\bar{u} = 1 - u$ being the fractions of photon momentum carried by the quak and anti-quark, respectively. The other scalar functions which are not present in Eqn.(4.33)-Eqn.(4.54) do not appear in QCD calculations upto two-particle twist-3 accuracy. Now, according to the LCSR matching condition (see Chapter-2 for details)

$$\Pi_{\Gamma\Gamma'}^{had,r}(p_p^2, P_e^2) = \Pi_{\Gamma\Gamma'}^{QCD,r}(p_p^2, P_e^2), \quad (4.55)$$

the sum rule for $F_{\Gamma\Gamma'}^r$ reads as

$$\lambda_p m_p^2 \frac{F_{\Gamma\Gamma'}^r(s, P_e^2)}{m_p^2 - p_p^2} = \int_0^{s_0} ds \frac{1}{\pi} \frac{\text{Im}\Pi_{\Gamma\Gamma'}^{r, QCD}(s, P_e^2)}{s - p_p^2}. \quad (4.56)$$

In order to suppress the effect of the heavier states and improve the stability of the sum rule, we perform Borel transformation with respect to p_p^2 as a final step (see Section-2.1.1 for details). Consequently, the final sum rule reads as,

$$F_{\Gamma\Gamma'}^r(s_0, P_e^2) = \frac{e^{\frac{m_p^2}{M^2}}}{\lambda_p m_p^2} \int_0^{s_0} ds e^{-\frac{s}{M^2}} \frac{1}{\pi} \text{Im}\Pi_{\Gamma\Gamma'}^{QCD, r}(s, P_e^2) \quad (4.57)$$

where M is the Borel mass and s_0 is the continuum threshold. These are the artefacts of the LCSR method, and have to be fixed such that the sum rule is saturated with the ground state and the heavy state contributions are properly suppressed. A typical rule of the thumb is to try and obtain at least 70% contribution to the correlation function from the ground state itself.

In order to compute these sum rules one needs an imaginary part of the QCD calculated correlation function collected in Eqns.(4.33-4.54) and substitute them in Eqn.(4.57) and then perform an integral over s . These can be incorporated by implementing the following substitutions in Eqns.(4.33-4.54) with $s = p_p^2$ and putting $k^2 = 0$, as the photon is on-shell

$$\int_0^1 du \frac{F(u)}{P^2} G(u, s) \rightarrow - \int_0^{u_0} du \frac{F(u)}{\bar{u}} e^{\frac{-\tilde{s}}{M^2}} G(u, \tilde{s}) \quad (4.58)$$

$$\begin{aligned} \int_0^1 du \frac{F(u)}{P^4} G(u, s) &\rightarrow \frac{e^{\frac{-s_0}{M^2}} F(u_0) G(s_0, u_0)}{P_e^2} \\ &+ \int_0^{u_0} du \frac{F(u)}{\bar{u}^2} \frac{e^{\frac{-\tilde{s}}{M^2}}}{M^2} \left(G(u, \tilde{s}) - M^2 \frac{\partial}{\partial \tilde{s}} G(u, \tilde{s}) \right) \end{aligned} \quad (4.59)$$

$$\begin{aligned}
\int_0^1 du \frac{F(u)}{P_e^6} G(u, s) &\rightarrow - \int_0^1 du \frac{F(u)}{2\bar{u}^2} \left[e^{\frac{-s_0}{M^2}} G(u, s_0) \frac{\partial}{\partial s_0} (\delta(\bar{u}s_0 - uP_e^2)) \right] \\
&+ \int_0^1 \frac{F(u)}{2\bar{u}^2} \left[\frac{\partial}{\partial s} \left(e^{\frac{-s}{M^2}} G(u, s) \right) \delta(\bar{u}s - uP_e^2) \right] \\
&- \int_0^{u_0} du \frac{F(u)}{2\bar{u}^3} \frac{\partial^2}{\partial \tilde{s}^2} \left(e^{\frac{-\tilde{s}}{M^2}} G(u, \tilde{s}) \right) \quad (4.60)
\end{aligned}$$

where $F(u)$ and $G(u, s)$ are some arbitrary functions of u and s ,

$$\tilde{s} = \frac{uP_e^2}{\bar{u}} \quad \text{and} \quad u_0 = \frac{s_0}{s_0 + P_e^2}. \quad (4.61)$$

These substitutions are consistent with [70]. After making these substitutions, we are now ready to perform the numerical analysis for the form factors using the sum rules provided in Eqn.(4.57).

4.3.1.2 Numerical Analysis

The values of various parameters used during the numerical calculations are collected in Appendix-D. The physical FFs, $A_{\Gamma\Gamma'}$, for $\Gamma\Gamma' = LL$ and LR are studied as a function of $P_e^2 = -p_e^2$ and the Borel mass M . These FFs can be found from different combinations of $F_{\Gamma\Gamma'}$'s as can be read from Eqn.(4.8) and Eqn.(4.23). As the photon is on-shell, we can put $k^2 = 0$. For the case of $\Gamma\Gamma' = LL$, there are only two possibilities to extract $A_{LL}(s_0, P_e^2)$ which are from the combination of F_{LL}^T and F_{LL}^{TP} with F_{LL}^{KPP} as F_{LL}^{PK} , F_{LL}^P , and F_{LL}^{PP} turn out to be zero. In Fig.(4.2), we show the variation of $A_{LL}^{TP+KPP}(s_0, P_e^2)$ with P_e^2 for three different values of the continuum threshold s_0 . In this Figure, we also show its variation with the Borel mass, M , for three different values of P_e^2 at fixed $s_0 = (1.44\text{GeV})^2$ which is equal to the Roper resonance. The combination $A_{LL}^{TP+KPP}(s_0, P_e^2)$ is found to be less stable against the variation in the parameters s_0 and M (as can be seen from Fig.(4.3)). Therefore, it is less reliable. However, on the face value, it is in broad agreement with A_{LL}^{TP+KPP} . As can be seen from the detailed expressions of these functions (Eqn.(4.33)-Eqn.(4.41)), the contributions coming due to condensate are quite important (even dominant in some cases). Thus, these contributions can not be simply ignored. For the case of $\Gamma\Gamma' = LR$, we have eight combinations in total as can

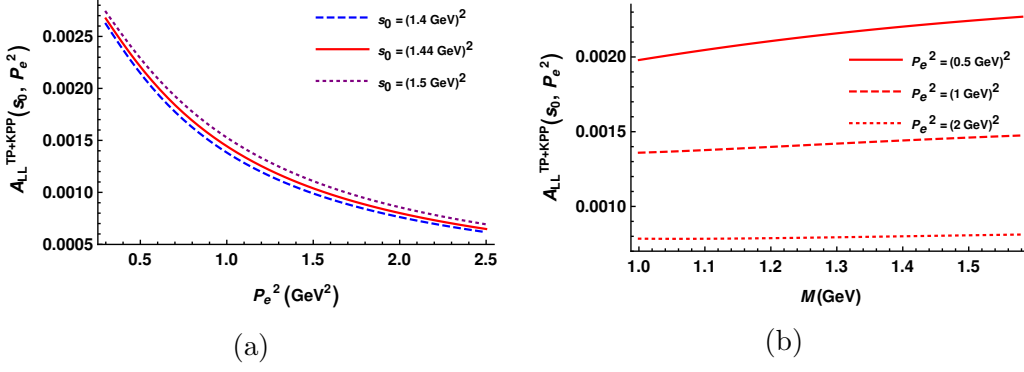


Figure 4.2: The physical FF, $A_{LL}(s_0, P_e^2)$ is calculated from the combination of F_{LL}^{TP} and F_{LL}^{KPP} employing photon DAs. Left panel: $A_{LL}^{TP+KPP}(s_0, P_e^2)$ vs P_e^2 is shown for three values of $s_0 = (1.4 \text{ GeV})^2$ (blue dashed), $s_0 = (1.44 \text{ GeV})^2$ (red solid) and $s_0 = (1.5 \text{ GeV})^2$ (purple dotted) at the Borel Mass, $M^2 = 2 \text{ GeV}^2$. Right Panel: $A_{LL}^{TP+KPP}(s_0, P_e^2)$ vs M is shown for three values of $P_e^2 = 0.5 \text{ GeV}^2$ (red solid), $P_e^2 = 1 \text{ GeV}^2$ (red dashed) and $P_e^2 = 2 \text{ GeV}^2$ (red dotted) at the continuum threshold, $s_0 = (1.44 \text{ GeV})^2$.

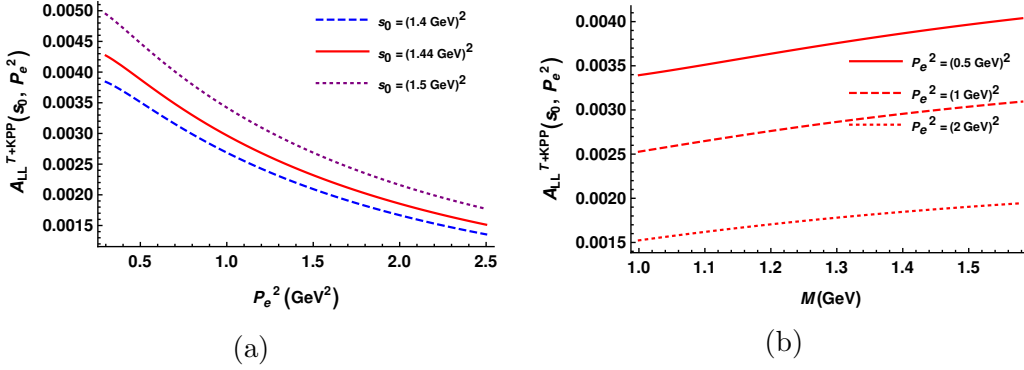


Figure 4.3: Same as Fig(4.2) but now with the combinations of F_{LL}^T and F_{LL}^{KPP} .

be read again from Eq.(4.8) and Eqn.(4.23). Moreover, for this case as well, the four combinations which involves F_{LR}^T are found to be less stable against s_0 and M and hence we discard them. The other four combinations involving F_{LR}^{TP} are shown in Fig.(4.4)-Fig.(4.7).

The values of the physical FFs, $A_{\Gamma\Gamma'}$ for $\Gamma\Gamma' = LL$ and $\Gamma\Gamma' = LR$, at $P_e^2 = 0.5 \text{ GeV}^2$ and $M^2 = 2 \text{ GeV}^2$ for $s_0 = (1.44 \text{ GeV})^2$ are found to be

$$\begin{aligned} A_{LL}^{T+KPP}(1.44^2, 0.5) &= (0.00388 \pm 0.00126) \text{ GeV}^2, \\ A_{LL}^{TP+KPP}(1.44^2, 0.5) &= (0.00221 \pm 0.00082) \text{ GeV}^2. \end{aligned} \quad (4.62)$$

¹LCSR calculations are trustworthy at $|Q^2| \rightarrow \infty$, where Q^2 is the momentum transferred squared. To be consistent with this requirement, in this case, we have chosen $Q^2 = P_e^2 = 0.5 \text{ GeV}^2$.

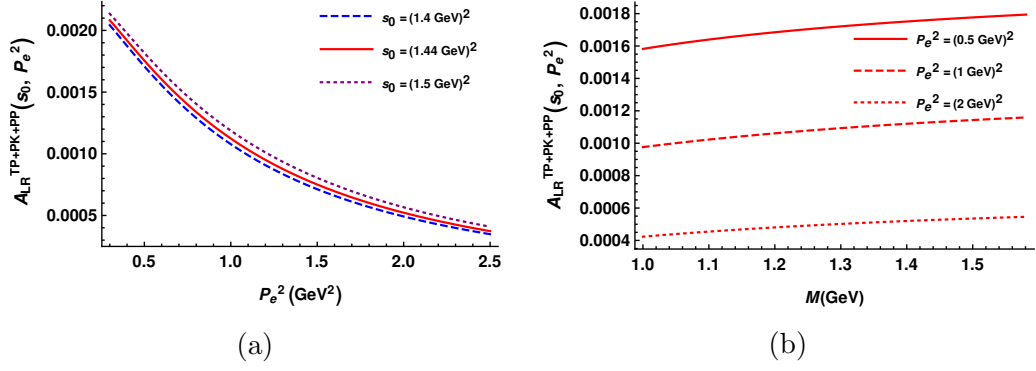


Figure 4.4: The physical FF, $A_{LR}(s_0, P_e^2)$ is calculated from the combination of F_{LR}^{TP} , F_{LR}^{PK} and F_{LR}^{PP} employing photon DAs. Left panel: $A_{LR}^{TP+PK+PP}(s_0, P_e^2)$ vs P_e^2 is shown for three values of $s_0 = (1.4 \text{ GeV})^2$ (blue dashed), $s_0 = (1.44 \text{ GeV})^2$ (red solid) and $s_0 = (1.5 \text{ GeV})^2$ (purple dotted) at the Borel Mass, $M^2 = 2 \text{ GeV}^2$. Right Panel: $A_{LR}^{TP+PK+PP}(s_0, P_e^2)$ vs M is shown for three values of $P_e^2 = 0.5 \text{ GeV}^2$ (red solid), $P_e^2 = 1 \text{ GeV}^2$ (red dashed) and $P_e^2 = 2 \text{ GeV}^2$ (red dotted) at the continuum threshold, $s_0 = (1.44 \text{ GeV})^2$.

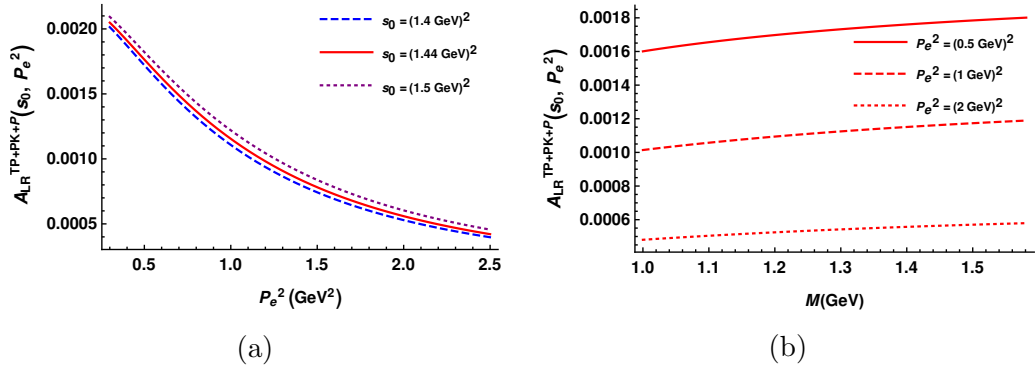


Figure 4.5: Same as Fig(4.4) but now with the combinations of F_{LR}^{TP} , F_{LR}^{PK} and F_{LR}^P .

$$\begin{aligned}
 A_{LR}^{TP+KPP+P}(1.44^2, 0.5) &= (0.00251 \pm 0.00118) \text{ GeV}^2, \\
 A_{LR}^{TP+KPP+PP}(1.44^2, 0.5) &= (0.00250 \pm 0.00118) \text{ GeV}^2 \\
 A_{LR}^{TP+PK+P}(1.4^2, 0.5) &= (0.00176 \pm 0.00123) \text{ GeV}^2, \\
 A_{LR}^{TP+PK+PP}(1.4^2, 0.5) &= (0.00176 \pm 0.00123) \text{ GeV}^2. \tag{4.63}
 \end{aligned}$$

From Eqn.(4.63), it is clearly evident that there is quite a good consistency in the form factor, A_{LR} , determined from different combinations. The uncertainties reported here are associated with the uncertainties in the values of the various parameters entering the sum rules except s_0 and M which we fixed to a certain value as mentioned above. These uncertainties are found to decrease with an

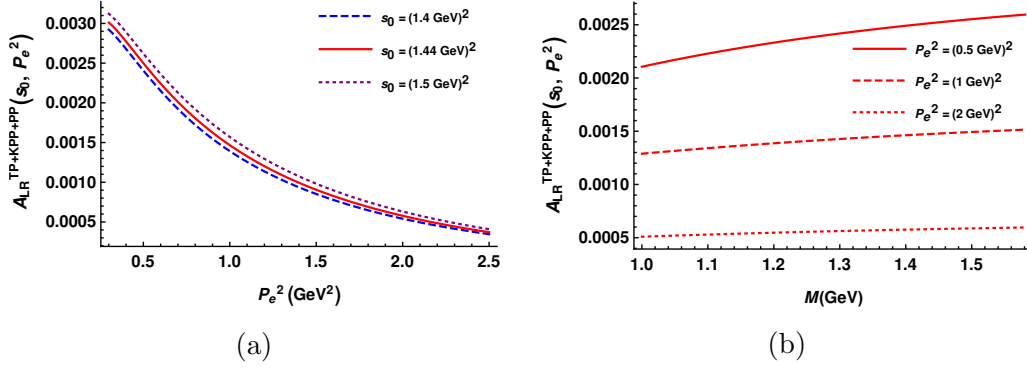


Figure 4.6: Same as Fig(4.4) but now with the combinations of F_{LR}^{TP} , F_{LR}^{KPP} and F_{LR}^{PP} .

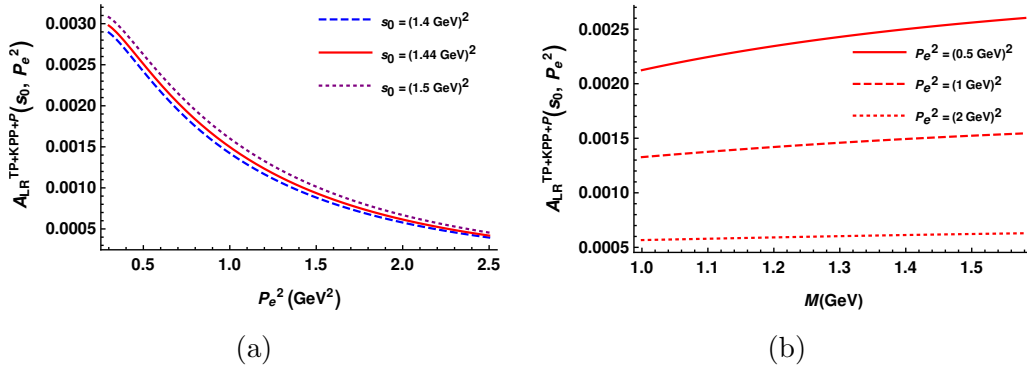


Figure 4.7: Same as Fig(4.4) but now with the combinations of F_{LR}^{TP} , F_{LR}^{KPP} and F_{LR}^P .

increase in P_e^2 for all the combinations. However, we have shown the error bands for $A_{LL}^{T+KPP}(s_0, P_e^2)$ and $A_{LR}^{T+KPP+P}(s_0, P_e^2)$ at $s_0 = (1.44 \text{ GeV})^2$ and $M^2 = 2 \text{ GeV}^2$ in Fig.(4.8) as the representative ones.

After discussing the first case in detail, let us now move to the other possibility for form factor calculation in LCSR framework using photon DAs.

4.3.2 Case-2: Using photon interpolation and proton DAs

In this case, we aim to calculate the physical form factors, $A_{\Gamma\Gamma'}$ by considering the correlation function where the photon state in Eqn.(4.7) is interpolated using the electromagnetic current, $j_{em}^\alpha(x)$. Such a correlation function (see Fig. (4.9))

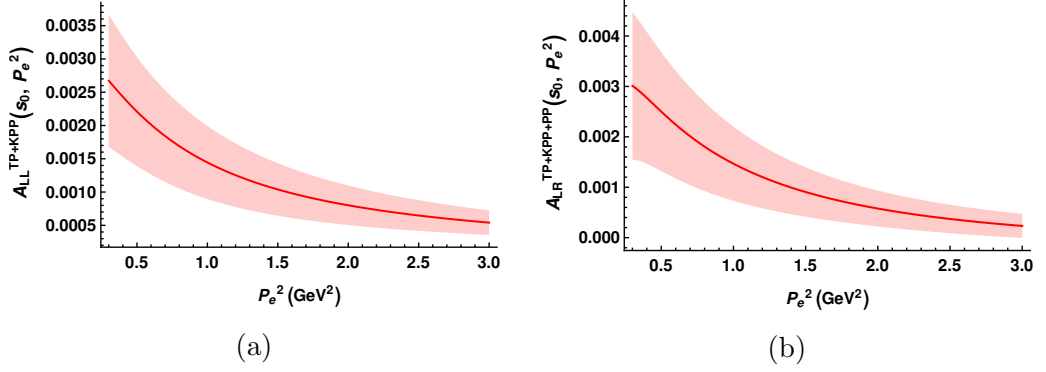


Figure 4.8: The physical FF, $A_{LL}^{TP+KPP}(s_0, P_e^2)$ (left pannel) and $A_{LR}^{TP+KPP+PP}(s_0, P_e^2)$ (right panel) vs P_e^2 are shown at $s_0 = (1.44 \text{ GeV})^2$ and $M^2 = 2 \text{ GeV}^2$ along with the uncertainties associated with the parameters involved in photon DAs. The bands represents the uncertainties.

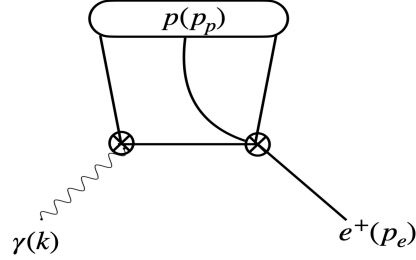


Figure 4.9: Feynman diagram which contributes to the light-cone expansion to proton decay to positron and photon in case-2 up to twist-3. The vertex on the left represents the electromagnetic current while the vertex on the right represents the dim-6 BNV operator. The encircled proton represents that the proton distribution amplitude will enter the LCSR computation.

reads as

$$H_{\Gamma\Gamma'}(p_p, p_e)u_p(p_p) = -ie\epsilon_\alpha^* \int d^4x e^{ik \cdot x} \langle 0 | T \{ j_{em}^\alpha(x) Q_{\Gamma\Gamma'}(0) \} | p(p_p) \rangle \quad (4.64)$$

where, $j_{em}^\alpha(x) = Q_d \bar{d}(x) \gamma^\alpha d(x) + Q_u \bar{u}(x) \gamma^\alpha u(x) - \bar{e}(x) \gamma^\alpha e(x)$, and the operator $Q_{\Gamma\Gamma'}$ is

$$Q_{\Gamma\Gamma'} = \epsilon^{abc} (d_a^T C P_\Gamma u_b) (P_{\Gamma'} u_c). \quad (4.65)$$

For $\Gamma\Gamma' = LL$ and $\Gamma\Gamma' = LR$, this operator can be rewritten using the generalised Fierz transformations [135] (discussed in Appendix-A) as

$$Q_{LL} = \frac{\epsilon^{abc}}{4} \left(2(P_L d_a)(\bar{u}_c^T P_L u_b) - \frac{1}{2}(\sigma_{\mu\nu} P_L d_a)(\bar{u}_c^T \sigma_{\mu\nu} P_L u_b) \right), \text{ and} \quad (4.66)$$

$$Q_{LR} = \frac{\epsilon^{abc}}{4} (2(\gamma_\mu P_L d_a)(\bar{u}_c^c \gamma^\mu P_L u_b)), \quad (4.67)$$

respectively². Now, in order to derive the sum rule, we need to compute the correlation function in Eq.(4.64) using perturbative QCD. For that, we need the time ordered product of j_{em}^α with Q_{LL} and Q_{RL} . These time ordered products can be written as a time product of $j_{em}^\alpha(x)$ with the operator $(\Gamma_A P_L d_a)(\bar{u}_c^c \Gamma^A P_L u_b)$ with $\Gamma_A = \{1, \sigma_{\mu\nu}\}$ and $\Gamma_A = \{\gamma_\mu\}$ for Q_{LL} and Q_{LR} , respectively. Therefore, for the QCD computation we need

$$\begin{aligned} & T\{j_{em}^\alpha(x) (\Gamma_A P_L d_a) (\bar{u}_c^c \Gamma^A P_L u_b)\} \\ &= \left[Q_u \left\{ \left(C \gamma^\alpha \tilde{S}_{ic}^u(x) \Gamma_A P_L \right)^{BF} (\Gamma^A P_L)^{CD} \left((u_i^T(x))^B u_b^F(0) d_a^D(0) \right) \right. \right. \\ &+ \left. \left(C \Gamma_A P_L S_{bi}(x) \gamma^\alpha \right)^{EB} (\Gamma^A P_L)^{CD} \left((u_c^T(0))^E u_b^B(x) d_a^D(0) \right) \right\} \\ &- \left. Q_d \left\{ (\Gamma_A S_{ai}^d(x) \gamma^\alpha)^{CB} (C \Gamma^A P_L)^{EF} \left((u_c^T(0))^E u_b^F(0) d_i^B(x) \right) \right\} \right] \end{aligned} \quad (4.68)$$

where capital alphabets (E, F, B, C, D) represent the Dirac indices, $\{a, b, c, i\}$ denote the color indices and superscript T refers to the transpose.

Now substitute Eqn.(4.68) in Eqn.(4.64) with $\Gamma_A = \{1, \sigma_{\mu\nu}\}$ and $\Gamma_A = \{\gamma_\mu\}$ for the case $\Gamma\Gamma' = LL$ and $\Gamma\Gamma' = LR$, respectively. After doing so, we are now left with the matrix element of the remaining three quark operator between the proton state and the vacuum. This matrix element can be parameterized in terms of proton DAs of varying twists [136]. In the present work, we consider only the leading twist-3 DAs (collected in Appendix-B). Using the various properties of these DAs (as discussed in Appendix-B), the correlation function in Eqn.(4.64) can be computed in perturbative QCD and results into

$$\begin{aligned} H_{\Gamma\Gamma'}^{QCD} u_p(p_p) &= \epsilon_\alpha^* P_{\Gamma'} \left[F_{\Gamma\Gamma'}^{1,QCD} \frac{p_p^\alpha \not{k}}{m_p^2} + F_{\Gamma\Gamma'}^{2,QCD} \frac{k^\alpha \not{k}}{m_p^2} + F_{\Gamma\Gamma'}^{3,QCD} \gamma^\alpha + F_{\Gamma\Gamma'}^{4,QCD} \frac{i\sigma^{\alpha\beta} k_\beta}{m_p} \right. \\ &+ \left. F_{\Gamma\Gamma'}^{5,QCD} \frac{p_p^\alpha}{m_p} + F_{\Gamma\Gamma'}^{6,QCD} \frac{k^\alpha}{m_p} \right] \end{aligned} \quad (4.69)$$

²The factor of $\frac{1}{2}$ in the second term of the r.h.s of Eqn.(4.66) was missed in [95] which reflects as differences in the analytical as well as numerical results for A_{LL} compared to [95]. However, this does not alter the numerical results much and the conclusions are more or less the same. We will be submitting an erratum reporting this correction soon.

where $F_{\Gamma\Gamma'}^n$, with $n = (1 \dots 6)$ are the scalar functions of $P'^2 = (p_p - k)^2$ and $K^2 = -k^2$ and these $F_{\Gamma\Gamma'}^n$, explicitly take the form

- For $\Gamma = \Gamma' = L$:

$$F_{LL}^{3,QCD}(p_p, k) = -\frac{em_p^2}{2} \int \mathcal{D}\alpha_i T_1(\alpha_i) \left[\frac{\alpha_3 Q_d}{2(k - \alpha_3 p_p)^2} + \frac{\alpha_1 Q_u}{(k - \alpha_1 p_p)^2} \right] \quad (4.70)$$

$$F_{LL}^{4,QCD}(p_p, k) = -\frac{em_p^2}{2} \int \mathcal{D}\alpha_i T_1(\alpha_i) \left[\frac{Q_d}{2(k - \alpha_3 p_p)^2} + \frac{Q_u}{(k - \alpha_1 p_p)^2} \right] \quad (4.71)$$

$$F_{LL}^{5,QCD}(p_p, k) = \frac{em_p^2}{2} \int \mathcal{D}\alpha_i T_1(\alpha_i) \left[\frac{\alpha_1 Q_u}{(k - \alpha_1 p_p)^2} - \frac{\alpha_3 Q_d}{(k - \alpha_3 p_p)^2} \right] \quad (4.72)$$

$$F_{LL}^{6,QCD}(p_p, k) = \frac{3Q_d em_p^2}{4} \int \mathcal{D}\alpha_i \frac{T_1(\alpha_i)}{(k - \alpha_3 p_p)^2} \quad (4.73)$$

- For $\Gamma = L$ and $\Gamma' = R$:

$$F_{LR}^{1,QCD}(p_p, k) = \frac{em_p^2}{2} \int \mathcal{D}\alpha_i \left[\frac{(V_1(\alpha_i) + A_1(\alpha_i)) Q_d}{(k - \alpha_3 p_p)^2} - \frac{(V_1(\alpha_i) - A_1(\alpha_i)) Q_u}{(k - \alpha_1 p_p)^2} \right] \quad (4.74)$$

$$F_{LR}^{3,QCD}(p_p, k) = -\frac{e}{2} \int \mathcal{D}\alpha_i \left[\frac{(V_1(\alpha_i) + A_1(\alpha_i)) Q_d (2p_p \cdot k - \alpha_3 m_p^2)}{2(k - \alpha_3 p_p)^2} + \frac{(V_1(\alpha_i) - A_1(\alpha_i)) Q_u (2\alpha_1 m_p^2 - p_p \cdot k)}{(k - \alpha_1 p_p)^2} \right] \quad (4.75)$$

$$F_{LR}^{4,QCD}(p_p, k) = -\frac{em_p^2}{2} \int \mathcal{D}\alpha_i \left[\frac{(V_1(\alpha_i) + A_1(\alpha_i)) Q_d}{2(k - \alpha_3 p_p)^2} + \frac{(V_1(\alpha_i) - A_1(\alpha_i)) Q_u}{(k - \alpha_1 p_p)^2} \right] \quad (4.76)$$

$$F_{LR}^{6,QCD}(p_p, k) = -\frac{em_p^2}{2} \int \mathcal{D}\alpha_i \left[\frac{(V_1(\alpha_i) + A_1(\alpha_i)) Q_d}{2(k - \alpha_3 p_p)^2} - \frac{(V_1(\alpha_i) - A_1(\alpha_i)) Q_u}{(k - \alpha_1 p_p)^2} \right] \quad (4.77)$$

where, V_1 , A_1 , and T_1 are the twist-3 light cone DAs of proton (collected in Appendix-B), and $\alpha_i = \{\alpha_1, \alpha_2, \alpha_3\}$ are the proton momentum fractions carried by up and down quarks inside the proton. $(k - \alpha_i p_p)^2$ can be expanded as $\alpha P'^2 - \bar{\alpha} K^2 - \alpha \bar{\alpha} m_p^2$ which will be useful for further computation. In this case also, some scalar functions do not appear up to twist-3 accuracy and hence are not reported here.

Moreover, to derive the sum rule, we need another representation for the correlation function in Eqn.(4.64) in terms of the hadronic states. For that, we insert a complete set of intermediate states with the quantum numbers of the proton state. To write the hadronic decomposition, we saturate it with the contribution coming from the lowest state i.e. the ground state of proton. Furthermore, we use the matrix element of the electromagnetic current between two proton state given by

$$\langle p(p_p - k) | j_\alpha^{em}(0) | p(p_p) \rangle = \bar{u}_p(p_p - k) \left[W_1(K^2) \gamma_\alpha - i \frac{\sigma_{\alpha\beta} k^\beta}{2m_p} W_2(K^2) \right] u_p(p_p). \quad (4.78)$$

where $W_1(K^2)$ and $W_2(K^2)$ are electromagnetic electric and magnetic form factors of the proton, respectively. The final hadronic decomposition obtained reads as

$$\begin{aligned} H_{\Gamma\Gamma'}^{had} u_p(p_p) &= -e\epsilon_\alpha^* \frac{P_{\Gamma'}}{4} \lambda m_p \frac{\not{p}_p - \not{k} + m_p}{(p_p - k)^2 - m_p^2} \left\{ \gamma^\alpha W_1(K^2) - \frac{i\sigma^{\alpha\beta} k_\beta}{2m_p} W_2(K^2) \right\} u_p(p_p) + \dots \\ &= \epsilon_\alpha^* P_{\Gamma'} \left[F_{\Gamma\Gamma'}^{1,had} \frac{p_p^\alpha \not{k}}{m_p^2} + F_{\Gamma\Gamma'}^{2,had} \frac{k^\alpha \not{k}}{m_p^2} + F_{\Gamma\Gamma'}^{3,had} \gamma^\alpha + F_{\Gamma\Gamma'}^{4,had} \frac{i\sigma^{\alpha\beta} k_\beta}{m_p} \right. \\ &\quad \left. + F_{\Gamma\Gamma'}^{5,had} \frac{p_p^\alpha}{m_p} + F_{\Gamma\Gamma'}^{6,had} \frac{k^\alpha}{m_p} \right] \end{aligned} \quad (4.79)$$

where ellipses represent the heavier state contributions, and λ represents the coupling strength of the proton interpolation current with the proton state such that $\lambda = \lambda'_p$ and $\lambda = -\lambda_p$ for $\Gamma\Gamma' = LL$ and $\Gamma\Gamma' = LR$, respectively (as defined in Eqn.(4.15) and Eqn.(4.17), respectively). $F_{\Gamma\Gamma'}^{n,had}$ with $n = 1, \dots, 6$ are the scalar

functions of $P'^2 = (p_p - k)^2 = p_e^2$ and $K^2 = -k^2$. They are related to $W_1(K^2)$ and $W_2(K^2)$ as

$$\begin{aligned}
F_{LL}^{1,had} &= \frac{-e}{4} m_p^2 \lambda'_p \frac{W_2(K^2)}{P'^2 - m_p^2}, & F_{LL}^{2,had} &= \frac{e}{4} m_p^2 \lambda'_p \frac{W_2(K^2)}{2(P'^2 - m_p^2)}, \\
F_{LL}^{3,had} &= -\frac{e}{8} \lambda'_p W_2(K^2), & F_{LL}^{4,had} &= \frac{e}{4} m_p^2 \lambda'_p \frac{W_1(K^2) + W_2(K^2)}{P'^2 - m_p^2}, \\
F_{LL}^{5,had} &= \frac{-e}{2} m_p^2 \lambda'_p \frac{W_1(K^2)}{P'^2 - m_p^2}, \text{ and} & F_{LL}^{6,had} &= \frac{e}{4} m_p^2 \lambda'_p \frac{W_1(K^2)}{P'^2 - m_p^2}.
\end{aligned} \tag{4.80}$$

There are similar relations between $F_{LR}^{n,had}$ and $W_{1,2}(K^2)$ which can be obtained by simply replacing λ'_p by $-\lambda_p$. The sum rule can then be computed for $W_{1,2}(K^2)$ by equating the two representations and using the quark hadron duality to suppress the heavier state contributions. As a final step we perform the Borel transformation on P'^2 and using the relations in Eqn.(4.80), we derive the final sum rules for $F_{\Gamma\Gamma'}^{1,4,5}$ using the sum rules for $W_{1,2}(K^2)$ which reads as

$$F_{\Gamma\Gamma'}^{1,4,5}(s_0, K^2) = -\frac{\text{Exp}\left(\frac{m_p^2}{M^2}\right)}{P'^2 - m_p^2} \int_0^{s_0} ds \text{Exp}\left(\frac{-s}{M^2}\right) \frac{1}{\pi} \text{Im}\left(F_{\Gamma\Gamma'}^{\{1,4,5\},QCD}(s, K^2)\right) \tag{4.81}$$

where s_0 and M are the continuum threshold and the Borel mass, respectively. Here, we provide sum rules only for $F_{\Gamma\Gamma'}^{1,4,5}$ as they are related to the physical form factors given in Eqn.(4.8). However, one can similarly write sum rules for other $F_{\Gamma\Gamma'}^{n,had}$. Similar to the previous case, to compute these sum rules, we need the imaginary part of $F_{\Gamma\Gamma'}^{\{1,4,5\},QCD}(s, K^2)$ (provided in Eqn.(4.70)-Eqn.(4.77)) and then have to integrate over s . These operations can be incorporated by a simple substitution using $s = (p_p - k)^2$ and $K^2 = -k^2$, given by

$$\int \mathcal{D}\alpha_i \frac{F(\alpha_i)}{(k - \alpha p_p)^2} \rightarrow -\int_{\alpha_0}^1 \mathcal{D}\alpha_i \frac{F(\alpha_i)}{\alpha} e^{\frac{-s_1}{M^2}} \tag{4.82}$$

where $\alpha = \{\alpha_1, \alpha_3\}$, $\mathcal{D}\alpha_i = d\alpha_1 d\alpha_2 d\alpha_3 \delta(1 - \alpha_1 - \alpha_2 - \alpha_3)$,

$$s_1 = \frac{\bar{\alpha} K^2 + \alpha \bar{\alpha} m_p^2}{\alpha}, \tag{4.83}$$

and

$$\alpha_0 = -\frac{K^2 - m_p^2 + s_0}{2m_p^2} + \frac{\sqrt{(K^2 + s_0)^2 + m_p^4 - 2m_p^2(s_0 - K^2)}}{2m_p^2}. \quad (4.84)$$

We are now all set to get numerical estimates for the physical form factors obtained using proton DAs upto twist-3.

4.3.2.1 Numerical Analysis

The physical form factors, $A_{\Gamma\Gamma'}$ are studied as a function of $K^2 = -k^2$ and the Borel mass, M at $P'^2 = m_e^2 = 0$. Using Eqn.(4.8) and Eqn.(4.80), it is easy to see that these FFs which are defined using a combination of $F_{\Gamma\Gamma'}^1$, $F_{\Gamma\Gamma'}^4$ and $F_{\Gamma\Gamma'}^5$, turn out to be proportional to $W_2(K^2)$, the magnetic form factor (as discussed above). It can be seen from Eqn.(4.80) that $W_2(K^2)$ can also be obtained using other combinations of $F_{\Gamma\Gamma'}^n$. However, it is found that these other combinations result in poor stability against the Borel mass, M . Therefore, the combination of $F_{\Gamma\Gamma'}^1$, $F_{\Gamma\Gamma'}^4$, and $F_{\Gamma\Gamma'}^5$, as defined in Eqn.(4.8) is considered to be the best estimate for these form factors and thus, we choose to show only this explicitly in Fig.(4.10) and Fig(4.11).

The values of the physical FFs, $A_{\Gamma\Gamma'}$ using this combination at $K^2 = 0.5 \text{ GeV}^2$ and $M^2 = 2 \text{ GeV}^2$ for $s_0 (= 1.44 \text{ GeV})^2$ are found to be

$$\begin{aligned} A_{LL}^{1+4+5}(1.44^2, 0.5) &= (0.00038 \pm 0.00021) \text{ GeV}^2, \\ A_{LR}^{1+4+5}(1.44^2, 0.5) &= (0.00174 \pm 0.00027) \text{ GeV}^2 \end{aligned} \quad (4.85)$$

Here again, the uncertainties are associated with the parameters involved in form factor calculations except s_0 and M , and are found to decrease with an increase in K^2 (as shown in Fig.(4.12)).

It is important to note here that, in the present case, the numerical value of the form factor A_{LL}^{1+4+5} is smaller than A_{LR}^{1+4+5} (also the form factors obtained in the previous case) by a factor of ~ 3 .

Another important thing to remark here is that, it is not possible to have a direct comparison between the form factors obtained here with the ones obtained in

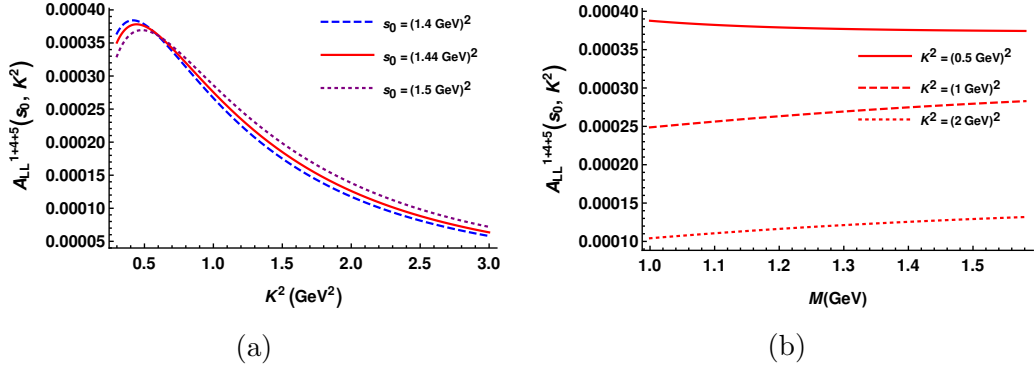


Figure 4.10: The physical FF, $A_{LL}(s_0, K^2)$ is calculated from the combination of F_{LL}^1 , F_{LL}^4 and F_{LL}^5 employing proton DAs. Left panel: $A_{LL}^{1+4+5}(s_0, K^2)$ vs K^2 is shown for three values of $s_0 = (1.4 \text{ GeV})^2$ (blue dotted), $s_0 = (1.44 \text{ GeV})^2$ (red solid) and $s_0 = (1.5 \text{ GeV})^2$ (blue dashed) at the Borel Mass, $M^2 = 2 \text{ GeV}^2$. Right Panel: $A_{LL}^{1+4+5}(s_0, K^2)$ vs M is shown for three values of $K^2 = 0.5 \text{ GeV}^2$ (red solid), $K^2 = 1 \text{ GeV}^2$ (red dashed) and $K^2 = 2 \text{ GeV}^2$ (red dotted) at the continuum threshold, $s_0 = (1.44 \text{ GeV})^2$.

case-1 where proton state was interpolated with Ioffe current and the photon DAs were used upto two particle twist-3 accuracy. The simple reason for it lies in the difference in the momentum transferred square in the two cases and the limitations of LCSR application to low momentum squared region (as discussed in previous case). Because of this the photon is taken to be far off-shell in the present case, while in the previous case the photon was taken on-shell. Moreover, the positron momentum squared in this case can be taken to $m_e^2 \approx 0$ while in the previous case it was taken to be 0.5 GeV^2 . Therefore, a direct comparison between the form factors obtained in the two cases is not straightforward and some kind of judicious extrapolation would be required in the two cases to meet the physical requirements and to have a proper comparison.

4.4 Discussion and Conclusions

In this chapter, we have discussed the computation of the form factors involved in the proton decay to a positron and a photon using the LCSR framework. This

³The numerical values of the form factor in Fig.(4.12 (b)) are slightly different from Fig.(4.11) as in the present case $(p_p - k)^2 = p_e^2$ is set to be equal to 0 GeV^2 . While, for Fig.(4.11), it has been set to 0.5 GeV^2 .

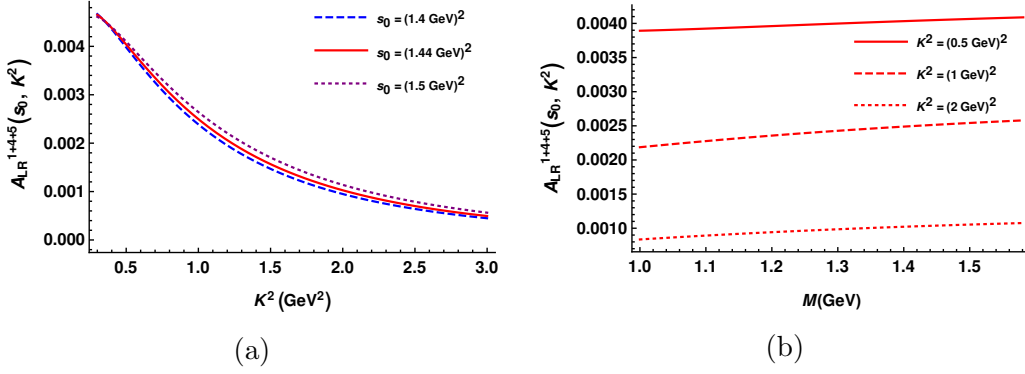


Figure 4.11: The physical FF, $A_{LR}(s_0, K^2)$ is calculated from the combination of F_{LR}^1 , F_{LR}^4 and F_{LR}^5 employing proton DAs. Left panel: $A_{LR}^{1+4+5}(s_0, K^2)$ vs K^2 is shown for three values of $s_0 = (1.4 \text{ GeV})^2$ (violate dotted), $s_0 = (1.44 \text{ GeV})^2$ (red solid) and $s_0 = (1.5 \text{ GeV})^2$ (blue dashed) at the Borel Mass, $M^2 = 2 \text{ GeV}^2$. Right Panel: $A_{LR}^{1+4+5}(s_0, K^2)$ vs M is shown for three values of $K^2 = 0.5 \text{ GeV}^2$ (red solid), $K^2 = 1 \text{ GeV}^2$ (red dashed) and $K^2 = 2 \text{ GeV}^2$ (red dotted) at the continuum threshold, $s_0 = (1.44 \text{ GeV})^2$.

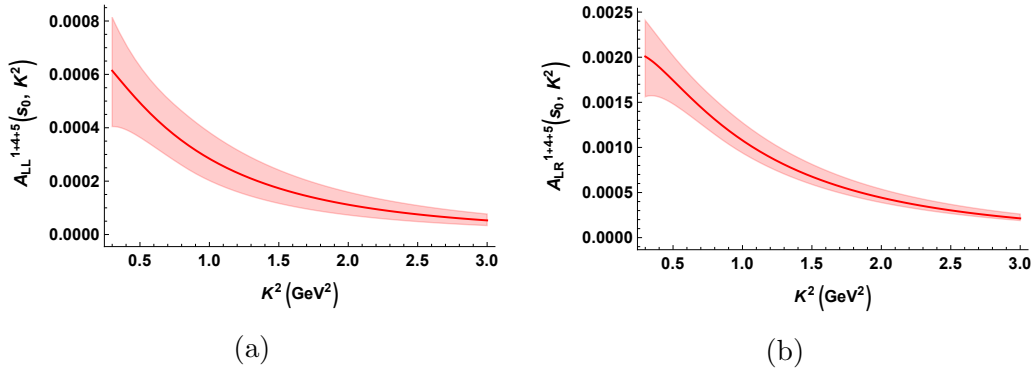


Figure 4.12: The physical FF, $A_{LL}^{1+4+5}(s_0, K^2)$ (left panel) and $A_{LR}^{1+4+5}(s_0, K^2)$ (right panel) vs K^2 are shown at $s_0 = (1.44 \text{ GeV})^2$ and $M^2 = 2 \text{ GeV}^2$ along with the uncertainties associated with the parameters involved in proton DAs. The bands represents the uncertainties ³.

should be viewed as a complimentary approach to lattice calculations, though, to the best of our knowledge, there is no lattice study so far for proton to gamma transition. This decay mode is found to have not attracted much attention. However, as briefly discussed in [124], the branching ratio for this mode is expected to be smaller than the $p \rightarrow \pi e^+$ mode, the very well studied mode, by a factor $\mathcal{O}(1/(\text{few tens}))$. As, it is not a huge suppression and keeping in mind that the nuclear absorption effects are not going to affect the radiative mode, it becomes important to remain optimistic about this mode. As a next step, it is important to have the relevant form factors computed in a reliable fashion. With that aim,

we discussed them in LCSR framework where they can be calculated either by interpolating the proton state and using the photon DAs (case 1) or by interpolating the photon state and using the proton DAs (case-2). In this chapter, we discussed both these cases one by one. In both the cases, the physical form factors (define in Eqn.(4.8)), which enter the amplitude and hence the decay rate of this radiative mode, are found to be related to the hadronic functions entering the parameterization of the correlator in the two cases. These hadronic functions have been systematically computed in LCSR framework and then the physical FFs have been determined using various combinations of them. In the first case, it was found that the hadronic functions entering the parameterization of the correlation function get important and, in some combinations, dominant contributions from condensates. Consequently, these contributions are important and if not considered, these would have led to erroneous results. The photon DAs used in this case were taken upto two-particle twist-3 accuracy. However, in case-2, at the order of twist-3 accuracy of the proton DAs, we did not encounter any contributions coming from the condensates.

Though, the physical FFs can be calculated using various combinations of these hadronic functions, not all the combinations were found to have good stability against the Borel mass and hence were discarded. For both the cases, we have explicitly shown the FFs obtained using the combinations with the best Borel stability.

The physical FFs in case-2 are found to have a factor of ~ 3 difference between each other and also to the FFs obtained in case-1. Though, as briefly discussed above, a straightforward comparison between the two cases is not possible due to differences in the choice of the momentum transferred square and the limitations of LCSR to attain the physical point. However, one can naively say that the FFs obtained in case-2 are more trustworthy on the basis of error analysis. The errors obtained in case-2 are much smaller than the errors encountered in case-1. The errors in case-2 are found to be as large as ($\sim 50\%$ for some combinations). Similar conclusions on errors were made in [118]. Nevertheless, a detailed analysis including higher twist effects is required. As for the case of baryon, the higher twist terms can have significant impact on the results obtained using LCSR as

discussed in Section-2.2.2. Moreover, it has been observed that the choice of interpolation current also plays a very crucial role [70]. For some choice(s), it has been seen that a particular FF may simply does not show up in the correlator. Along with this a proper mechanism for interpolating the LCSR result to the physical point i.e. $k^2 = 0$ and $p_e^2 = m_e^2 \approx 0$ is required to make any strong comments on the superiority of the two cases.

The results discussed here can also be utilised, with very less efforts, to compute the FFs and the branching ratios for process having μ^+ instead of e^+ in the final state. It is possible as the detailed expressions reported in Eqn.(4.33)-Eqn.(4.54) and Eqn.(4.70)-Eqn.(4.77) are written for non-zero positron mass and without assuming $k^2 = 0$. However, while computing the amplitude positron was considered massless and therefor there will be some extra contribution due to non-zero mass of the lepton while manipulating Eqn.(4.7) and Eqn.(4.8). These modes might turn out to be important as it was pointed out in a recent study [137] that in some GUT scenarios, where the scalar mediated contribution dominates over the gauge mediated ones, the decay channels with final states having second generation particles are more favoured. Thus, the radiative modes can be equally important and can provide complimentary information about the details of the underlying high energy theory.

Chapter 5

The heavy meson system and LCSR

After discussing the application of LCSR to light quark hadrons in Chapter-3 and Chapter-4, let us now move our attention to the processes involving heavy quarks like charm quark. In this regard, we discuss the decay of charmed mesons in this chapter. Firstly, we will discuss a baryon number violating (BNV) decay of charmed meson into an anti-proton and a positron, i.e. $D^0 \rightarrow \bar{p}e^+$. As discussed in the previous chapter, BNV processes are important as they can provide direct signature of new physics. This process is found to involve twelve independent form factors which we study using the framework of LCSR and find that some of these form factors attain large uncertainties (as large as 200%). These uncertainties are found to be majorly dominated by our lack of knowledge of the D-meson light cone distribution amplitudes. To get a better understanding on these DAs, in the later part of this chapter, we attempt to estimate w_0 , a parameter related to the first inverse moment of the D-meson DAs which enters directly in their definition. It can be estimated using the experimental data on the $D_q^* D_q \gamma$ (with $q = u, d, s$) coupling and comparing it with the results one obtains using LCSR for this coupling. This chapter is based on [138] and an ongoing project.

5.1 Introduction

As we know from the previous chapter, according to Sakharov conditions [94], baryon number violation (BNV) is one of the important criteria to explain the matter-anti-matter asymmetry of the Universe. Nonetheless, it is not allowed in the SM as the baryon number is a conserved quantity in the SM as a result of an accidental symmetry and motivates towards new physics. In that view, as already discussed in the previous chapter, looking at the BNV processes will be clear signature of BSM physics. Though, such processes are never observed, they are well motivated in various BSM scenarios like GUTs, SUSY, etc. and can be studied using higher dimensional baryon number violating effective operators (see Chapter-4). Experimentally, there are very stringent bounds on some of these decays like proton decay, decays of heavy mesons to baryons, etc [139]. Out of all the BNV processes, proton decay has got the most attention so far, theoretically (see for eg. [95], [112], [118] and references therein) as well as experimentally (see for eg. [126], [140] and references therein).

However, with advances in experimental facilities study of other modes are becoming more and more important. $D^0 \rightarrow \bar{p}e^+$ is one such mode with recently updated experimental bound on the branching fraction as $< 1.2 \times 10^{-6}$ [141]. Theoretically, this decay is possible via baryon number violating dim-6 effective operators. The major challenge in estimating the branching ratio is our lack of knowledge of the form factors involved. To the best of our knowledge, [142] is the only study which provides rough bounds on the branching ratio to be $\leq 1.1 \times 10^{-4} |C_{ucdl}^R|^2$, where C_{ucdl}^R is the Wilson coefficient corresponding to the relevant effective operator which we will discuss below, with no explicit discussion on the form factors involved. In this chapter, we will attempt to compute these form factors within LCSR framework using D-meson light cone distribution amplitudes using a general interpolation current for the proton state given in Eqn.(4.10).

The rest of the paper is devoted to the detailed discussion on the definition, computation, and numerical analysis of these form factors using LCSR. The following analysis proceeds parallel to the analysis of $p \rightarrow e^+\pi^0$ in LCSR framework

studied in [118] and more or less follows the same methodology and procedure as was followed in the previous chapter. Therefore, some details will be skipped. In Section-5.4, we will see that the numerical results on these form factors shows large uncertainties (as large as 200%). These uncertainties are found to be dominated by the uncertainties in w_0 , a parameter which enters the considered exponential model for the D-meson DAs and is related to the first inverse moment of these DAs. To address this issue, in later part of this chapter (Section-5.5 onwards), we attempt provide better estimate for this parameter by calculating $D_q^* D_q \gamma$ (with $q = u, d, s$) coupling using LCSR. The experimental value of this coupling can be estimated from the experimental data on the branching ratio of $D^* \rightarrow D_q \gamma$ decays. Our aim is to compare these experimental estimates with the theoretical estimates of these coupling and get an estimate on w_0 . This might help us in probing and developing a better understanding of the structure of D-meson.

5.2 Amplitude parameterization

As discussed above, one can compute BNV processes like $D^0 \rightarrow \bar{p}e^+$ in a model-independent way with the help of baryon number violating higher dimensional effective operators. Within the SM effective field theory (SMEFT), there are 4 types of dimension-6 operators which can lead to this process. The explicit forms of these operators are [128], [129], [143]

$$\begin{aligned}
\mathcal{O}_{ijkl}^{duq\ell} &= \epsilon_{abc} \epsilon_{\alpha\beta} (d_i^a C u_j^b) (q_k^{\alpha c} C \ell_l^\beta), & \mathcal{O}_{ijkl}^{qque} &= \epsilon_{abc} \epsilon_{\alpha\beta} (q_i^{\alpha a} C q_j^{\beta b}) (u_k^c C e_l) \\
\mathcal{O}_{ijkl}^{qqq\ell} &= \epsilon_{abc} \epsilon_{\alpha\beta} \epsilon_{\gamma\delta} (q_i^{\alpha a} C q_j^{\beta ab}) (q_k^{\gamma c} C \ell_l^\delta), & \mathcal{O}_{ijkl}^{duue} &= \epsilon_{abc} (d_i^a C u_j^b) (u_k^c C e_l)
\end{aligned}
\tag{5.1}$$

where $C = i\gamma^2\gamma^0$ represents the charge conjugation matrix, $\{i, j, k, l\}$ represent the flavour indices, $\{a, b, c\}$ are the color indices, $\{u, d\}$ represent the right-handed up and down quarks, and $\{q, \ell\}$ represent the left-hand doublets of quarks and leptons. These operators respect the SM gauge group, nonetheless, violate baryon number which is an accidental symmetry of the SM.

Using these operators and the generalised Fierz transformations (discussed in Appendix-A) [135], one can write the BNV Lagrangian which leads to the process $D^0 \rightarrow \bar{p}e^+$. Such a Lagrangian reads as

$$\mathcal{L}_{\not{B}}^{(6)} = \sum_{\Gamma, \Gamma'} c_{\Gamma\Gamma'}^A \mathcal{O}_{\Gamma\Gamma'}^A = \sum_{\Gamma'} c_{\Gamma'}^A \epsilon^{ijk} (d_i^T C P_{\Gamma} \Gamma_A u_j) (e^T C P_{\Gamma'} \Gamma^A c_k) \quad (5.2)$$

where superscript T represents the transpose, P_{Γ} and $P_{\Gamma'}$ are the chirality projection operators with $\{\Gamma, \Gamma'\} \in \{L, R\}$ and $\Gamma^A \in \{1, \gamma_{\mu}, \sigma^{\mu\nu}\}$ with $A \in \{S, V, T\}$. $c_{\Gamma\Gamma'}^A$ are the Wilson coefficients¹. The transition amplitude for $D^0 \rightarrow \bar{p}e^+$ is defined as the matrix element of this Lagrangian between the initial and the final states as

$$\mathcal{A}(D^0(p_D) \rightarrow \bar{p}(p_p)e^+(p_e)) = \sum_{\Gamma, \Gamma'} c_{\Gamma\Gamma'}^A \langle e^+(p_e)\bar{p}(p_p) | \mathcal{O}_{\Gamma\Gamma'}^A | D^0(p_D) \rangle \quad (5.3)$$

This amplitude can be factorized in terms of the leptonic and the hadronic parts as

$$\mathcal{A}(D^0(p_D) \rightarrow \bar{p}(p_p)e^+(p_e)) = \sum_{\Gamma, \Gamma'} c_{\Gamma\Gamma'}^A \bar{v}_e^c H_{\Gamma\Gamma'}^A v_p(p_p) \quad (5.4)$$

where, \bar{v}_e^c is the spinor corresponding to the positron and $H_{\Gamma\Gamma'}^A v_p(p_p)$ is the hadronic object of interest defined as

$$H_{\Gamma\Gamma'}^A v_p(p_p) = \langle \bar{p}(p_p) | \epsilon^{ijk} (d_i^T C \Gamma_A P_{\Gamma} u_j) (\Gamma^A P_{\Gamma'} c_k) | D^0(p_D) \rangle \quad (5.5)$$

Following the general parameterization in [118], this hadronic object can also be parameterized as

$$H_{\Gamma\Gamma'}^A v_p(p_p) = P_{\Gamma'} \left(F_{\Gamma\Gamma'}^{A,0}(p_e^2) + \not{p} F_{\Gamma\Gamma'}^{A,1}(p_e^2) \right) v_p(p_p) \quad (5.6)$$

where $F_{\Gamma\Gamma'}^{A,n}(p_e^2)$ are the form factors with $A \in \{S, V, T\}$ and $n \in \{0, 1\}$. As D-meson comprises of a heavy quark, we treat it in the framework of heavy quark effective theory (HQET) [144], [145]. $p_D^\mu = m_D v^\mu$ is the momentum of the D-

¹The Lagrangian is assumed to be expressed in terms of the physical fields at the charm scale and thus, $c_{\Gamma\Gamma'}^A$'s also include all the flavor and usual RG running effects.

meson with v being its velocity such that $v^2 = 1$.

Parity conservation in QCD relates these FFs

$$F_{LL}^{A,n} = F_{RR}^{A,n} \quad F_{LR}^{A,n} = F_{RL}^{A,n} \quad (5.7)$$

resulting in twelve independent FFs in this case. We will now compute these FFs in the framework of the light cone sum rules (LCSR).

Though the analysis is parallel to that in [118], there are two major differences in the two scenarios stemming from the difference in the number of the form factors and the type of mesons involved in the two cases. In the case of proton decay [118], there are two form factors and a light quark meson i.e. π^0 is involved. However, in the present case, we have D^0 -meson which brings in various challenges due to the presence of a heavy quark, and the very little knowledge about the light cone distribution amplitudes of heavy quark mesons. Along with that, the amplitude of $D^0 \rightarrow \bar{p}e^+$ involves twelve independent form factors (as discussed above) stemming as a result of the presence of more number of effective operators relevant to this decay as compared to the number of effective operators for the case of proton decay. Having pointed out these major differences in the two analysis, let us move to the discussion of the computation of these form factors using the method of LCSR.

5.3 Form Factors in LCSR

As discussed in Chapter-2, the starting object for a sum rule calculation is the identification of the relevant correlation function for the process. In the previous chapter, we saw that the interpolation current for the proton state is not unique and the determination of the form factors depends on the choice of the interpolation current used to define the correlation function. Therefore, in the present case we obtain the relevant correlation function by interpolating the anti-proton state in Eqn.(5.5) with the general interpolation current for the proton state

provided in Eqn.(4.10). Such a correlation function reads as

$$\Pi_{\Gamma\Gamma'}^A = i \int d^4x e^{ip_e \cdot x} \langle 0 | T \{ \bar{\chi}_t(0) \mathcal{Q}_{\Gamma\Gamma'}^A(x) \} | D^0(v) \rangle \quad (5.8)$$

where $\mathcal{Q}_{\Gamma\Gamma'}^A(x) = \epsilon^{ijk} (d_i^T C P_{\Gamma} \Gamma_A u_j) (P_{\Gamma'} \Gamma^A c_k)$, and $\bar{\chi}_t(0) = \chi_t^\dagger \gamma_0$ with $\chi_t(x) = [\epsilon^{lmn} (u_l^T(x) C \gamma_5 d_m(x)) u_n(x)] + t [\epsilon^{lmn} (u_l^T(x) C d_m(x)) \gamma_5 u_n(x)]$ being the proton interpolation current defined such that $\langle \bar{p}(p_p) | \chi_t(0) | 0 \rangle = m_p \lambda_p^t v_p(p_p)$ where, λ_p^t is a measure of the strength with which this current couples with the proton/antiproton state. $\{i,j,k\}$ denote the color indices.

To derive the sum rule from this correlation function, we require the two representation for this correlation function. First using the perturbative QCD in terms of OPE near the light cone and second directly in terms of the hadronic state resulting into the dispersion relation (as discussed in Chapter-2). In order to derive a representation directly in terms of hadronic states, we insert a complete set of intermediate states with the relevant quantum numbers. Once we separate the pole contribution coming from the lowest proton state, we get,

$$\begin{aligned} \Pi_{\Gamma\Gamma'}^{A, had} &= -m_p \lambda_p \bar{v}_p(p_p) [H_{\Gamma\Gamma'}] v_p(p_p) + \dots \\ &= iP_{\Gamma'} \left[\Pi_{\Gamma\Gamma'}^{A,S}(p_p^2, p_e^2) + \Pi_{\Gamma\Gamma'}^{A,V}(p_p^2, p_e^2) \not{p} + \Pi_{\Gamma\Gamma'}^{A,P}(p_p^2, p_e^2) \frac{\not{p}_p}{m_p} + \Pi_{\Gamma\Gamma'}^{A,VP}(p_p^2, p_e^2) \frac{\not{p} \not{p}_p}{m_p} \right] \end{aligned} \quad (5.9)$$

where ellipses represents are contribution of the heavier and continuum, $\Pi_{\Gamma\Gamma'}^{A,r}$ are the hadronic scalar function of p_p^2 and $P_e^2 = -p_e^2$ with $r = \{S, V, P, VP\}$. These functions can then be written in terms of the spectral densities which are related to the imaginary part of these functions itself. Explicitly, these spectral densities can be written as

$$\rho_{\Gamma\Gamma'}^{A,r, had}(s, P_e^2) = \lambda_p m_p^2 \delta(s - m_p^2) F_{\Gamma\Gamma'}^{A,r}(s, P_e^2) + \frac{1}{\pi} \text{Im} \left(\Pi_{\Gamma\Gamma'}^{A,r}(s, P_e^2) \right) \quad (5.10)$$

where, the first term corresponds to the pole contribution coming from the lowest energy state, i.e. the proton and the second term corresponds to the contribution of the heavier states and the continuum. $F_{\Gamma\Gamma'}^{A,r}(s, P_e^2)$ in the first terms are the

residues of the lowest energy states. These are the objects which we can compute using LCSR and are directly related to the form factors defined in Eqn.(5.6) i.e. $F_{\Gamma\Gamma'}^{A,n}(s, P_e^2)$ for the on-shell proton, i.e. $s = m_p^2$ as

$$\begin{aligned} -F_{\Gamma\Gamma'}^{A,S} &= F_{\Gamma\Gamma'}^{A,P} = F_{\Gamma\Gamma'}^{A,0} \\ -F_{\Gamma\Gamma'}^{A,V} &= F_{\Gamma\Gamma'}^{A,VP} = F_{\Gamma\Gamma'}^{A,1} \end{aligned} \quad (5.11)$$

Using the spectral density defined in Eqn.(5.10), the final dispersion relation for the hadronic scalar functions in Eqn.(5.9) reads as

$$\Pi_{\Gamma\Gamma'}^{A,r}(p_p^2, P_e^2) = \lambda_p m_p^2 \frac{F_{\Gamma\Gamma'}^{A,r}}{m_p^2 - p_p^2} + \int_{s_0^h}^{\infty} ds \frac{1}{\pi} \frac{\text{Im} \left(\Pi_{\Gamma\Gamma'}^{A,r}(s, P_e^2) \right)}{s - p_p^2} \quad (5.12)$$

where, s_0^h is the continuum threshold. The second term, coming from the heavier states and the continuum, can then be approximated using the quark hadron duality (see Section-2.1.1) according to which

$$\int_{s_0^h}^{\infty} ds \frac{1}{\pi} \frac{\text{Im} \left(\Pi_{\Gamma\Gamma'}^{A,r}(s, P_e^2) \right)}{s - p_p^2} \approx \int_{s_0}^{\infty} ds \frac{1}{\pi} \frac{\text{Im} \left(\Pi_{\Gamma\Gamma'}^{A,r,QCD}(s, P_e^2) \right)}{s - p_p^2} \quad (5.13)$$

where s_0 is also known as the continuum threshold and is not necessarily equals to s_0^h . We will discuss more about it in Section-5.4. $\Pi_{\Gamma\Gamma'}^{A,r,QCD}$ are the scalar functions (p_p^2 and P_e^2) to be calculated in perturbative QCD. We will discuss them below.

Now, after discussing the representation in terms of the hadronic states, we move to the representation which is calculated using perturbative QCD. To proceed further in this direction, we first need to solve the time ordered product of $\mathcal{Q}_{\Gamma\Gamma'}^A(x)$ and $\bar{\chi}_t(0)$ by contracting the fields and results into (see Fig. (5.1))

$$\begin{aligned} T \{ \bar{\chi}_t(0) \mathcal{Q}_{\Gamma\Gamma'}^A(x) \} &= -\epsilon^{lmn} \epsilon^{ijk} \left[(P_{\Gamma'} \Gamma^A c_i(x)) \left\{ \left(\bar{u}_l(0) \gamma_5 \tilde{S}_{mj}^d(x) P_{\Gamma} \Gamma_A S_{nk}^u(x) \right. \right. \right. \\ &\quad \left. \left. \left. + \bar{u}_l(0) \text{Tr} \left(\gamma_5 \tilde{S}_{mj}^d(x) P_{\Gamma} \Gamma_A S_{nk}^u(x) \right) \right) \right. \right. \\ &\quad \left. \left. + t \left(\bar{u}_l(0) \tilde{S}_{mj}^d(x) P_{\Gamma} \Gamma_A S_{nk}^u(x) \gamma_5 \right. \right. \right. \\ &\quad \left. \left. \left. + \bar{u}_l(0) \gamma_5 \text{Tr} \left(\tilde{S}_{mj}^d(x) P_{\Gamma} \Gamma_A S_{nk}^u(x) \right) \right) \right\} \right] \quad (5.14) \end{aligned}$$

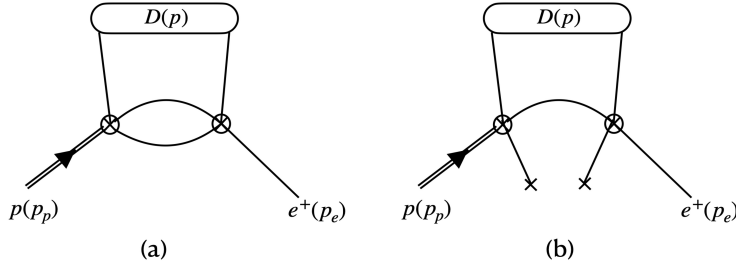


Figure 5.1: Feynman diagrams contributing to the light-cone expansion of the correlation function for $D^0 \rightarrow \bar{p}e^+$ decay to the leading order. The encircled D represents that the distribution amplitudes for D-meson enters the LCSR computation. The vertex on the left represents the proton interpolation current while the vertex on the right represents the dim-6 BNV operators. (a) represents the usual non-condensate contribution while (b) represents the considered contribution coming from the condensates.

where $\tilde{\Gamma} = CTC^{-1}$ and $S_{ij}^q(x)$ is the quark propagator at the light like separations given in Eqn.(4.28) and Eqn.(4.30), respectively. In the present analysis, we do not involve the contributions coming from the higher terms in the propagator due to one of more gluon emissions. Substituting it back in Eqn.(5.8), we end up having the matrix element of the quark bilinear between a vacuum and the D^0 -meson state. Such a bilinear is can be defined in terms of light cone distribution amplitudes (DAs) of D-meson as [146]

$$\begin{aligned} & \langle 0 | \bar{u}_\alpha(0)[x, 0]c_\beta(x) | D^0(v) \rangle \\ &= \frac{-if_D m_D}{4} \int_0^\infty dw e^{i w v \cdot x} \left[(1 + \not{x}) \left\{ \phi_+^D(w) - \frac{\phi_+^D(w) - \phi_-^D(w)}{2v \cdot x} \not{x} \right\} \gamma_5 \right]_{\beta\alpha} \end{aligned} \quad (5.15)$$

where f_D represents the decay constant of D-meson, $\phi_+^D(w)$ and $\phi_-^D(w)$ are the DAs of D-meson. These DAs are not very-well known and are parameterized using various models (see Appendix-B for details). For the present discussion we take the simplest exponential model parameterization for these DAs [72] which reads as

$$\phi_+^D(w) = \frac{1}{w_0^2} e^{-w/w_0}, \quad \phi_-^D(w) = \frac{1}{w_0} e^{-w/w_0} \quad (5.16)$$

where, w_0 is a model input parameter (we will discuss more about it below). Also, it is useful to define $\Phi_{\pm}^D(w)$ as

$$\Phi_{\pm}^D(w) = \int_0^w dt (\phi_+^D(t) - \phi_-^D(t)) \quad (5.17)$$

such that

$$\Phi_{\pm}^D(0) = \Phi_{\pm}^D(\infty) = 0, \text{ and } \frac{d\Phi_{\pm}^D(w)}{dw} = \phi_+^D(w) - \phi_-^D(w). \quad (5.18)$$

This definition along with the partial integral helps us in writing

$$\int_0^{\infty} dw e^{-i w v \cdot x} \frac{\phi_+^D(w) - \phi_-^D(w)}{2v \cdot x} = \frac{i}{2} \int_0^{\infty} dw e^{-i w v \cdot x} \Phi_{\pm}^D(w). \quad (5.19)$$

Finally, using the above definitions and the integrals collected in Appendix-A, we get the QCD representation of the correlation function defined in Eqn.(5.8) as

$$\begin{aligned} \Pi_{\Gamma\Gamma'}^{A,QCD} = i P_{\Gamma'} \left[\Pi_{\Gamma\Gamma'}^{A,S,QCD}(p_p^2, p_e^2) + \Pi_{\Gamma\Gamma'}^{A,V}(p_p^2, p_e^2) \not{v} + \Pi_{\Gamma\Gamma'}^{A,P}(p_p^2, p_e^2) \frac{\not{p}_p}{m_p} \right. \\ \left. + \Pi_{\Gamma\Gamma'}^{A,VP}(p_p^2, p_e^2) \frac{\not{v}\not{p}_p}{m_p} \right] \end{aligned} \quad (5.20)$$

Here, $\Pi_{\Gamma\Gamma'}^{A,S,QCD}(p_p^2, p_e^2)$ with $r = \{S, V, P, VP\}$ are the scalar functions of p_p^2 and p_e^2 that entered in Eqn.(5.13). The explicit forms for these function for $P_{\Gamma} = P_{\Gamma'} = P_L$, and $P_{\Gamma} = P_L$ and $P_{\Gamma'} = P_R$ are collected below (the choice we make for the independent form factors).

5.3.1 Case-1: $P_{\Gamma} = P_{\Gamma'} = P_L$

- For $\Gamma^A = 1$

$$\begin{aligned} \Pi_{LL}^{S,S} = \frac{f_D m_D}{8} \int_0^{\infty} dw \left[\frac{(t-1)}{4\pi^2} \{ (w + m_D) \Phi_{\pm}^D(w) + P^2 \phi_+^D(w) \} \ln(-P^2) \right. \\ \left. + \frac{\langle \bar{q}q \rangle (t-1)}{3} \left\{ \frac{(w + m_D) \phi_+^D(w)}{P^2} + \frac{\Phi_{\pm}^D(w)}{P^2} \right\} \right] \end{aligned} \quad (5.21)$$

$$\begin{aligned} \Pi_{LL}^{S,V} &= \frac{f_D m_D}{8} \int_0^\infty dw \left[\frac{3(t+1)}{8\pi^2} \{ (w+m_D)\Phi_\pm^D(w) + P^2\phi_+^D(w) \} \ln(-P^2) \right. \\ &\quad \left. - \frac{\langle \bar{q}q \rangle (t-1)}{3} \left\{ \frac{(w+m_D)\phi_+^D(w)}{P^2} + \frac{\Phi_\pm^D(w)}{P^2} \right\} \right] \end{aligned} \quad (5.22)$$

$$\Pi_{LL}^{S,P} = -m_p \frac{f_D m_D}{8} \int_0^\infty dw \left[\frac{3(t+1)}{8\pi^2} \Phi_\pm^D(w) \ln(-P^2) - \frac{\langle \bar{q}q \rangle (t-1)}{3} \frac{\phi_+^D(w)}{P^2} \right] \quad (5.23)$$

$$\Pi_{LL}^{S,VP} = -m_p \frac{f_D m_D}{8} \int_0^\infty dw \left[\frac{(t-1)}{4\pi^2} \Phi_\pm^D(w) \ln(-P^2) + \frac{\langle \bar{q}q \rangle (t-1)}{3} \frac{\phi_+^D(w)}{P^2} \right] \quad (5.24)$$

- For $\Gamma^A = \gamma_\mu$

$$\begin{aligned} \Pi_{LL}^{V,S} &= \frac{f_D m_D}{4} \int_0^\infty dw \left[\frac{(t-1)}{8\pi^2} \{ (w+m_D)\Phi_\pm^D(w) + P^2\phi_+^D(w) \} \ln(-P^2) \right. \\ &\quad \left. + \frac{\langle \bar{q}q \rangle}{3} \left\{ \frac{(t-1)\Phi_\pm^D(w)}{P^2} + \frac{(3+t)(w+m_D)\phi_+^D(w)}{P^2} - \frac{4(v.P)\phi_+^D(w)}{P^2} \right\} \right] \end{aligned} \quad (5.25)$$

$$\Pi_{LL}^{V,V} = -\frac{f_D m_D \langle \bar{q}q \rangle}{12} \int_0^\infty dw \left[\frac{(3+t)\Phi_\pm^D(w)}{P^2} - \frac{(w+m_D)}{P^2} \{ 2\phi_-^D(w) - (t+1)\phi_+^D(w) \} \right] \quad (5.26)$$

$$\Pi_{LL}^{V,P} = -m_p \frac{f_D m_D \langle \bar{q}q \rangle}{12} \int_0^\infty dw \left[\frac{1}{P^2} \{ 2\phi_-^D(w) - (t+1)\phi_+^D(w) \} \right] \quad (5.27)$$

$$\Pi_{LL}^{V,VP} = -m_p \frac{f_D m_D}{4} \int_0^\infty dw \left[\frac{(t-1)}{8\pi^2} \Phi_\pm^D(w) \ln(-P^2) + \frac{\langle \bar{q}q \rangle (t+3)}{3} \frac{\phi_+^D(w)}{P^2} \right] \quad (5.28)$$

- For $\Gamma^A = \sigma_{\mu\nu}$

$$\Pi_{LL}^{T,S} = \frac{f_D m_D \langle \bar{q}q \rangle (t-1)}{6} \int_0^\infty dw \left[\frac{1}{P^2} \{ 4\phi_+^D(w)(v.P - (w + m_D)) + 3\Phi_\pm^D(w) \} \right] \quad (5.29)$$

$$\begin{aligned} \Pi_{LL}^{T,V} = & \frac{f_D m_D}{2} \int_0^\infty dw \left[\frac{(t+1)}{4\pi^2} \left\{ \frac{\phi_+^D(w)}{6} (4(w + m_D)(v.P) - P^2) \right. \right. \\ & \left. \left. + \frac{3}{2} \Phi_\pm^D(w)(w + m_D) \right\} \ln(-P^2) - \frac{\langle \bar{q}q \rangle (t-1)}{3} \right. \\ & \left. \times \left\{ \frac{(w + m_D)(\phi_+^D(w) + 2\phi_-^D(w))}{P^2} - \frac{\Phi_\pm^D(w)}{P^2} \right\} \right] \quad (5.30) \end{aligned}$$

$$\begin{aligned} \Pi_{LL}^{T,P} = & -m_p \frac{f_D m_D}{2} \int_0^\infty dw \left[\frac{(t+1)}{4\pi^2} \left\{ \frac{3}{2} \Phi_\pm^D(w) + \frac{2(v.P)}{3} \phi_+^D(w) \right\} \ln(-P^2) \right. \\ & \left. - \frac{\langle \bar{q}q \rangle (t-1)}{3} \left\{ \frac{(\phi_+^D(w) + 2\phi_-^D(w))}{P^2} \right\} \right] \quad (5.31) \end{aligned}$$

$$\Pi_{LL}^{T,VP} = m_p \frac{f_D m_D \langle \bar{q}q \rangle (t-1)}{6} \int_0^\infty dw \left[\frac{\phi_+^D(w)}{P^2} \right] \quad (5.32)$$

5.3.2 Case-2: $P_\Gamma = P_L$ and $P'_\Gamma = P_R$

- For $\Gamma^A = 1$

$$\begin{aligned} \Pi_{LR}^{S,S} = & \frac{f_D m_D}{8} \int_0^\infty dw \left[\frac{3(t+1)}{8\pi^2} \{ (w + m_D)\Phi_\pm^D(w) + P^2\phi_+^D(w) \} \ln(-P^2) \right. \\ & \left. - \frac{\langle \bar{q}q \rangle (t-1)}{3} \left\{ \frac{(w + m_D)\phi_+^D(w)}{P^2} + \frac{\Phi_\pm^D(w)}{P^2} \right\} \right] \quad (5.33) \end{aligned}$$

$$\begin{aligned} \Pi_{LR}^{S,V} = & \frac{f_D m_D}{8} \int_0^\infty dw \left[\frac{(t-1)}{4\pi^2} \{ (w + m_D)\Phi_\pm^D(w) + P^2\phi_+^D(w) \} \ln(-P^2) \right. \\ & \left. + \frac{\langle \bar{q}q \rangle (t-1)}{3} \left\{ \frac{(w + m_D)\phi_+^D(w)}{P^2} + \frac{\Phi_\pm^D(w)}{P^2} \right\} \right] \quad (5.34) \end{aligned}$$

$$\Pi_{LR}^{S,P} = -m_p \frac{f_D m_D}{8} \int_0^\infty dw \left[\frac{(t-1)}{4\pi^2} \Phi_\pm^D(w) \ln(-P^2) + \frac{\langle \bar{q}q \rangle (t-1)}{3} \frac{\phi_+^D(w)}{P^2} \right] \quad (5.35)$$

$$\Pi_{LR}^{S,VP} = -m_p \frac{f_D m_D}{8} \int_0^\infty dw \left[\frac{3(t+1)}{8\pi^2} \Phi_\pm^D(w) \ln(-P^2) - \frac{\langle \bar{q}q \rangle (t-1)}{3} \frac{\phi_+^D(w)}{P^2} \right] \quad (5.36)$$

- For $\Gamma^A = \gamma_\mu$

$$\Pi_{LR}^{V,S} = \frac{f_D m_D \langle \bar{q}q \rangle}{12} \int_0^\infty dw \left[\frac{\phi_+^D(w)}{P^2} \{ (w + m_D) - (t+3)(v.P) \} - \frac{(t+2)\Phi_\pm^D(w)}{P^2} \right] \quad (5.37)$$

$$\begin{aligned} \Pi_{LR}^{V,V} = & -\frac{f_D m_D}{4} \int_0^\infty dw \left[\frac{(t-1)}{4\pi^2} \{ (w + m_D) \Phi_\pm^D(w) \right. \\ & \left. + \frac{\phi_+^D(w)}{6} (P^2 + 2(v.P)(w + m_D)) \right] \ln(-P^2) \\ & - \frac{\langle \bar{q}q \rangle}{3} \left\{ \frac{(w + m_D)}{P^2} (\phi_-^D(w)(t+3) + \phi_+^D(w)(t+1)) - \frac{\Phi_\pm^D(w)}{P^2} \right\} \end{aligned} \quad (5.38)$$

$$\begin{aligned} \Pi_{LR}^{V,P} = & m_p \frac{f_D m_D}{4} \int_0^\infty dw \left[\frac{(t-1)}{4\pi^2} \left\{ \frac{\phi_+^D(w)(v.P)}{3} + \Phi_\pm^D(w) \right\} \ln(-P^2) \right. \\ & \left. - \frac{\langle \bar{q}q \rangle}{3P^2} \{ \phi_-^D(w)(t+3) + \phi_+^D(w)(t+1) \} \right] \end{aligned} \quad (5.39)$$

$$\Pi_{LR}^{V,VP} = -m_p \frac{f_D m_D \langle \bar{q}q \rangle}{6} \int_0^\infty dw \frac{\phi_+^D(w)}{P^2} \quad (5.40)$$

- For $\Gamma^A = \sigma_{\mu\nu}$: All the correlation functions turns out to be zero.

with

$$\begin{aligned} P^2 &= (p_e + wv)^2 = ((w + m_D)v - p_p)^2 \\ &= w(w + m_D) - \frac{ws}{m_D} - \left(\frac{w + m_D}{m_D} \right) P_e^2 \end{aligned} \quad (5.41)$$

such that $s = p_p^2$ and $P_e^2 = -p_e^2$. Also, as $v^2 = 1$

$$\begin{aligned} (v.P) &= -(v.p_p - (w + m_D)) \\ &= \frac{2w + m_D}{2} - \frac{s + P_e^2}{2m_D}. \end{aligned} \quad (5.42)$$

Finally, after having both the representation given in Eqn.(5.12) and Eqn.(5.20) for the correlation function defined in Eqn.(5.8), we are ready to write the sum rule for the present case. It can be written by equating the two representations and using the statement of quark hadron duality given in Eqn.(5.13) to approximate the heavier states and continuum contributions. The final statement of the sum rule can then be written by performing Borel transformation to suppress the effect of these heavier states and continuum such that the sum rule is saturated with the lowest proton state. The final sum rule reads as,

$$F_{\Gamma\Gamma'}^{A,r}(P_e^2, s_0, M^2) = -\frac{e^{\frac{m_p^2}{M^2}}}{m_p^2 \lambda_p} \int_0^{s_0} ds e^{\frac{-s}{M^2}} \frac{1}{\pi} \text{Im} \left(\Pi_{\Gamma\Gamma'}^{A,r,QCD}(s, P_e^2) \right) \quad (5.43)$$

where M is the Borel mass. We will now discuss how to choose the values of M and s_0 and use them to get the numerical estimates for the form factors.

5.4 Results

The BNV process $D^0 \rightarrow \bar{p}e^+$ is found to involve twelve independent FFs. The analytic form of these form factors can be obtained using the sum rule for $F_{\Gamma\Gamma'}^{A,r}$ given in Eqn.(5.11) and the relations given in Eqn.(5.11). These FFs turns out to be dependent on two independent parameter, s_0 and M known as the continuum threshold and the Borel mass, respectively, and the momentum transferred square, $P_e^2 = -p_e^2$. The sum rule in Eqn.(5.43) is derived using the light cone

DAs of the D-meson and using a general interpolation current for the proton interpolation current. Now, in order to understand the dependence of these FFs on the choice of interpolation current, let us choose two different choices of this current namely, χ_{LA} and χ_{IO} defined in Eqn.(4.12) and Eqn.(4.14), respectively. These are the usually considered forms of proton interpolation current in lattice QCD and LCSR calculations (as discussed in previous chapter).

Moreover, in order to perform the numerical analysis, we need information on the values of s_0 and M . The values of these parameters are to be chosen such that the sum rule is saturated with the ground state contribution and the contribution coming from the continuum and the higher resonances should be well suppressed such that they do not contribute more than 30% to the result (see Chapter-2 for details). The value of s_0 must be close to the threshold of the continuum or the higher resonances such that the sum rule obtained is stable around its vicinity. we choose $s_0 = (1.44 \text{ GeV})^2$, the Roper resonance and show the dependence of FFs on s_0 by considering three different values of it in Figs.(5.2-5.5) for fixed $M = 2 \text{ GeV}$. This is the next resonance state after proton with the quantum numbers of the proton state. The form factors are found to have very small dependence on the variation of the value of s_0 in the vicinity of the Roper resonance. Moreover, for the value of M we find a range called Borel window such that the form factor is nearly stable in that range of M (as discussed in Chapter-2). We find these FFs to be most stable for $M^2 > 2 \text{ GeV}^2$ and show the Borel stability curves in the right panels of Figs.(5.2-5.5) where these FFs are plotted against the variation in $M^2 = (2 - 5) \text{ GeV}^2$ for three different values of P_e^2 equals to 0.1 GeV^2 , 0.5 GeV^2 , and 1 GeV^2 with fixed $s_0 = (1.44 \text{ GeV})^2$. The FFs are found to be very stable in this Borel window for all the sets.

As can be seen from Eqn.(5.11), each form factor can be calculated from two $F_{\Gamma\Gamma'}^{A,r}$ with $A = \{S, V, T\}$ and $r = \{S, V, P, VP\}$. In Fig.(5.2) and Fig.(5.3), we have shown the form factors $F_{LL}^{A,n}$ and $F_{LR}^{A,n}$, respectively with $n = 0, 1$ and $A = \{S, V, T\}$ using both combinations of $F_{LL}^{A,r}$ with $A = \{S, V, T\}$ and $r = \{S, V, P, VP\}$ and the χ_{IO} interpolation current for the proton state. Similarly, in Fig.(5.4) and Fig.(5.5), we show the FFs $F_{LL}^{A,n}$ and $F_{LR}^{A,n}$, respectively with $n = 0, 1$ and $A = \{S, V, T\}$ using both combinations of $F_{LL}^{A,r}$ with $A = \{S, V, T\}$

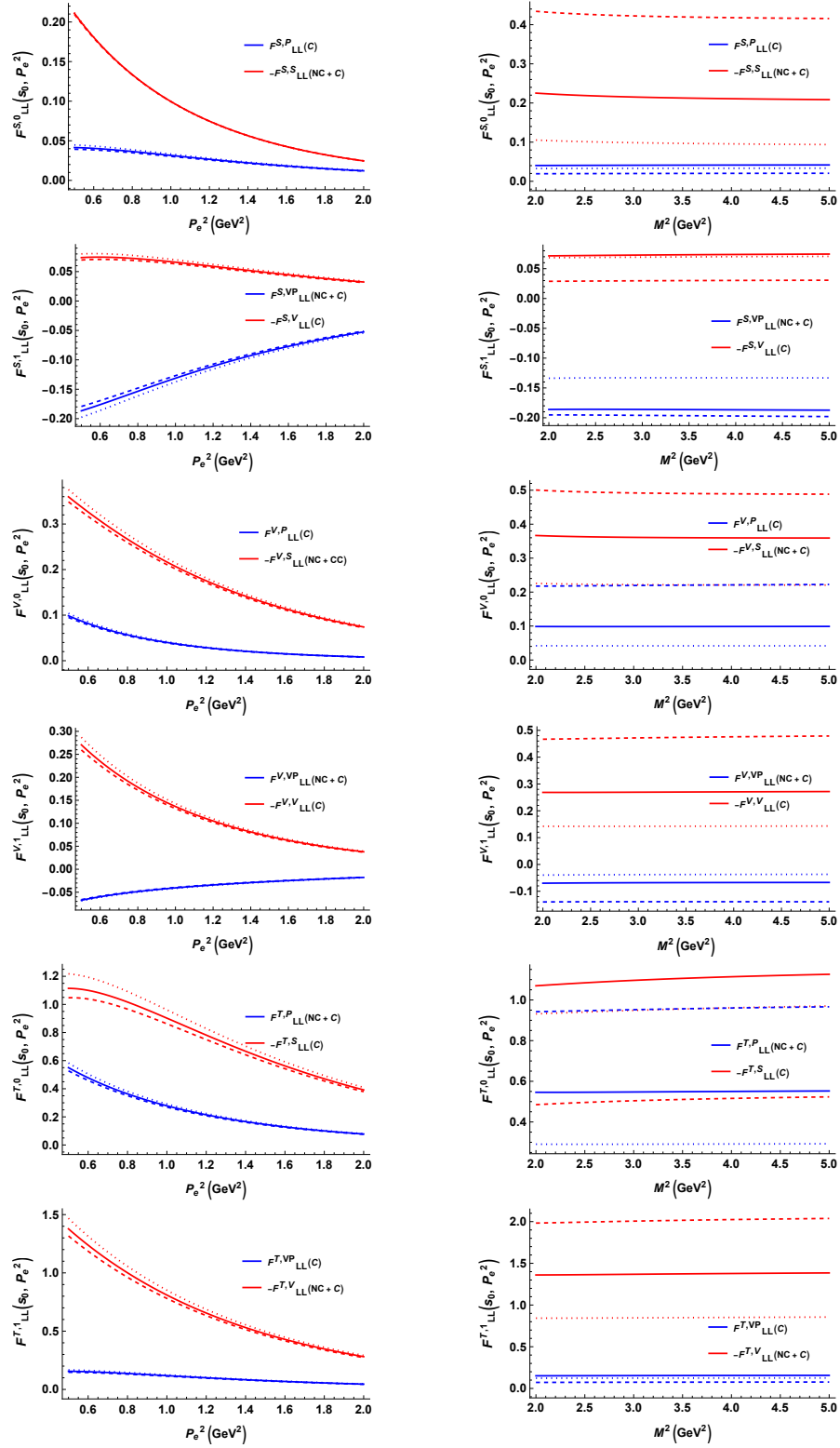


Figure 5.2: The FFs, $F_{LL}^{A,n}$ with $A \in \{S, V, T\}$ and $n \in \{0, 1\}$ are extracted from different combinations of $F_{LL}^{A,r}$ with $r \in \{S, V, P, VP\}$ using the proton interpolation current χ_{IO} . Left panel: We plot $F_{LL}^{A,n}$ vs P_e^2 for $s_0 = (1.4 \text{ GeV})^2$ (dashed), $s_0 = (1.44 \text{ GeV})^2$ (solid) and $s_0 = (1.5 \text{ GeV})^2$ (dotted) with $M = 2 \text{ GeV}$. Right panel: We plot $F_{LL}^{A,n}$ vs M^2 for $P_e^2 = 0.1 \text{ GeV}^2$ (dashed), $P_e^2 = 0.5 \text{ GeV}^2$ (solid) and $P_e^2 = 1 \text{ GeV}^2$ (dotted) with $s_0 = (1.44 \text{ GeV})^2$.

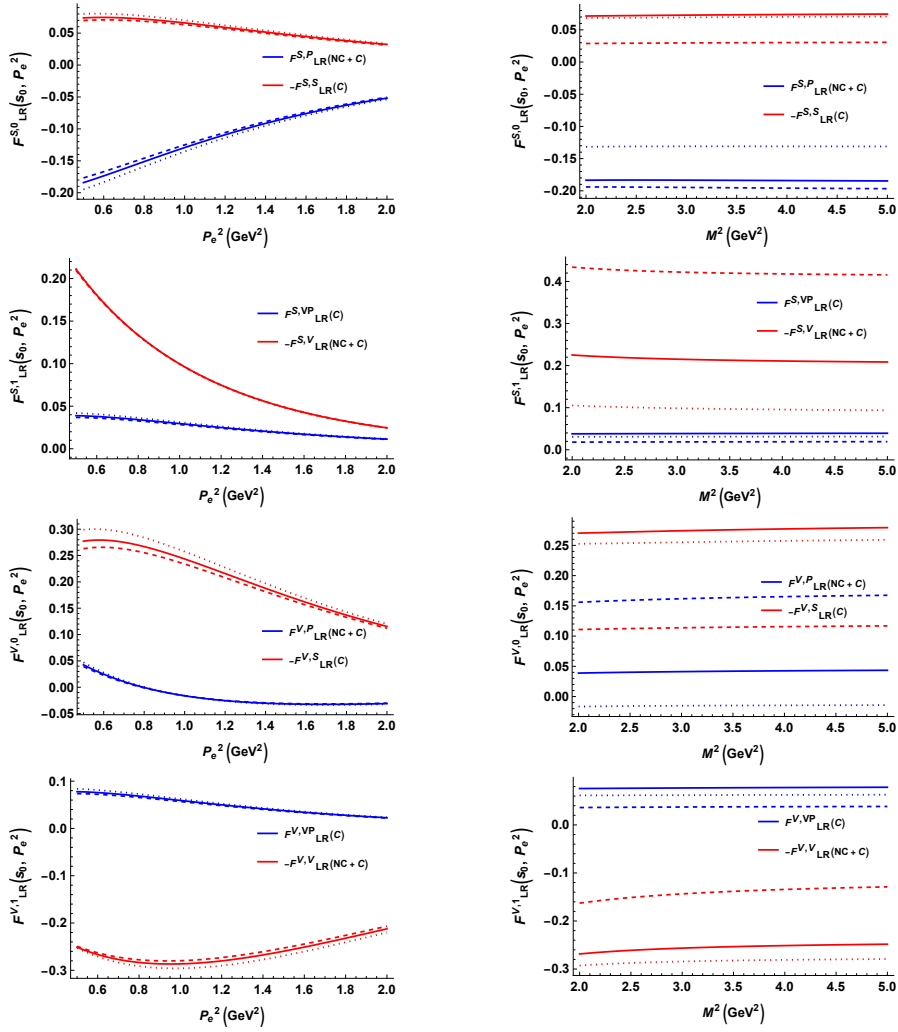
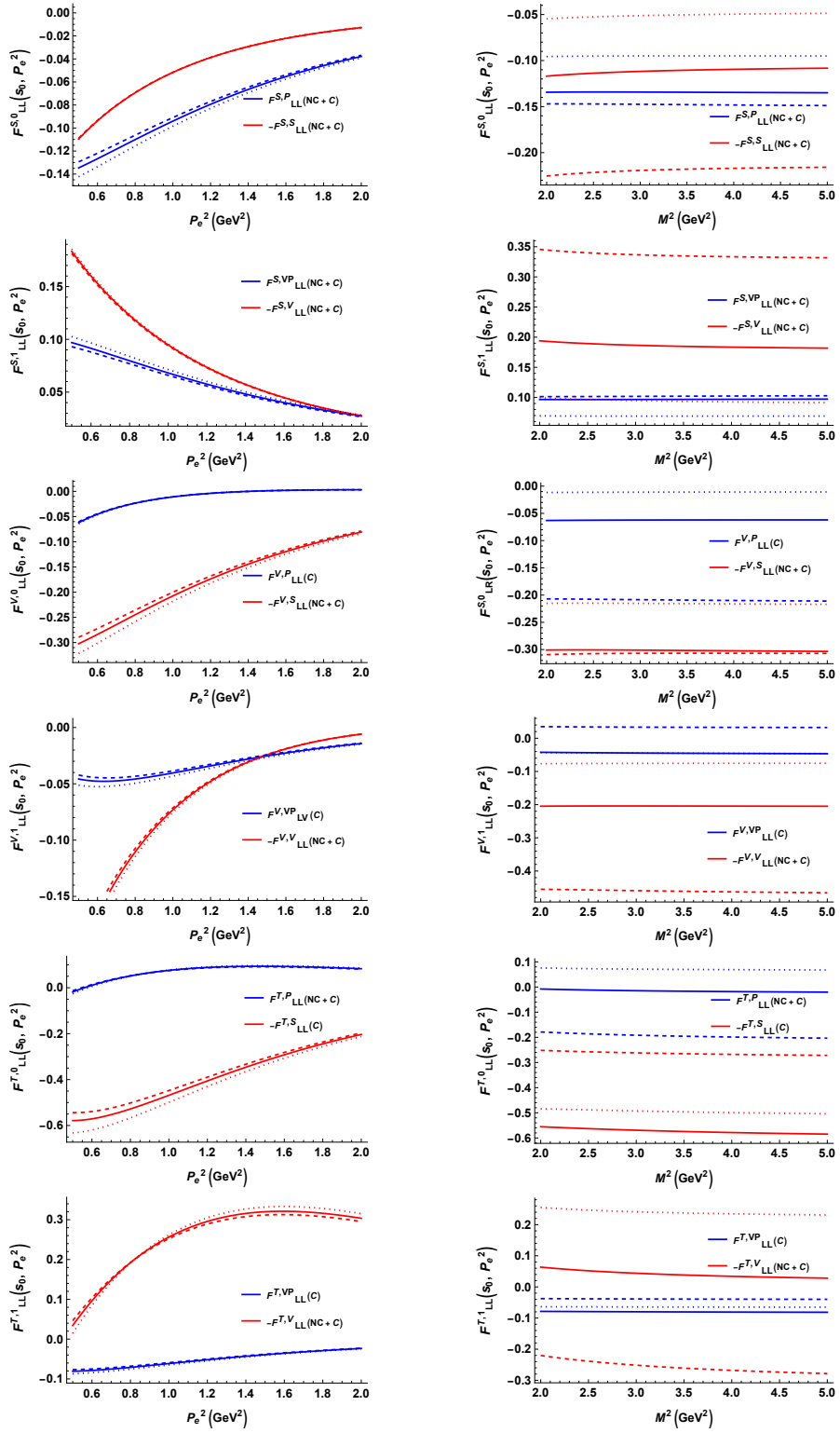


Figure 5.3: Same as Fig.(1) for $F_{LR}^{A,n}$ extracted from $F_{LR}^{A,r}$.

Figure 5.4: Same as Fig.(1) but for interpolation current, χ_{LA} .

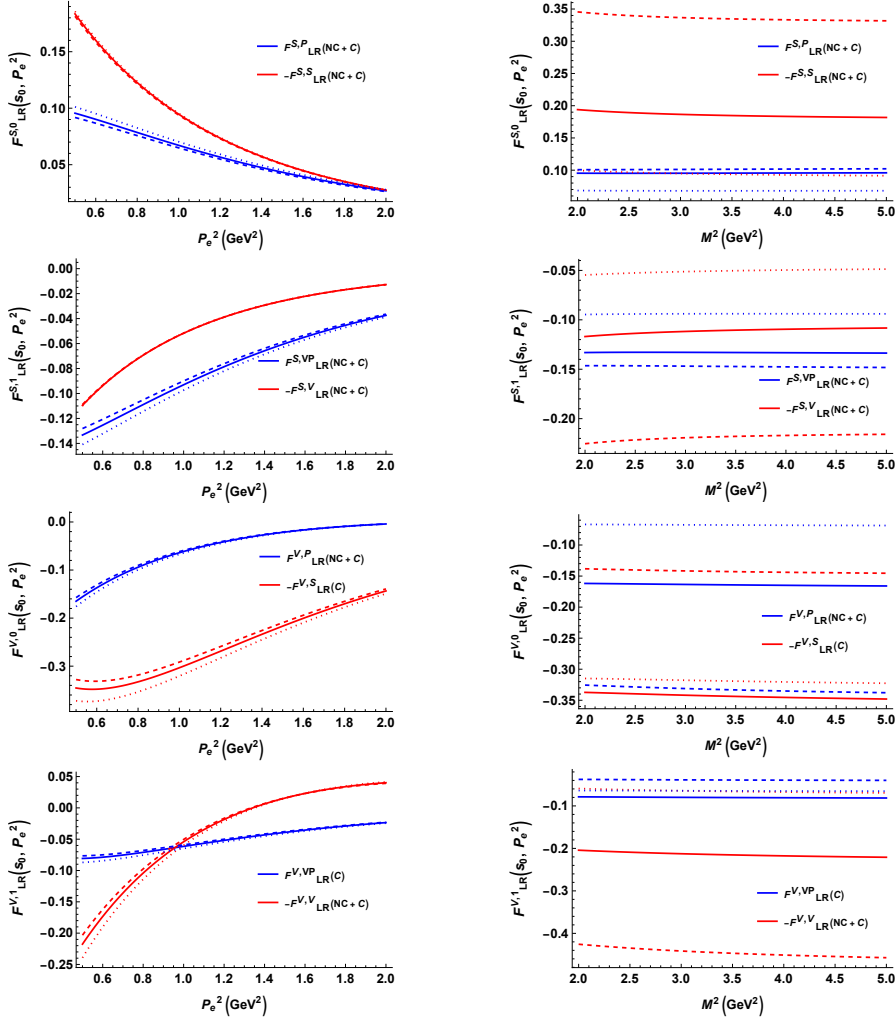


Figure 5.5: Same as Fig.(3) for $F_{LR}^{A,n}$ extracted from $F_{LR}^{A,r}$.

and $r = \{S, V, P, VP\}$ and the χ_{LA} interpolation current for the proton state. It is important to note that some of these $F_{\Gamma\Gamma'}^{A,r}$ get contributions only from the condensate terms due to which we found the difference in the extraction of the FFs using different combinations of $F_{\Gamma\Gamma'}^{A,r}$. In Figs.(5.2-5.5), we have labelled these different combinations with (C) and (NC+C) for having only the condensate contribution and having condensate as well as non-condensate contributions, respectively.

Furthermore we tabulate these form factors in Table-5.1 and Table-5.2 for χ_{IO} and χ_{LA} , respectively at $P_e^2 = 0.5 \text{ GeV}^2$, $s_0 = (1.44 \text{ GeV})^2$, and $M = 2 \text{ GeV}$. Two FFs, $F_{LR}^{T,0}$ and $F_{LR}^{T,1}$ are found to be explicitly zero in our analysis. The uncertainties in Table-5.1 and Table-5.2 are associated with the uncertainties in the values of the parameters used for the numerical analysis (collected in Appendix-

Case-1: ($P_T = P_{T'} = P_L$)			Case-2: ($P_T = P_L, P_{T'} = P_R$)		
Form Factor	Extracted from	Value (GeV) ²	Form Factor	Extracted from	Value (GeV) ²
$F_{LL}^{S,0}$	$F_{LL}^{S,S}$	0.211 ± 0.471	$F_{LR}^{S,0}$	$F_{LR}^{S,S}$	-0.106 ± 0.075
	$F_{LL}^{S,P}$	0.041 ± 0.036		$F_{LR}^{S,P}$	0.074 ± 0.143
$F_{LL}^{S,1}$	$F_{LL}^{S,V}$	0.074 ± 0.075	$F_{LR}^{S,1}$	$F_{LR}^{S,V}$	0.211 ± 0.471
	$F_{LL}^{S,VP}$	-0.187 ± 0.144		$F_{LR}^{S,VP}$	0.039 ± 0.033
$F_{LL}^{V,0}$	$F_{LL}^{V,S}$	0.360 ± 0.467	$F_{LR}^{V,0}$	$F_{LR}^{V,S}$	0.277 ± 0.227
	$F_{LL}^{V,P}$	0.099 ± 0.036		$F_{LR}^{V,P}$	0.043 ± 0.077
$F_{LL}^{V,1}$	$F_{LL}^{V,V}$	0.271 ± 0.097	$F_{LR}^{V,1}$	$F_{LR}^{V,V}$	-0.251 ± 0.341
	$F_{LL}^{V,VP}$	-0.067 ± 0.154		$F_{LR}^{V,VP}$	0.078 ± 0.067
$F_{LL}^{T,0}$	$F_{LL}^{T,S}$	1.114 ± 0.812	$F_{LR}^{T,0}$	$F_{LR}^{T,S}$	0
	$F_{LL}^{T,P}$	0.550 ± 0.256		$F_{LR}^{T,P}$	0
$F_{LL}^{T,1}$	$F_{LL}^{T,V}$	1.378 ± 0.629	$F_{LR}^{T,1}$	$F_{LR}^{T,V}$	0
	$F_{LL}^{T,VP}$	0.156 ± 0.133		$F_{LR}^{T,VP}$	0

Table 5.1: Tabulation of all the 12 independent FFs at $P_e^2 = 0.5 \text{ GeV}^2$ for $s_0 = (1.44 \text{ GeV})^2$ and $M = 2 \text{ GeV}$ calculated using the proton interpolation current χ_{IO} . The errors are associated with the errors in the parameters used for the numerical analysis.

Case-1: ($P_T = P_{T'} = P_L$)			Case-2: ($P_T = P_L, P_{T'} = P_R$)		
Form Factor	Extracted from	Value (GeV) ²	Form Factor	Extracted from	Value (GeV) ²
$F_{LL}^{S,0}$	$F_{LL}^{S,S}$	-0.110 ± 0.244	$F_{LR}^{S,0}$	$F_{LR}^{S,S}$	0.183 ± 0.363
	$F_{LL}^{S,P}$	-0.135 ± 0.109		$F_{LR}^{S,P}$	0.096 ± 0.074
$F_{LL}^{S,1}$	$F_{LL}^{S,V}$	0.183 ± 0.363	$F_{LR}^{S,1}$	$F_{LR}^{S,V}$	-0.110 ± 0.244
	$F_{LL}^{S,VP}$	0.097 ± 0.074		$F_{LR}^{S,VP}$	-0.133 ± 0.109
$F_{LL}^{V,0}$	$F_{LL}^{V,S}$	-0.302 ± 0.268	$F_{LR}^{V,0}$	$F_{LR}^{V,S}$	-0.345 ± 0.270
	$F_{LL}^{V,P}$	-0.062 ± 0.026		$F_{LR}^{V,P}$	-0.165 ± 0.088
$F_{LL}^{V,1}$	$F_{LL}^{V,V}$	-0.204 ± 0.072	$F_{LR}^{V,1}$	$F_{LR}^{V,V}$	0.218 ± 0.257
	$F_{LL}^{V,VP}$	-0.046 ± 0.125		$F_{LR}^{V,VP}$	0.081 ± 0.068
$F_{LL}^{T,0}$	$F_{LL}^{T,S}$	-0.578 ± 0.414	$F_{LR}^{T,0}$	$F_{LR}^{T,S}$	0
	$F_{LL}^{T,P}$	-0.018 ± 0.152		$F_{LR}^{T,P}$	0
$F_{LL}^{T,1}$	$F_{LL}^{T,V}$	-0.081 ± 0.405	$F_{LR}^{T,1}$	$F_{LR}^{T,V}$	0
	$F_{LL}^{T,VP}$	0.034 ± 0.068		$F_{LR}^{T,VP}$	0

Table 5.2: Tabulation of all the 12 independent FFs at $P_e^2 = 0.5 \text{ GeV}^2$ for $s_0 = (1.44 \text{ GeV})^2$ and $M = 2 \text{ GeV}$ calculated using the proton interpolation current χ_{LA} . The errors are associated with the errors in the parameters used for the numerical analysis.

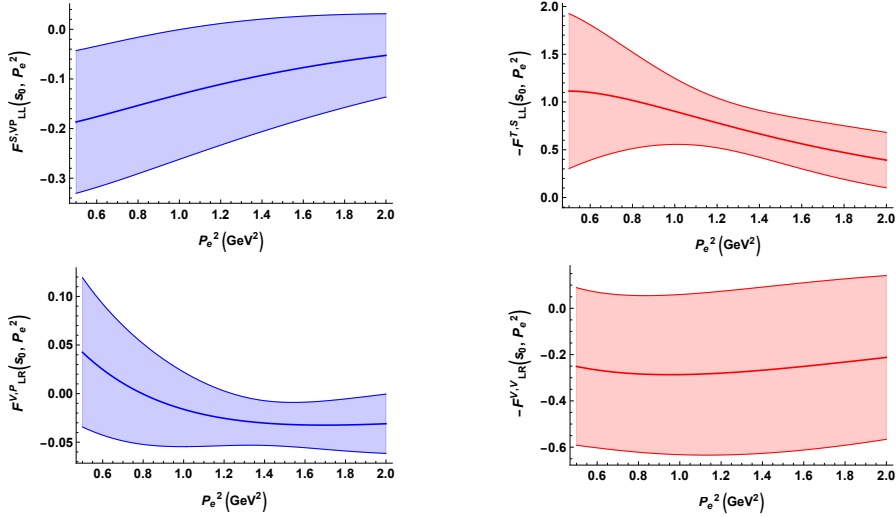


Figure 5.6: The representative graphs showing the variation of errors with P_e^2 for some $F_{\Gamma'}^{A,r}$ functions calculated using the proton interpolation current, χ_{IO} . The shaded regions represents the error band and the central line gives the calculated values of the $F_{\Gamma'}^{A,r}$ functions

D). Further uncertainties due to higher order effects and duality violations are not included here. Looking only at the uncertainties due to uncertainties in the parameter values are also worrisome as in some cases these uncertainties are as large as 200%. We have also plotted the uncertainties in $F_{\Gamma'}^{A,r}$ with P_e^2 using proton interpolations currents, χ_{IO} and χ_{LA} in Fig.(5.6) and Fig.(5.7) (only some representative graphs). These uncertainties are found to be mainly dominated by the uncertainties in w_0 which is a model input parameter in the DAs of D-meson. This parameter is related to the first inverse moment of these DAs, λ_D , defined as

$$\lambda_D^{-1}(\mu) = \int_0^\infty \frac{dw}{w} \phi_D^+(w, \mu) \quad (5.44)$$

where, μ is the normalization scale. This parameter can be very useful in probing and understanding the structure of D-meson. In the next section, we will discuss an attempt to have a better estimate on this parameter using the experimental data on the $D_q^* D_q \gamma$ coupling (with $q = u, d, s$) by equating them to the same couplings obtained using LCSR.

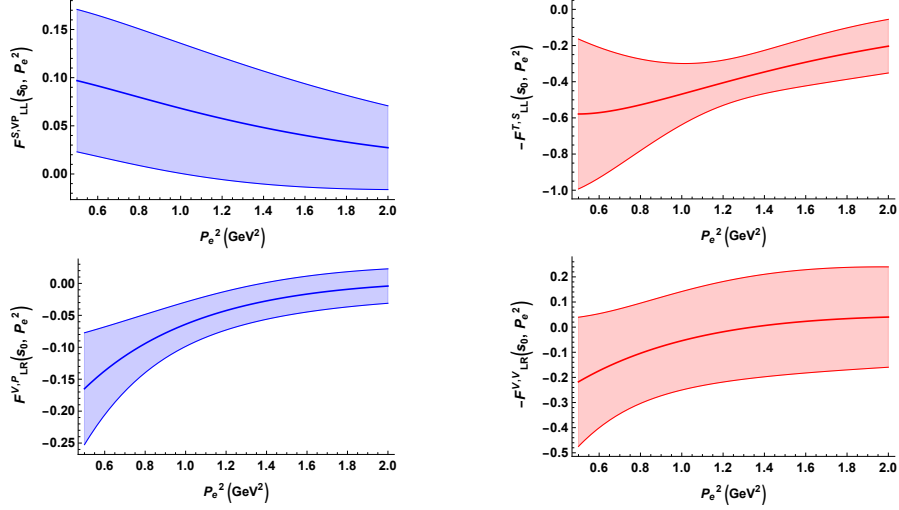


Figure 5.7: The representative graphs showing the variation of errors with P_e^2 for some $F_{\Gamma\Gamma'}^{A,r}$ functions calculated using the proton interpolation current, χ_{LA} . The shaded regions represents the error band and the central line gives the calculated values of the $F_{\Gamma\Gamma'}^{A,r}$ functions

5.5 $D^*D\gamma$: Probing the inner structure of the charm mesons

In this section, we will first look at the $D_q^*D_q\gamma$ (with $q=u,d,s$) coupling in the LCSR framework. Later we will see how we can use the experimental data on the branching ratios of $D_q^* \rightarrow D_q\gamma$ to obtain the value for this coupling, which in turn can be used to get an estimate for the parameter w_0 (see Eqn.(5.16)).

The amplitude for the radiative decay of D_q^* -meson to D_q -meson (with $q = u, d, s$) can be written as [147]

$$\mathcal{A}(D_q^*(p') \rightarrow D_q(p)\gamma(k)) = \langle D_q(p)\gamma(k) | D_q^* \rangle = g_{D_q} e \epsilon_{\mu\nu\rho\sigma} k^\rho \epsilon_\gamma^\sigma p^\nu \epsilon_{D_q^*}^\mu \quad (5.45)$$

where $p' = p + k$, g_{D_q} is the $D_q^*D_q\gamma$ coupling, $\epsilon_{\mu\nu\rho\sigma}$ is the Levi-civita tensor, e is the electric charge of the electron, and ϵ_γ^σ and $\epsilon_{D_q^*}^\mu$ are the polarization vectors for photon and D_q^* -meson, respectively. Using this amplitude and the two body phase space, the decay width of D_q^* -meson for this process can be calculated as

$$\Gamma(D_q^* \rightarrow D_q\gamma) = \frac{\alpha_{em} g_{D_q}^2 |\vec{k}|^3}{3} \quad (5.46)$$

where $\alpha_{em} = \frac{e^2}{4\pi}$ is the fine structure constant and

$$|\vec{k}| = \frac{m_{D_q^*}^2 - m_{D_q}^2}{2m_{D_q^*}} \quad (5.47)$$

with m_{D_q} and $m_{D_q^*}$ being the masses of D_q and D_q^* mesons, respectively. Now, in order to evaluate this coupling using the method of LCSR, we first need the relevant correlation function for this process. It can be obtained by interpolating the D_q^* -meson and photon with the D_q^* interpolation and electromagnetic currents, respectively. Such a correlation function reads as

$$T_{\mu\nu} = -ie \int d^4x e^{ik \cdot x} \langle D_q(p) | T \{ J_\mu^{em}(x) J_\nu^{D_q^*}(0) \} | 0 \rangle \quad (5.48)$$

where T represents the time ordering, and the currents $J_\mu^{em} = Q_c \bar{c}(x) \gamma_\mu c(x) + Q_q \bar{q}(x) \gamma_\mu q(x)$ and $j_\nu^{D_q^*} = \bar{c}(0) \gamma_\nu q(0)$ are the interpolation currents for the photon and D_q^* -meson states, respectively. Now, in order to derive the sum rule for the $D_q^* D_q \gamma$ coupling, we first calculate this correlation function using perturbative QCD. As the mass of strange and charm quarks can not be neglected, one need to employ the light cone propagator for the massive particle given by (see Appendix-B)

$$\begin{aligned} S_{ij}(x_1, x_2, m) &\equiv -i \langle 0 | T \{ q_i(x_1) \bar{q}_j(x_2) \} | 0 \rangle \\ &= \int \frac{d^4k}{(2\pi)^4} e^{-ik \cdot (x_1 - x_2)} \frac{\not{k} + m}{k^2 - m^2} \delta_{ij} + \dots \end{aligned} \quad (5.49)$$

where m represents the mass of the quark, and the ellipses represent higher order terms involving one or more gluon emissions and the condensate contributions. These are not considered in the present discussion. Next, using the parameterization of the matrix element of the bilinear operator between the vacuum and the D_q -meson state (in terms of the light cone DAs of D_q -meson given in Eqn.(5.15)), the representation of the correlation function in Eqn.(5.48) within

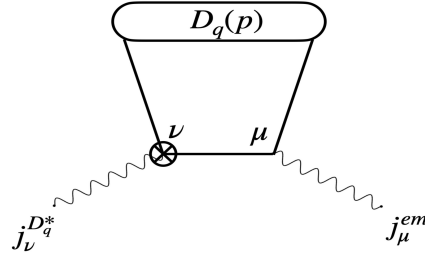


Figure 5.8: Feynman diagram contributing to the light-cone expansion of the correlation function for $D_q^* \rightarrow D_q \gamma$ up to leading order. The encircled D_q represents that the distribution amplitudes for D_q -meson enters the LCSR computation. The encircled vertex on the left represents the D_q^* interpolation current while the vertex on the right represents the electromagnetic current.

perturbative QCD reads as (see Fig. (5.8))

$$T_{\mu\nu}^{QCD}(p, k) = e f_{D_q} m_{D_q} \int_0^\infty dw \left[\phi_+^{D_q}(w) \left\{ \frac{Q_c}{(k-wv)^2 - m_c^2} + \frac{Q_q}{(k+vw)^2 - m_q^2} \right\} + \Phi_\pm^{D_q}(w) \left\{ \frac{Q_c m_c}{((k-wv)^2 - m_c^2)^2} + \frac{Q_q m_q}{((k+vw)^2 - m_q^2)^2} \right\} \right] \epsilon_{\mu\nu\alpha\beta} k^\alpha v^\beta \quad (5.50)$$

where $\phi_+^{D_q}(w)$ and $\Phi_\pm^{D_q}(w)$ are defined in Eqn.(5.16) and Eqn.(5.17), respectively. f_{D_q} and m_{D_q} are the decay constant and mass of the D_q -meson while m_c and m_q are the masses of the charm and $q = \{u, d, s\}$ quarks, respectively. v is the four velocity of the D_q -meson such that $p^\mu = m_{D_q} v^\mu$ and $v^2 = 1$.

Moreover, the representation of the correlation function given in Eqn.(5.48) in terms of hadronic states can be found by inserting hadron states with relevant quantum numbers and separating the contribution coming from the lowest energy state which is D_q^* itself in the present case. Therefore, the hadronic representation i.e. the dispersion relation reads as

$$T^{had}(p, k) = 2e \frac{f_{D_q^*} m_{D_q^*}}{m_{D_q} + m_{D_q^*}} \frac{G_{D_q D_q^*}(-k^2)}{(p+k)^2 - m_{D_q^*}^2} + \int_{m_{D_q^*}^2}^\infty ds \frac{1}{\pi} \frac{\text{Im}(T^{had}(s, -k^2))}{s - (p+k)^2} \quad (5.51)$$

where $f_{D_q^*}$ and $m_{D_q^*}$ are the decay constant and the mass of the D_q^* -meson, respectively, $\epsilon_\mu^{D_q^*}$ represents the polarisation vector for the D_q^* -meson, and $G_{D_q D_q^*}(K^2)$

with $K^2 = -k^2$ is the residue of the lowest energy term and dictates the dynamics of the electromagnetic transition of a D_q^* -meson into a D_q -meson defined by the following matrix element

$$\langle D_q(p) | j_{em}^\mu(0) | D_q^*(p+k) \rangle = \frac{2}{m_{D_q} + m_{D_q^*}} \epsilon_{\mu\rho\alpha\beta} \epsilon_\rho^{D_q^*} p_\alpha k_\beta G_{D_q^* D_q}(k^2) \quad (5.52)$$

In writing the first term of Eqn.(5.51), we have also using the following conventions

$$\langle D_q^*(p+k) | \bar{c}(0) \gamma_\nu q(0) | 0 \rangle = f_{D_q^*} m_{D_q^*} \epsilon_\nu^{*(D_q^*)}, \quad \text{and} \quad (5.53)$$

$$\epsilon_\rho^{(D_q^*)} \epsilon_\nu^{*(D_q^*)} = -g_{\rho\nu} + \frac{(p+k)_\rho (p+k)_\nu}{m_{D_q^*}^2}. \quad (5.54)$$

The second term in Eqn.(5.51) represents the contribution coming from the heavier states and the continuum where s_0^h is the continuum threshold. Now, we are ready to write the sum rule by equating the two representations and approximating the heavier states and continuum contributions using quark hadron duality (see Section-2.1.1). The final sum rule after performing the Borel transformation on $(p+k)^2$ reads as

$$G_{D_q^* D_q}(-k^2) = \frac{1}{f_{D_q^*} m_{D_q^*}} \int_0^{s_0} ds e^{\frac{(m_{D_q^*}^2 - s)}{M^2}} \frac{1}{\pi} \text{Im} (T^{QCD}(s, Q^2)) \quad (5.55)$$

where $T^{had}(p, k)$ can be obtained from $T_{\mu\nu}^{had}(p, k)$ as $T_{\mu\nu}^{had}(p, k) = T^{had}(p, k) \epsilon_{\mu\nu\alpha\beta} k^\alpha p^\beta$, and M is the Borel mass. The imaginary part of $T(s, K^2)$ can be obtained using the Cutkosky rule and the use of the following identities

$$\text{Im} \left(\frac{1}{P^2 - m^2} \right) = -\pi \delta(P^2 - m^2), \quad \text{and} \quad (5.56)$$

$$\text{Im} \left(\frac{1}{(P^2 - m^2)^2} \right) = \frac{-\pi}{k \cdot v - w} \left(\frac{\partial}{\partial w} \delta(P^2 - m^2) \right) \quad (5.57)$$

where $m = \{m_c, m_q\}$, and

$$P^2 = (k - wv)^2 = -K^2 \left(1 + \frac{w}{m_{D_q}} \right) + w^2 - w \frac{s}{m_{D_q}} + w m_{D_q} \quad (5.58)$$

with $s = (p + k)^2$. Similarly, for P'^2 given by

$$P'^2 = (k + wv)^2 = -K^2 \left(1 - \frac{w}{m_{D_q}} \right) + w^2 + w \frac{s}{m_{D_q}} - wm_{D_q} \quad (5.59)$$

one can simply replace P^2 by P'^2 in Eqn.(5.56) while Eqn.(5.57) will be slightly different such that

$$\text{Im} \left(\frac{1}{(P'^2 - m^2)^2} \right) = \frac{\pi}{k \cdot v + w} \left(\frac{\partial}{\partial w} \delta(P'^2 - m^2) \right). \quad (5.60)$$

Using these relations, one can then perform the integrations over w and s , and get the final LCSR extraction for $G_{D_q D_q^*}(K^2)$. The $D_q^* D_q \gamma$ coupling represented by g_{D_q} is Eqn.(5.45) can now be calculated using the sum rule for $G_{D_q D_q^*}(K^2)$ in Eqn.(5.55) as the two are related by

$$g_{D_q} = \frac{2}{m_{D_q} + m_{D_q^*}} G_{D_q D_q^*}(k^2 = 0) \quad (5.61)$$

where $\Gamma_{D_q^*}$ is the total decay width of the D_q^* -meson. If we have the experimental values for g_{D_q} , then it can help us in getting a direct estimate of w_0 .

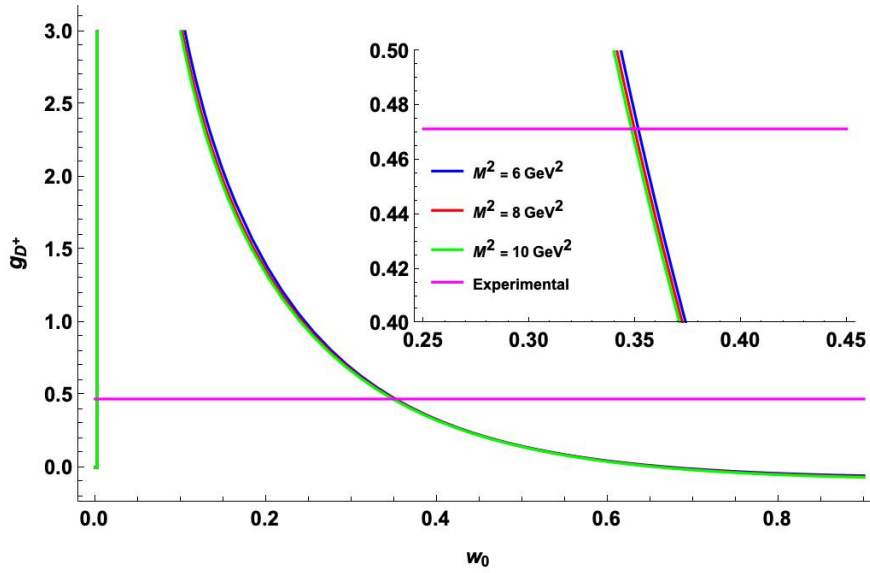
For that purpose we have collected the values of the branching ratios for $D_q^* \rightarrow D_q \gamma$ along with the total decay widths of the D_q^* -meson in Table-5.3 taken from [35], and also the couplings g_{D_q} determined from these experimental values or limits.

Now, as we have the experimental as well as theoretical curves for g_{D_q} as a

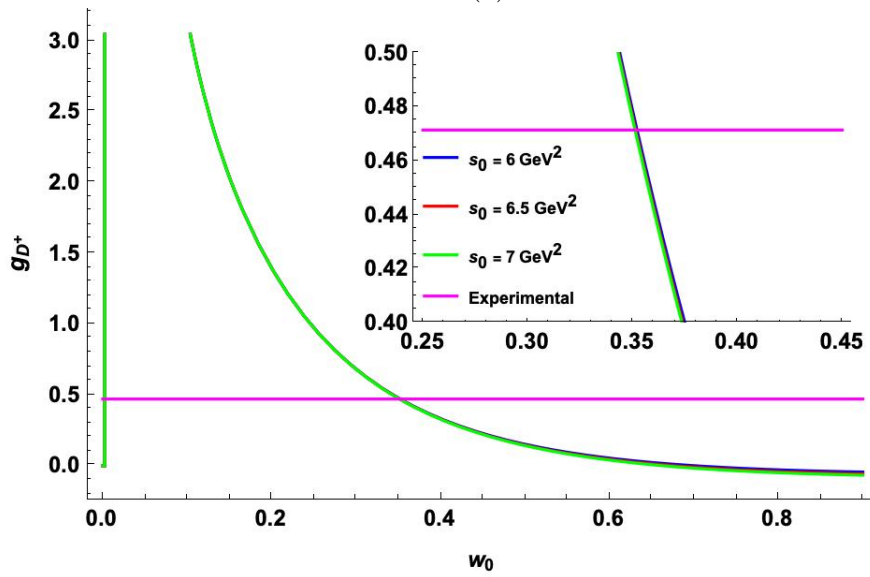
Channel	Branching ratio (%)	Total decay widths	g_{D_q}
$D^{*+} \rightarrow D^+ \gamma$	(1.6 ± 0.4)	(83.4 ± 1.8) KeV	0.47
$D^{*0} \rightarrow D^0 \gamma$	(35.3 ± 0.9)	< 2.1 MeV	< 10.98
$D_s^{*+} \rightarrow D_s^+ \gamma$	(93.5 ± 0.7)	< 1.9 MeV	< 16.27

Table 5.3: Tabulating the values of the branching ratios for $D_q^* \rightarrow D_q \gamma$ ($q = u, d, s$) decay and the total decay width of the D_q^* -mesons [35], along with the experimental estimation of the $D_q^* D_q \gamma$ coupling, g_{D_q} defined in Eqn.(5.46).

function of w_0 , the intersection point (see Fig. 5.9) provides the best value of w_0 . We infer $w_0 = 0.35$ GeV. The experimental uncertainties are found to be almost



(a)



(b)

Figure 5.9: Plots showing the variation of g_{D^+} as a function of w_0 : (a) for different values of M^2 and fixed $s_0 = 6.5 \text{ GeV}^2$, and (b) for different values of s_0 and fixed $M^2 = 6 \text{ GeV}^2$. The Magenta line represents the expected value of g_{D^+} using the experimental data as tabulated in Table-5.3 (Error bands are to be included).

negligible here. However, the theoretical uncertainties, which we expect to be small, are yet to be included. As can be seen from Table-5.3, the exact value of the total decay width is known only for D^{*+} -meson while for D^{*0} and D_s^{*+} , we only have the upper bounds. Thus for D^{*+} , an exact value for the coupling g_{D^+} has been extracted. To get an estimate for the total decay widths instead of the bounds, we plan to construct suitable ratios of the branching ratios of various process. However, the estimation of w_0 from experimental information on g_{D^+} in Fig.(5.9) already shows the power of this method in probing the inner structure of D -meson. We expect that the estimation of w_0 obtained using this method will act as a complimentary way to the method one opts to have estimates on the first inverse moment of B-meson DAs using data on $B \rightarrow \ell\nu_\ell\gamma$ mode. Such an approach can be used for D -meson system as well. Moreover, we expect our method to be sharper and better due to two reasons. Firstly, there are less complications involved due to presence of only one hadronic quantity here given by the $D_q^*D_q\gamma$ coupling, while for $D \rightarrow \ell\nu_\ell\gamma$ mode, there will be two form factors present. Secondly, our method will provide the exact value for this parameter while using $D \rightarrow \ell\nu_\ell\gamma$, one only gets a limit. Whether this expectation bears out or not can only be confirmed after complete analysis. This is an ongoing work and is expected to be completed in near future.

5.6 Conclusions and Discussion

In this chapter, we have discussed the application of LCSR to processes involving mesons with heavy quarks. To this purpose, we first considered the BNV decay of charmed meson to an anti-proton and a positron i.e. $D^0 \rightarrow \bar{p}e^+$. This process is found to involve twelve independent form factors. We discussed the evaluation of these form factors in LCSR framework using D-meson light cone distribution amplitudes in the exponential model parameterization and the general interpolation current for proton state. However, for numerical analysis we explicitly considered two forms of proton interpolation currents labelled as χ_{LA} and χ_{IO} provided in Eqn.(4.12) and Eqn.(4.14), respectively. It is found that each of these FFs can be extracted from two $F_{\Gamma}^{A,r}$ where $A = \{S, V, T\}$ and

$r = \{S, V, P, VP\}$, the residue functions of the lowest state contribution to the dispersion relation given in Eqn.(5.12). The relations between these functions and the form factors are provided in Eqn.(5.11). However, the extraction from the two are not found to match completely. We suspect two possible reasons for that. Firstly, some of $F_{\Gamma\Gamma'}^{A,r}$ are found to get contribution coming only from the condensate term of the propagator while others get contributions from both condensate and non-condensate terms. The case where both the combinations have condensate as well as non-condensate contributions, like for $F_{LL}^{S,0}$ and $F_{LL}^{S,1}$ for χ_{LA} case (see Fig.(5.4)), the extractions from the two combinations are found to be close to each other. Secondly, as the LCSR predictions are more trustworthy at large momentum transfers i.e. large P_e^2 , the extractions from different combinations might be different at low P_e^2 . At large P_e^2 , they are found to be approaching each other.

Furthermore, the uncertainties associated with the uncertainties in various parameters used in the numerical analysis are also computed. They are found to be very large (as large as 200% for some cases) as can be seen from Table-5.1 and Table-5.2, and also from Fig.(5.6) and Fig.(5.7). Even though the extractions of the FFs from the two combinations did not match, they are found to be numerically within the error bars of each other. Thus, these results provide reasonable estimates for these FFs which can be used in a specific model framework where $c_{\Gamma\Gamma'}^A$'s are known functions of heavy particle masses and couplings to obtain the bounds on the parameters of the theory. The uncertainties obtained are found to be dominated by the uncertainty in the model input parameter, w_0 in the DAs of D-meson. Therefore, a better understanding of these FFs demands a better understanding of D-meson DAs as well. The better understanding of these DAs are not required just for a better understanding of this particular mode but rather for other modes involving D-meson also like $D^0 \rightarrow \bar{\Lambda}e^+$ which can be studied straightforwardly using the same method. As experimental searches improve, it is important to have first estimates of these non-perturbative inputs as well as to reduce there uncertainties.

We then discussed an attempt to get a better understanding on these DAs. For that we have estimated the $D_q^* D_q \gamma$ (with $q = u, d, s$) coupling, which is a func-

tion of w_0 , in the framework of LCSR. These couplings can also be estimated using the experimental data on the branching ratios of $D_q^* \rightarrow D_q \gamma$ decays, and the total decay widths of the D_q^* -mesons. On equating these estimations, we have shown that one may indeed get a better estimate of the input parameter w_0 which is related to the first inverse moment of the D-meson DAs, λ_D . Therefore, it can help us in probing the structure of the D-meson. For the case of B-meson, one constrains the analogous inverse moment using the $B \rightarrow \ell \nu_\ell \gamma$ mode. Such an analysis provides only a limit on the value of the inverse moment and is rather complicated due to the presence of two form factors. A similar analysis can also be performed for D-meson. Our method to estimate λ_D can be considered a complimentary way to this approach and is rather simple and is expected to be give sharper results. Moreover, stronger conclusions can be made only after a complete analysis as stated above.

Chapter 6

Summary and Future Work

6.1 Summary

The theory of strong interactions is dictated by Quantum ChromoDynamics (QCD) at the fundamental level. It is a non-abelian gauge theory that leads to a special property of self-interactions amongst the gauge bosons called gluons. Due to these self-interactions of the gluon, QCD becomes complicated and shows a unique feature of asymptotic freedom as a result of renormalization, because of which QCD being a perturbative theory is applicable only at small distances or equivalently at large energies. As one tries to look at the phenomena happening at long distances or equivalently at small energy scales, perturbative QCD is no longer reliable. The colored quarks and gluons, the fundamental degrees of freedom of QCD, are no longer the degrees of freedom. Rather they form colorless bound states called hadrons as a result of color confinement. These hadrons are majorly of two types called mesons (the bound state of a quark and an anti-quark) and baryons (the bound state of three quarks). As QCD is a relativistic field theory, these hadronic bound states can not be explained simply by a description in terms of a potential or wave functions. Therefore, these hadrons are non-perturbative in nature with quarks and gluons interacting at scale Λ_{QCD} , the scale of hadronization, inside the hadrons.

Experimentally, one can detect only these colorless hadronic states and no free-colored quarks and gluons. Consequently, according to the scattering the-

ory, to have a theoretical prediction for any physical observable like scattering cross-section, decay width, etc., one needs to calculate the matrix elements of the quark-gluon operators between the hadronic states. Such matrix elements are called hadronic matrix elements (HMEs). These HMEs are of non-perturbative nature in general and hence can not be calculated perturbatively using QCD. These HMEs can be parameterized in terms of hadronic objects like form factors, decay constant, etc. which contains all the information of the dynamics of strong interactions responsible for hadron formation. This makes the calculation of these hadronic quantities very demanding as they are very essential quantities required to make any theoretical prediction as well as to understand the dynamics of strong interactions at small energies. These objects are not only necessary to make predictions within the SM, rather they are very crucial inputs to make any prediction for beyond the SM physics scenarios as well.

To date, there is no theory that can compute these hadronic objects accurately and precisely with the present computational and technical skills. Light Cone Sum Rules (LCSR) is a QCD-based model which attempts to calculate these hadronic quantities relying on analytic properties and unitarity of the correlation functions.

In this thesis, we have studied the applications of LCSR to various processes involving light pion, proton, photon, and D-mesons within and beyond the SM of particle physics.

The first application involved considers the radiative decay of tau to a pion, neutrino, and a photon. This process involves two time-like form factors named as the axial and the vector form factors. We have computed these form factors as the first-time application of LCSR to such a system up to twist-2 accuracy. We have also computed the structure-dependent parameter for the pion which is defined as the ratio of the axial to the vector form factor at zero momentum transfer. The prediction for this parameter matches well with the experimental determination of this parameter from the radiative decay of pion, including sign where differing results have been quoted in literature. Afterward, we presented the theoretical prediction for the decay width and the invariant mass spectrum

of the $\pi - \gamma$ system. We have found roughly 10% uncertainties due to the uncertainties in the numerical values of the input parameters. Further uncertainties of roughly 10% are expected due to higher twist effects and the duality violations which were not included in this study and have been left for future studies.

As a second application, we have discussed the form factors involved in the radiative proton decay. It is a baryon number violating process and hence is only possible in beyond the SM scenarios. It involves two independent form factors. This study presents a first-ever systematic estimation for these form factors. We have computed these form factors considering two cases. In the first case, the proton state is interpolated using the Ioffe current and we used the distribution amplitudes of the photon up to twist-3 accuracy. In the second case, the photon state is interpolated with the electromagnetic current and the distribution amplitudes for the proton state have been used up to twist-3 accuracy. The numerical values of both the form factors in the first case are found to be $\mathcal{O}(10^{-3})$ while in the second case the form factor, A_{LL} was found to be smaller than A_{LR} as well as the FFs calculated in case-1, by a factor ~ 3 . These two cases can not be simply compared because of the difference in the momentum transferred square variable in the two cases and the limitations of the LCSR framework in reaching the physical point. Moreover, the uncertainties are found to be lesser for the second case. Hence, the second case can be preferred on the basis of less uncertainties in the results. However, a careful analysis of both the cases including higher twist effects and using different interpolation currents for the proton state are required to make any concrete conclusion on the preference of a particular case that has been left for future investigations.

After discussing these hadronic systems consisting of light quarks, we moved to the system involving heavy quarks. For such systems, the distribution amplitudes are not very well known. There are some models which have been proposed for these DAs using heavy quark symmetry arguments. In this thesis, we have only considered the exponential model. As an application to the heavy meson system, we first considered the baryon number violating decay of D-meson to a proton and an electron. This process involves 12 independent form factors. We have computed these form factors for the first time using LCSR and provided

estimates for a general interpolation current for the proton state. These form factors can be very useful to develop a better understanding of various BSM models. In calculating these form factors, we have used the D-meson distribution amplitudes up to the leading twist in the exponential model. The FFs are found to have uncertainties as large as 200%. This error budget is found to be dominated by our lack of precise knowledge of these D-meson DAs. In order to get a better understanding of these DAs, we have attempted to fix the free parameter ω_0 in the D-meson DAs, which is related to the first inverse moment of the D-meson DAs, using the experimental data on the radiative decays of the D^* -mesons. These decay modes are expected to be very helpful in probing the structure of these heavy quark mesons systems.

6.2 Future Works

In future, we plan to study the rate and spectrum of radiative kaon decays i.e., $K^- \rightarrow \ell^- \nu_\ell \gamma$, where $\ell = \{e, \mu\}$ using the form factors estimated in the framework of LCSR. These decays are interesting which can be seen by looking at the branching ratios of the non-radiative and the radiative decay modes of kaon (collected in Table-6.1). There are two important points to notice here. First,

mode	Non-radiative		Radiative	
	$K^- \rightarrow e^- \nu_e$	$K^- \rightarrow \mu^- \nu_\mu$	$K^- \rightarrow e^- \nu_e \gamma$	$K^- \rightarrow \mu^- \nu_\mu \gamma$
Branching ratio	$(1.58 \pm 0.007) \times 10^{-5}$	$(63.56 \pm 0.11) \times 10^{-2}$	$(9.4 \pm 0.4) \times 10^{-6}$	$(6.2 \pm 0.8) \times 10^{-3}$

Table 6.1: Tabulating the branching ratios for the radiative and non-radiative decay modes of kaon to muon and electron (values taken from [35]).

the helicity suppression is lifted for the case of radiative decay. Second, which is more interesting, is the ratio of the branching ratio for the radiative decay to the non-radiative decay. This ratio turns out to be ($\mathcal{O}(10^{-2}) \approx \alpha_{em}$) for the muonic mode, as one might expect. However, for the electronic mode, this ratio is $\mathcal{O}(1)$. This leaves one wondering if there is any interesting physics hidden behind it or it is just an artifact of kinematics? To get an answer, we need information about the form factors involved in this decay. This decay also has two form factors like in the case of radiative pion decay. However, there are extra complications due to

large mass of kaon, m_K which can not be set to zero, unlike the case of the pion. We plan to compute these form factors within the LCSR framework overcoming the difficulties arising due to large mass of kaon. Finally, in this project we plan to find the branching ratios for both the muonic mode and the electronic mode and look for any interesting phenomena which may be causing the difference in the behaviour of these radiative modes compared to the non-radiative ones (as discussed above).

In a different project, we intend to study the radiative decay of Λ_b baryon using LCSR. This decay is loop induced in the SM and hence, is very sensitive to new physics. LHCb has observed this decay for the first time in 2019 and found the branching ratio to be $(7.1 \pm 1.5 \pm 0.6 \pm 0.7) \times 10^{-6}$ where, uncertainties are associated with statistics, systematics, and external measurements systematics, respectively [148]. This decay mode is considered to be an important channel to study the polarisation of photon in $b \rightarrow s\gamma$ transitions, since one can measure the helicity of Λ baryons which provides access to the helicity structure of these transitions. Theoretically, this mode has been studied in LCSR framework earlier two times [149], [150]. But, the LCSR analysis with the improved distribution amplitudes for Λ_b [150] is not found to be in agreement with the experimental results. However, the earlier predictions [149] are found to be agreeing well, resulting into a dilemma. Moreover, none of these studies considered the effect of photon emission from the spectator quark and the effect of charm loop inclusion which is found to be significant for the case of $B \rightarrow K^*\gamma$ and $B \rightarrow K^*\ell^+\ell^-$ transitions [151]. Both these effects can have impact on the LCSR results and might shed new light. Consequently, we intend to have a fresh computation of the FFs involved in the decay $\Lambda_b \rightarrow \Lambda\gamma$ in LCSR framework including the contributions coming from the above mentioned effects, and finally comparing the predictions on the branching ratio of $\Lambda_b \rightarrow \Lambda\gamma$ using these FFs with the experimental result in [148].

Apart from these, we plan to move our attention a little away from LCSR applications and devote some time to understand how to match lattice results, computed in specific schemes, to continuum calculations in the $\overline{\text{MS}}$ scheme.

Appendix A

Important definitions, identities and integrals

A.1 Important definitions

1. **Pauli matrices:** These are trace-less 2×2 matrices and are represented as σ_i with $i = 1, 2, 3$. These matrices act as the generators of $SU(2)$ gauge group. The explicit form of these matrices are:

$$\sigma_1 = \begin{pmatrix} 0 & 1 \\ 1 & 0 \end{pmatrix}, \quad \sigma_2 = \begin{pmatrix} 0 & -i \\ i & 0 \end{pmatrix}, \quad \text{and} \quad \sigma_3 = \begin{pmatrix} 1 & 0 \\ 0 & -1 \end{pmatrix}. \quad (\text{A.1})$$

2. **Gell-Mann Matrices:** These are trace-less 3×3 matrices and are represented as λ_i with $i = 1, \dots, 8$. These matrices act as the generators of $SU(3)$ gauge group. The explicit form of these matrices are:

$$\lambda_1 = \begin{pmatrix} 0 & 1 & 0 \\ 1 & 0 & 0 \\ 0 & 0 & 0 \end{pmatrix}, \quad \lambda_2 = \begin{pmatrix} 0 & -i & 0 \\ i & 0 & 0 \\ 0 & 0 & 0 \end{pmatrix}, \quad \lambda_3 = \begin{pmatrix} 1 & 0 & 0 \\ 0 & -1 & 0 \\ 0 & 0 & 0 \end{pmatrix},$$

$$\begin{aligned}
\lambda_4 &= \begin{pmatrix} 0 & 0 & 1 \\ 0 & 0 & 0 \\ 1 & 0 & 0 \end{pmatrix}, & \lambda_5 &= \begin{pmatrix} 0 & 0 & -i \\ 0 & 0 & 0 \\ i & 0 & 0 \end{pmatrix}, & \lambda_6 &= \begin{pmatrix} 0 & 0 & 0 \\ 0 & 0 & 1 \\ 0 & 1 & 0 \end{pmatrix}, \\
\lambda_7 &= \begin{pmatrix} 0 & 0 & 0 \\ 0 & 0 & -i \\ 0 & i & 0 \end{pmatrix}, & \text{and} & & \lambda_8 &= \frac{1}{\sqrt{3}} \begin{pmatrix} 1 & 0 & 0 \\ 0 & 1 & 0 \\ 0 & 0 & -2 \end{pmatrix}.
\end{aligned} \tag{A.2}$$

3. **The light cone coordinates:** A four vector, $p^\mu = (p^0, p^1, p^2, p^3)$, can be written in the light cone coordinates basis as

$$p^\mu = \frac{n^\mu}{2} \bar{n} \cdot p + \frac{\bar{n}^\mu}{2} n \cdot p + p_\perp^\mu \tag{A.3}$$

where n^μ and \bar{n}^μ are the light cone basis vectors such that

$$n^2 = 0, \quad \bar{n}^2 = 0, \quad n \cdot \bar{n} = 2. \tag{A.4}$$

where the last property defined the normalisation condition. A standard choice for these basis vectors is

$$n^\mu = (1, 0, 0, 1), \quad \bar{n}^\mu = (1, 0, 0, -1) \tag{A.5}$$

i.e. taking \bar{n}^μ in the opposite direction of n^μ . $p_\perp^\mu = (0, p_1, p_2, 0)$ is the component of p^μ which is perpendicular to both n^μ and \bar{n}^μ .

One usually represents the four vector in the light cone coordinates in Eqn.(A.3) by

$$p^\mu = (p^+, p^-, \vec{p}_\perp) \tag{A.6}$$

where the last entry is two-dimensional such that $|\vec{p}_\perp|^2 = -p_\perp^\mu p_{\perp\mu} = p_\perp^2$ i.e. the Euclidean $|\vec{p}_\perp|^2$ is negative of that of the Minkowskian p_\perp^2 . The

plus and the minus components are defined as

$$p^+ = p_+ \equiv n \cdot p, \quad p^- = p_- \equiv \bar{n} \cdot p \quad (\text{A.7})$$

In these coordinates, the four vector square is given by

$$p^2 = p^+ p^- + p_\perp^2 = p^+ p^- - \vec{p}_\perp^2 \quad (\text{A.8})$$

using the mostly negative signature for the metric tensor i.e. $g^{\mu\nu} = \text{diag}(1, -1, -1, -1)$. Furthermore, the metric tensor can also be decomposed as

$$g^{\mu\nu} = \frac{n^\mu \bar{n}^\nu}{2} + \frac{\bar{n}^\mu n^\nu}{2} + g_\perp^{\mu\nu}, \quad \text{and} \quad (\text{A.9})$$

the totally anti-symmetric tensor in the \perp space is defined as

$$\epsilon_\perp^{\mu\nu} = \frac{\epsilon^{\mu\nu\alpha\beta}}{2} \bar{n}_\alpha n_\beta \quad (\text{A.10})$$

A.2 Important identities

1. Chisholm Identity:

$$\gamma^\alpha \gamma^\beta \gamma^\mu = g^{\alpha\beta} \gamma^\mu - g^{\alpha\mu} \gamma^\beta + g^{\beta\mu} \gamma^\alpha - i \epsilon^{\alpha\beta\mu\nu} \gamma_\nu \gamma_5 \quad (\text{A.11})$$

2. For $\sigma^{\rho\sigma} = \frac{i}{2} [\gamma^\rho, \gamma^\sigma]$,

$$\gamma^\alpha \sigma^{\rho\sigma} = 2i g^{\alpha\rho} \gamma^\sigma - 2i \gamma^\rho g^{\alpha\sigma} + \sigma^{\rho\sigma} \gamma^\alpha \quad (\text{A.12})$$

3. According to the Cutkosky rule:

$$\text{Im} \frac{1}{p^2 - m^2} = -\pi \delta(p^2 - m^2) \theta(p_0) \quad (\text{A.13})$$

for a particle with mass m . $\theta(p_0)$ is replaced by $\theta(-p_0)$ for an anti-particle.

4. $\ln(-x) = \ln|x| - i\pi\theta(x)$

5. **Generalised Fierz identities:** The Fierz transforms [152] enable one to change the ordering of the spinors in an operator involved in weak-interactions as per the requirement of the problem. Also, the Fierz identities are the relations between the product of Dirac bilinears. For example, let us take a general product of these bilinears given as

$$[\bar{\psi}_1 \Gamma \psi_2] [\bar{\psi}_3 \Gamma' \psi_4] \quad (\text{A.14})$$

where Γ and Γ' are some structures of γ -matrices and ψ_n (with $n = 1 \dots 4$) are the Dirac spinors. These Dirac spinors can be arranged in $4! = 24$ different orderings. However, only 12 of these orderings will be relevant as the ordering of the bilinears is irrelevant which removes half of the combinations. Now to understand the Fierz identities which help us in attaining these ordering of spinors, let us take the basis of γ -matrices given as

$$\Gamma_X = \{\mathbb{1}, \gamma^\mu, \sigma^{\mu\nu}, i\gamma^\mu \gamma_5, \gamma_5\} \quad (\text{A.15})$$

for $\mu < \nu$ and $X = \{S, V, T, A, P\}$, respectively. Moreover, let us choose a shorthand notation to represent a bilinear given by

$$e_X^a(12) = \bar{\psi}_1 \Gamma_X^a \psi_2 \quad (\text{A.16})$$

where a represents the Lorentz index of the γ -matrices. The simplest form of the product of bilinear one can obtain is $e_X^a(12)e_{Xa}(34)$ which can be written in a convenient form for the final identities given by

$$e_X(1234) = n_X^2 e_X^a(12)e_{Xa}(34) \quad (\text{A.17})$$

where n_X is given by

$$n_X = \begin{cases} 1 & \text{if } X = S, V, P, \\ -i & \text{if } X = A, \\ \sqrt{2} & \text{if } X = T, \end{cases} \quad (\text{A.18})$$

Therefore, we have

$$\begin{aligned}
e_S(1234) &= [\bar{\psi}_1\psi_2] [\bar{\psi}_3\psi_4], \\
e_V(1234) &= [\bar{\psi}_1\gamma^\mu\psi_2] [\bar{\psi}_3\gamma_\mu\psi_4], \\
e_T(1234) &= [\bar{\psi}_1\sigma_{\mu\nu}\psi_2] [\bar{\psi}_3\sigma^{\mu\nu}\psi_4], \\
e_A(1234) &= [\bar{\psi}_1\gamma^\mu\gamma_5\psi_2] [\bar{\psi}_3\gamma_\mu\gamma_5\psi_4], \\
e_P(1234) &= [\bar{\psi}_1\gamma_5\psi_2] [\bar{\psi}_3\gamma_5\psi_4].
\end{aligned} \tag{A.19}$$

According to the generalised Fierz identities, different orderings are related as

$$e_X(1234) = \mathbf{K}_{XY} e_Y(abcd) \tag{A.20}$$

where $(abcd)$ represents all the 12 orderings and K_{XY} is the Fierz transformation matrix such that

(abcd)	(1234)	(1432)	(2 ^c 1 ^c 34)	(124 ^c 3 ^c)	(13 ^c 2 ^c 4)	(13 ^c 4 ^c 2)	(142 ^c 3 ^c)	(2 ^c 1 ^c 4 ^c 3 ^c)	(31 ^c 2 ^c 4)	(31 ^c 4 ^c 2)	(4 ^c 1 ^c 2 ^c 3 ^c)	(4 ^c 1 ^c 3 ^c 2)
K	1	F	S	S	SFS	SF	FS	1	SF	SFS	F	FS

where the superscript c represents the charge conjugation such that

$$\bar{\psi}^c = \psi^T C^{-1} \tag{A.21}$$

with C being the charge conjugation matrix such that $C^T = -C$ and the superscript T represents the transpose. The Fierz transformation matrices

are given by

$$\mathbf{F} = \frac{1}{4} \begin{pmatrix} 1 & 1 & \frac{1}{2} & -1 & 1 \\ 4 & -2 & 0 & -2 & -4 \\ 12 & 0 & -2 & 0 & 12 \\ -4 & -2 & 0 & -2 & 4 \\ 1 & -1 & \frac{1}{2} & 1 & 1 \end{pmatrix}, \quad \mathbf{S} = \begin{pmatrix} -1 & 0 & 0 & 0 & 0 \\ 0 & 1 & 0 & 0 & 0 \\ 0 & 0 & 1 & 0 & 0 \\ 0 & 0 & 0 & -1 & 0 \\ 0 & 0 & 0 & 0 & -1 \end{pmatrix}. \quad (\text{A.22})$$

The other transformation matrices can be obtained by simply multiplying these matrices. For more details on these generalised Fierz identities, we suggest the reader to look at [135] and the references therein.

A.3 Important integrals

In this section we collect all the useful integrals used through out this thesis. The general formula for these integrals in D-dimensions which usually appear in the sum rule calculations can be written using dimensional regularisation as [37],

$$\int d^D x e^{ipx} \frac{1}{(x^2)^n} = (-i) (-1)^n 2^{(D-2n)} \pi^{D/2} (-p^2)^{n-D/2} \frac{\Gamma(D/2 - n)}{\Gamma(n)} \quad (\text{A.23})$$

for $n \geq 1$, $p^2 < 0$. We can get the desired form of the integrals involved by differentiating it with respect to the four-momentum p_α . Various integrals that are used throughout this thesis are

$$\int d^4 x e^{ipx} \frac{x_\alpha}{x^4} = 2\pi^2 \frac{p_\alpha}{p^2}, \quad (\text{A.24})$$

$$\int d^4 x e^{ipx} \frac{x_\alpha}{x^2} = 8\pi^2 \frac{p_\alpha}{p^4}, \quad (\text{A.25})$$

$$\int d^4 x e^{ipx} \frac{x_\alpha x_\beta}{x^4} = -\frac{2i\pi^2}{p^2} \left(g_{\alpha\beta} - \frac{2p_\alpha p_\beta}{p^2} \right), \quad (\text{A.26})$$

$$\int d^4x e^{ipx} \frac{x_\alpha x_\beta}{x^2} = -\frac{8i\pi^2}{p^4} \left(g_{\alpha\beta} - \frac{4p_\alpha p_\beta}{p^2} \right), \quad (\text{A.27})$$

$$\int d^4x e^{ipx} \frac{x_\alpha}{x^6} = \frac{-\pi^2}{4} p_\alpha \ln(-p^2), \quad (\text{A.28})$$

$$\int d^4x e^{ipx} \frac{1}{x^6} = \frac{-i\pi^2}{8} p^2 \ln(-p^2), \quad (\text{A.29})$$

$$\int d^4x e^{ipx} \frac{x_\alpha x_\beta}{x^8} = \frac{-i\pi^2}{48} (p^2 g_{\alpha\beta} + 2p_\alpha p_\beta) \ln(-p^2), \text{ and} \quad (\text{A.30})$$

$$\int d^4x e^{ipx} \frac{x_\alpha x_\beta x_\mu}{x^8} = \frac{\pi^2}{24} \left(\frac{2p_\alpha p_\beta p_\mu}{p^2} - (p_\alpha g_{\beta\mu} + p_\beta g_{\alpha\mu} + p_\mu g_{\alpha\beta}) \ln(-p^2) \right). \quad (\text{A.31})$$

These integrals in general will have divergent terms proportional to p^2 . We choose to omit these terms as they goes to zero after Borel transformation.

Appendix B

Light cone propagator and distribution amplitudes

In this appendix, we discuss and collect the light cone propagator and the light cone distribution amplitudes of the light meson, photon, nucleon, and heavy mesons that are used throughout this thesis.

B.1 Light cone propagator

The gauge invariance demands the insertion of a path ordered Wilson line $([x_1, x_2])$ between $\bar{q}(x_1)$ and $q(x_2)$ in a non-local operator given by,

$$[x_1, x_2] = P \left\{ \exp \left(ig \int_{x_2}^{x_1} G_\mu^a(z) T^a dz^\mu \right) \right\} \quad (\text{B.1})$$

where G_μ^a represents the gluon field. With the use of fixed-point gauge given by $G_\mu^a x^\mu = 0$, the light cone expansion of the quark propagator is given by [153],

$$\begin{aligned} S_{ij}(x_1, x_2, m) &= -i \langle 0 | T \{ q_i(x_1) \bar{q}_j(x_2) \} | 0 \rangle \\ &= \int \frac{d^4 k}{(2\pi)^4} e^{-ik(x_1-x_2)} \left\{ \frac{\not{k} + m}{k^2 - m^2} \delta_{ij} - g_s \int_0^1 dv \mathbf{G}_{\mu\nu}^{ij}(vx_1 + (1-v)x_2) \right. \\ &\quad \left. \times \left[\frac{1}{2} \frac{\not{k} + m}{(k^2 - m^2)^2} \sigma^{\mu\nu} - \frac{1}{k^2 - m^2} v(x_1 - x_2)^\mu \gamma^\nu \right] \right\} \end{aligned} \quad (\text{B.2})$$

where $\mathbf{G}^{\mu\nu} = G_a^{\mu\nu} T^a = G_a^{\mu\nu} \frac{\lambda^a}{2}$ with $Tr(\lambda^a \lambda^b) = 2\delta^{ab}$ (defined in Eqn.(1.4))

It can be written in the mass-less limit as

$$S_{ij}(x_1, x_2, m)|_{m \rightarrow 0} = \frac{1}{2\pi^2} \left[\frac{\not{x}_1 - \not{x}_2}{(x_1 - x_2)^4} + \frac{2m}{2(x_1 - x_2)^2} \right] - \frac{1}{16\pi^2} \frac{(1}{(x_1 - x_2)^2} \\ \times \int_0^1 dv \mathbf{G}_{\alpha\beta}(vx_1 + (1-v)x_2) [(\not{x}_1 - \not{x}_2)\sigma_{\alpha\beta} - 4iv(x_1 - x_2)_\alpha \gamma_\beta]. \quad (\text{B.3})$$

While calculating the time-ordered product in Eqn.(B.3), we also have a normal ordered piece which in general perturbative field theories goes to zero. However, in the present case it does not go to zero but contains universal non-perturbative effects in terms of vacuum condensates. To understand it, let us consider the Taylor expansion of the normal ordered piece given by (taking $x_1 = x$ and $x_2 = 0$ for simplicity)

$$: q_i(x), \bar{q}_j(0) := : q_i(0), \bar{q}_j(0) : + x^\mu : \partial_\mu q_i(0), \bar{q}_j(0) : \\ + \frac{1}{2!} x^\mu x^\nu : \partial_\mu \partial_\nu q_i(0), \bar{q}_j(0) : + \dots \quad (\text{B.4})$$

To make this expansion gauge invariant, the partial derivative is to be replaced by the covariant gauge which reads as

$$D_\mu = \partial_\mu + ig_s \mathbf{G}_\mu \quad (\text{B.5})$$

where, the gauge field, \mathbf{G}_μ using the fixed point gauge is given by

$$\mathbf{G}_\mu(x) = -\frac{1}{2} \mathbf{G}_{\mu\nu}(0) x^\nu - \frac{1}{3} (\partial_\lambda \mathbf{G}_{\mu\nu}(0)) x^\lambda x^\nu + \dots \quad (\text{B.6})$$

Having done this, we find that this normal ordered piece does not goes to zero, but rather provides a correction to the propagator defined in Eqn.(B.3) in terms of vacuum condensates. Such a correction term in the mass-less limit reads as

$$\Delta S_{ij}(x_1, x_2, m) = -\frac{1}{12} \left[\left(\delta_{ij} + \frac{i}{4} m (x_1 - x_2)^\mu (\gamma_\mu)_{ji} + \mathcal{O}(m^2) \right) \langle \bar{q} q \rangle \right]$$

$$+ \frac{i}{16}(x_1 - x_2)^2 \left(\delta_{ij} + \frac{i}{6}m(x_1 - x_2)^\mu (\gamma_\mu)_{ji} + \mathcal{O}(m^2) \right) \langle \bar{q}g_s \mathbf{G} \cdot \sigma q \rangle \Big] + \dots \quad (\text{B.7})$$

where $\langle \bar{q}q \rangle$ is the quark condensate, and $\langle \bar{q}g_s \mathbf{G} \cdot \sigma q \rangle$, with $\mathbf{G} \cdot \sigma \equiv \mathbf{G}_{\mu\nu} \sigma^{\mu\nu}$, is a mixed condensate related to the quark condensate as

$$\langle \bar{q}g_s \mathbf{G} \cdot \sigma q \rangle = m_0^2 \langle \bar{q}q \rangle \quad (\text{B.8})$$

where m_0 is a parameter whose value is provided in Table-D.2. The ellipses in Eqn.(B.7) represent the contributions of higher dimensional condensates. One can look at [153], [154] for more details.

B.2 Light cone distribution amplitudes (DAs)

In this section we collect all the light cone distribution amplitudes used throughout this thesis for light mesons, photon, nucleon, and the heavy meson.

B.2.1 Light-Meson DAs

The light cone DAs of the light pseudoscalar mesons, P like π , K, are defined by the matrix elements of the axial-vector bilocal operator, expanded around the light cone i.e. $x_1^2 = x_2^2 = (x_1 - x_2)^2 = 0$ as [155]

$$\begin{aligned} \langle 0 | \bar{q}_2(x_2) \gamma_\mu \gamma_5 q_1(x_1) | P(p) \rangle = f_P \int_0^1 du e^{-i(ux_1 + \bar{u}px_2)} \left\{ ip_\mu (\phi(u) + (x_1 - x_2)^2 g_{1P}(u)) \right. \\ \left. + \left((x_1 - x_2)_\mu - \frac{p_\mu (x_1 - x_2)^2}{p(x_1 - x_2)} \right) g_{2P}(u) \right\} \quad (\text{B.9}) \end{aligned}$$

where u and $\bar{u} = 1 - u$ represents the momentum fractions of the meson P carried by the quark and the anti-quark, respectively, $\phi_P(u)$ represents the leading twist-2 DA used in Chapter-3 for pion, and $g_{1P}(u)$ and $g_{2P}(u)$ represents the twist-4 DAs (which are not considered in the discussions involved in this thesis.) These

DAs have the following normalisation conditions

$$\int_0^1 du \phi_P(u) = 1, \quad \int_0^1 du g_{2P}(u) = 0. \quad (\text{B.10})$$

These DAs can be derived using the conformal expansion as discussed in Section-2.2.2 and read as

$$\phi_\pi(u, \mu) = 6u\bar{u} \left[1 + \sum_{n=1} a_n^P(\mu) C_n^{3/2}(u - \bar{u}) \right]. \quad (\text{B.11})$$

where $C_n^{3/2}$ are the Gegenbauer polynomials given by

$$C_1^{3/2}(x) = 3x, \quad C_2^{3/2}(x) = -\frac{3}{2}(1 - 5x^2), \dots, \text{ and} \quad (\text{B.12})$$

a_n are the multiplicatively renormalizable coefficient defined as,

$$a_n^P(\mu) = a_n^P(\mu_0) \left(\frac{\alpha_s(\mu)}{\alpha_s(\mu_0)} \right)^{\gamma_n/\beta_0} \quad (\text{B.13})$$

with $\alpha_s = \frac{g_s^2}{4\pi}$ (g_s is the strong coupling constant), β_0 is the leading QCD β -function given as $\beta_0 = 11 - \frac{2}{3}N_F$, and

$$\gamma_n = \frac{4}{3} \left[-3 - \frac{2}{(n+1)(n+2)} + 4 \left(\sum_{k=1}^{(n+1)} \frac{1}{k} \right) \right]. \quad (\text{B.14})$$

For pion, a_n^π vanishes for odd values of n due to isospin symmetry.

Apart from the two-particle twist-4 DAs, g_{1P} and g_{2P} , there are four three-particle twist-4 DAs as well defined by the matrix elements of the quark-anti-quark and gluon operators taken between the vacuum and the meson state. Moreover, there exists 2 two particle and 1 three particle twist-3 DAs as well. These twist-3 and twist-4 DAs are related to each other via QCD equation of motion. We are not providing exact definitions and forms of these DAs here as they are not a part of this thesis. However, interested reader can find all of them collected in the appendix of [156].

B.2.2 Photon DAs

According to the QCD description of the radiative processes, a photon can be considered to contain a point-like electromagnetic component along with a soft hadronic component, as one would anticipate from the deep inelastic scattering experiments. Using the background field formalism, one can get better understanding on the hadronic component (see [71] and references therein for better understanding). In the presence of a constant electric field, the QCD vacuum can get magnetized due to the presence of the quarks and antiquarks in the QCD vacuum. This induced magnetisation will be proportional to the quark density, applied field, electric charge of the quarks and the magnetic susceptibility, χ of the quark condensate such that

$$\langle 0 | \bar{q} \sigma_{\mu\nu} q | 0 \rangle_F = e_q \chi \langle \bar{q} q \rangle F_{\mu\nu} \quad (\text{B.15})$$

where $\langle \bar{q} q \rangle$ represents the quark-anti-quark condensate, $F_{\mu\nu}$ represents the field strength tensor of the electromagnetic field, $e_q = e Q_q$ represents the charge of quark, and the subscript F represents that this vacuum expectation is taken when the electromagnetic field is present. Moreover, if we have a varying magnetic field instead of a constant one, the response of the vacuum becomes more complicated as it will be now sensitive to the separation between the quark and the anti-quark. For light like separations, the magnetic susceptibility gets substituted by the response function ϕ_γ . This function can be identified with the photon DA in the plane wave configuration and the infinite momentum frame. In such a configuration, the l.h.s of the above equation for a electromagnetic field varying at a certain frequency represents the probability amplitude for a real photon to get dissociated into a quark-anti-quark pair. After having a broad understanding of how one defines the DAs for photon, let us now collect the definitions and forms of photon DAs used throughout this thesis. However, a more complete list can be found in [71].

The photon DAs can be defined as the vacuum expectation value of the non-local quark-antiquark plus n gluons operator (when $n \geq 0$) with light-like separations in a complete analogy to the case of light meson. In this thesis, we considered

only the two particle i.e. quark-antiquark DAs of twist-2 and twist-3 which are defined as follows:

1. **Twist-2 DAs:** At twist-2, we have only one two-particle photon DA, $\phi_\gamma(u)$ which is defined as

$$\langle \gamma(k) | \bar{q}(0) \sigma_{\rho\sigma} q(x) | 0 \rangle = -ie_q \langle \bar{q}q \rangle (\epsilon_\rho k_\sigma - \epsilon_\sigma k_\rho) \int_0^1 du e^{i\bar{u}k \cdot x} \chi \phi_\gamma(u) \quad (\text{B.16})$$

where ϵ_μ is the polarisation vector of the photon, u and $\bar{u} = 1 - u$ are the momentum fractions carried by the quark and anti-quark, respectively. The photon DA, $\phi_\gamma(u)$ has the same form as of the twist-2 DA of pion defined in Eqn.(B.11) with the asymptotic form given by

$$\phi_\gamma^{asy}(u) = 6u(1 - u). \quad (\text{B.17})$$

2. **Twist-3 DAs:** At twist-3, there are four DAs out of which two are for two-particle. The other two are defined using the matrix element of three particles. The two-particle DAs are defined as

$$\langle \gamma(k) | \bar{q}(0) \gamma_\mu q(x) | 0 \rangle = e_q f_{3\gamma} \left(\epsilon_\mu^* - k_\mu \frac{\epsilon^* \cdot x}{k \cdot x} \right) \int_0^1 du e^{i\bar{u}k \cdot x} \psi^v(u, \mu) \quad (\text{B.18})$$

$$\langle \gamma(k) | \bar{q}(0) \gamma_\mu \gamma_5 q(x) | 0 \rangle = \frac{1}{4} e_q f_{3\gamma} \epsilon_{\mu\nu\alpha\beta} k^\alpha x^\beta \epsilon^{*\mu} \int_0^1 du e^{i\bar{u}k \cdot x} \psi^a(u, \mu) \quad (\text{B.19})$$

where, $f_{3\gamma}$ provides a natural mass scale for twist-3 DAs, $\psi^v(u)$ and $\psi^a(u)$.

The explicit form of these DAs are:

$$\psi^{(v)}(u) = 5(3\xi^2 - 1) + \frac{3}{64} (15\omega_\gamma^V - 5\omega_\gamma^A) (3 - 30\xi^2 + 35\xi^4) \quad (\text{B.20})$$

$$\psi^{(a)}(u) = (1 - \xi^2) (5\xi^2 - 1) \frac{5}{2} \left(1 + \frac{9}{16} \omega_\gamma^V - \frac{3}{16} \omega_\gamma^A \right) \quad (\text{B.21})$$

where, $\xi = 2u - 1$ and ω_γ^V & ω_γ^A corresponds to the local operators of dimension six. The values of these constants are provided in Appendix-D.

The integral of $\psi^v(\alpha)$ over α from 0 to u is defined as $\bar{\psi}^v(u)$ and reads as

$$\begin{aligned}\bar{\psi}^v(u) &= 2 \int_0^u d\alpha \psi^v(\alpha) \\ &= -20u\bar{u}\xi + \frac{15}{16} (\omega_\gamma^A - 3\omega_\gamma^V) u\bar{u}\xi (7\xi^2 - 3)\end{aligned}\quad (\text{B.22})$$

B.2.3 Nucleon DAs

The nucleon DAs are defined by the matrix element of the non-local three quark operator give by

$$\langle 0 | \epsilon^{abc} u_\alpha^a(a_1x) u_\beta^b(a_2x) d_\gamma^c(a_3x) | P(p, \lambda) \rangle \quad (\text{B.23})$$

where p and λ denote the momentum and helicity of the nucleon state, P , respectively, and u and d represents the up and down quarks. The Greek letters (α, β, γ) and the Latin letters (a, b, c) represents the Dirac and the color indices, respectively. a_i are some real numbers and z represents some light-like vector such that $z^2 = 0$.

Considering the Lorentz covariance, parity and spin of the nucleon, the above mentioned matrix element can be decomposed into 24 invariant functions, \mathcal{F}^i ($i = 1, \dots, 24$) in general such that

$$4 \langle 0 | \epsilon^{abc} u_\alpha^a(a_1x) u_\beta^b(a_2x) d_\gamma^c(a_3x) | P(p) \rangle = \sum_{i=1}^2 4\mathcal{F}^i(\{a_1, a_2, a_3\}, (p.x)) X_{\alpha\beta}^i Y_\gamma^i \quad (\text{B.24})$$

where $X_{\alpha\beta}^i$ and Y_γ^i are the gamma matrix structure, collected in Table-B.1 corresponding to each \mathcal{F}^i . The gamma matrix structures $X_{\alpha\beta}$ are such that

$$X_i^T = \begin{cases} X_i, & \mathcal{F}_i \in \mathcal{V}_i, \mathcal{T}_i \\ -X_i, & \mathcal{F}_i \in \mathcal{A}_i \end{cases} \quad (\text{B.25})$$

where superscript T represents transpose. The invariant functions, \mathcal{F}_i are the functions of $p.z$ and have the following symmetry property under the exchange

\mathcal{F}^i	$X_{\alpha\beta}$	Y_γ	\mathcal{F}^i	$X_{\alpha\beta}$	Y_γ
\mathcal{S}_1	$M(C)_{\alpha\beta}$	$(\gamma_5 N)_\gamma$	\mathcal{A}_3	$M(\gamma_\mu \gamma_5 C)_{\alpha\beta}$	$(\gamma^\mu N)_\gamma$
\mathcal{S}_2	$M^2(C)_{\alpha\beta}$	$(\not{z} \gamma_5 N)_\gamma$	\mathcal{A}_4	$M^2(\not{z} \gamma_5 C)_{\alpha\beta}$	$(N)_\gamma$
\mathcal{P}_1	$M(\gamma_5 C)_{\alpha\beta}$	$(N)_\gamma$	\mathcal{A}_5	$M^2(\gamma_\mu \gamma_5 C)_{\alpha\beta}$	$(i\sigma^{\mu\nu} z_\nu N)_\gamma$
\mathcal{P}_2	$M^2(\gamma_5 C)_{\alpha\beta}$	$(\not{z} N)_\gamma$	\mathcal{A}_6	$M^3(\not{z} \gamma_5 C)_{\alpha\beta}$	$(\not{z} N)_\gamma$
\mathcal{V}_1	$(\not{p} C)_{\alpha\beta}$	$(\gamma_5 N)_\gamma$	\mathcal{T}_1	$(p^\nu i\sigma_{\mu\nu} C)_{\alpha\beta}$	$(\gamma^\mu \gamma_5 N)_\gamma$
\mathcal{V}_2	$M(\not{p} C)_{\alpha\beta}$	$(\not{z} \gamma_5 N)_\gamma$	\mathcal{T}_2	$M(z^\mu p^\nu i\sigma_{\mu\nu} C)_{\alpha\beta}$	$(\gamma_5 N)_\gamma$
\mathcal{V}_3	$M(\gamma_\mu C)_{\alpha\beta}$	$(\gamma^\mu \gamma_5 N)_\gamma$	\mathcal{T}_3	$M(\sigma_{\mu\nu} C)_{\alpha\beta}$	$(\sigma^{\mu\nu} \gamma_5 N)_\gamma$
\mathcal{V}_4	$M^2(\not{z} C)_{\alpha\beta}$	$(\gamma_5 N)_\gamma$	\mathcal{T}_4	$(p^\nu \sigma_{\mu\nu} C)_{\alpha\beta}$	$(\sigma^{\mu\rho} z_\rho \gamma_5 N)_\gamma$
\mathcal{V}_5	$M^2(\gamma_\mu C)_{\alpha\beta}$	$(i\sigma^{\mu\nu} z_\nu \gamma_5 N)_\gamma$	\mathcal{T}_5	$M^2(z^\nu i\sigma_{\mu\nu} C)_{\alpha\beta}$	$(\gamma^\mu \gamma_5 N)_\gamma$
\mathcal{V}_6	$M^3(\not{z} C)_{\alpha\beta}$	$(\not{z} \gamma_5 N)_\gamma$	\mathcal{T}_6	$M^2(z^\mu p^\nu i\sigma_{\mu\nu} C)_{\alpha\beta}$	$(\not{z} \gamma_5 N)_\gamma$
\mathcal{A}_1	$(\not{p} \gamma_5 C)_{\alpha\beta}$	$(N)_\gamma$	\mathcal{T}_7	$M^2(\sigma_{\mu\nu} C)_{\alpha\beta}$	$(\sigma^{\mu\nu} \not{z} \gamma_5 N)_\gamma$
\mathcal{A}_2	$M(\not{p} \gamma_5 C)_{\alpha\beta}$	$(\not{z} N)_\gamma$	\mathcal{T}_8	$M^3(z^\nu \sigma_{\mu\nu} C)_{\alpha\beta}$	$(\sigma^{\mu\rho} z_\rho \gamma_5 N)_\gamma$

Table B.1: Tabulating the invariant functions and the gamma matrix structures that appear in the general decomposition of the matrix element of the non-local three quark operator which helps us define the nucleon DAs. Here, C is the charge conjugation matrix, M and N_γ are the mass and the spinor for the nucleon state, and $\sigma_{\mu\nu} = \frac{i}{2}[\gamma_\mu, \gamma_\nu]$.

of a_1 and a_2 ,

$$\mathcal{F}_i(\{a_1, a_2, a_3\}, (p_p \cdot x)) = \begin{cases} \mathcal{F}_i(\{a_2, a_1, a_3\}, (p_p \cdot x)), & \mathcal{F}_i \in \mathcal{V}_i, \mathcal{T}_i \\ -\mathcal{F}_i(\{a_2, a_1, a_3\}, (p_p \cdot x)), & \mathcal{F}_i \in \mathcal{A}_i \end{cases}. \quad (\text{B.26})$$

These functions are related to the light cone distribution amplitudes of the nucleon which can be seen by moving to the infinite momentum frame and decomposing the Dirac spinors in the good and the bad components as discussed in Section-2.2.2 (see [136] for the details). We do not discuss these relations for all 24 DAs here. However a twist classification of all the DAs can be found in Table-B.2.

In this thesis we have considered DAs upto twist-3 only, and hence we will discuss only them now. As can be seen from Table-B.2, there are three DAs upto twist-3: the vector, V_1 , the axial-vector, A_1 and the tensor, T_1 . These DAs

Type	twist-3	twist-4	twist-5	twist-6
Vector	V_1	V_2, V_3	V_4, V_5	V_6
Axial-vector	A_1	A_2, A_3	A_4, A_5	A_6
Tensor	T_1	T_2, T_3, T_4	T_5, T_6, T_7	T_8
Scalar		S_1	S_2	
Pseudo-scalar		P_1	P_2	

Table B.2: The twist classification of nucleon DAs.

can be represented as

$$\mathcal{F}^i(\{a_1, a_2, a_3\}, (p.x)) = \int_0^1 \mathcal{D}\alpha_i e^{-i\alpha_i a_i p.x} F^i(\alpha_1, \alpha_2, \alpha_3) \quad (\text{B.27})$$

where $\mathcal{D}\alpha_i = d\alpha_1 d\alpha_2 d\alpha_3 \delta(1 - \alpha_1 - \alpha_2 - \alpha_3)$ and α_i ($i = 1, 2, 3$) are the momentum fractions of the nucleon momentum carried by the three quarks.

These twist-3 DAs of the nucleon are related to the invariant functions in Eqn.(B.24) as

$$V_1 = \mathcal{V}_1, \quad A_1 = \mathcal{A}_1, \quad \text{and} \quad T_1 = \mathcal{T}_1. \quad (\text{B.28})$$

Therefore, one can directly use the parameterization in Eqn.(B.24) for computations upto twist-3. We suggest the reader to look at [136] for the relations of other DAs with the invariant functions in Eqn.(B.24). Moreover, it is important to point out that with the use of isospin symmetry, the number of independent DAs is reduced to eight from twenty four and there remains only one independent DA at twist-3 which is related to the DAs V_1 , A_1 and T_1 .

The explicit conformal expansion of V_1 , A_1 and T_1 DAs are

$$V_1(\alpha_i, \mu) = 120\alpha_1\alpha_2\alpha_3 [\phi_3^0(\mu) + \phi_3^+(\mu)(1 - 3\alpha_3)] \quad (\text{B.29})$$

$$A_1(\alpha_i, \mu) = 120\alpha_1\alpha_2\alpha_3(\alpha_2 - \alpha_1)\phi_3^-(\mu) \quad (\text{B.30})$$

$$T_1(\alpha_i, \mu) = 120\alpha_1\alpha_2\alpha_3 \left[\phi_3^0(\mu) + \frac{1}{2}(\phi_3^- - \phi_3^+)(\mu)(1 - \alpha_3) \right] \quad (\text{B.31})$$

where $\phi_3^0(\mu)$, $\phi_3^+(\mu)$, and $\phi_3^-(\mu)$ are the renormalisation scale, μ , dependent coefficients. They are available from QCD sum rules and are provided in Appendix-D.

B.2.4 Heavy meson DAs

Unlike the DAs of the light quark systems which we discussed above, the DAs for the heavy quark system can not be calculated using the conformal expansion. It is so because of the presence of heavy mass of the quark because of which the QCD Lagrangian does not obey the conformal symmetry any more. As a result, one uses heavy quark effective theory (HQET) to get define and obtain these DAs (see [72] and [157] for detailed discussion). These distribution amplitudes are defined using the matrix element of the bilocal operator involving a heavy quark taken between the vacuum and the heavy-meson state as

$$\begin{aligned} & \langle 0 | \bar{q}_\alpha(0)[x, 0] h_\beta(x) | M_h(v) \rangle \\ &= \frac{-i f_{M_h} m_{M_h}}{4} \int_0^\infty dw e^{i w v \cdot x} \left[(1 + \psi) \left\{ \phi_+^{M_h}(w) - \frac{\phi_+^{M_h}(w) - \phi_-^{M_h}(w)}{2v \cdot x} \not{x} \right\} \gamma_5 \right]_{\beta\alpha} \end{aligned} \quad (\text{B.32})$$

where q and h represents light and heavy quark, respectively. M_h is the heavy meson containing the heavy quark h . f_{M_h} and m_{M_h} are the decay constant and the mass of M_h -meson respectively. v is the velocity of the meson, and $\phi_+^{M_h}(w)$ and $\phi_-^{M_h}(w)$ are the DAs of M_h -meson. These DAs are not very-well known and have been parameterized using various models. For this thesis, we considered the simplest exponential model parameterization for these DAs [72] which reads as

$$\phi_+^{M_h}(w) = \frac{1}{w_0^2} e^{-w/w_0}, \quad \phi_-^{M_h}(w) = \frac{1}{w_0} e^{-w/w_0} \quad (\text{B.33})$$

where, w_0 is a model input parameter.

Appendix C

Kinematics for radiative tau decay

In this appendix, we discuss the kinematics involved in the decay width calculations of the radiative tau decay discussed in Chapter-3. We also provide the t-dependence of the intermediate vector bosons (ρ and a_1) in the end of this appendix.

C.1 Kinematics and decay width

As can be seen from Eqn.(3.46) and Eqn.(3.47), the total decay width for the process can be written as a sum of different components [87]: Γ_{IB} coming from $|\overline{\mathcal{A}_{IB}}|^2$, Γ_{SD} coming from $|\overline{\mathcal{A}_{SD}}|^2$ and Γ_{int} coming from $2\overline{\mathcal{R}e}(\overline{\mathcal{A}_{IB}^* \mathcal{A}_{SD}})$. Γ_{SD} can be further divided into three parts: Γ_{VV} coming from $|\overline{\mathcal{A}_v}|^2$, Γ_{AA} coming from $|\overline{\mathcal{A}_A}|^2$ and Γ_{AV} coming from $2\overline{\mathcal{R}e}(\overline{\mathcal{A}_V \mathcal{A}_A^*})$. Therefore, we can write

$$\begin{aligned}\Gamma_{all} &= \Gamma_{IB} + \Gamma_{int} + \Gamma_{SD}, \\ \Gamma_{SD} &= \Gamma_{VV} + \Gamma_{AV} + \Gamma_{AA}, \\ \Gamma_{int} &= \Gamma_{IB-A} + \Gamma_{IB-V}.\end{aligned}\tag{C.1}$$

Now, for convenience, we define the dimensionless variables x and y such that

$$x = \frac{2p_1 \cdot k}{m_\tau^2}, \quad \text{and} \quad y = \frac{2p_1 \cdot p_2}{m_\tau^2}. \quad (\text{C.2})$$

In the rest frame of tau-lepton, these variables, x and y are simply the energies of the photon and the pion, respectively in the units of $\frac{m_\tau}{2}$. The kinematical boundaries of these variables are given by,

$$0 \leq x \leq 1 - r_p^2, \quad 1 - x + \frac{r_p^2}{1 - x} \leq y \leq 1 + r_p^2 \quad (\text{C.3})$$

where $r_p^2 = \frac{m_\pi^2}{m_\tau^2}$. For the discussion in Chapter-3, we considered pion to be massless for form factor calculations thus, we must use $r_p \rightarrow 0$ in our final answers for consistency.

The variable t which provides the invariant mass square of the pion-photon system can be written in terms of x and y as

$$t = P^2 = (p_2 + k)^2 = m_\tau^2(x + y - 1) \quad \implies \quad P \cdot k = \frac{m_\tau^2}{2}(x + y - 1 - r_p^2), \quad (\text{C.4})$$

and the the differential decay width (provided in Eqn.(3.46)) in the rest frame of tau is given by

$$\frac{d^2\Gamma}{dxdy} = \frac{m_\tau}{256\pi^3} \overline{|\mathcal{A}|^2}, \quad (\text{C.5})$$

where $\overline{|\mathcal{A}|^2}$ is defined in Eqn.(3.47). Using the Mathematica package named FeynCalc [158]), we calculate these different contribution to the differential decay width as

$$\begin{aligned} \frac{d^2\Gamma_{IB}}{dxdy} &= \frac{\alpha}{2\pi} f_{IB}(x, y, r_p^2) \frac{\Gamma_{\tau^- \rightarrow \pi^- \nu_\tau}}{(1 - r_p^2)^2}, \\ \frac{d^2\Gamma_{SD}}{dxdy} &= \frac{\alpha}{8\pi} \frac{m_\tau^4}{f_\pi^2} \left\{ |F_V^{(\pi)}|^2 f_{VV}(x, y, r_p^2) + 2\mathcal{R}e(F_A^{(\pi)*} F_V^{(\pi)}) f_{AV}(x, y, r_p^2) \right. \\ &\quad \left. + |F_A^{(\pi)}|^2 f_{AA}(x, y, r_p^2) \right\} \frac{\Gamma_{\tau^- \rightarrow \pi^- \nu_\tau}}{(1 - r_p^2)^2}, \end{aligned} \quad (\text{C.6})$$

$$\frac{d^2\Gamma_{int}}{dxdy} = \frac{\alpha}{2\pi} \frac{m_\tau^2}{f_\pi} \left[f_{IB-V}(x, y, r_p^2) \mathcal{R}e(F_V^{(\pi)}) + f_{IB-A}(x, y, r_p^2) \mathcal{R}e(F_A^{(\pi)}) \right] \frac{\Gamma_{\tau^- \rightarrow \pi^- \nu_\tau}}{(1 - r_p^2)^2}, \quad (\text{C.7})$$

where $\alpha = \frac{e^2}{4\pi}$ is the fine structure constant, the functions $f_{IB}(x, y, r_p^2)$, $f_{VV}(x, y, r_p^2)$, $f_{AA}(x, y, r_p^2)$, $f_{IB-V}(x, y, r_p^2)$, and $f_{IB-A}(x, y, r_p^2)$ are

$$\begin{aligned}
f_{IB}(x, y, r_p^2) &= \frac{[r_p^4(x+2) - 2r_p^2(x+y) + (x+y-1)(2-3x+x^2+xy)](r_p^2-y+1)}{(r_p^2-x-y+1)^2x^2}, \\
f_{VV}(x, y, r_p^2) &= -[r_p^4(x+y) + 2r_p^2(1-y)(x+y) + (x+y-1)(-x+x^2-y+y^2)], \\
f_{AV}(x, y, r_p^2) &= -[r_p^2(x+y) + (1-x-y)(y-x)](r_p^2-x-y+1), \\
f_{AA}(x, y, r_p^2) &= f_{VV}(x, y, r_p^2), \\
f_{IB-V}(x, y, r_p^2) &= -\frac{(r_p^2-x-y+1)(r_p^2-y+1)}{x}, \\
f_{IB-A}(x, y, r_p^2) &= -\frac{[r_p^4 - 2r_p^2(x+y) + (1-x+y)(x+y-1)](r_p^2-y+1)}{(r_p^2-x-y+1)x},
\end{aligned} \tag{C.8}$$

and $\Gamma_{\tau^- \rightarrow \pi^- \nu_\tau}$ represents the non-radiative decay width given by

$$\Gamma_{\tau^- \rightarrow \pi^- \nu_\tau} = \frac{G_F^2 |V_{ud}|^2 f_\pi^2}{8\pi} m_\tau^3 (1-r_p^2)^2. \tag{C.9}$$

Using the double differential decay width given in Eqn.(C.5) and integrating over y , we get the photon spectrum for the process. Furthermore, the integration over x gives the total decay width for radiative tau decay. While integrating over x , the IB contribution receives infrared divergences because of zero mass of the photon. These divergences can be fixed by putting a threshold on the minimum energy of the emitted photon. Moreover, the SD contribution does not face any such divergence and hence can be integrated over the full phase space. Therefore, the total decay width for the process reads as

$$\Gamma(\tau^- \rightarrow \pi^- \nu_\tau \gamma) = \int_{x_0}^{1-r_p^2} dx \int_{1-x+\frac{r_p^2}{1-x}}^{1+r_p^2} dy \frac{d^2\Gamma}{dxdy} \tag{C.10}$$

where, x_0 is the minimum energy cut for the photon energy in unit of $\frac{m_\tau}{2}$ used to get rid of the IR divergences discussed above.

Finally, to get the invariant mass spectrum of $\pi - \gamma$ system, we define another

dimensionless variable z (as used in ref-[87]) as,

$$z = \frac{t}{m_\tau^2} = x + y - 1. \quad (\text{C.11})$$

The kinematical boundaries for this new variable are given by

$$z - r_p^2 \leq x \leq 1 - \frac{r_p^2}{z}, \quad r_p^2 \leq z \leq 1. \quad (\text{C.12})$$

The invariant mass spectrum of $\pi-\gamma$ system can then be obtained by substituting y in terms of z in Eqn.(C.5) and integrating over x . Hence, the $\pi-\gamma$ spectrum is defined as

$$\frac{d\Gamma}{dz} = \int_{z-r_p^2}^{1-\frac{r_p^2}{z}} dx \frac{d^2\Gamma}{dxdy}(x, y = z - x + 1). \quad (\text{C.13})$$

C.2 t-dependence of decay width of intermediate vector mesons

The t-dependence of decay widths of ρ and a_1 mesons are given by [93],

$$\Gamma_\rho(t) = \Gamma_\rho \frac{m_\rho^2 p^3}{p_\rho^3 t} \quad (\text{C.14})$$

with, $2p = (t - 4m_\pi^2)^{1/2}$ and $2p_\rho = (m_\rho^2 - 4m_\pi^2)^{1/2}$.

$$\Gamma_{a_1}(t) = \frac{m_{a_1} \Gamma_{a_1}}{\sqrt{t}} \frac{g(t)}{g(m_{a_1}^2)} \quad (\text{C.15})$$

with,

$$g(t) = \begin{cases} 4.1(t - 9m_\pi^2)^3(1 - 3.3(t - 9m_\pi^2) + 5.8(t - 9m_\pi^2)^2) & \text{if } t < (m_\rho + m_\pi)^2 \\ t(1.623 + \frac{10.38}{t} - \frac{9.38}{t^2} + \frac{0.65}{t^3}) & \text{else} \end{cases}$$

Appendix D

Numerical values of various parameters

In this Appendix, we collect the numerical values along with the errors of all the parameters used throughout this thesis. The values are tabulated chapterwise. In Table-D.1, we collected the numerical values of various parameters used while studying the radiative decay of tau lepton in Chapter-3 along with their symbolic representations. Similarly, the values used for the numerical analysis in Chapter-4 and Chapter-5 are collected in Table-D.2 and Table-D.3, respectively.

¹The value of the fine structure constant is taken at the scale m_τ and the decay width of a_1 meson is taken to the central value of the range given in [73].

²The decay constant for D^0 meson is not known. We have used the decay constant for D^+ meson here.

S.No.	Parameter	Symbol	Value used	References
1.	Fine structure constant	α	$\frac{1}{133.6}$	-
2.	Fermi's Constant	G_F	$1.166 \times 10^{-5} \text{ GeV}^{-2}$	[73]
3.	Mass of τ -lepton	m_τ	$(1776.86 \pm 0.12) \text{ MeV}$	[73]
4.	Pion decay constant	f_π	$(130.41 \pm 0.23) \text{ MeV}$	-
5.	CKM Matrix element	V_{ud}	(0.9745 ± 0.0001)	[73]
6.	Mass of ρ -meson	m_ρ	$(775.26 \pm 0.25) \text{ MeV}$	[73]
7.	Decay width of ρ -meson	Γ_ρ	$(149.1 \pm 0.8) \text{ MeV}$	[73]
8.	Mass of a_1 -meson	m_{a_1}	$(1230 \pm 40) \text{ MeV}$	[73]
9.	Decay width of a_1 -meson	Γ_{a_1}	$(425 \pm 175) \text{ MeV}$	[73]
10.	Vector form factor	$F_V^{(\pi)}(0)$	0.0254 ± 0.0017	[73]
11.	Axial-vector form factor	$F_A^{(\pi)}(0)$	0.0119 ± 0.0001	[73]
12.	$\alpha_s(1 \text{ GeV})$	$\alpha_s(1 \text{ GeV})$	~ 0.7	-
13.	$\alpha_s(m_\tau)$	$\alpha_s(m_\tau)$	0.325	-
14.	$a_2(1 \text{ GeV})$	$a_2(1 \text{ GeV})$	0.12	-

Table D.1: The numerical values of various parameters used in the numerical analysis performed for the form factor and decay width calculations for radiative tau decay¹.

S.No.	Parameter	Symbol	Value Used	Reference
1.	Proton mass	m_p	0.938 GeV	[35]
2.	Fine Structure Constant	$\alpha = \frac{e^2}{4\pi}$	$\frac{1}{137}$	[35]
3.	Quark condensate	$\langle \bar{q}q \rangle$	$-((256 \pm 2) \text{ MeV})^3$	[118]
4.	m_0^2	m_0^2	$(0.8 \pm 0.2) \text{ GeV}^2$	[118]
5.	Magnetic Susceptibility	χ	$(3.08 \pm 0.02) \text{ GeV}^{-2}$	[71]
6.	$f_{3\gamma}$	$f_{3\gamma}$	$-(4 \pm 2) \times 10^{-3} \text{ GeV}^2$	[71]
7.	ω_γ^v	ω_γ^v	3.8 ± 1.8	[71]
8.	ω_γ^a	ω_γ^a	-2.1 ± 1.0	[71]
9.	λ'_p	λ'_p	$(5.4 \pm 1.9) \times 10^{-2} \text{ GeV}^2$	[70]
10.	λ_p	λ_p	$-(2.7 \pm 0.9) \times 10^{-2} \text{ GeV}^2$	[70]
11.	$\phi_3^0(1\text{GeV})$	$\phi_3^0(1\text{GeV})$	$(5.3 \pm 0.5) \times 10^{-3} \text{ GeV}^2$	[136]
12.	$\tilde{\phi}_3^+(1\text{GeV}) = \frac{\phi_3^+}{\phi_3^0}$	$\tilde{\phi}_3^+(1\text{GeV})$	1.1 ± 0.3	[136]
13.	$\tilde{\phi}_3^-(1\text{GeV}) = \frac{\phi_3^-}{\phi_3^0}$	$\tilde{\phi}_3^-(1\text{GeV})$	4.0 ± 1.5	[136]

Table D.2: The numerical values of various parameters used during the numerical analysis of both the cases considered in Chapter-4 for determination of the form factors involved in radiative proton decay.

S.No.	Parameter	Symbol	Value Used	Reference
1.	Proton mass	m_p	0.938 GeV	[139]
2.	Quark condensate	$\langle \bar{q}q \rangle$	$-((256 \pm 2) \text{ MeV})^3$	[118]
3.	D-meson decay constant	f_D	$(0.212 \pm 0.001) \text{ GeV}^2$	[139]
4.	D-meson mass	m_D	1.864 GeV	[139]
5.	λ_{p1}	λ_{p1}	$(-0.027 \pm 0.009) \text{ GeV}^2$	[70]
6.	λ_{p2}	λ_{p2}	$(-0.013 \pm 0.004) \text{ GeV}^2$	[134]
7.	w_0	w_0	$(0.45 \pm 0.3) \text{ GeV}$	[159]

Table D.3: The numerical values of the parameters used during numerical analysis for the form factors involved in $D^0 \rightarrow \bar{p}e^+$ and $D_q^* D_q \gamma$, with $q = \{u, d, s\}$, coupling discussed in Chapter-5 ².

Bibliography

- [1] J. M. Cline, “Baryogenesis,” in *Les Houches Summer School - Session 86: Particle Physics and Cosmology: The Fabric of Spacetime*, Sep. 2006. arXiv: hep-ph/0609145.
- [2] S. Davidson, E. Nardi, and Y. Nir, “Leptogenesis,” *Phys. Rept.*, vol. 466, pp. 105–177, 2008. DOI: 10.1016/j.physrep.2008.06.002. arXiv: 0802.2962 [hep-ph].
- [3] S. M. Bilenky and S. T. Petcov, “Massive Neutrinos and Neutrino Oscillations,” *Rev. Mod. Phys.*, vol. 59, p. 671, 1987, [Erratum: Rev.Mod.Phys. 61, 169 (1989), Erratum: Rev.Mod.Phys. 60, 575–575 (1988)]. DOI: 10.1103/RevModPhys.59.671.
- [4] R. N. Mohapatra and A. Y. Smirnov, “Neutrino Mass and New Physics,” *Ann. Rev. Nucl. Part. Sci.*, vol. 56, K. Anagnostopoulos, I. Antoniadis, G. Fanourakis, *et al.*, Eds., pp. 569–628, 2006. DOI: 10.1146/annurev.nucl.56.080805.140534. arXiv: hep-ph/0603118.
- [5] G. Bertone and D. Hooper, “History of dark matter,” *Rev. Mod. Phys.*, vol. 90, no. 4, p. 045002, 2018. DOI: 10.1103/RevModPhys.90.045002. arXiv: 1605.04909 [astro-ph.CO].
- [6] E. Oks, “Brief review of recent advances in understanding dark matter and dark energy,” *New Astron. Rev.*, vol. 93, p. 101632, 2021. DOI: 10.1016/j.newar.2021.101632. arXiv: 2111.00363 [astro-ph.CO].
- [7] G. C. Branco, L. Lavoura, and J. P. Silva, *CP Violation*. 1999, vol. 103.

- [8] Y. Grossman and P. Tanedo, “Just a Taste: Lectures on Flavor Physics,” in *Theoretical Advanced Study Institute in Elementary Particle Physics: Anticipating the Next Discoveries in Particle Physics*, 2018, pp. 109–295. DOI: 10.1142/9789813233348_0004. arXiv: 1711.03624 [hep-ph].
- [9] B. Abi *et al.*, “Measurement of the Positive Muon Anomalous Magnetic Moment to 0.46 ppm,” *Phys. Rev. Lett.*, vol. 126, no. 14, p. 141 801, 2021. DOI: 10.1103/PhysRevLett.126.141801. arXiv: 2104.03281 [hep-ex].
- [10] T. Aoyama *et al.*, “The anomalous magnetic moment of the muon in the Standard Model,” *Phys. Rept.*, vol. 887, pp. 1–166, 2020. DOI: 10.1016/j.physrep.2020.07.006. arXiv: 2006.04822 [hep-ph].
- [11] A. A. Petrov, *Indirect Searches for New Physics*. Boca Raton: CRC Press, May 2021, ISBN: 978-1-351-17601-9. DOI: 10.1201/9781351176019.
- [12] A. J. Buras, “Weak Hamiltonian, CP violation and rare decays,” in *Les Houches Summer School in Theoretical Physics, Session 68: Probing the Standard Model of Particle Interactions*, Jun. 1998, pp. 281–539. arXiv: hep-ph/9806471.
- [13] G. Hiller and F. Kruger, “More model-independent analysis of $b \rightarrow s$ processes,” *Phys. Rev. D*, vol. 69, p. 074 020, 2004. DOI: 10.1103/PhysRevD.69.074020. arXiv: hep-ph/0310219.
- [14] D. London and J. Matias, “ B Flavour Anomalies: 2021 Theoretical Status Report,” Oct. 2021. DOI: 10.1146/annurev-nucl-102020-090209. arXiv: 2110.13270 [hep-ph].
- [15] S. L. Glashow, “Partial Symmetries of Weak Interactions,” *Nucl. Phys.*, vol. 22, pp. 579–588, 1961. DOI: 10.1016/0029-5582(61)90469-2.
- [16] A. Salam and J. C. Ward, “Electromagnetic and weak interactions,” *Phys. Lett.*, vol. 13, pp. 168–171, 1964. DOI: 10.1016/0031-9163(64)90711-5.
- [17] S. Weinberg, “A Model of Leptons,” *Phys. Rev. Lett.*, vol. 19, pp. 1264–1266, 1967. DOI: 10.1103/PhysRevLett.19.1264.

- [18] M. Gell-Mann, “The interpretation of the new particles as displaced charge multiplets,” *Nuovo Cim.*, vol. 4, no. S2, pp. 848–866, 1956. DOI: 10.1007/BF02748000.
- [19] T. Nakano and K. Nishijima, “Charge Independence for V-particles,” *Prog. Theor. Phys.*, vol. 10, pp. 581–582, 1953. DOI: 10.1143/PTP.10.581.
- [20] F. Englert and R. Brout, “Broken Symmetry and the Mass of Gauge Vector Mesons,” *Phys. Rev. Lett.*, vol. 13, J. C. Taylor, Ed., pp. 321–323, 1964. DOI: 10.1103/PhysRevLett.13.321.
- [21] P. W. Higgs, “Broken symmetries, massless particles and gauge fields,” *Phys. Lett.*, vol. 12, pp. 132–133, 1964. DOI: 10.1016/0031-9163(64)91136-9.
- [22] ———, “Broken Symmetries and the Masses of Gauge Bosons,” *Phys. Rev. Lett.*, vol. 13, J. C. Taylor, Ed., pp. 508–509, 1964. DOI: 10.1103/PhysRevLett.13.508.
- [23] G. S. Guralnik, C. R. Hagen, and T. W. B. Kibble, “Global Conservation Laws and Massless Particles,” *Phys. Rev. Lett.*, vol. 13, J. C. Taylor, Ed., pp. 585–587, 1964. DOI: 10.1103/PhysRevLett.13.585.
- [24] P. W. Higgs, “Spontaneous Symmetry Breakdown without Massless Bosons,” *Phys. Rev.*, vol. 145, pp. 1156–1163, 1966. DOI: 10.1103/PhysRev.145.1156.
- [25] T. W. B. Kibble, “Symmetry breaking in nonAbelian gauge theories,” *Phys. Rev.*, vol. 155, J. C. Taylor, Ed., pp. 1554–1561, 1967. DOI: 10.1103/PhysRev.155.1554.
- [26] S. Chatrchyan *et al.*, “Observation of a New Boson at a Mass of 125 GeV with the CMS Experiment at the LHC,” *Phys. Lett. B*, vol. 716, pp. 30–61, 2012. DOI: 10.1016/j.physletb.2012.08.021. arXiv: 1207.7235 [hep-ex].

- [27] G. Aad *et al.*, “Observation of a new particle in the search for the Standard Model Higgs boson with the ATLAS detector at the LHC,” *Phys. Lett. B*, vol. 716, pp. 1–29, 2012. DOI: 10.1016/j.physletb.2012.08.020. arXiv: 1207.7214 [hep-ex].
- [28] N. Cabibbo, “Unitary Symmetry and Leptonic Decays,” *Phys. Rev. Lett.*, vol. 10, pp. 531–533, 1963. DOI: 10.1103/PhysRevLett.10.531.
- [29] M. Kobayashi and T. Maskawa, “CP Violation in the Renormalizable Theory of Weak Interaction,” *Prog. Theor. Phys.*, vol. 49, pp. 652–657, 1973. DOI: 10.1143/PTP.49.652.
- [30] M. D. Schwartz, *Quantum Field Theory and the Standard Model*. Cambridge University Press, Mar. 2014, ISBN: 978-1-107-03473-0, 978-1-107-03473-0.
- [31] T. Muta, *Foundations of quantum chromodynamics: An Introduction to perturbative methods in gauge theories*. 1987, vol. 5.
- [32] C. Amsler, *The Quark Structure of Hadrons: An Introduction to the Phenomenology and Spectroscopy*. Cham: Springer, 2018, vol. 949, ISBN: 978-3-319-98526-8, 978-3-319-98527-5. DOI: 10.1007/978-3-319-98527-5.
- [33] L. B. Okun, *Leptons and Quarks: Special Edition Commemorating the Discovery of the Higgs Boson*. Amsterdam, Netherlands: North-Holland, 1982, ISBN: 978-981-4603-14-0, 978-981-4603-00-3, 978-0-444-86924-1. DOI: 10.1142/9162.
- [34] C. Itzykson and J. B. Zuber, *Quantum Field Theory*, ser. International Series In Pure and Applied Physics. New York: McGraw-Hill, 1980, ISBN: 978-0-486-44568-7.
- [35] P. Zyla *et al.*, “Review of Particle Physics,” *PTEP*, vol. 2020, no. 8, p. 083C01, 2020. DOI: 10.1093/ptep/ptaa104.
- [36] L. Maiani and A. Pilloni, “GGI Lectures on Exotic Hadrons,” Jul. 2022. arXiv: 2207.05141 [hep-ph].

- [37] A. Khodjamirian, *Hadron Form Factors: From Basic Phenomenology to QCD Sum Rules*. Boca Raton, FL, USA: CRC Press, Taylor & Francis Group, 2020, ISBN: 978-1-138-30675-2, 978-1-315-14200-5.
- [38] D. Akers, “Constituent quark model and new particles,” Mar. 2003. arXiv: hep-ph/0303139.
- [39] A. Chodos, R. L. Jaffe, K. Johnson, C. B. Thorn, and V. F. Weisskopf, “A New Extended Model of Hadrons,” *Phys. Rev. D*, vol. 9, pp. 3471–3495, 1974. DOI: 10.1103/PhysRevD.9.3471.
- [40] S. Weinberg, “Phenomenological Lagrangians,” *Physica A*, vol. 96, no. 1-2, S. Deser, Ed., pp. 327–340, 1979. DOI: 10.1016/0378-4371(79)90223-1.
- [41] A. Pich, “Chiral perturbation theory,” *Rept. Prog. Phys.*, vol. 58, pp. 563–610, 1995. DOI: 10.1088/0034-4885/58/6/001. arXiv: hep-ph/9502366.
- [42] G. Colangelo and G. Isidori, “An Introduction to ChPT,” *Frascati Phys. Ser.*, vol. 18, G. Panzeri, Ed., pp. 333–376, 2000. arXiv: hep-ph/0101264.
- [43] H. Leutwyler, “Chiral dynamics,” M. Shifman and B. Ioffe, Eds., pp. 271–316, Aug. 2000. DOI: 10.1142/9789812810458_0012. arXiv: hep-ph/0008124.
- [44] G. S. Bali, “QCD forces and heavy quark bound states,” *Phys. Rept.*, vol. 343, pp. 1–136, 2001. DOI: 10.1016/S0370-1573(00)00079-X. arXiv: hep-ph/0001312.
- [45] R. Gupta, “Introduction to lattice QCD: Course,” in *Les Houches Summer School in Theoretical Physics, Session 68: Probing the Standard Model of Particle Interactions*, Jul. 1997, pp. 83–219. arXiv: hep-lat/9807028.
- [46] N. H. Christ, R. Friedberg, and T. D. Lee, “GAUGE THEORY ON A RANDOM LATTICE,” *Nucl. Phys. B*, vol. 210, J. Julve and M. Ramón-Medrano, Eds., p. 310, 1982. DOI: 10.1016/0550-3213(82)90123-7.
- [47] P. Colangelo and A. Khodjamirian, “QCD sum rules, a modern perspective,” M. Shifman and B. Ioffe, Eds., pp. 1495–1576, Oct. 2000. DOI: 10.1142/9789812810458_0033. arXiv: hep-ph/0010175.

- [48] M. A. Shifman, A. Vainshtein, and V. I. Zakharov, “QCD and Resonance Physics. Theoretical Foundations,” *Nucl. Phys. B*, vol. 147, pp. 385–447, 1979. DOI: 10.1016/0550-3213(79)90022-1.
- [49] M. A. Shifman, “Snapshots of hadrons or the story of how the vacuum medium determines the properties of the classical mesons which are produced, live and die in the QCD vacuum,” *Prog. Theor. Phys. Suppl.*, vol. 131, pp. 1–71, 1998. DOI: 10.1143/PTPS.131.1. arXiv: hep-ph/9802214.
- [50] A. Khodjamirian, T. Mannel, and N. Offen, “Form-factors from light-cone sum rules with B-meson distribution amplitudes,” *Phys. Rev. D*, vol. 75, p. 054013, 2007. DOI: 10.1103/PhysRevD.75.054013. arXiv: hep-ph/0611193.
- [51] A. V. Manohar, “Introduction to Effective Field Theories,” S. Davidson, P. Gambino, M. Laine, M. Neubert, and C. Salomon, Eds., Apr. 2018. DOI: 10.1093/oso/9780198855743.003.0002. arXiv: 1804.05863 [hep-ph].
- [52] P. Colangelo and A. Khodjamirian, “QCD sum rules, a modern perspective,” M. Shifman and B. Ioffe, Eds., pp. 1495–1576, Oct. 2000. DOI: 10.1142/9789812810458_0033. arXiv: hep-ph/0010175.
- [53] K. G. Wilson, “Nonlagrangian models of current algebra,” *Phys. Rev.*, vol. 179, pp. 1499–1512, 1969. DOI: 10.1103/PhysRev.179.1499.
- [54] H. A. Kramers, “La diffusion de la lumiere par les atomes,” in *Atti Cong. Intern. Fisica (Transactions of Volta Centenary Congress) Como*, vol. 2, 1927, pp. 545–557.
- [55] R. de L. Kronig, “On the theory of dispersion of x-rays,” *J. Opt. Soc. Am.*, vol. 12, no. 6, pp. 547–557, Jun. 1926. DOI: 10.1364/JOSA.12.000547. [Online]. Available: <http://opg.optica.org/abstract.cfm?URI=josa-12-6-547>.
- [56] R. Zwicky, “A brief Introduction to Dispersion Relations and Analyticity,” in *Quantum Field Theory at the Limits: from Strong Fields to Heavy*

- Quarks*, 2017, pp. 93–120. DOI: 10.3204/DESY-PROC-2016-04/Zwicky. arXiv: 1610.06090 [hep-ph].
- [57] G. Kallen, “On the definition of the Renormalization Constants in Quantum Electrodynamics,” *Helv. Phys. Acta*, vol. 25, no. 4, C. Jarlskog, Ed., p. 417, 1952. DOI: 10.1007/978-3-319-00627-7_90.
- [58] H. Lehmann, “On the Properties of propagation functions and renormalization constants of quantized fields,” *Nuovo Cim.*, vol. 11, pp. 342–357, 1954. DOI: 10.1007/BF02783624.
- [59] M. A. Shifman, “Quark hadron duality,” in *8th International Symposium on Heavy Flavor Physics*, vol. 3, Singapore: World Scientific, Jul. 2000, pp. 1447–1494. DOI: 10.1142/9789812810458_0032. arXiv: hep-ph/0009131.
- [60] B. Chibisov, R. D. Dikeman, M. A. Shifman, and N. Uraltsev, “Operator product expansion, heavy quarks, QCD duality and its violations,” *Int. J. Mod. Phys. A*, vol. 12, pp. 2075–2133, 1997. DOI: 10.1142/S0217751X97001316. arXiv: hep-ph/9605465.
- [61] D. Boito, I. Caprini, M. Golterman, K. Maltman, and S. Peris, “Hyperasymptotics and quark-hadron duality violations in QCD,” *Phys. Rev. D*, vol. 97, no. 5, p. 054007, 2018. DOI: 10.1103/PhysRevD.97.054007. arXiv: 1711.10316 [hep-ph].
- [62] É. Borel, “Mémoire sur les séries divergentes,” fr, *Annales scientifiques de l’École Normale Supérieure*, vol. 3e série, 16, pp. 9–131, 1899. DOI: 10.24033/asens.463. [Online]. Available: <http://www.numdam.org/articles/10.24033/asens.463/>.
- [63] I. Novak and S. Olejnik, “BOUND STATE PERTURBATION METHOD VIA SVZ SUM RULES IN QUANTUM MECHANICS,” *Czech. J. Phys. B*, vol. 35, pp. 1067–1083, 1985, [Addendum: *Czech.J.Phys.B* 36, 655–658 (1986)]. DOI: 10.1007/BF01597498.

- [64] V. M. Braun, “Light cone sum rules,” in *4th International Workshop on Progress in Heavy Quark Physics*, Sep. 1997, pp. 105–118. arXiv: hep-ph/9801222.
- [65] V. L. Chernyak and A. R. Zhitnitsky, “Asymptotic Behavior of Exclusive Processes in QCD,” *Phys. Rept.*, vol. 112, p. 173, 1984. DOI: 10.1016/0370-1573(84)90126-1.
- [66] G. P. Lepage and S. J. Brodsky, “Exclusive Processes in Perturbative Quantum Chromodynamics,” *Phys. Rev. D*, vol. 22, p. 2157, 1980. DOI: 10.1103/PhysRevD.22.2157.
- [67] R. A. Brandt and G. Preparata, “Operator product expansions near the light cone,” *Nucl. Phys. B*, vol. 27, pp. 541–567, 1971. DOI: 10.1016/0550-3213(71)90265-3.
- [68] F. A. C. Porkert, “Meson distribution amplitudes,” Ph.D. dissertation, Regensburg U., 2019.
- [69] V. M. Braun, G. P. Korchemsky, and D. Müller, “The Uses of conformal symmetry in QCD,” *Prog. Part. Nucl. Phys.*, vol. 51, pp. 311–398, 2003. DOI: 10.1016/S0146-6410(03)90004-4. arXiv: hep-ph/0306057.
- [70] V. M. Braun, A. Lenz, and M. Wittmann, “Nucleon Form Factors in QCD,” *Phys. Rev. D*, vol. 73, p. 094019, 2006. DOI: 10.1103/PhysRevD.73.094019. arXiv: hep-ph/0604050.
- [71] P. Ball, V. M. Braun, and N. Kivel, “Photon distribution amplitudes in QCD,” *Nucl. Phys. B*, vol. 649, pp. 263–296, 2003. DOI: 10.1016/S0550-3213(02)01017-9. arXiv: hep-ph/0207307.
- [72] A. G. Grozin and M. Neubert, “Asymptotics of heavy meson form-factors,” *Phys. Rev. D*, vol. 55, pp. 272–290, 1997. DOI: 10.1103/PhysRevD.55.272. arXiv: hep-ph/9607366.
- [73] P. D. Group, “Review of particle physics,” *PRD* 98,030001, 2018.
- [74] A. Bansal and N. Mahajan, “Phenomenology of $\tau^- \rightarrow \pi^- \nu_\tau \gamma$ using light cone sum rules,” *Phys. Rev. D*, vol. 103, no. 5, p. 056017, 2021. DOI: 10.1103/PhysRevD.103.056017. arXiv: 2010.00549 [hep-ph].

- [75] B. Barish and R. Stroynowski, “The Physics of the tau Lepton,” *Phys. Rept.*, vol. 157, p. 1, 1988. DOI: 10.1016/0370-1573(88)90103-2.
- [76] S. Gentile and M. Pohl, “Physics of τ leptons,” *Phys. Rept.*, vol. 274, pp. 287–376, 1996. DOI: 10.1016/0370-1573(96)00002-6.
- [77] A. Stahl, “Physics with tau leptons,” *Springer Tracts Mod. Phys.*, vol. 160, pp. 1–316, 2000. DOI: 10.1007/BFb0109630.
- [78] M. Davier, A. Hocker, and Z. Zhang, “The Physics of Hadronic Tau Decays,” *Rev. Mod. Phys.*, vol. 78, pp. 1043–1109, 2006. DOI: 10.1103/RevModPhys.78.1043. arXiv: hep-ph/0507078.
- [79] A. Pich, “Precision Tau Physics,” *Prog. Part. Nucl. Phys.*, vol. 75, pp. 41–85, 2014. DOI: 10.1016/j.pnpnp.2013.11.002. arXiv: 1310.7922 [hep-ph].
- [80] J. H. Kim and L. Resnick, “ τ radiative decay and pion structure form factors,” *Phys. Rev. D*, vol. 21, no. 5, pp. 1330–1333, Mar. 1980. DOI: 10.1103/PhysRevD.21.1330.
- [81] Y. Ivanov, A. Osipov, and M. Volkov, “Radiative decay tau \rightarrow tau-neutrino pi gamma,” *Phys. Lett. B*, vol. 242, pp. 498–502, 1990. DOI: 10.1016/0370-2693(90)91801-H.
- [82] R. Decker and M. Finkemeier, “Radiative corrections to the decay tau \rightarrow pi (K) tau-neutrino. 2,” *Phys. Lett. B*, vol. 334, pp. 199–202, 1994. DOI: 10.1016/0370-2693(94)90611-4.
- [83] C. Geng and C. Lih, “Tau radiative decays in the light front quark model,” *Phys. Rev. D*, vol. 68, p. 093001, 2003. DOI: 10.1103/PhysRevD.68.093001. arXiv: hep-ph/0310161.
- [84] Z.-H. Guo and P. Roig, “One meson radiative tau decays,” *Phys. Rev. D*, vol. 82, p. 113016, 2010. DOI: 10.1103/PhysRevD.82.113016. arXiv: 1009.2542 [hep-ph].
- [85] V. Cirigliano, G. Ecker, and H. Neufeld, “Radiative tau decay and the magnetic moment of the muon,” *JHEP*, vol. 08, p. 002, 2002. DOI: 10.1088/1126-6708/2002/08/002. arXiv: hep-ph/0207310.

- [86] S. Banerjee, “Analysis of radiative τ decays,” *Phys. Rev. D*, vol. 34, pp. 2080–2087, 7 Oct. 1986. DOI: 10.1103/PhysRevD.34.2080. [Online]. Available: <https://link.aps.org/doi/10.1103/PhysRevD.34.2080>.
- [87] R. Decker and M. Finkemeier, “Radiative tau decays with one pseudoscalar meson,” *Phys. Rev. D*, vol. 48, pp. 4203–4215, 1993, [Addendum: *Phys.Rev.D* 50, 7079–7081 (1994)]. DOI: 10.1103/PhysRevD.48.4203. arXiv: [hep-ph/9302286](https://arxiv.org/abs/hep-ph/9302286).
- [88] A. Khodjamirian and D. Wyler, “Counting contact terms in $B \rightarrow V$ gamma decays,” Nov. 2001. DOI: 10.1142/9789812777478_0014. arXiv: [hep-ph/0111249](https://arxiv.org/abs/hep-ph/0111249).
- [89] K. Kawarabayashi and M. Suzuki, “Partially conserved axial vector current and the decays of vector mesons,” *Phys. Rev. Lett.*, vol. 16, p. 255, 1966. DOI: 10.1103/PhysRevLett.16.255.
- [90] Riazuddin and Fayyazuddin, “Algebra of current components and decay widths of rho and K^* mesons,” *Phys. Rev.*, vol. 147, pp. 1071–1073, 1966. DOI: 10.1103/PhysRev.147.1071.
- [91] M. Gonzalez-Alonso, A. Pich, and J. Prades, “Violation of Quark-Hadron Duality and Spectral Chiral Moments in QCD,” *Phys. Rev. D*, vol. 81, p. 074007, 2010. DOI: 10.1103/PhysRevD.81.074007. arXiv: 1001.2269 [hep-ph].
- [92] C. A. Dominguez, L. A. Hernandez, K. Schilcher, and H. Spiesberger, “Tests of quark-hadron duality in tau-decays,” *Mod. Phys. Lett. A*, vol. 31, no. 31, p. 1630036, 2016. DOI: 10.1142/S0217732316300366. arXiv: 1607.02048 [hep-ph].
- [93] J. H. Kuhn and A. Santamaria, “Tau decays to pions,” *Z. Phys. C*, vol. 48, pp. 445–452, 1990. DOI: 10.1007/BF01572024.
- [94] A. D. Sakharov, “Violation of CP Invariance, C asymmetry, and baryon asymmetry of the universe,” *Pisma Zh. Eksp. Teor. Fiz.*, vol. 5, pp. 32–35, 1967. DOI: 10.1070/PU1991v034n05ABEH002497.

- [95] A. Bansal and N. Mahajan, “Light cone sum rules and form factors for $p \rightarrow e^+ \gamma$,” *JHEP*, vol. 06, p. 161, 2022. DOI: 10.1007/JHEP06(2022)161. arXiv: 2204.03448 [hep-ph].
- [96] J. C. Pati and A. Salam, “Unified Lepton-Hadron Symmetry and a Gauge Theory of the Basic Interactions,” *Phys. Rev. D*, vol. 8, pp. 1240–1251, 1973. DOI: 10.1103/PhysRevD.8.1240.
- [97] H. Georgi and S. L. Glashow, “Unity of All Elementary Particle Forces,” *Phys. Rev. Lett.*, vol. 32, pp. 438–441, 1974. DOI: 10.1103/PhysRevLett.32.438.
- [98] H. P. Nilles, “Supersymmetry, Supergravity and Particle Physics,” *Phys. Rept.*, vol. 110, pp. 1–162, 1984. DOI: 10.1016/0370-1573(84)90008-5.
- [99] D. E. Morrissey and M. J. Ramsey-Musolf, “Electroweak baryogenesis,” *New J. Phys.*, vol. 14, p. 125003, 2012. DOI: 10.1088/1367-2630/14/12/125003. arXiv: 1206.2942 [hep-ph].
- [100] P. Fileviez Perez, “New Paradigm for Baryon and Lepton Number Violation,” *Phys. Rept.*, vol. 597, pp. 1–30, 2015. DOI: 10.1016/j.physrep.2015.09.001. arXiv: 1501.01886 [hep-ph].
- [101] H. E. Haber and G. L. Kane, “The Search for Supersymmetry: Probing Physics Beyond the Standard Model,” *Phys. Rept.*, vol. 117, pp. 75–263, 1985. DOI: 10.1016/0370-1573(85)90051-1.
- [102] N. Chamoun, F. Domingo, and H. K. Dreiner, “Nucleon decay in the R-parity violating MSSM,” *Phys. Rev. D*, vol. 104, no. 1, p. 015020, 2021. DOI: 10.1103/PhysRevD.104.015020. arXiv: 2012.11623 [hep-ph].
- [103] K. R. Dienes, E. Dudas, and T. Gherghetta, “Extra space-time dimensions and unification,” *Phys. Lett. B*, vol. 436, pp. 55–65, 1998. DOI: 10.1016/S0370-2693(98)00977-0. arXiv: hep-ph/9803466.
- [104] R. H. Brandenberger, A.-C. Davis, and A. M. Matheson, “Cosmic Strings and Baryogenesis,” *Phys. Lett. B*, vol. 218, pp. 304–308, 1989. DOI: 10.1016/0370-2693(89)91586-4.

- [105] B. Fornal and B. Shams Es Haghi, “Baryon and Lepton Number Violation from Gravitational Waves,” *Phys. Rev. D*, vol. 102, no. 11, p. 115 037, 2020. DOI: 10 . 1103 / PhysRevD . 102 . 115037. arXiv: 2008 . 05111 [hep-ph].
- [106] C. Murgui and M. B. Wise, “Scalar leptoquarks, baryon number violation, and Pati-Salam symmetry,” *Phys. Rev. D*, vol. 104, no. 3, p. 035 017, 2021. DOI: 10.1103/PhysRevD.104.035017. arXiv: 2105.14029 [hep-ph].
- [107] P. Nath and P. Fileviez Perez, “Proton stability in grand unified theories, in strings and in branes,” *Phys. Rept.*, vol. 441, pp. 191–317, 2007. DOI: 10.1016/j.physrep.2007.02.010. arXiv: hep-ph/0601023.
- [108] P. Langacker, “Grand Unified Theories and Proton Decay,” *Phys. Rept.*, vol. 72, p. 185, 1981. DOI: 10.1016/0370-1573(81)90059-4.
- [109] P. H. Frampton, “A novel viewpoint of Proton Decay,” Dec. 2021. arXiv: 2112.10720 [hep-ph].
- [110] J. Hisano, “Proton Decay in SUSY GUTs,” Feb. 2022. arXiv: 2202.01404 [hep-ph].
- [111] Y. Aoki, C. Dawson, J. Noaki, and A. Soni, “Proton decay matrix elements with domain-wall fermions,” *Phys. Rev. D*, vol. 75, p. 014 507, 2007. DOI: 10.1103/PhysRevD.75.014507. arXiv: hep-lat/0607002.
- [112] Y. Aoki, T. Izubuchi, E. Shintani, and A. Soni, “Improved lattice computation of proton decay matrix elements,” *Phys. Rev. D*, vol. 96, no. 1, p. 014 506, 2017. DOI: 10.1103/PhysRevD.96.014506. arXiv: 1705.01338 [hep-lat].
- [113] V. S. Berezinsky, B. L. Ioffe, and Y. I. Kogan, “The Calculation of Matrix Element for Proton Decay,” *Phys. Lett. B*, vol. 105, p. 33, 1981. DOI: 10.1016/0370-2693(81)90034-4.
- [114] N. Isgur and M. B. Wise, “On the Consistency of Chiral Symmetry and the Quark Model in Proton Decay,” *Phys. Lett. B*, vol. 117, pp. 179–184, 1982. DOI: 10.1016/0370-2693(82)90542-1.

- [115] A. M. Din, G. Girardi, and P. Sorba, “A Bag Model Calculation of the Nucleon Lifetime in Grand Unified Theories,” *Phys. Lett. B*, vol. 91, pp. 77–80, 1980. DOI: 10.1016/0370-2693(80)90665-6.
- [116] M. B. Gavela, A. Le Yaouanc, L. Oliver, O. Pene, and J. C. Raynal, “Calculation of Proton Decay in the Nonrelativistic Quark Model,” *Phys. Rev. D*, vol. 23, pp. 1580–1590, 1981. DOI: 10.1103/PhysRevD.23.1580.
- [117] M. Machacek, “The Decay Modes of the Proton,” *Nucl. Phys. B*, vol. 159, pp. 37–55, 1979. DOI: 10.1016/0550-3213(79)90325-0.
- [118] U. Haisch and A. Hala, “Light-cone sum rules for proton decay,” *JHEP*, vol. 05, p. 258, 2021. DOI: 10.1007/JHEP05(2021)258. arXiv: 2103.13928 [hep-ph].
- [119] M. R. Krishnaswamy, M. G. K. Menon, N. K. Mondal, *et al.*, “Candidate Events for Nucleon Decay in the Kolar Gold Field Experiment,” *Phys. Lett. B*, vol. 106, pp. 339–346, 1981. DOI: 10.1016/0370-2693(81)90549-9.
- [120] G. Battistoni *et al.*, “The Nussex Detector,” *Nucl. Instrum. Meth. A*, vol. 245, p. 277, 1986. DOI: 10.1016/0168-9002(86)91261-1.
- [121] J. L. Thron, “The Soudan-II Proton Decay Experiment,” *Nucl. Instrum. Meth. A*, vol. 283, pp. 642–645, 1989. DOI: 10.1016/0168-9002(89)91432-0.
- [122] K. S. Hirata *et al.*, “Experimental Limits on Nucleon Lifetime for Lepton + Meson Decay Modes,” *Phys. Lett. B*, vol. 220, pp. 308–316, 1989. DOI: 10.1016/0370-2693(89)90058-0.
- [123] K. Abe *et al.*, “Search for proton decay via $p \rightarrow e^+\pi^0$ and $p \rightarrow \mu^+\pi^0$ in 0.31 megaton-years exposure of the Super-Kamiokande water Cherenkov detector,” *Phys. Rev. D*, vol. 95, no. 1, p. 012004, 2017. DOI: 10.1103/PhysRevD.95.012004. arXiv: 1610.03597 [hep-ex].
- [124] D. Silverman and A. Soni, “The Decay Proton $\rightarrow e^+\gamma$ in Grand Unified Gauge Theories,” *Phys. Lett. B*, vol. 100, pp. 131–134, 1981. DOI: 10.1016/0370-2693(81)90759-0.

- [125] J. O. Eeg and I. Picek, “Relevance of the 3 q Annihilation and the Radiative Proton Decay,” *Phys. Lett. B*, vol. 112, pp. 59–62, 1982. DOI: 10.1016/0370-2693(82)90905-4.
- [126] P. S. B. Dev *et al.*, “Searches for Baryon Number Violation in Neutrino Experiments: A White Paper,” Mar. 2022. arXiv: 2203.08771 [hep-ex].
- [127] V. Takhistov, “Review of Nucleon Decay Searches at Super-Kamiokande,” in *51st Rencontres de Moriond on EW Interactions and Unified Theories*, 2016, pp. 437–444. arXiv: 1605.03235 [hep-ex].
- [128] S. Weinberg, “Baryon and Lepton Nonconserving Processes,” *Phys. Rev. Lett.*, vol. 43, pp. 1566–1570, 1979. DOI: 10.1103/PhysRevLett.43.1566.
- [129] F. Wilczek and A. Zee, “Operator Analysis of Nucleon Decay,” *Phys. Rev. Lett.*, vol. 43, pp. 1571–1573, 1979. DOI: 10.1103/PhysRevLett.43.1571.
- [130] M. Claudson, M. B. Wise, and L. J. Hall, “Chiral Lagrangian for Deep Mine Physics,” *Nucl. Phys. B*, vol. 195, pp. 297–307, 1982. DOI: 10.1016/0550-3213(82)90401-1.
- [131] S. Chadha and M. Daniel, “Chiral Lagrangian Calculation of Nucleon Decay Modes Induced by $d = 5$ Supersymmetric Operators,” *Nucl. Phys. B*, vol. 229, pp. 105–114, 1983. DOI: 10.1016/0550-3213(83)90355-3.
- [132] N. G. Deshpande and G. Eilam, “FLAVOR CHANGING ELECTROMAGNETIC TRANSITIONS,” *Phys. Rev. D*, vol. 26, p. 2463, 1982. DOI: 10.1103/PhysRevD.26.2463.
- [133] B. L. Ioffe, “ON THE CHOICE OF QUARK CURRENTS IN THE QCD SUM RULES FOR BARYON MASSES,” *Z. Phys. C*, vol. 18, p. 67, 1983. DOI: 10.1007/BF01571709.
- [134] D. B. Leinweber, “Nucleon properties from unconventional interpolating fields,” *Phys. Rev. D*, vol. 51, pp. 6383–6393, 1995. DOI: 10.1103/PhysRevD.51.6383. arXiv: nucl-th/9406001.
- [135] J. F. Nieves and P. B. Pal, “Generalized Fierz identities,” *Am. J. Phys.*, vol. 72, pp. 1100–1108, 2004. DOI: 10.1119/1.1757445. arXiv: hep-ph/0306087.

- [136] V. Braun, R. J. Fries, N. Mahnke, and E. Stein, “Higher twist distribution amplitudes of the nucleon in QCD,” *Nucl. Phys. B*, vol. 589, pp. 381–409, 2000, [Erratum: *Nucl.Phys.B* 607, 433–433 (2001)]. DOI: 10.1016/S0550-3213(00)00516-2. arXiv: hep-ph/0007279.
- [137] K. M. Patel and S. K. Shukla, “Anatomy of scalar mediated proton decays in $SO(10)$ models,” Mar. 2022. arXiv: 2203.07748 [hep-ph].
- [138] A. Bansal, “ $D^0 \rightarrow \bar{p}e^+$ Form Factors in LCSR,” May 2022. arXiv: 2205.13564 [hep-ph].
- [139] P. A. Zyla *et al.*, “Review of Particle Physics,” *PTEP*, vol. 2020, no. 8, p. 083C01, 2020. DOI: 10.1093/ptep/ptaa104.
- [140] M. Tanaka *et al.*, “Search for proton decay into three charged leptons in 0.37 megaton-years exposure of the Super-Kamiokande,” *Phys. Rev. D*, vol. 101, no. 5, p. 052011, 2020. DOI: 10.1103/PhysRevD.101.052011. arXiv: 2001.08011 [hep-ex].
- [141] M. Ablikim *et al.*, “Search for baryon- and lepton-number violating decays $D^0 \rightarrow \bar{p}e^+$ and $D^0 \rightarrow pe^-$,” *Phys. Rev. D*, vol. 105, no. 3, p. 032006, 2022. DOI: 10.1103/PhysRevD.105.032006. arXiv: 2112.10972 [hep-ex].
- [142] W.-S. Hou, M. Nagashima, and A. Soddu, “Baryon number violation involving higher generations,” *Phys. Rev. D*, vol. 72, p. 095001, 2005. DOI: 10.1103/PhysRevD.72.095001. arXiv: hep-ph/0509006.
- [143] L. F. Abbott and M. B. Wise, “The Effective Hamiltonian for Nucleon Decay,” *Phys. Rev. D*, vol. 22, p. 2208, 1980. DOI: 10.1103/PhysRevD.22.2208.
- [144] H. D. Politzer and M. B. Wise, “Effective Field Theory Approach to Processes Involving Both Light and Heavy Fields,” *Phys. Lett. B*, vol. 208, pp. 504–507, 1988. DOI: 10.1016/0370-2693(88)90656-9.
- [145] A. V. Manohar and M. B. Wise, *Heavy quark physics*. 2000, vol. 10, ISBN: 978-0-521-03757-0.

- [146] M. Beneke, T. Feldmann, and D. Seidel, “Exclusive radiative and electroweak $b \rightarrow d$ and $b \rightarrow s$ penguin decays at NLO,” *Eur. Phys. J. C*, vol. 41, pp. 173–188, 2005. DOI: 10.1140/epjc/s2005-02181-5. arXiv: hep-ph/0412400.
- [147] J. F. Amundson, C. G. Boyd, E. E. Jenkins, *et al.*, “Radiative D^* decay using heavy quark and chiral symmetry,” *Phys. Lett. B*, vol. 296, pp. 415–419, 1992. DOI: 10.1016/0370-2693(92)91341-6. arXiv: hep-ph/9209241.
- [148] R. Aaij *et al.*, “Measurement of the photon polarization in $\Lambda_b^0 \rightarrow \Lambda \gamma$ decays,” *Phys. Rev. D*, vol. 105, no. 5, p. L051104, 2022. DOI: 10.1103/PhysRevD.105.L051104. arXiv: 2111.10194 [hep-ex].
- [149] Y.-m. Wang, Y. Li, and C.-D. Lu, “Rare Decays of $\Lambda(b) \rightarrow \Lambda + \gamma$ and $\Lambda(b) \rightarrow \Lambda + l^+ l^-$ in the Light-cone Sum Rules,” *Eur. Phys. J. C*, vol. 59, pp. 861–882, 2009. DOI: 10.1140/epjc/s10052-008-0846-5. arXiv: 0804.0648 [hep-ph].
- [150] L.-F. Gan, Y.-L. Liu, W.-B. Chen, and M.-Q. Huang, “Improved Light-cone QCD Sum Rule Analysis Of The Rare Decays $\Lambda_b \rightarrow \Lambda \gamma$ And $\Lambda_b \rightarrow \Lambda l^+ l^-$,” *Commun. Theor. Phys.*, vol. 58, pp. 872–882, 2012. DOI: 10.1088/0253-6102/58/6/14. arXiv: 1212.4671 [hep-ph].
- [151] A. Khodjamirian, T. Mannel, A. A. Pivovarov, and Y. .-. Wang, “Charm-loop effect in $B \rightarrow K^{(*)} \ell^+ \ell^-$ and $B \rightarrow K^* \gamma$,” *JHEP*, vol. 09, p. 089, 2010. DOI: 10.1007/JHEP09(2010)089. arXiv: 1006.4945 [hep-ph].
- [152] M. Fierz, “Zur fermischen theorie des β -zerfalls,” *Zeitschrift für Physik*, vol. 104, no. 7, pp. 553–565, 1937.
- [153] V. A. Novikov, M. A. Shifman, A. I. Vainshtein, and V. I. Zakharov, “Calculations in External Fields in Quantum Chromodynamics. Technical Review,” *Fortsch. Phys.*, vol. 32, p. 585, 1984.
- [154] C. A. Dominguez, *Quantum Chromodynamics Sum Rules*, ser. Springer-Briefs in Physics. Cham: Springer International Publishing, 2018. DOI: 10.1007/978-3-319-97722-5.

- [155] V. M. Braun and I. E. Filyanov, “Conformal Invariance and Pion Wave Functions of Nonleading Twist,” *Z. Phys. C*, vol. 48, pp. 239–248, 1990. DOI: 10.1007/BF01554472.
- [156] J. Bijnens and A. Khodjamirian, “Exploring light cone sum rules for pion and kaon form-factors,” *Eur. Phys. J. C*, vol. 26, pp. 67–79, 2002. DOI: 10.1140/epjc/s2002-01042-1. arXiv: hep-ph/0206252.
- [157] A. G. Grozin, “B-meson distribution amplitudes,” *Int. J. Mod. Phys. A*, vol. 20, pp. 7451–7484, 2005. DOI: 10.1142/S0217751X05028570. arXiv: hep-ph/0506226.
- [158] V. Shtabovenko, R. Mertig, and F. Orellana, “FeynCalc 9.3: New features and improvements,” *Comput. Phys. Commun.*, vol. 256, p. 107478, 2020. DOI: 10.1016/j.cpc.2020.107478. arXiv: 2001.04407 [hep-ph].
- [159] T. Feldmann, B. Müller, and D. Seidel, “ $D \rightarrow \rho \ell^+ \ell^-$ decays in the QCD factorization approach,” *JHEP*, vol. 08, p. 105, 2017. DOI: 10.1007/JHEP08(2017)105. arXiv: 1705.05891 [hep-ph].

Phenomenology of $\tau^- \rightarrow \pi^- \nu_\tau \gamma$ using light cone sum rules

Anshika Bansal^{1,2,*} and Namit Mahajan^{1,†}

¹Physical Research Laboratory, Navrangpura, Ahmedabad, 380009, India

²Indian Institute of Technology Gandhinagar, Gandhinagar 382424, India

 (Received 17 October 2020; accepted 25 February 2021; published 22 March 2021)

We present the study of radiative tau decay ($\tau^- \rightarrow \pi^- \nu_\tau \gamma$), computing the structure dependent contribution using light cone sum rules. This decay includes the same form factors as the radiative pion decay with the crucial difference that the momentum transfer squared, t , between the pion-photon system is positive, which makes these form factors timelike and also as t can now take values up to m_τ^2 , it can produce real hadronic resonances. The analytical form for these form factors has been calculated using the light cone sum rules method and the invariant mass spectrum in the $\pi - \gamma$ system and the decay width are presented. The structure dependent parameter, γ , the ratio of the axial vector to vector form factor is found to be in good agreement with the experimental determination.

DOI: [10.1103/PhysRevD.103.056017](https://doi.org/10.1103/PhysRevD.103.056017)

I. INTRODUCTION

τ is the heaviest lepton with $m_\tau = 1776.86 \pm 0.12$ MeV [1] and has numerous decay channels because of its heavy mass (see for example [2–6] for different aspects of τ lepton physics). It is the only lepton which can decay into hadrons. Theoretically, the electroweak part is reasonably well established while one is still lacking in developing a proper methodology to understand the strong interactions. The study of hadronic τ decays helps us to understand the dynamics of strong interaction involved in the hadronization of QCD currents in a cleaner environment

In particular, we are interested in the study of radiative tau decay in the present work, i.e., $\tau^- \rightarrow \pi^- \nu_\tau \gamma$. The branching ratio of $\tau^- \rightarrow \pi^- \nu_\tau$ is $(10.82 \pm 0.05)\%$ [1]. Hence, one expects the branching ratio for radiative tau decay to be $\mathcal{O}(10^{-3})$. To get a sense for this expectation, one can write the branching ratio as a product of branching ratios of $\tau \rightarrow \rho \nu_\tau$ and $\rho \rightarrow \pi \gamma$, and using the values from [1], one gets $\sim 10^{-3}$, which is about 10^{-2} of the nonradiative branching ratio. Even though the branching ratio is not very small, these decays are not observed experimentally yet which makes the study of this mode important.

The decay amplitude of this process includes two contributions [7–11]:

- (i) *Internal bremsstrahlung (IB)*: The contribution coming from the emission from either the incoming or the outgoing particles. This contribution can be calculated trivially with the use of scalar QED for the pointlike charged pion while the emission from the τ leg is calculated straightforwardly using QED. Diagrammatically this is shown in (a) and (b) of Fig. 1.
- (ii) *Structure dependent (SD)*: This contribution is governed by the strong interactions and contains nontrivial parts. The pion can no longer be taken as a pointlike particle. The partonic structure will play a role. This contribution appears because of the hadronization of $J^P = 1^- (\gamma^\mu)$ and $1^+ (\gamma^\mu \gamma_5)$ intermediate quark-antiquark currents of the matrix element [(c) of Fig. 1] and hence depends on the long distance dynamics. Using the Lorentz symmetry, it can be parametrized by vector and axial-vector form factors $F_V^{(\pi)}$ and $F_A^{(\pi)}$, respectively. These form factors encode the information of strong dynamics involved in the hadronization of these currents and their evaluation requires a nonperturbative treatment such as light cone sum rules (LCSR), chiral perturbation theory χ PT or lattice QCD. The SD contribution also includes a contact term (CT), which emerges as a consequence of gauge invariance and graphically represented in (d) of Fig. 1.

The explicit form of these contributions will be calculated in Sec. II where we will see that the IB part consists of two contributions: one independent of m_τ and another proportional to m_τ . The m_τ independent contribution turns out to

*anshika@prl.res.in
†nmahajan@prl.res.in

Published by the American Physical Society under the terms of the [Creative Commons Attribution 4.0 International license](https://creativecommons.org/licenses/by/4.0/). Further distribution of this work must maintain attribution to the author(s) and the published article's title, journal citation, and DOI. Funded by SCOAP³.

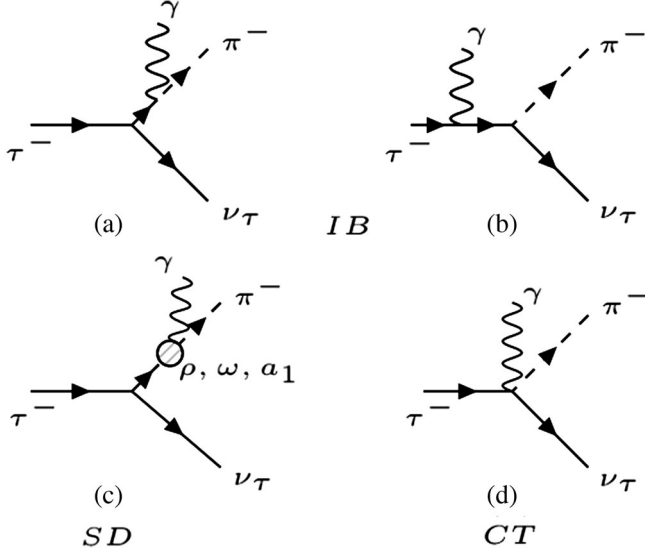


FIG. 1. Feynman diagrams showing different contributions to the radiative tau decay. (a) and (b) represent the IB contribution, (c) represents the SD contribution and (d) represents the CT contribution.

be equal and opposite to the CT contribution and hence gets canceled in the total amplitude.

The amplitude for the process of interest is related to that of the radiative pion decay by crossing symmetry with a major difference that comes at the level of kinematics as the square of the momentum transferred between the pion-photon and leptonic system can now take values up to m_τ^2 , while in the radiative pion decay, it can take values only up to m_π^2 which is almost negligible. Also, as both pion and photon are in the final state, the form factors involved in this process are timelike, and hence complicated, unlike the form factors involved in the radiative pion decay which are spacelike. As a consequence, the light flavored mesons will be created on shell and give resonant structures in the pion-photon invariant mass spectrum.

Hence to understand this process, the main task is to calculate the timelike form factors involved in the process. These form factors probe the structure of the pion. The information about the pion structure can be obtained by determining the ratio of $F_A^{(\pi)}(0)$ to $F_V^{(\pi)}(0)$ which is defined as the structure dependent parameter, γ , i.e., $\gamma = \frac{F_A^{(\pi)}(0)}{F_V^{(\pi)}(0)}$. We

know the values of $F_A^{(\pi)}(0)$ and $F_V^{(\pi)}(0)$ from the experimental determination of radiative pion decay to be equal to (0.0119 ± 0.0001) and (0.0254 ± 0.0017) , respectively [1], which results in the value of γ equal to (0.4685 ± 0.0353) . The value of γ , which is the ratio of form factors evaluated at zero momentum transfer, will be the same for radiative tau and pion decays. The calculation of radiative tau decay helps in determining this structure dependent parameter theoretically in a consistent way. This decay is also useful to understand the light-by-light hadronic contribution to the

muon anomalous magnetic moment, $(g-2)_\mu$ [12]. In [13], the authors have discussed how this decay can provide the means for the tau neutrino mass determination. These gauge invariant form factors for the radiative tau decay have been parametrized using Breit-Wigner-type resonances [14], light front quark model [10] and resonance χ PT [11] in the past.

The differences in the literature stem from the vastly different approaches adopted to determine or estimate the form factors, which affect the predictions for the rate and spectrum, as well as extraction of γ , including the sign. As an example, whenever the resonances are included via the Breit-Wigner method, a suspecting issue always is the relative phase between the different contributions. The main aim of this paper is to calculate these form factors using the method of LCSR in a consistent way.

The rest of the paper is organized as follows; in Sec. II, we present the amplitude calculation for the process and explicitly write the forms of different contributions mentioned above. In Sec. III, we present the calculation of the form factors using the method of LCSR and in Sec. IV we report our results. Finally, in Sec. V we conclude our results with some remarks. Various definitions and conventions used are reported in Appendix A. The values of various parameters used for numerical calculation are collected in Appendix B and the kinematical details are provided in Appendix C.

II. AMPLITUDE COMPUTATION

A photon can be emitted by any charged particle. Hence in the present case, the photon can be emitted from either the pion or tau lepton, as shown in Fig. 1. The pion is a composite object with a quark-antiquark pair. Therefore, the internal structure of the pion will also contribute to the process. This gives rise to two nonperturbative form factors. As mentioned above, the amplitude of radiative tau decay includes various contributions: internal bremsstrahlung (IB), structure dependent (SD) and contact term (CT). The IB contribution comes from the emission of the photon from tau and pion (considering pion to be the point object). The SD contribution comes from the emission of the photon from the internal structure of the pion. The contact term is an interesting effective contribution and has its origin in the gauge invariance of a QED amplitude [15]. We follow this approach here.

The amplitude of the process $\tau^-(p_1) \rightarrow \pi^-(p_2)\nu_\tau(p_3) \times \gamma(k)$ can be written as (employing the low energy four-Fermi effective Hamiltonian obtained by integrating out the heavy W boson)

$$\mathcal{A}(\tau^- \rightarrow \pi^- \nu_\tau \gamma) = \frac{G_F}{\sqrt{2}} V_{ud} \langle \pi^- \nu_\tau \gamma | (\bar{\nu}_\tau \Gamma^\mu \tau) (\bar{d} \Gamma_\mu u) | \tau^- \rangle, \quad (1)$$

where $\Gamma^\mu = \gamma^\mu (1 - \gamma_5)$.

This amplitude can be factorized in two parts; one where the photon is emitted from the final state pion and another where the photon gets emitted from the initial state tau lepton:

$$\begin{aligned} \mathcal{A}(\tau^- \rightarrow \pi^- \nu_\tau \gamma) &= \frac{G_F}{\sqrt{2}} V_{ud} [\langle \pi^- \gamma | (\bar{d} \Gamma_\mu u) | 0 \rangle \langle \nu_\tau | (\bar{\nu}_\tau \Gamma^\mu \tau) | \tau^- \rangle \\ &\quad + \langle \nu_\tau \gamma | (\bar{\nu}_\tau \Gamma^\mu \tau) | \tau^- \rangle \langle \pi^- | (\bar{d} \Gamma_\mu u) | 0 \rangle] \\ &= \frac{G_F}{\sqrt{2}} V_{ud} \left[-ie \epsilon_\alpha^* (\bar{u}_\nu \Gamma_\mu u_\tau) \right. \\ &\quad \times \int d^4 x e^{ikx} \langle \pi^- | T \{ j_{\text{em}}^\alpha(x) \bar{d} \Gamma^\mu u(0) \} | 0 \rangle \\ &\quad \left. - e f_\pi p_{2\mu} \epsilon_\alpha^* \int d^4 x e^{ikx} \langle \nu_\tau | T \{ j_{\text{em}}^\alpha(x) \bar{\nu}_\tau \Gamma^\mu \tau(0) \} | \tau^- \rangle \right], \quad (2) \end{aligned}$$

where $j_{\text{em}}^\alpha(x) = Q_\psi \bar{\psi}(x) \gamma^\alpha \psi(x) = -\bar{\tau} \gamma^\alpha \tau + Q_u \bar{u} \gamma^\alpha u + Q_d \bar{d} \gamma^\alpha d$ and f_π is the pion decay constant. The conventions and definitions are given in Appendix A. This factorization of the amplitude holds for energetic photons and at the leading order in $\frac{1}{m_\tau}$ and α_{em} .

For the computation of the first term of Eq. (2), define the hadronic matrix element as

$$T^{\alpha\mu}(p_2, k) = i \int d^4 x e^{ikx} \langle \pi^- | T \{ j_{\text{em}}^\alpha(x) \bar{d} \Gamma^\mu u(0) \} | 0 \rangle. \quad (3)$$

Using the conservation of electromagnetic current, one can apply the Ward identity which results in

$$k_\alpha T^{\alpha\mu}(p_2, k) = \langle \pi^- | \bar{d}(0) \Gamma^\mu u(0) | 0 \rangle = i f_\pi p_2^\mu \quad (4)$$

in the momentum space.

Also, one can write the hadronic matrix element [defined in Eq. (3)] using the general covariant decomposition in terms of the pion and photon momentum, i.e., p_2 and k respectively, as

$$\begin{aligned} T^{\alpha\mu}(p_2, k) &= A g^{\alpha\mu} + B p_2^\alpha p_2^\mu + C p_2^\alpha k^\mu + D k^\alpha p_2^\mu \\ &\quad + E k^\alpha k^\mu + i F_V^{(\pi)} \epsilon^{\alpha\mu\beta\nu} p_{2\beta} k_\nu, \quad (5) \end{aligned}$$

where $A, B, C, D, E, F_V^{(\pi)}$ are gauge invariant scalar functions of $(p_2 + k)^2$. Contraction of Eq. (5) with k_α results in (for on-shell photon $k^2 = 0$ and the Levi-Civita tensor is antisymmetric in α and ν)

$$k_\alpha T^{\alpha\mu}(p_2, k) = A k^\mu + B(p_2 \cdot k) p_2^\mu + C(p_2 \cdot k) k^\mu. \quad (6)$$

On equating Eqs. (4) and (6), we get

$$C = \frac{-A}{(p_2 \cdot k)}, \quad \text{and} \quad B = \frac{i f_\pi}{(p_2 \cdot k)} \quad (7)$$

which results in the final form of hadronic matrix element to be

$$\begin{aligned} T^{\alpha\mu}(p_2, k) &= F_A^{(\pi)} [g^{\alpha\mu}(P \cdot k) - P^\alpha k^\mu] + i F_V^{(\pi)} \epsilon^{\alpha\mu\beta\nu} P_\beta k_\nu \\ &\quad - i f_\pi g^{\alpha\mu} + i f_\pi \frac{P^\alpha P^\mu}{P \cdot k}. \quad (8) \end{aligned}$$

Here, $F_A^{(\pi)} = \frac{A + i f_\pi}{P \cdot k}$ and $P = p_1 - p_3 = p_2 + k$ and $p_2 \cdot k = P \cdot k$. Hence, the first term in Eq. (2) reads

$$\begin{aligned} &\langle \pi^- \gamma | \bar{d} \Gamma_\mu u | 0 \rangle \langle \nu_\tau | \bar{\nu}_\tau \Gamma^\mu \tau | \tau^- \rangle \\ &= i e \epsilon^{*\alpha} [\bar{u}_\nu \Gamma^\mu u_\tau] [i F_A^{(\pi)} \{g_{\alpha\mu}(P \cdot k) - P_\alpha k_\mu\} - F_V^{(\pi)} \epsilon_{\alpha\mu\beta\nu} P^\beta k^\nu] \\ &\quad + i e \epsilon^{*\mu} f_\pi \bar{u}_\nu \Gamma_\mu u_\tau - i e f_\pi \frac{\epsilon^* \cdot P}{P \cdot k} \bar{u}_\nu \not{P} (1 - \gamma_5) u_\tau. \quad (9) \end{aligned}$$

The second term in Eq. (2), using QED Feynman rules, takes the form

$$\begin{aligned} &\langle \nu_\tau \gamma | \bar{\nu}_\tau \Gamma^\mu \tau | \tau^- \rangle \langle \pi^- | \bar{d} \Gamma_\mu u | 0 \rangle \\ &= -i e f_\pi \bar{u}_\nu(p_3) \not{\epsilon}^* (1 - \gamma_5) u_\tau(p_1) \\ &\quad + \frac{i e f_\pi m_\tau}{2 p_1 \cdot k} \{ \bar{u}_\nu(p_3) [(2 \epsilon^* \cdot p_1) - \not{k} \not{\epsilon}^*] (1 + \gamma_5) u_\tau(p_1) \}. \quad (10) \end{aligned}$$

Adding the two, the final form of the amplitude is

$$\begin{aligned} \mathcal{A}(\tau^- \rightarrow \pi^- \nu_\tau \gamma) &= \frac{G_F}{\sqrt{2}} V_{ud} \left[i e \epsilon^{*\alpha} (\bar{u}_\nu \Gamma^\mu u_\tau) \{ i F_A^{(\pi)} [g_{\alpha\mu}(P \cdot k) - P_\mu k_\alpha] \right. \\ &\quad \left. - F_V^{(\pi)} \epsilon_{\alpha\mu\beta\nu} P^\beta k^\nu \} + i e f_\pi m_\tau \bar{u}_\nu \left\{ \frac{\epsilon^* \cdot p_1}{p_1 \cdot k} - \frac{\not{k} \not{\epsilon}^*}{2 p_1 \cdot k} - \frac{\epsilon^* \cdot p_2}{p_2 \cdot k} \right\} \right. \\ &\quad \left. \times (1 + \gamma_5) u_\tau \right]. \quad (11) \end{aligned}$$

Here, $F_A^{(\pi)}$ and $F_V^{(\pi)}$ are the gauge invariant axial-vector and vector form factors, respectively. The contact term appears explicitly by the use of Ward identity and cancels against the m_τ independent contribution of photon emission from τ .

For further simplification, we have divided the full amplitude as

$$\mathcal{A}(\tau^- \rightarrow \pi^- \nu_\tau \gamma) = \mathcal{A}_{\text{IB}} + \mathcal{A}_V + \mathcal{A}_A = \mathcal{A}_{\text{IB}} + \mathcal{A}_{\text{SD}}. \quad (12)$$

Here,

$$\begin{aligned} \mathcal{A}_{\text{IB}} &= \frac{G_F}{\sqrt{2}} V_{ud} \left[i e f_\pi m_\tau \bar{u}_\nu \left\{ \frac{\epsilon^* \cdot p_1}{p_1 \cdot k} - \frac{\not{k} \not{\epsilon}^*}{2 p_1 \cdot k} - \frac{\epsilon^* \cdot p_2}{p_2 \cdot k} \right\} \right. \\ &\quad \left. \times (1 + \gamma_5) u_\tau \right], \quad (13) \end{aligned}$$

$$\mathcal{A}_V = -\frac{G_F}{\sqrt{2}} V_{ud} [i e \epsilon^{*\alpha} (\bar{u}_\nu \Gamma^\mu u_\tau) (F_V^{(\pi)} \epsilon_{\alpha\mu\beta\nu} P^\beta k^\nu)], \quad \text{and} \quad (14)$$

$$\mathcal{A}_A = \frac{G_F}{\sqrt{2}} V_{ud} [i e \epsilon^{*\alpha} (\bar{u}_\nu \Gamma^\mu u_\tau) (i F_A^{(\pi)} [g_{\alpha\mu}(P \cdot k) - P_\mu k_\alpha])]. \quad (15)$$

\mathcal{A}_V and \mathcal{A}_A combined gives the structure dependent contribution, while \mathcal{A}_{IB} is the internal bremsstrahlung contribution.

III. FORM FACTORS IN LCSR FRAMEWORK

In the previous section, we saw that the amplitude of the radiative tau decay depends on two gauge invariant form factors; $F_A^{(\pi)}$ and $F_V^{(\pi)}$. These form factors are the non-perturbative objects and need a nonperturbative treatment. In this section, we will calculate these form factors using the method of LCSR.

The method of sum rules was developed in 1979 by Shifman, Vainshtein and Zakharov (SVZ) [16,17]. Their basic idea was to use the analytic properties of a correlation function [treated in the framework of operator product expansion (OPE)] to derive the hadronic parameter involved in a process. Below we briefly outline the method (for details, see [18–20]).

The important tools for deriving the sum rules are dispersion relation, operator product expansion (OPE), quark-hadron duality and the Borel transformation. The dispersion relation relates the real part of the correlation function to its imaginary part using Cauchy's integral formula. According to OPE, the correlation function can be written as a sum of products of long distance matrix elements of operators of increasing dimension and short distance Wilson coefficients which can be calculated using perturbation theory. The higher dimension operators capture the information of QCD vacuum fields in the form of vacuum condensates. Both dispersion relation and OPE give the same physics and hence can be equated.

Operationally, quark hadron duality means

$$q^2 \int_{s_0^h}^{\infty} ds \frac{\rho^h(s)}{s(s-q^2)} \simeq \frac{q^2}{\pi} \int_{4m^2}^{\infty} ds \frac{\text{Im}\Pi^{\text{(pert)}}(s)}{s(s-q^2)}. \quad (16)$$

Here, ρ^h is the hadronic spectral density function, while $\Pi^{\text{pert}}(s)$ [or $\Pi^{\text{QCD}}(s)$] is the perturbatively calculated correlation function. We will use this duality approximation below.

As the correlation function has contributions from all the resonance states as well as the continuum, one performs Borel transformation to suppress the effect of higher resonances and continuum. Mathematically, the Borel transform is given by

$$\begin{aligned} \Pi(M^2) &\equiv \mathcal{B}_{M^2} \Pi(k^2) \\ &= \lim_{-k^2, n \rightarrow \infty, -k^2/n = M^2} \frac{(-k^2)^{(n+1)}}{n!} \left(\frac{d}{dk^2} \right)^n \Pi(k^2), \end{aligned} \quad (17)$$

where M is known as the Borel parameter.

It was noticed that these SVZ sum rules have some limitations such as the OPE upsets the power counting in large Q^2 and that, even after performing the Borel transformation, practical calculations suffer from unsuppressed contributions. These limitations can be overcome by using light cone sum rules (LCSR). In LCSR, one expands the products of the currents near the light cone. LCSR give vacuum-to-hadron correlation function while by SVZ sum rules one gets vacuum-to-vacuum correlation functions. In LCSR, OPE at short distances is replaced by systematic expansion in the transverse direction in the infinite momentum frame.

In the light cone limit, the bilocal operator sandwiched between the pion state and vacuum is expressed as

$$\begin{aligned} \langle \pi^0(p) | \bar{u}(y) \gamma_\mu \gamma_5 u(x) | 0 \rangle_{x^2=0} \\ = -i f_\pi p_\mu \int_0^1 du e^{i(u p_2 \cdot y + \bar{u} p \cdot x)} \phi(u, \mu), \end{aligned} \quad (18)$$

where $\bar{u} = 1 - u$ and $\phi(u, \mu)$ is leading twist-2 distribution amplitude given by

$$\phi_\pi(u, \mu) = 6u\bar{u} \left[1 + \sum_{n=2,4,\dots} a_n(\mu) C_n^{3/2}(u - \bar{u}) \right]. \quad (19)$$

Here, $C_n^{3/2}$ are the Gegenbauer polynomials and a_n is the multiplicatively renormalizable coefficient defined as

$$a_n(\mu) = a_n(\mu_0) \left(\frac{\alpha_s(\mu)}{\alpha_s(\mu_0)} \right)^{\gamma_n/\beta_0} \quad (20)$$

with $\alpha_s = \frac{g_s^2}{4\pi}$ (g_s is the strong coupling constant), β_0 is the leading QCD β function and

$$\gamma_n = \frac{4}{3} \left[-3 - \frac{2}{(n+1)(n+2)} + 4 \left(\sum_{k=1}^{(n+1)} \frac{1}{k} \right) \right]. \quad (21)$$

The remaining process for computation is the same as for SVZ sum rules. We are now ready to derive the form factors, $F_V^{(\pi)}$ and $F_A^{(\pi)}$, using this technique.

As we know, these form factors arise from the computation of the hadronic matrix element defined in Eq. (3), i.e.,

$$T^{\alpha\mu}(p_2, k) = i \int d^4x e^{ikx} \langle \pi^- | T \{ Q_u \bar{u} \gamma^\alpha u(x) \bar{d} \Gamma^\mu u(0) + Q_d \bar{d} \gamma^\alpha d(x) \bar{d} \Gamma^\mu u(0) \} | 0 \rangle, \quad (22)$$

where Q_u and Q_d are the charges of up and down quark respectively in units of e . Using the definitions and identities given in Appendix A, we get

$$T^{\alpha\mu}(p_2, k) = if_\pi \int d^4x \frac{e^{ikx}}{2\pi^2 x^4} \int_0^1 du \phi(u, \mu) [i\epsilon^{\mu\beta\alpha\rho} x_\beta p_{2\rho} (Q_u e^{i\bar{u}p_2x} + Q_d e^{iup_2x}) + (x^\mu p_2^\alpha - g^{\mu\alpha}(x \cdot p_2) + x^\alpha p_2^\mu) (Q_u e^{i\bar{u}p_2x} - Q_d e^{iup_2x})], \quad (23)$$

where, as mentioned above, $\phi(u, \mu)$ is the pion distribution amplitude and $\bar{u} = 1 - u$. The integration over x results in

$$T^{\alpha\mu}(P, k) = if_\pi \left[\frac{i\epsilon^{\mu\beta\alpha\rho}}{3} P_\rho k_\beta \int_0^1 du \frac{\phi(u, \mu)}{P^2 \bar{u} + k^2 u} + 2\{P^\alpha P^\mu - (P \cdot k)g^{\mu\alpha}\} \int_0^1 du \frac{\phi(u, \mu)\bar{u}}{P^2 \bar{u} + k^2 u} - \{g^{\mu\alpha}(P \cdot k) - P^\alpha k^\mu\} \left\{ \int_0^1 du \phi(u, \mu) \left(\frac{1 - 2\bar{u}}{P^2 \bar{u} + k^2 u} \right) \right\} \right]. \quad (24)$$

Here, $p_2 + k = P$ and we have used the fact that the distribution amplitude is a symmetric function of u and \bar{u} .

A comparison with the general decomposition of the hadronic tensor given in Eq. (8) yields the following forms of vector and axial-vector form factors from QCD calculation:

$$F_V^{\text{QCD}}(t) = \frac{if_\pi}{3} \int_0^1 du \frac{\phi(u, \mu)}{t\bar{u} + k^2 u} \Rightarrow \frac{1}{\pi} \text{Im}\{F_V^{\text{QCD}}(t)\} = \frac{if_\pi}{3} \int_0^1 du \phi(u, \mu) \delta(t\bar{u} + k^2 u), \quad \text{and} \quad (25)$$

$$F_A^{\text{QCD}}(t) = -if_\pi \int_0^1 du \phi(u, \mu) \left(\frac{1 - 2\bar{u}}{t\bar{u} + k^2 u} \right) \Rightarrow \frac{1}{\pi} \text{Im}\{F_A^{\text{QCD}}(t)\} = -if_\pi \int_0^1 du \phi(u, \mu) (1 - 2\bar{u}) \delta(t\bar{u} + k^2 u). \quad (26)$$

Here, $t \equiv P^2 = (p_2 + k)^2 = (p_1 - p_3)^2$ is the invariant mass square of the photon-pion system.

Now, after computing the perturbative QCD contribution, the analytic properties of this hadronic matrix element are used to derive the contribution of various hadronic states. It will get contributions from (ρ , ω , a_1 -mesons)+ higher resonances and the continuum. In the present case, contributions coming from ρ , ω , a_1 -mesons will saturate the sum rules and thus will be the focus here.¹

Considering the matrix element $\langle \pi^- | T\{j_{\text{em}}^\alpha(x) j_{\text{ew}}^\mu(0)\} | 0 \rangle$ and inserting a complete set of states, we get

$$\langle \pi^- | T\{j_{\text{em}}^\alpha(x) j_{\text{ew}}^\mu(0)\} | 0 \rangle = \langle \pi^- | j_{\text{em}}^\alpha(x) | n \rangle \langle n | j_{\text{ew}}^\mu(0) | 0 \rangle, \quad (27)$$

where $|n\rangle = |\rho\rangle + |\omega\rangle + |a_1\rangle + \text{higher resonances} + \text{continuum}$.

(i) ρ and ω -meson contribution: The ρ -meson contribution will come from

$$\langle \pi^- (p_2) | j_{\text{em}}^\alpha(x) | \rho(p_2 + k) \rangle \langle \rho(p_2 + k) | j_{\text{ew}}^\mu(0) | 0 \rangle. \quad (28)$$

Using the definitions given in Appendix A,

¹The contribution of the higher resonances, at the present level of accuracy, is roughly 20% of these resonances because of the Borel suppression.

$$\langle \pi^- (p_2) | j_{\text{em}}^\alpha(x) | \rho(p_2 + k) \rangle \langle \rho(p_2 + k) | j_{\text{ew}}^\mu(0) | 0 \rangle = im_\rho f_\rho \epsilon^{\alpha\lambda\beta\nu} g_\lambda^\mu p_{2\beta} k_\nu F_{\rho\pi}(k^2), \quad (29)$$

where m_ρ and f_ρ are the mass and decay constant of the ρ meson respectively. Neglecting the very small difference between the masses of ρ and ω , the contribution of ω will be equal to the contribution of ρ and hence multiplying ρ contribution by a factor of 2 will incorporate the contribution of the ω meson.

(ii) a_1 -meson contribution: The a_1 -meson contribution will come from

$$\langle \pi^- (p_2) | j_{\text{em}}^\alpha(x) | a_1(p_2 + k) \rangle \langle a_1(p_2 + k) | j_{\text{ew}}^\mu(0) | 0 \rangle, \quad (30)$$

which results in

$$\langle \pi^- (p_2) | j_{\text{em}}^\alpha(x) | a_1(p_2 + k) \rangle \langle a_1(p_2 + k) | j_{\text{ew}}^\mu(0) | 0 \rangle = im_{a_1} f_{a_1} [2p_2 \cdot k g^{\alpha\mu} - 2p_2^\alpha k^\mu] G_{a_1\pi}(k^2) \quad (31)$$

using the definitions given in Appendix A. Here, m_{a_1} and f_{a_1} are the mass and decay constant of the a_1 meson respectively.

Here, $F_{\rho\pi}(G_{a_1\pi})$ captures the physics of transition of the $\rho(a_1)$ meson to the π meson. Using the optical theorem in Eq. (3), we get

$$2\text{Im}\{T^{\alpha\mu}(p_2, k)\} = \sum_n \langle \pi^- | j_{\text{em}}^\alpha(x) | n \rangle \langle n | j_{\text{ew}}^\mu | 0 \rangle d\tau_n (2\pi)^4 \delta^4(k - p_n), \quad (32)$$

and from Cauchy's theorem,

$$T(k^2) = \frac{1}{\pi} \int_{t_{\min}}^{\infty} ds \frac{\text{Im}\{T(s)\}}{s - k^2 - i\epsilon}. \quad (33)$$

Substituting the contributions of ρ and a_1 , we get

$$\begin{aligned} T^{\alpha\mu}(p_2, k) &= \frac{2im_\rho f_\rho \epsilon^{\alpha\lambda\beta\nu} g_\lambda^\mu p_{2\beta} k_\nu F_{\rho\pi}(k^2)}{m_\rho^2 - (p_2 + k)^2 - im_\rho \Gamma_\rho} \\ &+ \frac{im_{a_1} f_{a_1} [2p_2 \cdot k g^{\alpha\mu} - 2p_2^\alpha k^\mu] G_{a_1\pi}(k^2)}{m_{a_1}^2 - (p_2 + k)^2 - im_{a_1} \Gamma_{a_1}} \\ &+ \frac{1}{\pi} \int_{s_0^h}^{\infty} ds \frac{\text{Im}\{T^{\alpha\mu}(s, k)\}}{s - k^2 - i\epsilon}. \end{aligned} \quad (34)$$

Here, s_0^h is the threshold of the lowest continuum state and Γ_ρ and Γ_{a_1} are the decay widths of ρ and a_1 mesons, respectively. This is the dispersion relation which relates the imaginary part to the real part. Now, the light cone sum rules can be derived by taking the form of $F_V^{(\pi)}(t)$ from this dispersion relation and equating it with the form obtained in Eq. (25), i.e.,

$$\begin{aligned} \frac{2m_\rho f_\rho F_{\rho\pi}(k^2)}{m_\rho^2 - t - im_\rho \Gamma_\rho} + \frac{1}{\pi} \int_{s_0^h}^{\infty} ds \frac{\text{Im}\{F_V(s)\}}{s - t - i\epsilon} \\ = \frac{if_\pi}{3} \int_0^1 du \frac{\phi(u, \mu)}{t\bar{u} + k^2 u}. \end{aligned} \quad (35)$$

Using the duality approximation and the Cauchy's integral,

$$\begin{aligned} \frac{1}{\pi} \int_{s_0}^{\infty} ds \frac{\text{Im}\{F_V(s, k)\}}{s - t - i\epsilon} &= \frac{1}{\pi} \int_{s_0'}^{\infty} ds \frac{\text{Im}\{F_V^{\text{QCD}}(s, k)\}}{s - t - i\epsilon} \\ &= \frac{if_\pi}{3} \int_{u_0}^1 du \frac{\phi(u)}{t\bar{u} + k^2 u}, \end{aligned} \quad (36)$$

with $u_0 = \frac{s_0}{k^2 + s_0} = 1$ (as $k^2 = 0$). As a result, the sum rule for $F_V^{(\pi)}(t)$ turns out to be

$$\frac{2m_\rho f_\rho F_{\rho\pi}(k^2)}{m_\rho^2 - t} = \frac{if_\pi}{3} \int_0^{u_0} du \frac{\phi(u)}{t\bar{u} + k^2 u}. \quad (37)$$

Similarly, by equating the form of $F_A^{(\pi)}(t)$ obtained from the dispersion relation with the form given in Eq. (26) and using the duality approximation, the sum rule for $F_A^{(\pi)}(t)$ reads

$$\frac{2im_{a_1} f_{a_1} G_{a_1\pi}(k^2)}{m_{a_1}^2 - t} = -if_\pi \int_0^{u_0} \phi(u) \left(\frac{1 - 2\bar{u}}{t\bar{u} + k^2 u} \right). \quad (38)$$

After Borelization and substituting these sum rules back in Eq. (34), we get the following analytical forms for $F_V^{(\pi)}$ and $F_A^{(\pi)}$:

$$F_V^{(\pi)}(t) = -i \frac{f_\pi}{3(m_\rho^2 - t - im_\rho \Gamma_\rho)} \int_0^1 du \frac{\phi(u)}{\bar{u}} e^{\frac{m_\rho^2}{M^2}}, \quad (39)$$

$$F_A^{(\pi)}(t) = -i \frac{f_\pi}{m_{a_1}^2 - t - im_{a_1} \Gamma_{a_1}} \int_0^1 \frac{\phi(u)}{\bar{u}} (1 - 2\bar{u}) e^{\frac{m_{a_1}^2}{M^2}}. \quad (40)$$

Here, M is the Borel parameter and we have used the on-shell condition for the photon (i.e., $k^2 = 0$).²

For the present calculation, we will use the asymptotic form (where $\mu \rightarrow \infty$) and the Chernyak-Zhitnisky form (where the C_2 term will be considered) of the pion distribution amplitude given in Eq. (19). Explicitly these forms are given by

$$\phi_\pi^{\text{asym}}(u, \mu) = 6u\bar{u}, \quad \text{and} \quad (41)$$

$$\phi_\pi^{\text{CZ}}(u, \mu) = 6u\bar{u} \left[1 + \frac{3a_2(\mu)}{2} \{5(u - \bar{u})^2 - 1\} \right], \quad (42)$$

where $a_2(\mu)$ is defined in Eq. (20) with $n = 2$. All the structure dependent information of the pion involved in the radiative tau decay is contained in the ratio of the axial vector form factor and the vector form factor at zero invariant mass square of the photon-pion system, i.e.,

$$\gamma = \frac{F_A^{(\pi)}(0)}{F_V^{(\pi)}(0)}, \quad (43)$$

where γ is known as the structure dependent parameter (SDP). The vector form factor at $t = 0$ can be related to the anomaly term (or Wess-Zumino-Witten term) in the $\pi\gamma\gamma$ vertex [$1/(4\pi^2 f_\pi)$]. Using what is referred to as KSFR-II relation [21,22], $m_\rho^2 = 2g_{\rho\pi\pi}^2 f_\pi^2$, along with the assumptions of universality of ρ coupling ($g_{\rho\pi\pi} = g_{\rho NN} = g_{\rho\gamma} = g = 2\pi\sqrt{3/N_c}$) and ρ meson dominance of the pion electromagnetic form factor, one finds the right form emerging from $F_V^{(\pi)}(0)$, up to the overall factor $e^{\frac{m_\rho^2}{M^2}}$ which should tend to unity. As we see later, the choice of the Borel parameter that provides a stable window, trivially yields unity for this factor within a few percent.

²It is to be noted that these form factors have dimension of inverse mass and there is an extra factor of $-i$ due to the way initial amplitude is defined: $\mathcal{A}(\tau^- \rightarrow \pi^- \nu_\tau \gamma)$ instead of $i\mathcal{A}(\tau^- \rightarrow \pi^- \nu_\tau \gamma)$ as is often done.

Before discussing the results, it may be worthwhile to ponder over possible duality violations. Such contributions arise from our use of perturbatively evaluated spectral functions, imaginary parts of the form factors here, over the entire kinematical range. It is notoriously difficult to exactly quantify the magnitude of such duality violating terms. However, it is rather important to have some estimate or an educated guess since these would otherwise cause large uncertainties in the final results. For the case at hand, the perturbative effects occur at $1/Q$, where hard scale $Q \sim m_\tau$ while the time scale over which the partons come together to form final hadrons $\sim Q/\Lambda_{\text{QCD}}^2$. One possible way to evaluate the duality violations could be to use an instanton model, where the light quark amplitudes will be suppressed. A rough calculation yields a quantity that in the Euclidean domain has the form $\text{Exp}[-Q\rho]/Q^n$, where ρ denotes the mean instanton size. Analytically continued to the Minkowski space, this would have an oscillating factor multiplied by negative powers of the energy released in the hard process m_τ . Alternatively, one could assume a comb of hadronic resonances that would contribute and carry out the algebra. Both lead to similar conclusions that the violations are $\sim 10\%$ [23] (also see [24,25] for detailed analyses for inclusive tau decays). This is the typical duality violation contribution that we expect, though a more detailed calculation can reveal the actual amount of such violations.

IV. RESULTS

The analytic expressions for the vector and axial-vector form factors calculated using LCSR are given in Eqs. (39) and (40). Both of these form factors have the asymptotic $\frac{1}{t}$ dependence on the invariant mass squared, t of the photon pion system, as expected from QCD in the perturbative (asymptotic) regime. We have used two forms of pion distribution amplitude; the asymptotic form and the CZ form as given in Eqs. (41) and (42), respectively. The structure dependent parameter defined in Eq. (43) is also calculated using both forms for pion distribution amplitudes. The values of the various parameters used for the numerical computation are collected in Appendix B. The form factors depend on the value of the Borel parameter, M , and hence also the structure dependent parameter, γ . Figure 2 shows the variation of $F_A^{(\pi)}(0)$, $F_V^{(\pi)}(0)$ and SDP (γ) with the variation in the value of M . The variation of the observables with M dictates the model dependence here. As can be seen from the plot, all the observables are quite stable in the chosen Borel window. The value of γ for $M = 3.35$ GeV is 0.469 (using CZ distribution amplitude) which matches well, including the sign, with the experimental value of γ obtained from the radiative pion decay [1].

Further, we calculate the decay width contribution for the radiative tau decay using $M = 3.35$ GeV and the form

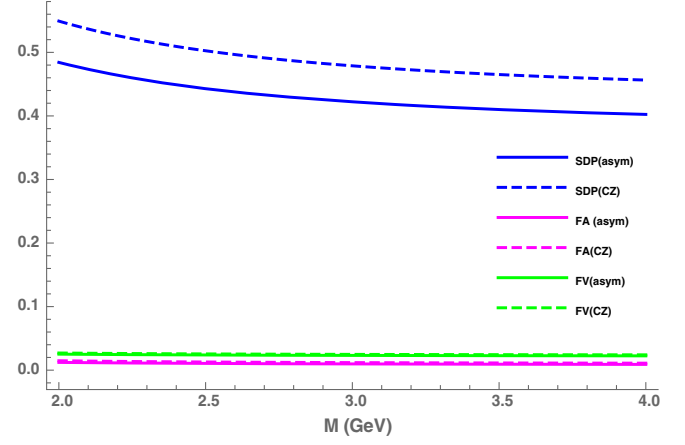


FIG. 2. The dependence of structure dependent parameter (SDP), $F_A^{(\pi)}(0)$ and $F_V^{(\pi)}(0)$ on the Borel parameter M (in GeV units) is shown in blue, magenta and green, respectively. In this plot, form factors have been multiplied by im_π to make them dimensionless in and take care of the extra $-i$ in the form factors as noted in footnote 1.

factors given in Eqs. (39) and (40). The differential decay rate for the radiative tau decay is given by

$$d\Gamma(\tau^- \rightarrow \pi^- \nu_\tau \gamma) = \frac{1}{512\pi^5} E_\tau \delta^{(4)}(k + p_2 + p_3 - p_1) \overline{|\mathcal{A}|^2} \frac{d^3 k d^3 p_2 d^3 p_3}{E_\gamma E_\pi E_\nu}, \quad (44)$$

where E_τ , E_π , E_γ , E_ν are the energies of tau lepton, pion, photon and neutrino, respectively. $\overline{|\mathcal{A}|^2}$ is the spin averaged square of the amplitude which has been calculated in Sec. II.

In terms of the functions used in Eq. (12),

$$\overline{|\mathcal{A}|^2} = \overline{|\mathcal{A}_{\text{IB}}|^2} + \overline{|\mathcal{A}_{\text{SD}}|^2} + 2\text{Re}\{\overline{\mathcal{A}_{\text{IB}}^* \mathcal{A}_{\text{SD}}}\}, \quad (45)$$

where $\overline{|\mathcal{A}_{\text{SD}}|^2} = \overline{|\mathcal{A}_A|^2} + \overline{|\mathcal{A}_V|^2} + 2\text{Re}\{\overline{\mathcal{A}_A^* \mathcal{A}_V}\}$.

The kinematical details to compute the decay rate can be found in Appendix C.

The structure dependent contribution to the photon spectrum is shown in Fig. 3 using both forms of pion distribution amplitudes. The IB contribution suffers from the infrared divergences which can be taken care of by putting a threshold on the photon energy. Figure 4 shows the threshold energy dependence of the IB contribution as well as the full decay width of the radiative tau decay. The SD contribution is free from any kind of divergences.

$F_A^{(\pi)}(t)$ gets a contribution from the a_1 meson while $F_V^{(\pi)}(t)$ from the ρ (and ω) meson. Figure 5 shows the SD contribution to the invariant mass spectrum of the $\pi - \gamma$ system. The higher and sharper peak corresponds to the contribution coming from the vector mesons while the

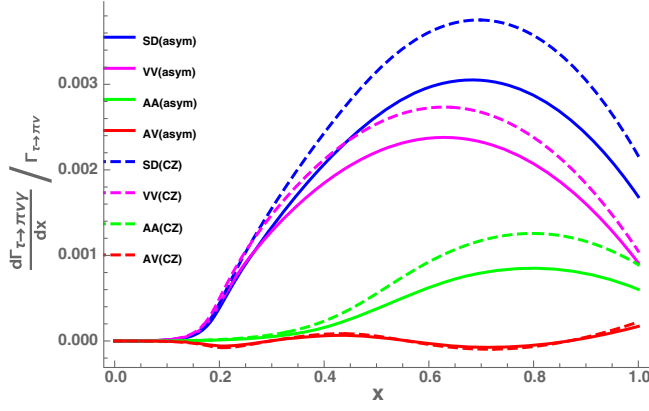


FIG. 3. The total structure dependent contribution (blue) to the photon spectrum is shown along with the individual contributions from the vector (magenta), axial vector (green) and the interference (red) of the two are also shown for the two distribution amplitudes. Solid lines are for asymptotic distribution amplitude while dashed ones are for Chernyak-Zitnisky distribution amplitude.

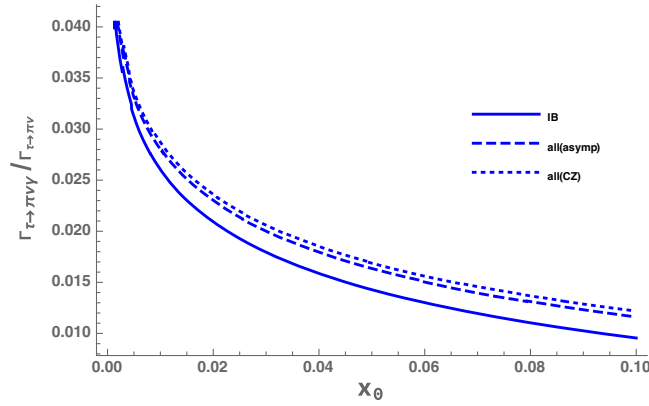
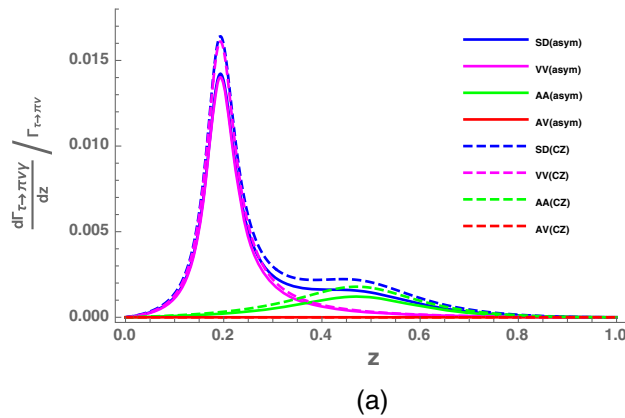
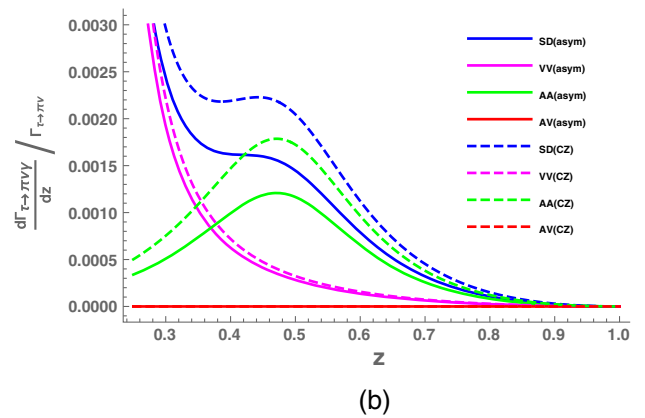


FIG. 4. The dependence of the IB (solid) contribution on the minimum energy threshold of the photon is shown here. Along with that, the same dependence for total decay width including form factors using asymptotic (dashed) and CZ (dotted) pion distribution amplitude is also shown.



(a)



(b)

FIG. 5. (a) The structure dependent contribution (blue) to the invariant mass spectrum of the $\pi - \gamma$ system is shown here for asymptotic (solid) and Chernyak-Zhitnisky (dashed) pion distribution amplitudes. The contribution from the vector (magenta), axial vector (green) and the interference (red) of the two is also shown. (b) Zoomed in version of (a).

shorter and broader peak corresponds to the axial vector contribution. The vector contribution to the total decay width dominates over the axial-vector contribution.

As ρ and a_1 -mesons are not very narrow, the effect of t dependence of the widths is also studied using the prescription provided in [26]. The t dependence of Γ_ρ does not have a significant effect as it is not that wide while the effect of Γ_{a_1} is clearly visible as one can see from Fig. 6. The explicit forms of t dependence of the decay widths are collected in Appendix A. We have also computed the effect of decay width of a_1 -meson Γ_{a_1} , as it has huge uncertainty, and found that the decay width of the radiative tau decay decreases with an increase in Γ_{a_1} . The results reported here are calculated using $\Gamma_{a_1} = 425$ MeV.

Figure 7 represents all the contributions to the invariant mass spectrum of the $\pi - \gamma$ system. The IB contribution dominates at the low photon energy for which we have used the minimum energy threshold of 50 MeV.

After integrating over the full phase space and applying an energy threshold of 50 MeV for the IB contribution, we get the following values for the different contributions to the decay width (normalized to the nonradiative decay width Eq. (C8), i.e., $\bar{\Gamma} = \Gamma(\tau \rightarrow \pi\gamma) / \Gamma(\tau \rightarrow \pi\nu)$):

(i) Asymptotic pion distribution amplitude:

$$\begin{aligned} \bar{\Gamma}_{\text{IB}} &= 1.36 \times 10^{-2}, & \bar{\Gamma}_{\text{VV}} &= (1.47 \pm 0.06) \times 10^{-3}, \\ \bar{\Gamma}_{\text{AA}} &= (3.97 \pm 2.45) \times 10^{-4}, & \bar{\Gamma}_{\text{AV}} &\approx 0 \\ \bar{\Gamma}_{\text{SD}} &= (1.87 \pm 0.30) \times 10^{-3}, \\ \bar{\Gamma}_{\text{int}} &= (3.82 \pm 2.14) \times 10^{-4}, \\ \bar{\Gamma}_{\text{all}} &= (1.56 \pm 0.04) \times 10^{-2}. \end{aligned}$$

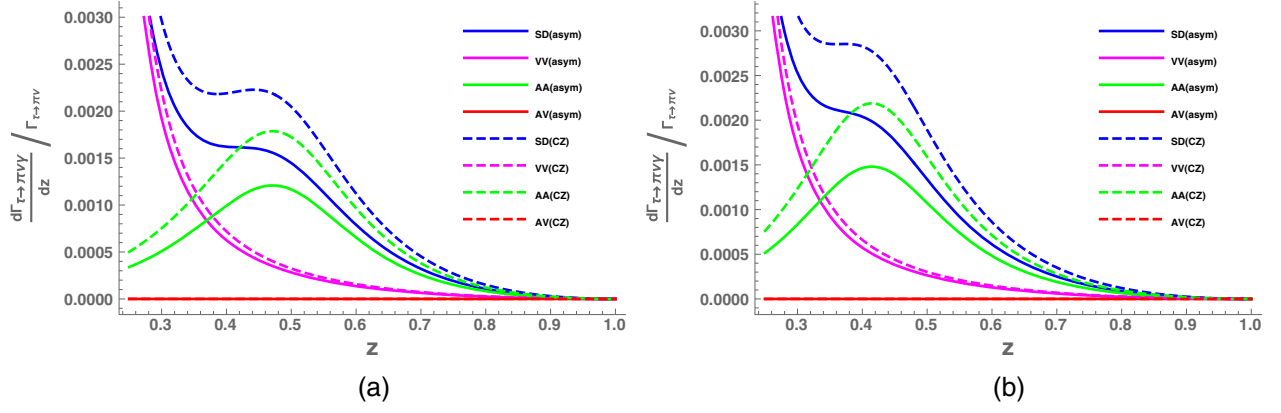


FIG. 6. The SD contribution (blue) considering (a) Γ_ρ and Γ_{a_1} to be constant and (b) the t dependence of Γ_ρ and Γ_{a_1} is shown here for asymptotic (solid) and Chernyak-Zhitnisky (dashed) pion distribution amplitudes. The contribution from the vector (magenta), axial vector (green) and the interference (red) of the two is also shown.

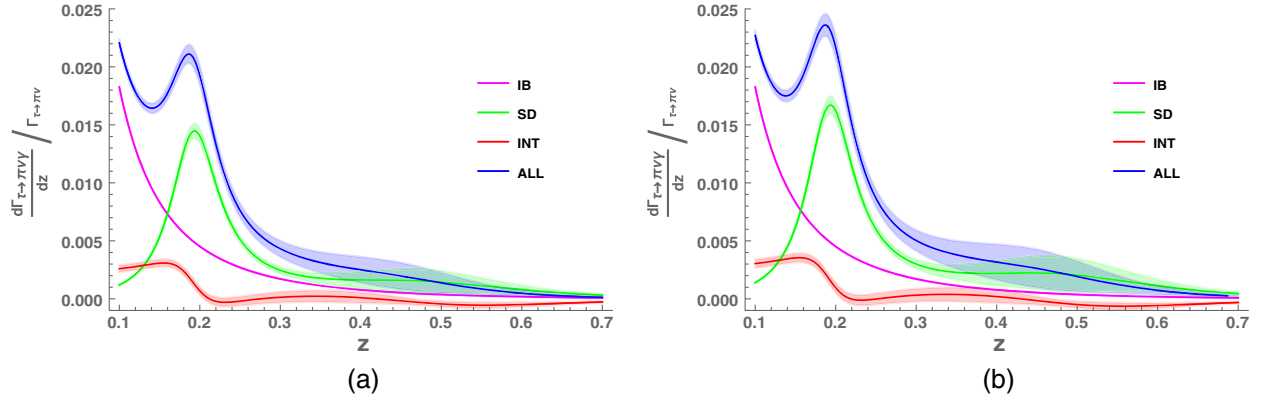


FIG. 7. The invariant mass spectrum of the $\pi - \gamma$ system for radiative tau decay is shown here considering (a) asymptotic and (b) CZ pion distribution amplitude. The contributions from the IB (magenta), SD (green) and the interference (red) of the two is also shown. The shaded region shows the uncertainties.

(ii) CZ pion distribution amplitude:

$$\begin{aligned} \bar{\Gamma}_{IB} &= 1.36 \times 10^{-2}, & \bar{\Gamma}_{VV} &= (1.70 \pm 0.07) \times 10^{-3}, \\ \bar{\Gamma}_{AA} &= (5.91 \pm 3.62) \times 10^{-4}, & \bar{\Gamma}_{AV} &\approx 0 \\ \bar{\Gamma}_{SD} &= (2.29 \pm 0.43) \times 10^{-3}, \\ \bar{\Gamma}_{\text{int}} &= (4.90 \pm 2.60) \times 10^{-4}, \\ \bar{\Gamma}_{\text{all}} &= (1.61 \pm 0.06) \times 10^{-2}. \end{aligned}$$

Since we consider radiative rate normalized to the non-radiative one, the uncertainty in IB contribution is negligible compared to the SD contribution which dominates the error budget, therefore no uncertainty is shown for the IB part. The final uncertainties are about 10%. From the above it is evident that there is a dependence on the form of the distribution amplitude chosen to evaluate these form factors. However, the difference is not too large, which is reassuring.

Having obtained detailed predictions for the pion in the final state, it is also instructive to have an estimate of the decay width for the kaon in the final state. Again, normalizing to the appropriate nonradiative width, and employing the asymptotic distribution amplitude (keeping the Borel parameter, $M = 3.35$ GeV), we get

$$\bar{\Gamma}^K = \Gamma(\tau \rightarrow K\nu\gamma)/\Gamma(\tau \rightarrow K\nu) \sim 8 \times 10^{-3}. \quad (46)$$

This (appropriately normalized) rate is roughly half of that for the pion.

V. DISCUSSION AND CONCLUSIONS

In the present paper, we have provided detailed predictions for the rate and photon spectrum for the process $\tau^- \rightarrow \pi^- \nu_\tau \gamma$. Employing Ward identity from the beginning, the amplitude was written so as to include the contact term which is necessitated by gauge invariance. The decay involves two timelike form factors. These have been calculated in the present work employing the light cone

sum rules, to twist-2 accuracy. The form factors, which automatically via the dispersion relations, encode the contributions from the vector and axial-vector mesons, have the right asymptotic behavior expected from perturbative QCD. The ratio of the axial-vector to vector form factor at zero momentum transfer defines the pion structure dependent parameter, γ . Our evaluation of this parameter, along with the sign, matches very well with the experimental value obtained from $\pi \rightarrow \ell \nu \gamma$, where the relevant pion-photon form factors, unlike the present case, are spacelike. The obtained values for the normalized rate and the photon spectrum are similar to those obtained in [11]. This provides a cross-check on the theoretical predictions employing a totally different method for computing the nonperturbative quantities. We have also provided an estimate for the appropriately normalized rate with kaon in the final state instead of a pion. This normalized rate is approximately half of that for the pion. The present study employed distribution amplitudes to twist-2 accuracy. The uncertainties reported here are the uncertainties associated with the uncertainties of the various parameters used. There will be further uncertainties associated with quark hadron duality approximation, and higher twist and higher order contributions. The pion is considered to be massless here. The effect of such an assumption is less than 1% on the values of the form factors. The uncertainties associated with quark hadron duality violation, like in inclusive tau decays are expected to be at 10% level, and can be calculated in a particular model to parametrize the spectral density. Precise calculations of these duality violations is indeed an important missing piece but is out of the scope of the present work. It would be interesting to consider both higher twist contributions as well as contributions higher order in α_s . These can have a significant impact on the phenomenology of radiative one meson tau decays.

APPENDIX A: CONVENTIONS, DEFINITIONS AND IDENTITIES

Here, we are reporting the various conventions and definitions used for the sake of completeness,

1. The matrix element of the pion is defined as

$$\langle \pi^-(p_2) | (\bar{d}\gamma^\mu(1-\gamma_5)u) | 0 \rangle = if_\pi p_2^\mu, \quad (\text{A1})$$

where f_π is the pion decay constant.

2. The outgoing photon state can be obtained by the use of a creation operator on the vacuum which results in

$$\begin{aligned} & \langle \nu_\tau \gamma | \bar{\nu}_\tau \gamma_\mu (1-\gamma_5) | \tau^- \rangle \\ &= -ie\epsilon_\mu^* \int d^4x e^{ikx} \langle \nu_\tau | T \{ j_{\text{em}}^\alpha(x) \bar{\nu}_\tau \Gamma_\mu \tau(0) \} | \tau^- \rangle, \end{aligned} \quad (\text{A2})$$

where $j_{\text{em}}^\alpha(x) = Q_u \bar{\psi} \gamma^\alpha \psi(x) = -\bar{\tau} \gamma^\alpha \tau + Q_u \bar{u} \gamma^\alpha u + Q_d \bar{d} \gamma^\alpha d$ is the electromagnetic current. Q_u and Q_d are the electromagnetic charges of u and d quarks, respectively in the units of e .

3. The commutator of the electromagnetic charge operator and electroweak current of the pion is given by

$$\begin{aligned} & [j_{\text{em}}^0(x), \bar{d}\Gamma^\mu u(0)] \\ &= -Q_u \delta^3(x) \bar{d}(0) \Gamma^\mu u(x) + Q_d \delta^3(x) \bar{d}(x) \Gamma^\mu u(0). \end{aligned} \quad (\text{A3})$$

4. The propagator of the massless fermions in position space is given by,

$$\begin{aligned} iS_0(x) &= \langle 0 | T \{ u(x) \bar{u}(0) \} | 0 \rangle \\ &= \frac{i\not{x}}{2\pi^2 x^4} = -\langle 0 | T \{ u(0) \bar{u}(x) \} | 0 \rangle. \end{aligned} \quad (\text{A4})$$

5. $\gamma_\mu \gamma_\beta \gamma_\alpha = g_{\mu\beta} \gamma_\alpha - g_{\mu\alpha} \gamma_\beta + g_{\beta\alpha} \gamma_\mu - i\epsilon_{\mu\beta\alpha\rho} \gamma^\rho \gamma_5$.
6. The leading order expansion (twist-2) of the matrix element $\langle \pi^-(p_2) | \bar{d}(y) \gamma_\mu \gamma_5 u(x) | 0 \rangle$ in the light cone limit ($x^2 = 0$) is given by

$$\begin{aligned} & \langle \pi^-(p_2) | \bar{d}(y) \gamma_\mu \gamma_5 u(x) | 0 \rangle \\ &= if_\pi p_{2\mu} \int_0^1 du e^{i(up_2 y + \bar{u} p_2 x)} \phi(u, \mu), \end{aligned} \quad (\text{A5})$$

where $\bar{u} = 1 - u$ and $\phi(u, \mu)$ is pion distribution amplitude of twist-2.

7. The matrix elements of ρ and a_1 mesons are defined as

$$\langle V(p_2 + k) | \bar{d}\gamma_\mu u | 0 \rangle = -im_V f_V \epsilon_\mu^{(V)*} \quad (\text{A6})$$

$$\langle \pi^-(p_2) | j_{\text{em}}^\alpha(x) | \rho(p_2 + k) \rangle = \epsilon^{\alpha\lambda\beta\nu} \epsilon_\lambda^{(\rho)} p_{2\beta} k_\nu F_{\rho\pi}(k^2) \quad (\text{A7})$$

$$\begin{aligned} & \langle \pi^-(p_2) | j_{\text{em}}^\mu(x) | a_1(p_2 + k) \rangle \\ &= [(2p_2 - k) \cdot k g^{\mu\lambda} - (2p_2 - k)^\mu k^\lambda] \epsilon_\lambda^{(a_1)*} G_{a_1\pi}(k^2), \end{aligned} \quad (\text{A8})$$

where V can be ρ or a_1 meson, m_V and f_V are the mass and decay constant of the V meson, respectively. $\epsilon_\lambda^{(\rho)}$ and $\epsilon_\lambda^{(a_1)*}$ are the polarization vectors of ρ and a_1 meson, respectively. $F_{\rho\pi}(k^2)$ and $G_{a_1\pi}(k^2)$ are the scalar functions of k^2 which contains the information of $\rho \rightarrow \pi$ and $a_1 \rightarrow \pi$ transitions, respectively.

8. The sum over polarization of ρ or a_1 meson is given by

$$\epsilon_\lambda^{(V)} \epsilon_\nu^{(V)*} = -g_{\lambda\nu} + \frac{(p_2 + k)_\lambda (p_2 + k)_\nu}{m_V^2}. \quad (\text{A9})$$

9. The t dependence of the decay widths of ρ and a_1 mesons are given by [26]

$$\Gamma_\rho(t) = \Gamma_\rho \frac{m_\rho^2 p^3}{p_\rho^3 t} \quad (\text{A10})$$

with $2p = (t - 4m_\pi^2)^{1/2}$ and $2p_\rho = (m_\rho^2 - 4m_\pi^2)^{1/2}$:

$$\Gamma_{a_1}(t) = \frac{m_{a_1} \Gamma_{a_1}}{\sqrt{t}} \frac{g(t)}{g(m_{a_1}^2)} \quad (\text{A11})$$

with

$$g(t) = \begin{cases} 4.1(t - 9m_\pi^2)^3(1 - 3.3(t - 9m_\pi^2) + 5.8(t - 9m_\pi^2)^2) & \text{if } t < (m_\rho + m_\pi)^2 \\ t \left(1.623 + \frac{10.38}{t} - \frac{9.38}{t^2} + \frac{0.65}{t^3} \right) & \text{else.} \end{cases}$$

APPENDIX B: VALUES OF PARAMETERS USED

Here, we tabulate the values of the various parameters used for numerical calculation.

S.No.	Parameter	Symbol	Value
1.	Fine structure constant	α	$\frac{1}{133.6}$
2.	Fermi's constant	G_F	$1.166 \times 10^{-5} \text{ GeV}^{-2}$ [1]
3.	Mass of τ lepton	m_τ	$(1776.86 \pm 0.12) \text{ MeV}$ [1]
4.	Pion decay constant	f_π	$(130.41 \pm 0.23) \text{ MeV}$
5.	CKM matrix element	V_{ud}	(0.9745 ± 0.0001) [1]
6.	Mass of ρ meson	m_ρ	$(775.26 \pm 0.25) \text{ MeV}$ [1]
7.	Decay width of ρ meson	Γ_ρ	$(149.1 \pm 0.8) \text{ MeV}$ [1]
8.	Mass of a_1 meson	m_{a_1}	$(1230 \pm 40) \text{ MeV}$ [1]
9.	Decay width of a_1 meson	Γ_{a_1}	$(425 \pm 175) \text{ MeV}$ [1]
10.	Vector form factor	$F_V^{(\pi)}(0)$	0.0254 ± 0.0017 [1]
11.	Axial-vector form factor	$F_A^{(\pi)}(0)$	0.0119 ± 0.0001 [1]
12.	$\alpha_s(1 \text{ GeV})$	$\alpha_s(1 \text{ GeV})$	~ 0.7
13.	$\alpha_s(m_\tau)$	$\alpha_s(m_\tau)$	0.325
14.	$a_2(1 \text{ GeV})$	$a_2(1 \text{ GeV})$	0.12

The value of the fine structure constant is taken at the scale m_τ and the decay width of the a_1 meson is taken to the central value of the range given in [1].

APPENDIX C: KINEMATICS AND DECAY WIDTH

The differential decay width can be written as a sum of different components [14]: Γ_{IB} coming from $|\mathcal{A}_{\text{IB}}|^2$, Γ_{SD} coming from $|\mathcal{A}_{\text{SD}}|^2$ and Γ_{int} coming from $2\text{Re}(\mathcal{A}_{\text{IB}}^* \mathcal{A}_{\text{SD}})$. Γ_{SD} is further divided into three parts: Γ_{VV} coming from $|\mathcal{A}_V|^2$, Γ_{AA} coming from $|\mathcal{A}_A|^2$ and Γ_{AV} coming from $2\text{Re}(\mathcal{A}_V \mathcal{A}_A^*)$:

$$\begin{aligned} \Gamma_{\text{all}} &= \Gamma_{\text{IB}} + \Gamma_{\text{int}} + \Gamma_{\text{SD}}, \\ \Gamma_{\text{SD}} &= \Gamma_{\text{VV}} + \Gamma_{\text{AV}} + \Gamma_{\text{AA}}, \\ \Gamma_{\text{int}} &= \Gamma_{\text{IB-A}} + \Gamma_{\text{IB-V}}. \end{aligned} \quad (\text{C1})$$

For convenience, we use the dimensionless variables x and y defined as

$$x = \frac{2p_1 \cdot k}{m_\tau^2}, \quad y = \frac{2p_1 \cdot p_2}{m_\tau^2}. \quad (\text{C2})$$

In the rest frame of tau, x and y are simply the energies of photon and pion respectively in units of $\frac{m_\tau}{2}$. The kinematical boundaries of x and y are given by

$$0 \leq x \leq 1 - r_p^2, \quad 1 - x + \frac{r_p^2}{1-x} \leq y \leq 1 + r_p^2, \quad (\text{C3})$$

where $r_p^2 = \frac{m_\pi^2}{m_\tau^2}$. We have considered pion to be massless for form factor calculations and hence we will use $r_p \rightarrow 0$ in our final answers.

The variable t , the invariant mass square of the pion-photon system, can be written in terms of x and y as

$$\begin{aligned} t = P^2 &= (p_2 + k)^2 = m_\tau^2(x + y - 1) \\ \Rightarrow P \cdot k &= \frac{m_\tau^2}{2}(x + y - 1 - r_p^2). \end{aligned} \quad (\text{C4})$$

In terms of variables x and y , the differential decay width in the rest frame of tau is

$$\frac{d^2\Gamma}{dx dy} = \frac{m_\tau}{256\pi^3} \overline{|\mathcal{A}|^2}, \quad (\text{C5})$$

where different contributions to the differential decay width are (calculated using FeynCalc [27])

$$\begin{aligned}
\frac{d^2\Gamma_{\text{IB}}}{dx dy} &= \frac{\alpha}{2\pi} f_{\text{IB}}(x, y, r_p^2) \frac{\Gamma_{\tau^- \rightarrow \pi^- \nu_\tau}}{(1 - r_p^2)^2}, \\
\frac{d^2\Gamma_{\text{SD}}}{dx dy} &= \frac{\alpha}{8\pi} \frac{m_\tau^4}{f_\pi^2} \{ |F_V^{(\pi)}|^2 f_{V_V}(x, y, r_p^2) + 2\mathcal{R}e(F_A^{(\pi)*} F_V^{(\pi)}) f_{A_V}(x, y, r_p^2) + |F_A^{(\pi)}|^2 f_{A_A}(x, y, r_p^2) \} \frac{\Gamma_{\tau^- \rightarrow \pi^- \nu_\tau}}{(1 - r_p^2)^2}, \\
\frac{d^2\Gamma_{\text{int}}}{dx dy} &= \frac{\alpha}{2\pi} \frac{m_\tau^2}{f_\pi} [f_{\text{IB-V}}(x, y, r_p^2) \mathcal{R}e(F_V^{(\pi)}) + f_{\text{IB-A}}(x, y, r_p^2) \mathcal{R}e(F_A^{(\pi)})] \frac{\Gamma_{\tau^- \rightarrow \pi^- \nu_\tau}}{(1 - r_p^2)^2}, \tag{C6}
\end{aligned}$$

with $\alpha = \frac{e^2}{4\pi}$, being the fine structure constant,

$$\begin{aligned}
f_{\text{IB}}(x, y, r_p^2) &= \frac{[r_p^4(x+2) - 2r_p^2(x+y) + (x+y-1)(2-3x+x^2+xy)](r_p^2-y+1)}{(r_p^2-x-y+1)^2 x^2}, \\
f_{V_V}(x, y, r_p^2) &= -[r_p^4(x+y) + 2r_p^2(1-y)(x+y) + (x+y-1)(-x+x^2-y+y^2)], \\
f_{A_V}(x, y, r_p^2) &= -[r_p^2(x+y) + (1-x-y)(y-x)](r_p^2-x-y+1), \\
f_{A_A}(x, y, r_p^2) &= f_{V_V}(x, y, r_p^2), \\
f_{\text{IB-V}}(x, y, r_p^2) &= -\frac{(r_p^2-x-y+1)(r_p^2-y+1)}{x}, \\
f_{\text{IB-A}}(x, y, r_p^2) &= -\frac{[r_p^4 - 2r_p^2(x+y) + (1-x+y)(x+y-1)](r_p^2-y+1)}{(r_p^2-x-y+1)x}, \tag{C7}
\end{aligned}$$

and $\Gamma_{\tau^- \rightarrow \pi^- \nu_\tau}$ is the nonradiative decay width given by

$$\Gamma_{\tau^- \rightarrow \pi^- \nu_\tau} = \frac{G_F^2 |V_{ud}|^2 f_\pi^2}{8\pi} m_\tau^3 (1 - r_p^2)^2. \tag{C8}$$

The photon spectrum is obtained by integrating over y . Integration over x will give the total decay width for radiative tau decay. The IB contribution has the infrared divergences which can be fixed by putting a threshold on the minimum energy of the emitted photon. The SD contribution does not face any such divergence and hence can be integrated over the full phase space:

$$\Gamma(\tau^- \rightarrow \pi^- \nu_\tau \gamma) = \int_{x_0}^{1-r_p^2} dx \int_{1-x+\frac{r_p^2}{1-x}}^{1+r_p^2} dy \frac{d^2\Gamma}{dx dy}, \tag{C9}$$

where x_0 is the minimum energy cut for the photon energy in the unit of $\frac{m_\pi}{2}$.

To get the invariant mass spectrum of the $\pi\gamma$ system, define another dimensionless variable z (as used in Ref. [14]) as

$$z = \frac{t}{m_\tau^2} = x + y - 1. \tag{C10}$$

The kinematical boundaries for the new variable are

$$z - r_p^2 \leq x \leq 1 - \frac{r_p^2}{z}, \quad r_p^2 \leq z \leq 1. \tag{C11}$$

The $\pi\gamma$ spectrum can be obtained by substituting y in terms of z in $\frac{d^2\Gamma}{dx dy}$ and integrating it over x , i.e.,

$$\frac{d\Gamma}{dz} = \int_{z-r_p^2}^{1-\frac{r_p^2}{z}} dx \frac{d^2\Gamma}{dx dy}(x, y = z - x + 1). \tag{C12}$$

-
- [1] M. Tanabashi *et al.* (Particle Data Group), Review of particle physics, *Phys. Rev. D* **98**, 030001 (2018).
[2] B. C. Barish and R. Stroynowski, The physics of the tau lepton, *Phys. Rep.* **157**, 1 (1988).
[3] S. Gentile and M. Pohl, Physics of τ leptons, *Phys. Rep.* **274**, 287 (1996).

- [4] A. Stahl, Physics with tau leptons, *Springer Tracts Mod. Phys.* **160**, 1 (2000).
[5] M. Davier, A. Hocker, and Z. Zhang, The physics of hadronic tau decays, *Rev. Mod. Phys.* **78**, 1043 (2006).
[6] A. Pich, Precision tau physics, *Prog. Part. Nucl. Phys.* **75**, 41 (2014).

- [7] J. H. Kim and L. Resnick, τ radiative decay and pion structure form factors, *Phys. Rev. D* **21**, 1330 (1980).
- [8] Yu. P. Ivanov, A. A. Osipov, and M. K. Volkov, Radiative decay $\tau \rightarrow \tau \nu_\tau \pi \gamma$, *Phys. Lett. B* **242**, 498 (1990).
- [9] R. Decker and M. Finkemeier, Radiative corrections to the decay $\tau \rightarrow \pi(K) \tau \nu_\tau$, *Phys. Lett. B* **334**, 199 (1994).
- [10] C. Q. Geng and C. C. Lih, Tau radiative decays in the light front quark model, *Phys. Rev. D* **68**, 093001 (2003).
- [11] Z.-H. Guo and P. Roig, One meson radiative tau decays, *Phys. Rev. D* **82**, 113016 (2010).
- [12] V. Cirigliano, G. Ecker, and H. Neufeld, Radiative tau decay and the magnetic moment of the muon, *J. High Energy Phys.* **08** (2002) 002.
- [13] S. Banerjee, Analysis of radiative τ decays, *Phys. Rev. D* **34**, 2080 (1986).
- [14] R. Decker and M. Finkemeier, Radiative tau decays with one pseudoscalar meson, *Phys. Rev. D* **48**, 4203 (1993); Addendum to “Radiative τ decays with one pseudoscalar meson”, *Phys. Rev. D* **50**, 7079 (1994).
- [15] A. Khodjamirian and D. Wyler, Counting contact terms in $B \rightarrow V$ gamma decays, in *From Integrable Models to Gauge Theories* (World Scientific, 2001), pp. 227–241, https://doi.org/10.1142/9789812777478_0014.
- [16] M. A. Shifman, A. I. Vainshtein, and V. I. Zakharov, QCD and resonance physics. theoretical foundations, *Nucl. Phys.* **B147**, 385 (1979).
- [17] M. A. Shifman, A. I. Vainshtein, and V. I. Zakharov, QCD and resonance physics: Applications, *Nucl. Phys.* **B147**, 448 (1979).
- [18] P. Colangelo and A. Khodjamirian, QCD Sum Rules, a Modern Perspective, in *At The Frontier of Particle Physics* (World Scientific, 2000), pp. 1495–1576, https://doi.org/10.1142/9789812810458_0033.
- [19] V. M. Braun, Light cone sum rules, in the *4th International Workshop on Progress in Heavy Quark Physics* (1997), pp. 105–118 [arXiv:hep-ph/9801222].
- [20] M. A. Shifman, Snapshots of hadrons or the story of how the vacuum medium determines the properties of the classical mesons which are produced, live and die in the QCD vacuum, *Prog. Theor. Phys. Suppl.* **131**, 1 (1998).
- [21] K. Kawarabayashi and M. Suzuki, Partially Conserved Axial Vector Current and the Decays of Vector Mesons, *Phys. Rev. Lett.* **16**, 255 (1966).
- [22] Riazuddin and Fayyazuddin, Algebra of current components and decay widths of rho and K^* mesons, *Phys. Rev.* **147**, 1071 (1966).
- [23] M. A. Shifman, Quark Hadron Duality, in *8th International Symposium on Heavy Flavor Physics*, Vol. 3 (World Scientific, Singapore, 2000), pp. 1447–1494, https://doi.org/10.1142/9789812810458_0032.
- [24] M. Gonzalez-Alonso, A. Pich, and J. Prades, Violation of quark-hadron duality and spectral chiral moments in QCD, *Phys. Rev. D* **81**, 074007 (2010).
- [25] C. A. Dominguez, L. A. Hernandez, K. Schilcher, and H. Spiesberger, Tests of quark-hadron duality in tau-decays, *Mod. Phys. Lett. A* **31**, 1630036 (2016).
- [26] J. H. Kuhn and A. Santamaria, Tau decays to pions, *Z. Phys. C* **48**, 445 (1990).
- [27] V. Shtabovenko, R. Mertig, and F. Orellana, FeynCalc 9.3: New features and improvements, *Comput. Phys. Commun.* **256**, 107478 (2020).

Light cone sum rules and form factors for $p \rightarrow e^+ \gamma$

Anshika Bansal^{a,b,1} and Namit Mahajan^a

^a*Theoretical physics division, Physical Research Laboratory,
Navrangpura, Ahmedabad, India*

^b*Physics Department, Indian Institute of Technology, Gandhinagar,
Palaj, Gandhinagar, India*

E-mail: anshika@prl.res.in, nmahajan@prl.res.in

ABSTRACT: Proton decay is a baryon number violating process, and hence is forbidden in the Standard Model (SM) of particle physics. Baryon number violation is expected to be an important criteria to explain the matter-anti-matter asymmetry of the universe. Any detection of the proton decay will be a direct evidence of physics beyond the SM. In SMEFT, proton decay is possible via baryon number violating dimension-6 operators. In this work, we pay attention to the decay channel $p \rightarrow e^+ \gamma$ which is expected to be an experimentally cleaner channel due to less nuclear absorption. The gauge invariant amplitude of this process involves two form factors. We calculate these form factors in the framework of light cone sum rules (LCSR) using photon DAs upto two particle twist-3 accuracy as well as proton DAs of twist-3 accuracy. We find that the form factors calculated using photon DAs are more reliable.

KEYWORDS: Nonperturbative Effects, Properties of Hadrons, Baryon/Lepton Number Violation, Grand Unification

ARXIV EPRINT: [2204.03448](https://arxiv.org/abs/2204.03448)

¹Corresponding author.

Contents

1	Introduction	1
2	Amplitude computation	3
3	Form factors in the LCSR framework	4
3.1	Case-1: using proton interpolation and photon DAs	5
3.1.1	Numerical analysis	8
3.2	Case-2: using photon interpolation and proton DAs	11
3.2.1	Numerical analysis	14
4	Discussion and conclusions	16
A	Distribution amplitudes (DAs)	17
A.1	Proton DAs	17
A.2	Photon DAs	17
B	Correlation functions for case-1 (employing photon DAs)	18
C	Correlation functions for case-2 (employing proton DAs)	20
D	Conventions, definitions and identities	21
D.1	Definitions and conventions	21
D.2	Useful identities and integrals	21
D.3	Borel Transformations	22
E	Values of parameters used	23

1 Introduction

In particle physics, the Standard Model (SM) of strong and electro-weak interactions is the most successful model of particle interactions. In the SM, baryon number conservation is an accidental global symmetry at the classical level. In 1967, Sakharov proposed that baryon number violation is one of the important criteria to explain the matter-anti matter asymmetry of the universe [1]. Baryon number violation at the perturbative level is well motivated in the theories of grand unification (GUTs), supersymmetry, models of baryogenesis, model building in string theory and in theories with extra dimensions, etc (see for example [2–12] and references therein). Proton decay is a baryon number violating process. Any observation of it is a direct indication of physics beyond the SM. This makes

proton decay a crucial test of such models and an important window to understand the nature of matter unification.

In the case of GUTs, quarks and leptons fall in the common multiplets and hence can lead to proton decay at the tree level via the exchange of superheavy gauge bosons or scalar and/or vector leptoquarks. This makes it possible to write the effective baryon and lepton number violating operators of dim-6 by integrating out these heavy fields, such that they are consistent with the SM gauge symmetry. These effective operators are found to conserve $B - L$ which implies that a proton always decays into an antilepton (or antineutrino) (see [13–16] for reviews on proton decays).

$p \rightarrow e^+\pi^0$ is the most favoured channel in several GUTs models. As with any process involving hadrons, proton decay modes like $p \rightarrow e^+\pi^0$ require hadronic matrix elements, the form factors, to be computed within some framework or at least properly estimated. This mode has been studied using various models of QCD, such as relativistic quark model, QCD sum rules, effective chiral theory, lattice QCD, [17–23]. Very recently, it has been studied in the framework of light cone sum rules [24]. Another decay channel which is found to have strong constraints is the radiative mode: $p \rightarrow e^+\gamma$. The radiative mode is expected to be suppressed by α_{em} . In [25], it is been studied within SU(5) GUT set up. They pointed out that it might be a more feasible channel experimentally as there will be less nuclear absorption. The form factors have been evaluated with a simple harmonic oscillator potential as a model for binding the quarks inside the proton. In [26], it was studied in the framework of bag model and they concluded that it is not a feasible channel for experiments as the decay rate is small. The experimental facilities have been advancing over the time (see [27] for a review of different experiments and expected sensitivities expected at future experiments) and hence a reanalysis of this mode is required, including a fresh attempt at evaluation of the involved form factors.

Experimentally, Kolar Gold Field [28], NUSEX [29], SOUDAN [30], Kamiokande [31], etc, were designed to detect the proton decay. At present, the Super-Kamiokande, the largest proton water Cherenkov detector, is the most sensitive detector and has put the most stringent lower bounds on the partial life times for the proton decays, $\tau_p > 10^{34}$ years [32]. The lower bound for the radiative proton decay modes $p \rightarrow e^+\gamma$ and $p \rightarrow \mu^+\gamma$ are $\tau_p > 6.7 \times 10^{32}$ years and $\tau_p > 4.8 \times 10^{32}$ years, respectively [33]. In the Water-Cherenkov experiments, such as Super-Kamiokande, the decay products of the proton are measured approximately at rest which makes the relevant energy scale for the process to be the proton mass (see [34] for a review on Super-Kamiokande).

At these energy scales, a perturbative description for the hadronic transitions is not possible in QCD because of quark confinement. Hence, we need alternative ways to get an estimate of the hadronic matrix elements which can help us in probing the baryon-number violating physics with the help of experimental data. Light Cone Sum Rules (LCSR) is one such interesting framework which helps us to predict the hadronic matrix elements at the proton mass scales using the analytic properties of the correlation functions (see for example [35–40] for details). In this work, we study the $p \rightarrow e^+\gamma$ in the framework of LCSR.

The rest of the paper is organised as follows: in section 2, we discuss the general parametrisation of the amplitude for the decay in terms of the form factor and define

the physical FFs involved. In section 3, we discuss the computation of these form factors in the framework of LCSR. Here, we discuss the two cases: firstly, the use of photon distribution amplitudes and interpolating the proton state; and secondly, the use of proton distribution amplitudes and interpolating the photon state. In this section, we also discuss the numerical results obtained in both the cases. section 4 is dedicated to discussion of the results and conclusions. This paper consists of five appendices. In appendix-A, we collect the distribution amplitudes (DAs) of proton and photon upto the desired twist. appendix-B and appendix-C are dedicated to collect the correlation functions computed in QCD for the case employing photon DAs and proton DAs, respectively. In appendix-D, we provide some useful identities and integrals along with definitions and conventions used throughout the paper. Finally, we tabulate the numerical values of all the important parameters involved during numerical analysis in appendix-E.

2 Amplitude computation

Proton decay is a baryon number violating process. Though baryon number is a good symmetry in the SM, one can write higher dimensional effective operators which allow the proton to decay. In a beyond the SM scenario, like GUTs, proton decay is possible even at tree level via an exchange of heavy gauge bosons or leptoquarks. On integrating out these heavy particles, one obtains the baryon number violating dim-6 SMEFT lagrangian which preserves the $SU(3)_C \times SU(2)_L \times U(1)_Y$ invariance [41–44].

$$\mathcal{L}_{\not{B}}^{(6)} = \sum_{\Gamma, \Gamma'} c_{\Gamma\Gamma'} \mathcal{O}_{\Gamma\Gamma'} = \sum_{\Gamma, \Gamma'} c_{\Gamma\Gamma'} \epsilon^{abc} \left(\bar{d}_a^c P_{\Gamma} u_b \right) \left(\bar{e}^c P_{\Gamma'} u_c \right) \quad (2.1)$$

Here, $\Gamma, \Gamma' \in \{L, R\}$ are the chirality projections. $c_{\Gamma\Gamma'}$ are the Wilson coefficients. $C = i\gamma^2\gamma^0$ is the charge conjugation matrix and a, b, c are the colour indices. It is worth pointing out at this juncture that the above effective lagrangian is assumed to be expressed in terms of the physical quark and lepton fields at the relevant scale. This means that all the flavour mixing and perturbative renormalization group (RG) effects together with the short distance information, are collectively lumped in the Wilson coefficients $c_{\Gamma\Gamma'}$. Since the aim of the present work is to systematically evaluate the corresponding form factors relevant for the radiative mode, the exact details of these effects are not particularly relevant here, and therefore not discussed further. It should be straightforward to explicitly express these dependencies in a concrete model of proton decay.

The transition amplitude for $p \rightarrow e^+ + \gamma$ is the matrix element of the dim-6 lagrangian given in eq.-(2.1) between the initial and the final states.

$$\begin{aligned} \mathcal{A} \left(p(p_p) \rightarrow e^+(p_e) \gamma(k) \right) &= \sum_{\Gamma\Gamma'} c_{\Gamma\Gamma'} \left\langle e^+(p_e) \gamma(k) \left| \mathcal{O}_{\Gamma\Gamma'} \right| p(p_p) \right\rangle \\ &= \sum_{\Gamma\Gamma'} c_{\Gamma\Gamma'} \left\langle e^+(p_e) \gamma(k) \left| \epsilon^{abc} \left(\bar{d}_a^c P_{\Gamma} u_b \right) \left(\bar{e}^c P_{\Gamma'} u_c \right) \right| p(p_p) \right\rangle \quad (2.2) \end{aligned}$$

As mentioned above, all the flavour effects are absorbed in the Wilson coefficients, $c_{\Gamma\Gamma'}$. On demanding the gauge invariance, this amplitude can be parametrised as

$$\mathcal{A}\left(p(p_p) \rightarrow e^+(p_e)\gamma(k)\right) = \sum_{\Gamma\Gamma'} c_{\Gamma\Gamma'} \bar{v}_e^c P_{\Gamma'} \left\{ \epsilon_{\alpha^*} A_{\Gamma\Gamma'} \frac{i\sigma^{\alpha\beta} k_\beta}{m_p} \right\} u_p(p_p). \quad (2.3)$$

where $A_{\Gamma\Gamma'}$ are the non-perturbative form factors. Parity conservation in QCD relates the different form factors relevant for the process:

$$A_{LL} = -A_{RR} \quad A_{LR} = -A_{RL}. \quad (2.4)$$

Hence, this process involves only two independent gauge invariant form factors. For the present study, we choose them to be A_{LL} and A_{LR} . Clearly, the main hurdle in obtaining the branching ratio is the knowledge of the form factors. All other factors are known once a given model of particle physics leading to proton decay is chosen.

The photon can be emitted either from the proton or the positron. The photon emission from positron can be trivially calculated and is not explicitly written as it does not contribute to the dipole transition depicted above. The photon emission from proton involves the photon emission from both u and d-quarks and contributes to the form factors. The study of these FFs in the framework of LCSR is the subject of the present study. The transition matrix element for the photon emission from proton can be factorised in the leptonic and hadronic parts as

$$\left\langle e^+(p_e)\gamma(k) \left| \mathcal{O}_{\Gamma\Gamma'} \right| p(p_p) \right\rangle = \bar{v}_e^c(p_e) H_{\Gamma\Gamma'}(p_P, p_e) u_p(p_p). \quad (2.5)$$

We choose to parametrise the hadronic matrix element $H_{\Gamma\Gamma'} u_p(p_p)$ as (see [45] for general parametrisation of the vertex for $b \rightarrow s\gamma$ transition):

$$\begin{aligned} & H_{\Gamma\Gamma'}(p_P, p_e) u_p(p_p) \\ &= \left\langle \gamma(k) \left| \epsilon^{abc} \left(d_a^T C P_\Gamma u_b \right) (P_{\Gamma'} u_c) \right| p(p_p) \right\rangle \\ &= P_{\Gamma'} \epsilon_\mu^* \left[F_{\Gamma\Gamma'}^1 \frac{\not{k} p_p^\mu}{m_p^2} + F_{\Gamma\Gamma'}^2 \frac{\not{k} k^\mu}{m_p^2} + F_{\Gamma\Gamma'}^3 \gamma^\mu + i F_{\Gamma\Gamma'}^4 \frac{\sigma^{\mu\nu} k_\nu}{m_p} + F_{\Gamma\Gamma'}^5 \frac{p_p^\mu}{m_p} + F_{\Gamma\Gamma'}^6 \frac{k^\mu}{m_p} \right] u_p(p_p) \end{aligned} \quad (2.6)$$

The physical FFs, $A_{\Gamma\Gamma'}$ are then related to $F_{\Gamma\Gamma'}^n$, with $n = \{1, 2, 3, 4, 5\}$, considering positron to be massless as,

$$A_{\Gamma\Gamma'} = \frac{F_{\Gamma\Gamma'}^1}{2} + F_{\Gamma\Gamma'}^4 + \frac{F_{\Gamma\Gamma'}^5}{2}. \quad (2.7)$$

3 Form factors in the LCSR framework

To compute the FFs, $A_{\Gamma\Gamma'}$, in LCSR framework, we need to compute the hadronic matrix element given in eq. (2.6) in QCD. For that there are two possibilities:

1. Interpolating the proton state and using the photon distribution amplitudes (DAs).
2. Interpolating the photon state and using the proton distribution amplitudes (DAs).

We will discuss here both these approaches one by one with an aim to be finally able to compare the outcomes from both in order to gain deeper insights into the underlying non-perturbative dynamics.

3.1 Case-1: using proton interpolation and photon DAs

The interpolation current for the proton state is not unique. For the present study, we choose it to be

$$\chi(x) = \epsilon^{abc} \left(u^{aT}(x) C \gamma_\mu u^b(x) \right) \gamma_5 \gamma^\mu d^c(x). \quad (3.1)$$

Here C is the charge conjugation matrix, $\{a, b, c\}$ are the color indices and the superscript T denotes the transpose. This current is popularly known as the Ioffe current [46] and is defined such that,

$$\langle 0 | \chi(0) | p(p_p) \rangle = m_p \lambda_p u_p(p_p) \quad (3.2)$$

where, m_p is the mass of proton, $u_p(p_p)$ is the proton spinor and λ_p is the interaction strength of this interpolation current with the proton state.

In literature, this current is found to provide the maximum stability against the Borel mass, the parameter introduced in LCSR computations [47]. The Ioffe current is a linear combination of

$$\chi_1(x) = \epsilon^{abc} \left(u^{Ta}(x) C \gamma_5 d^b(x) \right) u^c(x) \quad \text{and} \quad \chi_2(x) = \epsilon^{abc} \left(u^{Ta}(x) C d^b(x) \right) \gamma_5 u^c(x) \quad (3.3)$$

such that $\chi(x) = 2(\chi_2 - \chi_1)$ after performing Fierz transformation (see for example [48]). χ_1 is the common choice of interpolation current employed in Lattice QCD computations. On interpolating the proton state using the Ioffe current, the correlation function to be computed reads as

$$\Pi_{\Gamma\Gamma'}(p_p, p_e) = i \int d^4x e^{ip_e \cdot x} \langle \gamma(k) | T \{ Q_{\Gamma\Gamma'}(x) \bar{\chi}(0) \} | 0 \rangle. \quad (3.4)$$

Here, $\bar{\chi}(0) \equiv \chi^\dagger(0) \gamma^0$, $Q_{\Gamma\Gamma'}(x) = \epsilon^{abc} \left(d_a^T C P_\Gamma u_b \right) (P_{\Gamma'} u_C)$ and T denotes the time ordering.

One can get the hadronic parametrisation of this correlation function by inserting a complete set of intermediate states with the same quantum numbers as the proton and isolating the pole contribution of the proton state as,

$$\begin{aligned} \Pi_{\Gamma\Gamma'}^{had}(p_p, p_e) &= -\frac{m_p \lambda_p}{p_p^2 - m_p^2} H_{\Gamma\Gamma'}(p_e, p_p) (\not{p}_p + m_p) + \dots \\ &= \epsilon_\mu^* P_{\Gamma'} \left[\Pi_{\Gamma\Gamma'}^{had,PK} \frac{\not{k} p_p^\mu}{m_p^2} + \Pi_{\Gamma\Gamma'}^{had,KK} \frac{\not{k} k^\mu}{m_p^2} + \Pi_{\Gamma\Gamma'}^{had,V} \gamma^\mu + \Pi_{\Gamma\Gamma'}^{had,T} \frac{i\sigma^{\mu\nu} k_\nu}{m_p} + \Pi_{\Gamma\Gamma'}^{had,P} \frac{p_p^\mu}{m_p} \right. \\ &\quad + \Pi_{\Gamma\Gamma'}^{had,K} \frac{k^\mu}{m_p} + \Pi_{\Gamma\Gamma'}^{had,KPP} \frac{\not{k} p_p^\mu \not{p}_p}{m_p^3} + \Pi_{\Gamma\Gamma'}^{had,KKP} \frac{k^\mu \not{k} \not{p}_p}{m_p^3} + \Pi_{\Gamma\Gamma'}^{had,VP} \frac{\gamma^\mu \not{p}_p}{m_p} \\ &\quad \left. + \Pi_{\Gamma\Gamma'}^{had,TP} \frac{i\sigma^{\mu\nu} k_\nu \not{p}_p}{m_p^2} + \Pi_{\Gamma\Gamma'}^{had,PP} \frac{\not{p}_p p_p^\mu}{m_p^2} + \Pi_{\Gamma\Gamma'}^{had,KP} \frac{k^\mu \not{p}_p}{m_p^2} \right]. \quad (3.5) \end{aligned}$$

The ellipsis above represent the heavy states i.e. excited states and continuum, contributions. The 12 Dirac structures in eq. (3.5) can be used to derive the form factors A_{LL} and A_{LR} .

$\Pi_{\Gamma\Gamma'}^{had,r}$ with $r = \{PK, KK, V, T, P, K, KPP, KKP, VP, TP, PP, KP\}$ are the scalar functions of p_p^2 and $P_e^2 = -p_e^2$ and can be parametrised in terms of spectral densities using the dispersion relation given by,

$$\Pi_{\Gamma\Gamma'}^{had,r}(p_p^2, P_e^2) = \int_0^\infty ds \frac{\rho_{\Gamma\Gamma'}^{had,r}(s, P_e^2)}{s - p_p^2}. \quad (3.6)$$

where, $\rho_{\Gamma\Gamma'}^{had,r}(s, P_e^2)$ are the spectral densities given by,

$$\rho_{\Gamma\Gamma'}^{had,r}(s, P_e^2) = \frac{1}{\pi} \text{Im} \Pi_{\Gamma\Gamma'}^{had,r}(s + i\epsilon, P_e^2) \quad (3.7)$$

These spectral densities can also be written by separating the pole contribution and the heavy states contributions as

$$\rho_{\Gamma\Gamma'}^{had,r}(s, P_e^2) = \lambda_p m_p^2 \delta(s - m_p^2) F_{\Gamma\Gamma'}^r(s, P_e^2) + \rho_{\Gamma\Gamma'}^{heavy,r}(s, P_e^2). \quad (3.8)$$

where $F_{\Gamma\Gamma'}^r(s, P_e^2)$ can be related to $F_{\Gamma\Gamma'}^n(s, P_e^2)$ for $s = m_p^2$ i.e proton being onshell which is ensured by the delta function. These relations reads as,

$$\begin{aligned} F_{\Gamma\Gamma'}^{PK}(s, P_e^2) &= F_{\Gamma\Gamma'}^{KPP}(s, P_e^2) = F_{\Gamma\Gamma'}^1(s, P_e^2), & F_{\Gamma\Gamma'}^{KK}(s, P_e^2) &= F_{\Gamma\Gamma'}^{KKP}(s, P_e^2) = F_{\Gamma\Gamma'}^2(s, P_e^2), \\ F_{\Gamma\Gamma'}^V(s, P_e^2) &= F_{\Gamma\Gamma'}^{VP}(s, P_e^2) = F_{\Gamma\Gamma'}^3(s, P_e^2), & F_{\Gamma\Gamma'}^T(s, P_e^2) &= F_{\Gamma\Gamma'}^{TP}(s, P_e^2) = F_{\Gamma\Gamma'}^4(s, P_e^2), \\ F_{\Gamma\Gamma'}^P(s, P_e^2) &= F_{\Gamma\Gamma'}^{PP}(s, P_e^2) = F_{\Gamma\Gamma'}^5(s, P_e^2), & F_{\Gamma\Gamma'}^K(s, P_e^2) &= F_{\Gamma\Gamma'}^{KP}(s, P_e^2) = F_{\Gamma\Gamma'}^6(s, P_e^2). \end{aligned} \quad (3.9)$$

Using the assumptions of the quark-hadron duality, the spectral densities of the heavy states, $\rho_{\Gamma\Gamma'}^{heavy,r}(s, P_e^2)$, can be approximated to the spectral densities computed using the quantum chromodynamics (QCD) as,

$$\int_{s_0}^\infty ds \frac{\rho_{\Gamma\Gamma'}^{heavy,r}(s, P_e^2)}{s - p_p^2} \approx \int_{s_0}^\infty ds \frac{\rho_{\Gamma\Gamma'}^{QCD,r}(s, P_e^2)}{s - p_p^2} = \int_{s_0}^\infty ds \frac{1}{\pi} \frac{\text{Im}(\Pi_{\Gamma\Gamma'}^{QCD,r}(s, P_e^2))}{s - p_p^2} \quad (3.10)$$

with s_0 being the continuum threshold which is a free parameter and is expected to be chosen below or equal to the lightest excitation but well above the ground state. In the present case, the lightest excitation state is the Roper resonance with mass of 1.44 GeV. To compute the contribution of the spectral densities due to heavier states one needs to compute the correlation functions $\Pi_{\Gamma\Gamma'}^r(s, P_e^2)$ in QCD.

In QCD, the time ordered product in eq. (3.4) can be computed by partially contracting the quark fields as,

$$\begin{aligned} T\{Q_{\Gamma\Gamma'}(x)\bar{\chi}(0)\} &= -\frac{1}{2} \epsilon^{lmn} \epsilon^{ijk} P_{\Gamma'} \left[(\bar{u}_l(0) \Gamma_A u_i(x)) \left\{ \Gamma_A \gamma_\mu \tilde{S}_{jm}^{(u)}(x) P_\Gamma S_{nk}^{(d)}(x) \gamma^\mu \gamma_5 \dots \right. \right. \\ &\quad \left. \left. + \dots S_{jm}^{(u)}(x) \gamma_\mu \tilde{\Gamma}_A P_\Gamma S_{nk}^{(d)}(x) \gamma^\mu \gamma_5 \right\} \right. \\ &\quad \left. + (\bar{d}_l(0) \Gamma_A d_i(x)) \left\{ S_{kn}^{(u)}(x) \gamma_\mu \tilde{S}_{jm}^{(u)}(x) P_\Gamma \Gamma_A \gamma^\mu \gamma_5 \right\} \right]. \end{aligned} \quad (3.11)$$

Here, we have employed the completeness relation given by,

$$q(x)\bar{q}(0) = \frac{-1}{4} (\bar{q}(0)\Gamma_A q(x)) \Gamma^A \quad (3.12)$$

with, $q = \{u, d\}$ and the chosen basis of gamma matrices is

$$\Gamma_A = \left\{ 1, \gamma_5, \gamma^\rho, i\gamma_\rho\gamma_5, \frac{1}{\sqrt{2}}\sigma^{\rho\sigma} \right\}. \quad (3.13)$$

Further, $\tilde{\Gamma}_A = C\Gamma_A^T C^{-1} = \eta_i \Gamma_A$ with $C = i\gamma^2\gamma^0$ and,

$$\eta_i = \begin{cases} 1, & \Gamma_A = 1, i\gamma_5, \gamma_\mu\gamma_5 \\ -1, & \Gamma_A = \gamma_\mu, \sigma_{\mu\nu} \end{cases} \quad (3.14)$$

$S^{ij}(x)$ is the quark propagator at the light like separations. In the massless limit, it is given by,

$$S_{ij}(x) = \frac{i\not{x}}{2\pi^2 x^4} \delta_{ij} - \frac{\langle \bar{q}q \rangle}{12} \delta_{ij} \left(1 + \frac{m_0^2 x^2}{16} \right) + \dots \quad (3.15)$$

Here, $\langle \bar{q}q \rangle$ is the quark condensate. Ellipses denote higher terms with one or more gluon exchanges which are not considered in this work. m_0 is associated with the mixed condensate as

$$\langle \bar{q}g_s G \cdot \sigma q \rangle = m_0^2 \langle \bar{q}q \rangle \quad (3.16)$$

where $G \cdot \sigma = G_{\mu\nu} \sigma^{\mu\nu}$. After performing the partial integrals, we are left with the matrix elements of two or more particle (quarks and gluons) operators which had been found to be written in terms of light cone distribution amplitudes (DAs) of photon of varying twist [49]. In the present work, we only consider the two particle DAs of twist-2 and twist-3 and leave a more detailed analysis of three-particle twist-3 and higher twist DAs (which are expected to be small) for future works.

The definitions of the DAs are collected in appendix-A. It is important to note here that at twist-2 there is only one DA, $\phi_\gamma(u, \mu)$ which appears in the matrix element of two quark operator with $\Gamma_A = \frac{1}{\sqrt{2}}\sigma^{\rho\sigma}$. At twist-3, there are 2 two-particle DAs which appears for $\Gamma_A = \{\gamma_\rho, i\gamma_\rho\gamma_5\}$ (for details look at appendix-A). On substituting the partial contractions of the time ordered product of quarks, eq. (3.11) and the two-particle twist-2 and twist-3 DAs of the photon and summing up all the contributions, we get the analytic structure of the correlation function defined in eq. (3.5) in QCD as,

$$\begin{aligned} \Pi_{\Gamma\Gamma'}^{QCD}(p_p, p_e) = \epsilon_\mu^* P_{\Gamma'} \left[\right. & \Pi_{\Gamma\Gamma'}^{QCD,PK} \frac{\not{k} p_p^\mu}{m_p^2} + \Pi_{\Gamma\Gamma'}^{QCD,KK} \frac{\not{k} k^\mu}{m_p^2} + \Pi_{\Gamma\Gamma'}^{QCD,V} \gamma^\mu + \Pi_{\Gamma\Gamma'}^{QCD,T} \frac{i\sigma^{\mu\nu} k_\nu}{m_p} \\ & + \Pi_{\Gamma\Gamma'}^{QCD,P} \frac{p_p^\mu}{m_p} + \Pi_{\Gamma\Gamma'}^{QCD,K} \frac{k^\mu}{m_p} + \Pi_{\Gamma\Gamma'}^{QCD,KPP} \frac{\not{k} p_p^\mu \not{p}_p}{m_p^3} + \Pi_{\Gamma\Gamma'}^{QCD,KKP} \frac{k^\mu \not{k} \not{p}_p}{m_p^3} \\ & \left. + \Pi_{\Gamma\Gamma'}^{QCD,VP} \frac{\gamma^\mu \not{p}_p}{m_p} + \Pi_{\Gamma\Gamma'}^{QCD,TP} \frac{i\sigma^{\mu\nu} k_\nu \not{p}_p}{m_p^2} + \Pi_{\Gamma\Gamma'}^{QCD,PP} \frac{\not{p}_p p_p^\mu}{m_p^2} + \Pi_{\Gamma\Gamma'}^{QCD,KP} \frac{k^\mu \not{p}_p}{m_p^2} \right] \quad (3.17) \end{aligned}$$

$\Pi_{\Gamma\Gamma'}^{QCD,r}$ are the scalar functions of p_p^2 and P_e^2 . The analytic expressions for these functions are lengthy and hence are provided in appendix-B. We also provide several useful identities and integrals in appendix-D. According to the light cone sum rule matching condition,

$$\Pi_{\Gamma\Gamma'}^{had,r}(p_p^2, P_e^2) = \Pi_{\Gamma\Gamma'}^{QCD,r}(p_p^2, P_e^2) \quad (3.18)$$

Using the above relations, the final sum rule for $F_{\Gamma\Gamma'}^r$ reads as

$$\lambda_p m_p^2 \frac{F_{\Gamma\Gamma'}^r(s, P_e^2)}{m_p^2 - p_p^2} = \int_0^{s_0} ds \frac{1}{\pi} \frac{\text{Im} \Pi_{\Gamma\Gamma'}^{r,QCD}(s, P_e^2)}{s - p_p^2} \quad (3.19)$$

To suppress the effect of the heavy states, we perform the Borel transformation with respect to p_p^2 . After Borel transformation the sum rule reads as (see appendix-D for details),

$$F_{\Gamma\Gamma'}^r(s_0, P_e^2) = \frac{e^{\frac{m_p^2}{M^2}}}{\lambda_p m_p^2} \int_0^{s_0} ds e^{-\frac{s}{M^2}} \frac{1}{\pi} \text{Im} \Pi_{\Gamma\Gamma'}^{QCD,r}(s, P_e^2) \quad (3.20)$$

Here M is the Borel mass and s_0 is the continuum threshold. These are the artefacts of the LCSR method, and have to be fixed such that the sum rule is saturated with the ground state and the heavy state contributions are properly suppressed. A typical rule of the thumb is to try and obtain at least 70% contribution to the correlation function from the ground state itself. The details on these parameters is given in the next section.

3.1.1 Numerical analysis

The values of various parameters used during the numerical calculations are provided in appendix-E. The physical FFs, $A_{\Gamma\Gamma'}$, for $\Gamma\Gamma' = LL$ and LR are studied as a function of $P_e^2 = -p_e^2$ and the Borel mass M . These FFs can be found from different combinations of $F_{\Gamma\Gamma'}$'s as can be read from eq. (2.7) and eq. (3.9). As the photon is onshell, we put $k^2 = 0$. For the case of $\Gamma\Gamma' = LL$, we have only two possibilities to extract $A_{LL}(s_0, P_e^2)$ which are from the combination of $F_{\Gamma\Gamma'}^T$ and $F_{\Gamma\Gamma'}^{TP}$ with $F_{\Gamma\Gamma'}^{KPP}$ as $F_{\Gamma\Gamma'}^{PK}$, $F_{\Gamma\Gamma'}^P$, and $F_{\Gamma\Gamma'}^{PP}$ turns out to be zero in this case. In figure 1, we show the variation of $A_{LL}^{TP+KPP}(s_0, P_e^2)$ with P_e^2 for three different values of the continuum threshold s_0 . In this figure, we also show its variation with the Borel mass, M for three different values of P_e^2 at fixed $s_0 = (1.44\text{GeV})^2$ which is equal to the Roper resonance. The combination $A_{LL}^{T+KPP}(s_0, P_e^2)$ is found to be less stable when varying the parameters s_0 and M (as can be seen from figure 2) and hence is less reliable. On the face value, it is in broad agreement with A_{LL}^{TP+KPP} . As can be seen from the detailed expressions of these functions (listed in appendix-B), condensate contributions are quite important (and also dominant in some cases), and therefore can't be simply ignored. For the case of $\Gamma\Gamma' = LR$, we have a total of eight combinations as can again be read from eq. (2.7) and eq. (3.9). For this case as well, the four combinations which involves $F_{\Gamma\Gamma'}^T$ are found to be less stable against s_0 and M and hence we do not show them here. The other four combinations involving $F_{\Gamma\Gamma'}^{TP}$ are shown in figure 3-figure 6.

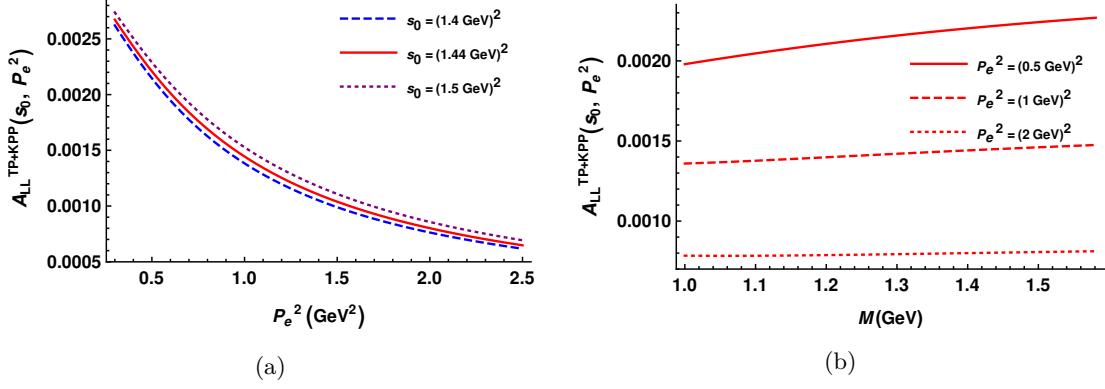


Figure 1. The physical FF, $A_{LL}(s_0, P_e^2)$ is calculated from the combination of F_{LL}^{TP} and F_{LL}^{KPP} employing photon DAs. Left panel: $A_{LL}^{TP+KPP}(s_0, P_e^2)$ vs P_e^2 is shown for three values of $s_0 = (1.4 \text{ GeV})^2$ (violate dotted), $s_0 = (1.44 \text{ GeV})^2$ (red solid) and $s_0 = (1.5 \text{ GeV})^2$ (blue dashed) at the Borel Mass, $M^2 = 2 \text{ GeV}^2$. Right Panel: $A_{LL}^{TP+KPP}(s_0, P_e^2)$ vs M is shown for three values of $P_e^2 = 0.5 \text{ GeV}^2$ (red solid), $P_e^2 = 1 \text{ GeV}^2$ (red dashed) and $P_e^2 = 2 \text{ GeV}^2$ (red dotted) at the continuum threshold, $s_0 = (1.44 \text{ GeV})^2$.

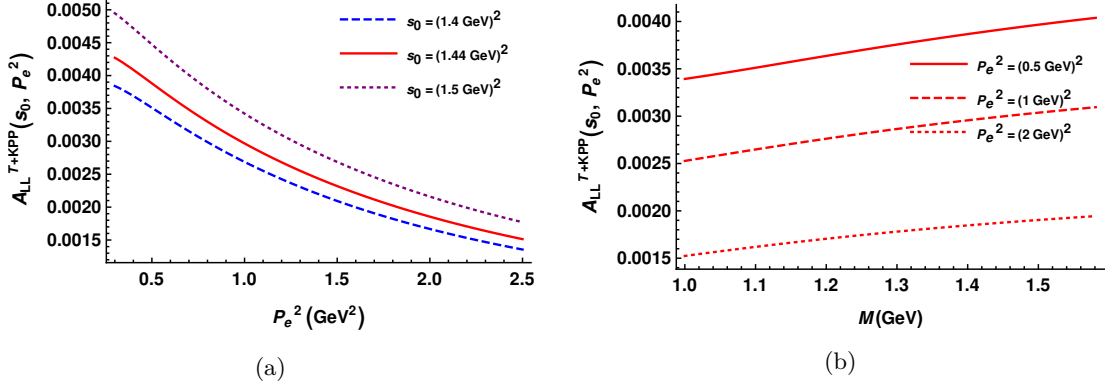


Figure 2. Same as figure 1 but now with the combinations of F_{LL}^T and F_{LL}^{KPP} .

The values of the physical FFs, $A_{\Gamma\Gamma'}$ at $P_e^2 = 0.5 \text{ GeV}^2$,¹ and $M^2 = 2 \text{ GeV}^2$ for $s_0 = (1.44 \text{ GeV})^2$ are found to be:

$$\begin{aligned} A_{LL}^{T+KPP}(1.44^2, 0.5) &= (0.00388 \pm 0.00126) \text{ GeV}^2, \\ A_{LL}^{TP+KPP}(1.44^2, 0.5) &= (0.00221 \pm 0.00082) \text{ GeV}^2. \end{aligned} \quad (3.21)$$

$$\begin{aligned} A_{LR}^{TP+KPP+P}(1.44^2, 0.5) &= (0.00251 \pm 0.00118) \text{ GeV}^2, \\ A_{LR}^{TP+KPP+PP}(1.44^2, 0.5) &= (0.00250 \pm 0.00118) \text{ GeV}^2 \\ A_{LR}^{TP+PK+P}(1.4^2, 0.5) &= (0.00176 \pm 0.00123) \text{ GeV}^2, \\ A_{LR}^{TP+PK+PP}(1.4^2, 0.5) &= (0.00176 \pm 0.00123) \text{ GeV}^2. \end{aligned} \quad (3.22)$$

From the above equations, it is clearly evident that there is quite good consistency in the form factor, A_{LR} , determined from different combinations. The uncertainties are associated with the uncertainties in the values of parameters entering the DAs. These uncertainties

¹LCSR calculations are trustworthy at $|Q^2| \rightarrow \infty$, where Q^2 is the momentum transferred squared. To be consistent with this requirement, in this case, we have chosen $Q^2 = P_e^2 = 0.5 \text{ GeV}^2$.

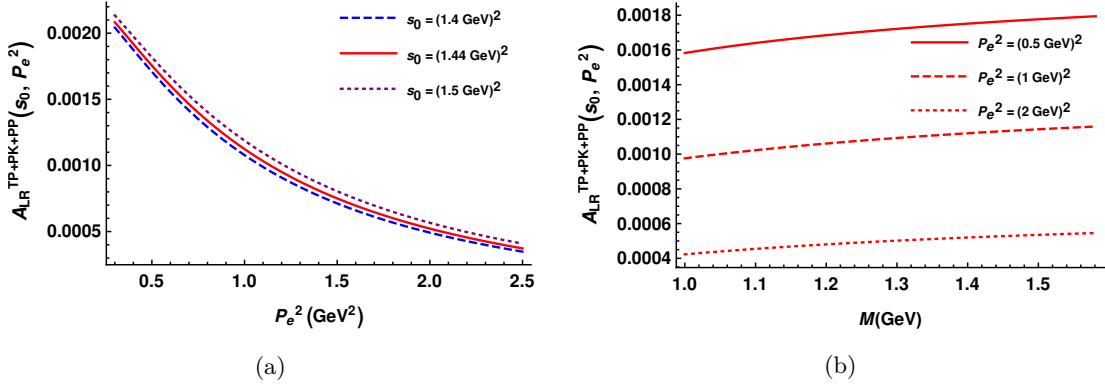


Figure 3. The physical FF, $A_{LR}(s_0, P_e^2)$ is calculated from the combination of F_{LR}^{TP} , F_{LR}^{PK} and F_{LR}^{PP} employing photon DAs. Left panel: $A_{LR}^{TP+PK+PP}(s_0, P_e^2)$ vs P_e^2 is shown for three values of $s_0 = (1.4 \text{ GeV})^2$ (violate dotted), $s_0 = (1.44 \text{ GeV})^2$ (red solid) and $s_0 = (1.5 \text{ GeV})^2$ (blue dashed) at the Borel Mass, $M^2 = 2 \text{ GeV}^2$. Right Panel: $A_{LR}^{TP+PK+PP}(s_0, P_e^2)$ vs M is shown for three values of $P_e^2 = 0.5 \text{ GeV}^2$ (red solid), $P_e^2 = 1 \text{ GeV}^2$ (red dashed) and $P_e^2 = 2 \text{ GeV}^2$ (red dotted) at the continuum threshold, $s_0 = (1.44 \text{ GeV})^2$.

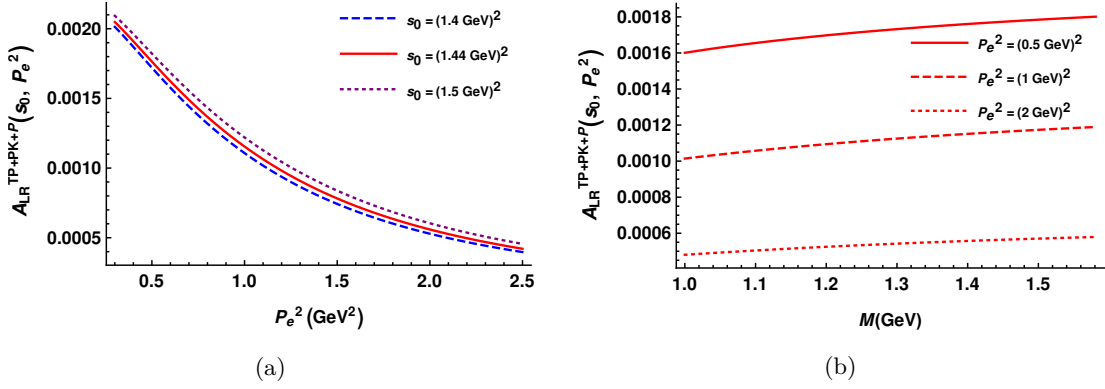


Figure 4. Same as figure 3 but now with the combinations of F_{LR}^{TP} , F_{LR}^{PK} and F_{LR}^P .

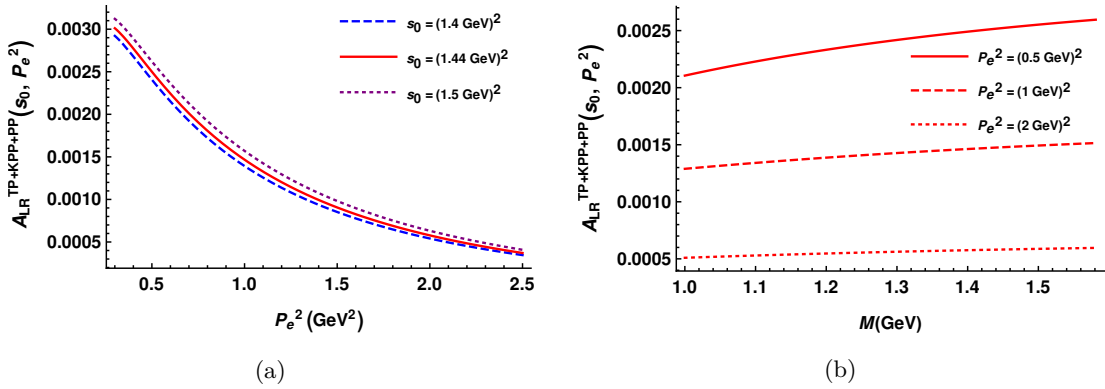


Figure 5. Same as figure 3 but now with the combinations of F_{LR}^{TP} , F_{LR}^{KPP} and F_{LR}^{PP} .

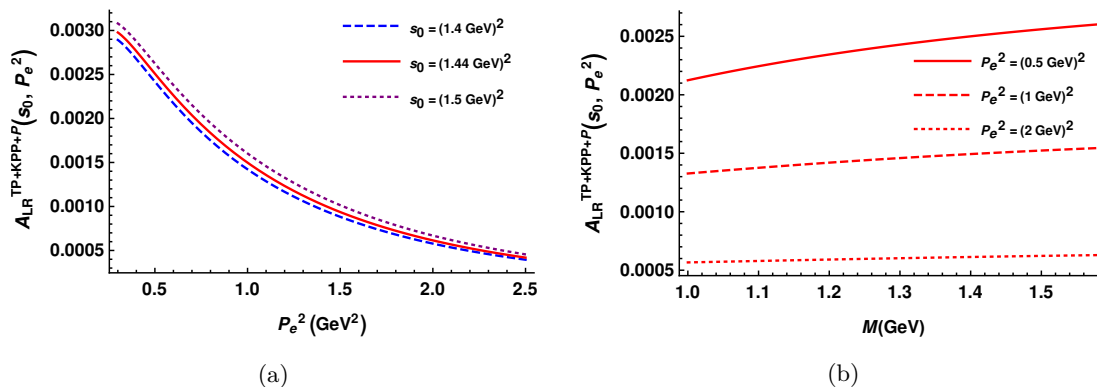


Figure 6. Same as figure 3 but now with the combinations of F_{LR}^{TP} , F_{LR}^{KPP} and F_{LR}^P .

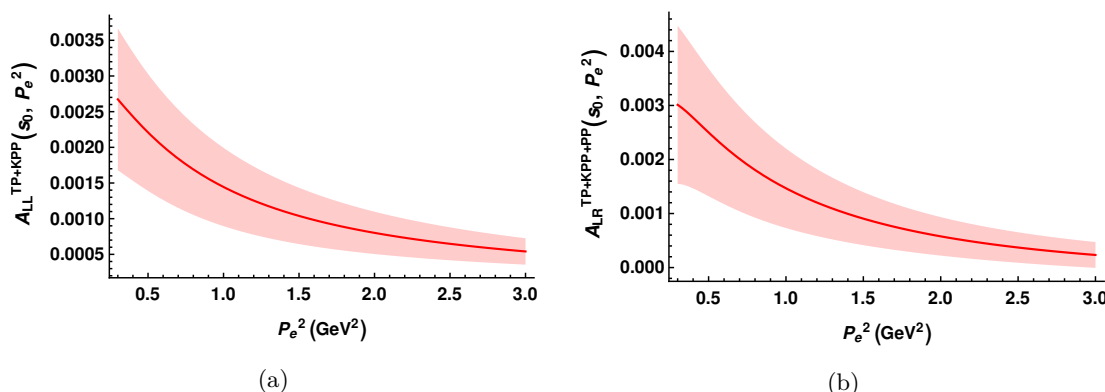


Figure 7. The physical FF, $A_{LL}^{TP+KPP}(s_0, P_e^2)$ (left pannel) and $A_{LR}^{TP+KPP+PP}(s_0, P_e^2)$ (right pannel) vs P_e^2 are shown at $s_0 = (1.44 \text{ GeV})^2$ and $M^2 = 2 \text{ GeV}^2$ along with the uncertainties associated with the parameters involved in photon DAs. The bands represents the uncertainties.

are found to decrease with an increase in P_e^2 as shown in figure 7 for $A_{LL}^{TP+KPP}(s_0, P_e^2)$ and $A_{LR}^{TP+KPP+PP}(s_0, P_e^2)$ as the representative FFs at $s_0 = (1.44 \text{ GeV})^2$ and $M^2 = 2 \text{ GeV}^2$.

3.2 Case-2: using photon interpolation and proton DAs

Having worked through the details with the proton state being interpolated, we next seek to determine the relevant form factors, but this time employing the distribution amplitudes of the proton. Then, on interpolating the photon state, the hadronic matrix element in eq. (2.6) reads as,

$$H_{\Gamma\Gamma'}(p_p, p_e)u_p(p_p) = -ie\epsilon_\alpha^* \int d^4x e^{ik \cdot x} \langle 0 | T \{ j_{em}^\alpha(x) Q_{\Gamma\Gamma'}(0) \} | p(p_p) \rangle \quad (3.23)$$

where, $j_{em}^\alpha(x) = Q_d \bar{d}(x) \gamma^\alpha d(x) + Q_u \bar{u}(x) \gamma^\alpha u(x) - \bar{e}(x) \gamma^\alpha e(x)$ is the electromagnetic current and

$$Q_{\Gamma\Gamma'} = \epsilon^{abc} \left(d_a^T C P_\Gamma u_b \right) (P_{\Gamma'} u_c). \quad (3.24)$$

Using the generalized Fierz transformations [50], it can be written as,

$$Q_{LL} = \frac{\epsilon^{abc}}{4} \left(2(P_L d_a)(\bar{u}_c^c P_L u_b) - (\sigma_{\mu\nu} P_L d_a)(\bar{u}_c^c \sigma_{\mu\nu} P_L u_b) \right), \text{ and} \quad (3.25)$$

$$Q_{LR} = \frac{\epsilon^{abc}}{4} (2(\gamma_\mu P_L d_a)(\bar{u}_c^c \gamma^\mu P_L u_b)). \quad (3.26)$$

As discussed above, to get the sum rule, we need to calculate the correlation function in eq. (3.23) in QCD. To get the time ordered product of the electromagnetic current with Q_{LL} and Q_{RL} we need

$$\begin{aligned} & T \left\{ j_{em}^\alpha(x) (\Gamma_A P_L d_a) (\bar{u}_c^c \Gamma^A P_L u_b) \right\} \\ &= \left[Q_u \left\{ (C \gamma^\alpha \tilde{S}_{ic}^u(x) \Gamma_A P_L)^{BF} (\Gamma^A P_L)^{CD} \left((u_i^T(x))^B u_b^F(0) d_a^D(0) \right) \right. \right. \\ &\quad \left. \left. + (C \Gamma_A P_L S_{bi}(x) \gamma^\alpha)^{EB} (\Gamma^A P_L)^{CD} \left((u_c^T(0))^E u_b^B(x) d_a^D(0) \right) \right\} \right. \\ &\quad \left. - Q_d \left\{ (\Gamma_A S_{ai}^d(x) \gamma^\alpha)^{CB} (C \Gamma^A P_L)^{EF} \left((u_c^T(0))^E u_b^F(0) d_i^B(x) \right) \right\} \right] \end{aligned} \quad (3.27)$$

Here, capital alphabets (E, F, B, C, D) are the Dirac indices, $\{a, b, c, i\}$ are the color indices and superscript T denotes the transpose. $\Gamma_A = \{1, \sigma_{\mu\nu}\}$ and $\Gamma_A = \{\gamma_\mu\}$ for the case of LL and LR , respectively. The matrix element of the remaining three quark operator between the proton state and the vacuum can be parametrised in terms of proton DAs of varying twists [51]. In the present work, we consider only the leading twist-3 DAs (given in appendix-A), which can be defined by,

$$4 \langle 0 | \epsilon^{abc} u_\alpha^a(a_1 x) u_\beta^b(a_2 x) d_\gamma^c(a_3 x) | P(p) \rangle = \sum_i \mathcal{F}^i(\{a_1, a_2, a_3\}, (p.x)) X_{\alpha\beta}^i Y_\gamma^i \quad (3.28)$$

where,

\mathcal{F}^i	$X_{\alpha\beta}$	Y_γ
\mathcal{V}_1	$(\not{p} C)_{\alpha\beta}$	$(\gamma_5 u_p)_\gamma$
\mathcal{A}_1	$(\not{p} \gamma_5 C)_{\alpha\beta}$	$(u_p)_\gamma$
\mathcal{T}_1	$(p_p^\nu i \sigma_{\mu\nu} C)_{\alpha\beta}$	$(\gamma^\mu \gamma_5 u_p)_\gamma$

such that

$$X_i^T = \begin{cases} X_i, & \mathcal{F}_i \in \mathcal{V}_i, \mathcal{T}_i \\ -X_i, & \mathcal{F}_i \in \mathcal{A}_i \end{cases} \quad (3.29)$$

where, superscript T represents transpose. The DAs, \mathcal{F}_i , have the following symmetry under the exchange of a_1 and a_2 ,

$$\mathcal{F}_i(\{a_1, a_2, a_3\}, (p_p.x)) = \begin{cases} \mathcal{F}_i(\{a_2, a_1, a_3\}, (p_p.x)), & \mathcal{F}_i \in \mathcal{V}_i, \mathcal{T}_i \\ -\mathcal{F}_i(\{a_2, a_1, a_3\}, (p_p.x)), & \mathcal{F}_i \in \mathcal{A}_i \end{cases} \quad (3.30)$$

and

$$\mathcal{F}^i(\{a_1, a_2, a_3\}, (p.x)) = \int_0^1 \mathcal{D}\alpha_i e^{-i\alpha_i a_i p.x} F^i(\alpha_1, \alpha_2, \alpha_3) \quad (3.31)$$

with $\mathcal{D}\alpha_i = d\alpha_1 d\alpha_2 d\alpha_3 \delta(1 - \alpha_1 - \alpha_2 - \alpha_3)$.

Using these DAs and considering the photon emission from the u- and d-quark, the correlation function in eq. (3.23) turns out to be,

$$\begin{aligned}
 & H_{\Gamma\Gamma'}^{QCD} u_p(p_p) \\
 &= \epsilon_\alpha^* P_{\Gamma'} \left[F_{\Gamma'}^{1,QCD} \frac{p_p^\alpha \not{k}}{m_p^2} + F_{\Gamma'}^{2,QCD} \frac{k^\alpha \not{k}}{m_p^2} + F_{\Gamma'}^{3,QCD} \gamma^\alpha + F_{\Gamma'}^{4,QCD} \frac{i\sigma^{\alpha\beta} k_\beta}{m_p} \right. \\
 & \quad \left. + F_{\Gamma'}^{5,QCD} \frac{p_p^\alpha}{m_p} + F_{\Gamma'}^{6,QCD} \frac{k^\alpha}{m_p} \right] \quad (3.32)
 \end{aligned}$$

Here, $F_{\Gamma\Gamma'}$ are the scalar functions of $P'^2 = (p_p - k)^2$ and $K^2 = -k^2$, and are provided in appendix-C. Upon saturating with the intermediate lowest state, the hadronic decomposition reads as,

$$\begin{aligned}
 & H_{\Gamma\Gamma'}^{had} u_p(p_p) \\
 &= -e\epsilon_\alpha^* \frac{P'_\Gamma}{4} \lambda m_p \frac{\not{p}_p - \not{k} + m_p}{(p_p - k)^2 - m_p^2} \left\{ \gamma^\alpha W_1(K^2) - \frac{i\sigma^{\alpha\beta} k_\beta}{2m_p} W_2(K^2) \right\} u_p(p_p) + \dots \\
 &= \epsilon_\alpha^* P_{\Gamma'} \left[F_{\Gamma'}^{1,had} \frac{p_p^\alpha \not{k}}{m_p^2} + F_{\Gamma'}^{2,had} \frac{k^\alpha \not{k}}{m_p^2} + F_{\Gamma'}^{3,had} \gamma^\alpha + F_{\Gamma'}^{4,had} \frac{i\sigma^{\alpha\beta} k_\beta}{m_p} + F_{\Gamma'}^{5,had} \frac{p_p^\alpha}{m_p} + F_{\Gamma'}^{6,had} \frac{k^\alpha}{m_p} \right] \quad (3.33)
 \end{aligned}$$

Here, ellipses represent the contribution from the heavy states and λ is the coupling strength of the proton interpolation current with the proton state. $\lambda = \lambda'_p$ and $\lambda = -\lambda_p$ for $\Gamma\Gamma' = LL$ and $\Gamma\Gamma' = LR$, respectively and are defined in eq. (D.2) and eq. (D.4), respectively. $W_1(K^2)$ and $W_2(K^2)$ are the electromagnetic electric and magnetic form factors of the proton and are defined as,

$$\langle p(p_p - k) | j_\alpha^{em}(0) | p(p_p) \rangle = \bar{u}_p(p_p - k) \left[W_1(K^2) \gamma_\alpha - i \frac{\sigma_{\alpha\beta} k^\beta}{2m_p} W_2(K^2) \right] u_p(p_p). \quad (3.34)$$

The scalar functions $F_{\Gamma\Gamma'}^{had,n}$ (for $n = 1, 2, 3, 4, 5, 6$) of P'^2 and K^2 are related to $W_1(K^2)$ and $W_2(K^2)$ via following relations:

$$\begin{aligned}
 F_{LL}^{1,had} &= \frac{-e}{4} m_p^2 \lambda'_p \frac{W_2(K^2)}{P'^2 - m_p^2} & F_{LL}^{2,had} &= \frac{e}{4} m_p^2 \lambda'_p \frac{W_2(K^2)}{2(P'^2 - m_p^2)} \\
 F_{LL}^{3,had} &= -\frac{e}{8} \lambda'_p W_2(K^2) & F_{LL}^{4,had} &= \frac{e}{4} m_p^2 \lambda'_p \frac{W_1(K^2) + W_2(K^2)}{P'^2 - m_p^2} \\
 F_{LL}^{5,had} &= \frac{-e}{2} m_p^2 \lambda'_p \frac{W_1(K^2)}{P'^2 - m_p^2} & F_{LL}^{6,had} &= \frac{e}{4} m_p^2 \lambda'_p \frac{W_1(K^2)}{P'^2 - m_p^2} \quad (3.35)
 \end{aligned}$$

There will be similar relations between $F_{LR}^{n,had}$ and $W_{1,2}(K^2)$ with λ'_p replaced by $-\lambda_p$. From eq. (2.7), we know $F_{\Gamma\Gamma'}^{1,4,5}$ are required to calculate the physical FFs, $A_{\Gamma\Gamma'}$. For $F_{\Gamma\Gamma'}^{1,4,5}$, after using the quark hadron duality and Borel transformation, the sum rule condition

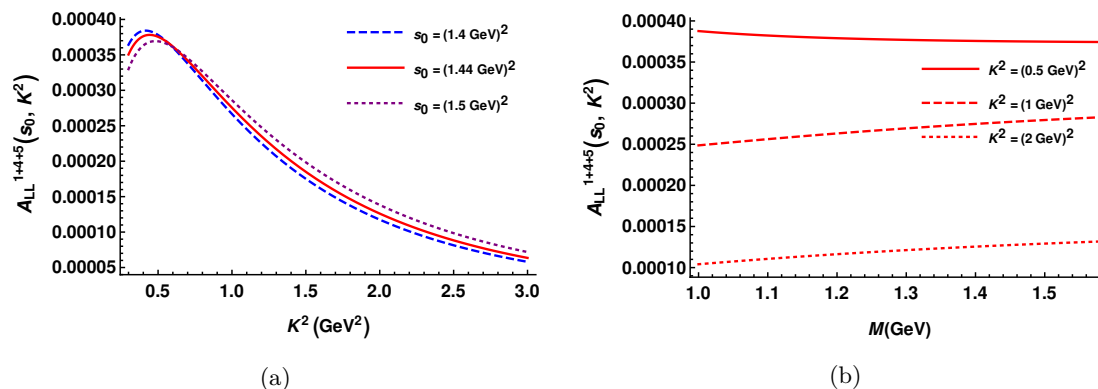


Figure 8. The physical FF, $A_{LL}(s_0, K^2)$ is calculated from the combination of F_{LL}^1 , F_{LL}^4 and F_{LL}^5 employing proton DAs. Left panel: $A_{LL}^{1+4+5}(s_0, K^2)$ vs K^2 is shown for three values of $s_0 = (1.4 \text{ GeV})^2$ (blue dotted), $s_0 = (1.44 \text{ GeV})^2$ (red solid) and $s_0 = (1.5 \text{ GeV})^2$ (blue dashed) at the Borel Mass, $M^2 = 2 \text{ GeV}^2$. Right Panel: $A_{LL}^{1+4+5}(s_0, K^2)$ vs M is shown for three values of $K^2 = 0.5 \text{ GeV}^2$ (red solid), $K^2 = 1 \text{ GeV}^2$ (red dashed) and $K^2 = 2 \text{ GeV}^2$ (red dotted) at the continuum threshold, $s_0 = (1.44 \text{ GeV})^2$.

reads as,

$$F_{\Gamma\Gamma'}^{1,4,5}(s_0, K^2) = -\frac{\text{Exp}\left(\frac{m_p^2}{M^2}\right)}{P'^2 - m_p^2} \int_0^{s_0} ds \text{Exp}\left(\frac{-s}{M^2}\right) \frac{1}{\pi} \text{Im}\left(F_{\Gamma\Gamma'}^{\{1,4,5\}, QCD}(s, K^2)\right) \quad (3.36)$$

3.2.1 Numerical analysis

The physical FFs, $A_{\Gamma\Gamma'}$ are studied as a function of $K^2 = -k^2$ and the Borel mass, M at $P'^2 = m_e^2 = 0$. Using eq. (2.7) and eq. (3.35), one can see that the physical form factors are proportional to $W_2(K^2)$ which can be calculated using other combinations of $F_{\Gamma\Gamma'}^n$, as well. We have found that the most stable one against the Borel mass is obtained from the combination of $F_{\Gamma\Gamma'}^1$, $F_{\Gamma\Gamma'}^4$, and $F_{\Gamma\Gamma'}^5$ as defined in eq. (2.7). We thus choose to show this explicitly in figure 8 and figure 9. We would also like to remark that a direct comparison of the form factors obtained here with those obtained when the proton is interpolated and photon DAs are used is not possible. The simple reason being that in the present case, the photon is far off-shell while in the previous case photon is on-shell and hence, in our view, the form factors so obtained in the previous case are better suited for a phenomenological analysis. The value of the physical FFs, $A_{\Gamma\Gamma'}$ at $K^2 = 0.5 \text{ GeV}^2$ and $M^2 = 2 \text{ GeV}^2$ for $s_0 = (1.44 \text{ GeV})^2$ from the combination of $F_{\Gamma\Gamma'}^{1,4,5}$ are found to be

$$\begin{aligned} A_{LL}^{1+4+5}(1.44^2, 0.5) &= (0.00038 \pm 0.00021) \text{ GeV}^2, \\ A_{LR}^{1+4+5}(1.44^2, 0.5) &= (0.00174 \pm 0.00027) \text{ GeV}^2 \end{aligned} \quad (3.37)$$

Here again, the uncertainties are associated with the parameters involved in the DAs and are found to decrease with an increase in K^2 (as shown in figure 10).

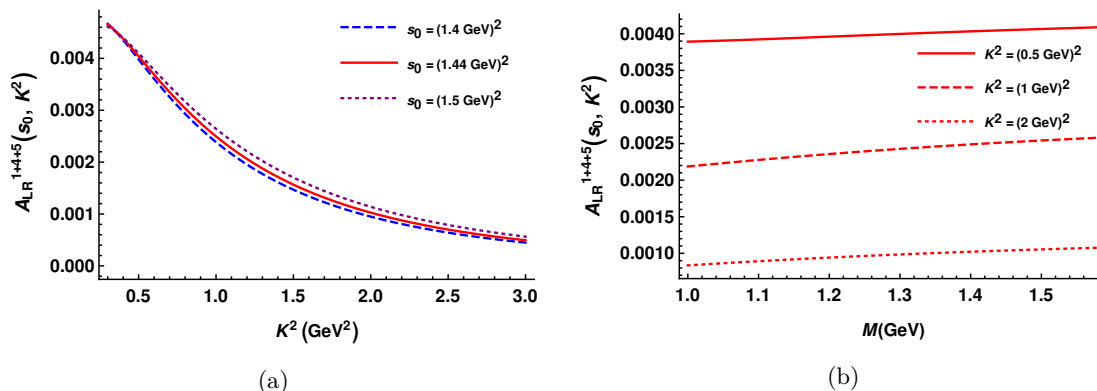


Figure 9. The physical FF, $A_{LR}(s_0, K^2)$ is calculated from the combination of F_{LR}^1 , F_{LR}^4 and F_{LR}^5 employing proton DAs. Left panel: $A_{LR}^{1+4+5}(s_0, K^2)$ vs K^2 is shown for three values of $s_0 = (1.4 \text{ GeV})^2$ (blue dotted), $s_0 = (1.44 \text{ GeV})^2$ (red solid) and $s_0 = (1.5 \text{ GeV})^2$ (purple dashed) at the Borel Mass, $M^2 = 2 \text{ GeV}^2$. Right Panel: $A_{LR}^{1+4+5}(s_0, K^2)$ vs M is shown for three values of $K^2 = 0.5 \text{ GeV}^2$ (red solid), $K^2 = 1 \text{ GeV}^2$ (red dashed) and $K^2 = 2 \text{ GeV}^2$ (red dotted) at the continuum threshold, $s_0 = (1.44 \text{ GeV})^2$.

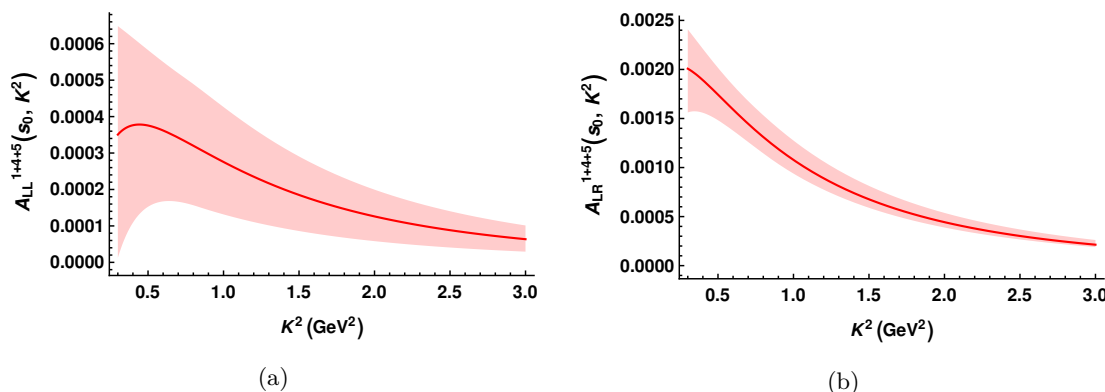


Figure 10. The physical FF, $A_{LL}^{1+4+5}(s_0, K^2)$ (left panel) and $A_{LR}^{1+4+5}(s_0, K^2)$ (right panel) vs K^2 are shown at $s_0 = (1.44 \text{ GeV})^2$ and $M^2 = 2 \text{ GeV}^2$ along with the uncertainties associated with the parameters involved in proton DAs. The bands represent the uncertainties.²

In the present case, some kind of judicious extrapolation would be required. There is another issue that is worth pointing out. When employing proton (or nucleon) DAs while computing the electromagnetic form factors of the nucleons, it has been observed that the choice of the interpolation current plays a crucial role [47]. For some choice(s), particular form factors simply don't actually show up in the correlator calculation. In the case at hand, the four quark operator, with the positron field factored out, can be thought of as an analog of an interpolating current. Thus, it seems that differences or ambiguities similar to the above discussion are perhaps at play even here as the form factor A_{LL} in figure 8 is about an order of magnitude smaller than A_{LR} , and also with the form factors determined with photon DAs. As its value itself is smaller by an order, the errors in its value are large.

²The numerical values of the form factor in 10b are slightly different from figure 9 as in the present case $(p_p - k)^2 = p_e^2$ is set to be equal to 0 GeV^2 . While for figure 9, it has been set to 0.5 GeV^2 .

4 Discussion and conclusions

In this work, we have computed the form factors involved in the proton decay to a positron and a photon using the LCSR framework. This should be viewed as a complimentary approach to lattice calculations, though, to the best of our knowledge, no lattice study exists for proton to gamma transition. This decay mode has not attracted much attention. However, as briefly discussed in [25], the branching ratio for this mode is expected to be smaller than the $p \rightarrow \pi e^+$ mode by a factor $\mathcal{O}(1/(\text{few tens}))$. This is not a huge suppression and keeping in mind that the nuclear absorption effects are not going to affect the radiative mode, it is important to remain optimistic about this mode. The next important task is to have the relevant form factors computed in a reliable fashion. Choosing to work in the framework of light cone sum rules, these form factors can be calculated either by interpolating the proton state and using the photon DAs or by interpolating the photon state and using the proton DAs. We have considered both these scenarios one by one. The physical form factors that would enter the decay rate for the radiative process can be determined from different combinations of hadronic functions that can be systematically computed. In the case when photon DAs are employed for computing the correlation functions, we find that the condensate contributions do turn out to be important and dominant for specific hadronic functions. Thus, not having considered these would have led to erroneous results. In the case of proton DAs, at the order in twist employed for the present calculations, condensate contributions do not appear. For both the cases, we have explicitly shown the form factors for the combinations that present the best Borel stability. As we have briefly discussed above, in our opinion, the form factors determined using photon distribution amplitudes (Case-1) are more trustworthy. This also motivates for more detailed studies employing proton DAs in order to gain better insight into the issues, including investigating the effect of the condensates at twist-4 and higher. In the first case i.e., when photon DAs are employed, the calculations performed do not include three particle twist-3 contributions. This is justified at the level of precision needed at present as these contributions are expected to be about an order of magnitude smaller than those already included since two-particle twist-3 contributions are found to be typically an order of magnitude smaller. We find that the typical errors on form factors are in the range (30 – 40)% while for some combinations, errors turns out to be larger ($\sim 50\%$). Similar conclusions on error are reached in [24].

The detailed expressions for all the hadronic correlators are listed in the appendices and are exact in the sense that they are written for non-zero positron mass and without assuming $k^2 = 0$. While computing the amplitude we have assumed positron to be massless. Some extra contributions will arise due to non-zero lepton mass while manipulating eq. (3) and eq. (7). Thus, with very little effort, these can be utilised to compute form factors and thus branching ratio if there is μ^+ instead of e^+ in the final state. Some Final states with second generation particles may be favoured channels in scenarios where the scalar mediated contribution dominates over the gauge mediated one (see for example [52] for a recent study pointing out this feature). The radiative modes thus become equally important and can provide complimentary information about the details of the underlying high energy theory.

A Distribution amplitudes (DAs)

A.1 Proton DAs

Considering the Lorentz covariance, parity and spin of the nucleon, the matrix element of three quark operator between the vacuum and the nucleon state can be decomposed into 24 invariant functions in general. These functions are related to the light cone distribution amplitudes of the proton (see [51] for the details). At twist-3, there are three DAs (eq. (3.28)): the vector, V_1 , the axial-vector, A_1 and the tensor, T_1 . The explicit conformal expansion of these DAs are:

$$V_1(\alpha_i, \mu) = 120\alpha_1\alpha_2\alpha_3 \left[\phi_3^0(\mu) + \phi_3^+(\mu)(1 - 3\alpha_3) \right] \quad (\text{A.1})$$

$$A_1(\alpha_i, \mu) = 120\alpha_1\alpha_2\alpha_3 (\alpha_2 - \alpha_1) \phi_3^-(\mu) \quad (\text{A.2})$$

$$T_1(\alpha_i, \mu) = 120\alpha_1\alpha_2\alpha_3 \left[\phi_3^0(\mu) + \frac{1}{2} (\phi_3^- - \phi_3^+) (\mu) (1 - \alpha_3) \right] \quad (\text{A.3})$$

Here, α_i ($i = 1, 2, 3$) are the momentum fractions of the nucleon momentum carried by the three quarks. $\phi_3^0(\mu)$, $\phi_3^+(\mu)$, and $\phi_3^-(\mu)$ are the renormalisation scale, μ , dependent coefficients. They are available from QCD sum rules and are provided in appendix-E

A.2 Photon DAs

The photon DAs are defined as the vacuum expectation value of the non-local quark-antiquark plus n gluons operator (when $n \geq 0$) with light-like separations. We have considered only the two particle i.e. quark-antiquark DAs of twist-2 and twist-3 in the present work which are defined as follows:

1. Twist-2 DAs: at twist-2, we have only one two-particle DA, $\phi_\gamma(u)$ which is defined as

$$\langle \gamma(k) | \bar{q}(0) \sigma_{\rho\sigma} q(x) | 0 \rangle = -ie_q \langle \bar{q}q \rangle (\epsilon_\rho k_\sigma - \epsilon_\sigma k_\rho) \int_0^1 du e^{i\bar{u}k \cdot x} \chi \phi_\gamma(u). \quad (\text{A.4})$$

Here, $\langle \bar{q}q \rangle$ is the quark condensate, ϵ_μ is the polarisation vector of the photon, $e_q = Q_q e$ is the electric charge of the quark and χ is the magnetic susceptibility. u and $\bar{u} = 1 - u$ are the momentum fractions carried by the quark and anti-quark, respectively. $\phi_\gamma(u)$ is the photon DA of twist-2. The asymptotic form of this DA is

$$\phi_\gamma^{asy}(u) = 6u(1 - u) \quad (\text{A.5})$$

2. Twist-3 DAs: at twist-3, there are four DAs out of which two are two-particle DAs and two are three particle DAs. The two particle DAs are defined as

$$\langle \gamma(k) | \bar{q}(0) \gamma_\mu q(x) | 0 \rangle = e_q f_{3\gamma} \left(\epsilon_\mu^* - k_\mu \frac{\epsilon^* \cdot x}{k \cdot x} \right) \int_0^1 du e^{i\bar{u}k \cdot x} \psi^v(u, \mu) \quad (\text{A.6})$$

$$\langle \gamma(k) | \bar{q}(0) \gamma_\mu \gamma_5 q(x) | 0 \rangle = \frac{1}{4} e_q f_{3\gamma} \epsilon_{\mu\nu\alpha\beta} k^\alpha x^\beta \epsilon^{*\mu} \int_0^1 du e^{i\bar{u}k \cdot x} \psi^a(u, \mu) \quad (\text{A.7})$$

where, $f_{3\gamma}$ provides a natural mass scale for twist-3 DAs $\psi^v(u)$ and $\psi^a(u)$. The explicit form of these DAs are:

$$\psi^{(v)}(u) = 5 \left(3\xi^2 - 1 \right) + \frac{3}{64} \left(15\omega_\gamma^V - 5\omega_\gamma^A \right) \left(3 - 30\xi^2 + 35\xi^4 \right) \quad (\text{A.8})$$

$$\psi^{(a)}(u) = \left(1 - \xi^2 \right) \left(5\xi^2 - 1 \right) \frac{5}{2} \left(1 + \frac{9}{16}\omega_\gamma^V - \frac{3}{16}\omega_\gamma^A \right) \quad (\text{A.9})$$

where, $\xi = 2u - 1$ and ω_γ^V & ω_γ^A corresponds to the local operators of dimension six. The values of these constants are provided in appendix-E. Twice the integral of $\psi^v(\alpha)$ over α from 0 to u is defined as $\bar{\psi}^v(u)$ and is given by

$$\begin{aligned} \bar{\psi}^v(u) &= 2 \int_0^u d\alpha \psi^v(\alpha) \\ &= -20u\bar{u}\xi + \frac{15}{16} \left(\omega_\gamma^A - 3\omega_\gamma^V \right) u\bar{u}\xi \left(7\xi^2 - 3 \right) \end{aligned} \quad (\text{A.10})$$

For photon DAs of higher twist and DAs corresponding to three or more particles, one can look at [49].

B Correlation functions for case-1 (employing photon DAs)

In this appendix, we collect the analytic results of the correlation functions $\Pi_{\Gamma\Gamma'}^r(p_e, p_p)$ computed in QCD.

$$\begin{aligned} \Pi_{LL}^{QCD,T}(p_e, p_p) &= -em_p \langle \bar{q}q \rangle \int_0^1 du \left[\frac{3Q_u\chi}{16\pi^2} \phi_\gamma(u) P^2 \ln(-P^2) + \frac{f_{3\gamma}(Q_u - Q_d)}{6} \left\{ \frac{1}{P^2} \left(1 + \frac{m_0^2}{4P^2} \right) \right. \right. \\ &\quad \left. \left. \times \left(u\psi^{(v)}(u) - \frac{\bar{\psi}^{(v)}(u)}{2} \right) + \frac{\psi^a(u)}{2P^4} \left(1 + \frac{m_0^2}{2P^2} \right) (uk \cdot p_p - p_p^2) \right\} \right] \end{aligned} \quad (\text{B.1})$$

$$\Pi_{LL}^{QCD,TP}(p_e, p_p) = \frac{em_p^2 \langle \bar{q}q \rangle^2 \chi}{6} (Q_u - Q_d) \int_0^1 du \left[\frac{\phi_\gamma(u)}{P^2} \left(1 + \frac{m_0^2}{4P^2} \right) \right] \quad (\text{B.2})$$

$$\Pi_{LL}^{QCD,KK}(p_e, p_p) = -\frac{em_p^2 \langle \bar{q}q \rangle^2 \chi}{6} (Q_u - Q_d) \int_0^1 du \left[\frac{\phi_\gamma(u)}{P^2} \left(1 + \frac{m_0^2}{4P^2} \right) \right] \quad (\text{B.3})$$

$$\Pi_{LL}^{QCD,V}(p_e, p_p) = \frac{e \langle \bar{q}q \rangle^2 \chi}{6} (Q_u - Q_d) \int_0^1 du \left[uk^2 \frac{\phi_\gamma(u)}{P^2} \left(1 + \frac{m_0^2}{4P^2} \right) \right] \quad (\text{B.4})$$

$$\begin{aligned} \Pi_{LL}^{QCD,VP}(p_e, p_p) &= -\frac{em_p f_{3\gamma} \langle \bar{q}q \rangle}{6} (Q_u - Q_d) \int_0^1 du \left[\frac{\psi^v(u)}{P^2} \left(1 + \frac{m_0^2}{4P^2} \right) - (k \cdot p_p - uk^2) \right. \\ &\quad \left. \times \frac{\psi^a(u)}{2P^4} \left(1 + \frac{m_0^2}{2P^2} \right) \right] \end{aligned} \quad (\text{B.5})$$

$$\begin{aligned} \Pi_{LL}^{QCD,K}(p_e, p_p) &= \frac{em_p f_{3\gamma} \langle \bar{q}q \rangle}{6} (Q_u - Q_d) \int_0^1 du \left[\frac{1}{P^2} \left(1 + \frac{m_0^2}{4P^2} \left(u\psi^v(u) + \frac{\bar{\psi}^v(u)}{2} \right) \right) \right. \\ &\quad \left. - \left(uk^2 \bar{\psi}^v(u) + u(p_p \cdot k) \psi^a(u) \right) \frac{1}{P^4} \left(1 + \frac{m_0^2}{2P^2} \right) \right] \end{aligned} \quad (\text{B.6})$$

$$\Pi_{LL}^{QCD,KPP}(p_e, p_p) = -\frac{em_p^3 f_{3\gamma} \langle \bar{q}q \rangle}{12} (Q_u - Q_d) \int_0^1 du \frac{2\bar{\psi}^v(u) + \psi^a(u)}{P^4} \left(1 + \frac{m_0^2}{2P^2}\right) \quad (\text{B.7})$$

$$\Pi_{LL}^{QCD,P}(p_e, p_p) = \frac{em_p f_{3\gamma} \langle \bar{q}q \rangle}{12} (Q_u - Q_d) \int_0^1 du \frac{uk^2(2\bar{\psi}^v(u) + \psi^a(u))}{P^4} \left(1 + \frac{m_0^2}{2P^2}\right) \quad (\text{B.8})$$

$$\Pi_{LL}^{QCD,KKP}(p_e, p_p) = \frac{em_p^3 f_{3\gamma} \langle \bar{q}q \rangle}{12} (Q_u - Q_d) \int_0^1 du \frac{u\psi^a(u)}{P^4} \left(1 + \frac{m_0^2}{2P^2}\right) \quad (\text{B.9})$$

$$\begin{aligned} \Pi_{LR}^{QCD,T}(p_e, p_p) &= \frac{em_p \langle \bar{q}q \rangle}{6} \int_0^1 du \left[\frac{Q_d}{8\pi^2} \chi \phi_\gamma(u) (5P^2 + 2u(p_p \cdot k - uk^2)) \ln(-P^2) \right. \\ &\quad \left. + f_{3\gamma} Q_u (p_p^2 - up_p \cdot k) \frac{\psi^a(u)}{P^4} \left(1 + \frac{m_0^2}{2P^2}\right) \right] \end{aligned} \quad (\text{B.10})$$

$$\Pi_{LR}^{QCD,KPP}(p_e, p_p) = -\frac{em_p^3 \langle \bar{q}q \rangle}{6} \int_0^1 du \left[\frac{Q_d}{4\pi^2} \chi \phi_\gamma(u) \ln(-P^2) + f_{3\gamma} Q_u \frac{\psi^a(u)}{P^4} \left(1 + \frac{m_0^2}{2P^2}\right) \right] \quad (\text{B.11})$$

$$\Pi_{LR}^{QCD,KKP}(p_e, p_p) = \frac{em_p^3 \langle \bar{q}q \rangle}{6} \int_0^1 du \left[\frac{Q_d}{4\pi^2} \chi u \phi_\gamma(u) \ln(-P^2) + f_{3\gamma} Q_u \frac{u\psi^a(u)}{P^4} \left(1 + \frac{m_0^2}{2P^2}\right) \right] \quad (\text{B.12})$$

$$\begin{aligned} \Pi_{LR}^{QCD,P}(p_e, p_p) &= \frac{em_p \langle \bar{q}q \rangle}{3} \int_0^1 du \left[\frac{Q_d}{8\pi^2} \chi uk^2 \phi_\gamma(u) \ln(-P^2) - f_{3\gamma} Q_u \left\{ \frac{\psi^v(u)}{P^2} \left(1 + \frac{m_0^2}{4P^2}\right) \right. \right. \\ &\quad \left. \left. + \left(\bar{\psi}^v(u)(k \cdot p_p - uk^2) - \frac{uk^2 \psi^a(u)}{2} \right) \frac{1}{P^4} \left(1 + \frac{m_0^2}{2P^2}\right) \right\} \right] \end{aligned} \quad (\text{B.13})$$

$$\begin{aligned} \Pi_{LR}^{QCD,K}(p_e, p_p) &= -\frac{em_p \langle \bar{q}q \rangle}{3} \int_0^1 du \left[\frac{Q_d}{8\pi^2} \chi u (p_p \cdot k) \phi_\gamma(u) \ln(-P^2) - f_{3\gamma} Q_u \right. \\ &\quad \times \left\{ \left(u\psi^v(u) + \frac{\bar{\psi}^v(u)}{2} \right) \frac{1}{P^2} \left(1 + \frac{m_0^2}{4P^2}\right) \right. \\ &\quad \left. \left. + \left(u(k \cdot p_p - uk^2) \bar{\psi}^v(u) - \frac{u(p_p \cdot k) \psi^a(u)}{2} \right) \frac{1}{P^4} \left(1 + \frac{m_0^2}{2P^2}\right) \right\} \right] \end{aligned} \quad (\text{B.14})$$

$$\begin{aligned} \Pi_{LR}^{QCD,VP}(p_e, p_p) &= \frac{em_p \langle \bar{q}q \rangle}{6} \int_0^1 du (p_p \cdot k - uk^2) \left[\frac{Q_d}{4\pi^2} \chi \phi_\gamma(u) \ln(-P^2) \right. \\ &\quad \left. + f_{3\gamma} Q_u \frac{\psi^a(u)}{P^4} \left(1 + \frac{m_0^2}{2P^2}\right) \right] \end{aligned} \quad (\text{B.15})$$

$$\Pi_{LR}^{QCD,TP}(p_e, p_p) = em_p^2 \int_0^1 du \left[\frac{\langle \bar{q}q \rangle^2 \chi Q_u \phi_\gamma(u)}{3 P^2} \left(1 + \frac{m_0^2}{4P^2}\right) + \frac{f_{3\gamma} Q_u \psi^a(u) \ln(-P^2)}{16\pi^2} \right] \quad (\text{B.16})$$

$$\begin{aligned} \Pi_{LR}^{QCD,V}(p_e, p_p) &= e \int_0^1 du \left[\frac{\langle \bar{q}q \rangle^2 \chi Q_u (p_p \cdot k) \phi_\gamma(u)}{3 P^2} \left(1 + \frac{m_0^2}{4P^2}\right) + \frac{f_{3\gamma}}{16\pi^2} \left\{ \frac{1}{3} \left((7Q_u + Q_d) \psi^v(u) P^2 \right. \right. \right. \\ &\quad \left. \left. - (Q_u + Q_d) \bar{\psi}^v(u) (p_p \cdot k - uk^2) \right) + Q_u \psi^a(u) (p_p \cdot k) \right\} \ln(-P^2) \right] \end{aligned} \quad (\text{B.17})$$

$$\begin{aligned} \Pi_{LR}^{QCD,PK}(p_e, p_p) = & -em_p^2 \int_0^1 du \left[\frac{\langle \bar{q}q \rangle^2 \chi Q_u \phi_\gamma(u)}{3 P^2} \left(1 + \frac{m_0^2}{4P^2} \right) + \frac{f_{3\gamma}}{16\pi^2} \left\{ \frac{1}{3} (2(Q_u + Q_d) \right. \right. \\ & \times u\psi^v(u) + (7Q_u + Q_d)\bar{\psi}^v(u) + Q_u\psi^a(u) \left. \left. \right\} \ln(-P^2) \right. \\ & \left. + \frac{2(Q_u + Q_d)}{3P^2} u (p_p \cdot k - uk^2) \bar{\psi}^v(u) \right] \end{aligned} \quad (\text{B.18})$$

$$\Pi_{LR}^{QCD,PP}(p_e, p_p) = \frac{em_p^2 f_{3\gamma}}{24\pi^2} (Q_u + Q_d) \int_0^1 du \left[\psi^v(u) \ln(-P^2) + (p_p \cdot k - uk^2) \frac{\bar{\psi}^v(u)}{P^2} \right] \quad (\text{B.19})$$

$$\begin{aligned} \Pi_{LR}^{QCD,KP}(p_e, p_p) = & -\frac{em_p^2 f_{3\gamma}}{24\pi^2} (Q_u + Q_d) \int_0^1 du \left[(u\psi^v(u) + \bar{\psi}^v(u)) \ln(-P^2) \right. \\ & \left. + (p_p \cdot k - uk^2) \frac{u\bar{\psi}^v(u)}{P^2} \right] \end{aligned} \quad (\text{B.20})$$

$$\begin{aligned} \Pi_{LR}^{QCD,KK}(p_e, p_p) = & \frac{em_p^2 f_{3\gamma}}{24\pi^2} \int_0^1 du u^2 \left[\left\{ (Q_u + Q_d)\psi^v(u) + (4Q_u + Q_d) \frac{\bar{\psi}^v(u)}{u} \right\} \ln(-P^2) \right. \\ & \left. + (Q_u + Q_d)(p_p \cdot k - uk^2) \frac{\bar{\psi}^v(u)}{P^2} \right] \end{aligned} \quad (\text{B.21})$$

Here, $P^2 = (p_p - uk)^2 = (p_e + uk)^2 = \bar{u}p_p^2 - uP_e^2 - u\bar{u}k^2$. The remaining correlation functions does not appear in QCD calculations upto the twist accuracy we have considered. We perform the Borel transform on p_p^2 to get the final sum rules.

C Correlation functions for case-2 (employing proton DAs)

In this appendix, we collect the analytic results for the correlation functions $F_{\Gamma\Gamma'}^n(p_p, k)$ computed in QCD.

$$F_{LL}^{3,QCD}(p_p, k) = -\frac{em_p^2}{2} \int \mathcal{D}\alpha_i T_1(\alpha_i) \left[\frac{\alpha_3 Q_d}{(k - \alpha_3 p_p)^2} + \frac{\alpha_1 Q_u}{(k - \alpha_1 p_p)^2} \right] \quad (\text{C.1})$$

$$F_{LL}^{4,QCD}(p_p, k) = -\frac{em_p^2}{2} \int \mathcal{D}\alpha_i T_1(\alpha_i) \left[\frac{Q_d}{(k - \alpha_3 p_p)^2} + \frac{Q_u}{(k - \alpha_1 p_p)^2} \right] \quad (\text{C.2})$$

$$F_{LL}^{5,QCD}(p_p, k) = \frac{em_p^2}{2} \int \mathcal{D}\alpha_i T_1(\alpha_i) \left[\frac{\alpha_1 Q_u}{(k - \alpha_1 p_p)^2} - \frac{2\alpha_3 Q_d}{(k - \alpha_3 p_p)^2} \right] \quad (\text{C.3})$$

$$F_{LL}^{6,QCD}(p_p, k) = \frac{3Q_d em_p^2}{2} \int \mathcal{D}\alpha_i \frac{T_1(\alpha_i)}{(k - \alpha_3 p_p)^2} \quad (\text{C.4})$$

$$F_{LR}^{1,QCD}(p_p, k) = \frac{em_p^2}{2} \int \mathcal{D}\alpha_i \left[\frac{(V_1(\alpha_i) + A_1(\alpha_i)) Q_d}{(k - \alpha_3 p_p)^2} - \frac{(V_1(\alpha_i) - A_1(\alpha_i)) Q_u}{(k - \alpha_1 p_p)^2} \right] \quad (\text{C.5})$$

$$\begin{aligned} F_{LR}^{3,QCD}(p_p, k) = & -\frac{e}{2} \int \mathcal{D}\alpha_i \left[\frac{(V_1(\alpha_i) + A_1(\alpha_i)) Q_d (2p_p \cdot k - \alpha_3 m_p^2)}{2(k - \alpha_3 p_p)^2} \right. \\ & \left. + \frac{(V_1(\alpha_i) - A_1(\alpha_i)) Q_u (2\alpha_1 m_p^2 - p_p \cdot k)}{(k - \alpha_1 p_p)^2} \right] \end{aligned} \quad (\text{C.6})$$

$$F_{LR}^{4,QCD}(p_p, k) = -\frac{em_p^2}{2} \int \mathcal{D}\alpha_i \left[\frac{(V_1(\alpha_i) + A_1(\alpha_i)) Q_d}{2(k - \alpha_3 p_p)^2} + \frac{(V_1(\alpha_i) - A_1(\alpha_i)) Q_u}{(k - \alpha_1 p_p)^2} \right] \quad (C.7)$$

$$F_{LR}^{6,QCD}(p_p, k) = -\frac{em_p^2}{2} \int \mathcal{D}\alpha_i \left[\frac{(V_1(\alpha_i) + A_1(\alpha_i)) Q_d}{2(k - \alpha_3 p_p)^2} - \frac{(V_1(\alpha_i) - A_1(\alpha_i)) Q_u}{(k - \alpha_1 p_p)^2} \right] \quad (C.8)$$

The remaining correlation functions does not appear in QCD calculations upto the twist accuary we have considered. In this case, the Borel transformation will be performed on $P'^2 = (p_p - k)^2 = p_e^2$.

D Conventions, definitions and identities

D.1 Definitions and conventions

As discussed in section-3.1, the interpolation current for proton state is not unique. The Ioffe current, $\chi(x)$ as defined in eq. (3.1) is the linear combination of $\chi_1(x)$ and $\chi_2(x)$ defined in eq.(3.3) as,

$$\chi(x) = 2(\chi_2 - \chi_1) \quad (D.1)$$

such that,

$$\langle 0 | \chi(0) | p(p_p) \rangle = m_p \lambda_p u_p(p_p). \quad (D.2)$$

There is another interpolation current as a linear combination of these two currents defined as,

$$\begin{aligned} \chi'(x) &= 2(\chi_2 + \chi_1) \\ &= \frac{1}{2} \epsilon^{abc} \left(u^{Ta}(x) C \sigma_{\mu\nu} u^b(x) \right) \sigma^{\mu\nu} \gamma_5 d^c(x) \end{aligned} \quad (D.3)$$

such that,

$$\langle 0 | \chi'(0) | p(p_p) \rangle = m_p \lambda'_p u_p(p_p) \quad (D.4)$$

D.2 Useful identities and integrals

- **Identities:**

1. For $\sigma = \frac{i}{2} [\gamma^\rho, \gamma^\sigma]$,

$$\gamma^\alpha \sigma^{\rho\sigma} = 2i g^{\alpha\rho} \gamma^\sigma - 2i \gamma^\rho g^{\alpha\sigma} + \sigma^{\rho\sigma} \gamma^\alpha \quad (D.5)$$

2. Chisholm Identity:

$$\gamma^\alpha \gamma^\beta \gamma^\mu = g^{\alpha\beta} \gamma^\mu - g^{\alpha\mu} \gamma^\beta + g^{\beta\mu} \gamma^\alpha - i \epsilon^{\alpha\beta\mu\nu} \gamma_\nu \gamma_5 \quad (D.6)$$

- **Integrals:** in D dimensions using dimensional regularisation, the formula for general integrations involved in the correlation function is given by [39],

$$\int d^D x e^{ipx} \frac{1}{(x^2)^n} = (-i) (-1)^n 2^{(D-2n)} \pi^{D/2} (-p^2)^{n-D/2} \frac{\Gamma(D/2 - n)}{\Gamma(n)} \quad (D.7)$$

for $n \geq 1, p^2 < 0$. On differentiating it over the four-momentum p_α , we get the desired form of the integrals involved in our calculations.

$$\begin{aligned}
 \int d^4x e^{ipx} \frac{x_\alpha}{x^4} &= 2\pi^2 \frac{p_\alpha}{p^2}, \\
 \int d^4x e^{ipx} \frac{x_\alpha}{x^2} &= 8\pi^2 \frac{p_\alpha}{p^4} \\
 \int d^4x e^{ipx} \frac{x_\alpha x_\beta}{x^4} &= -\frac{2i\pi^2}{p^2} \left(g_{\alpha\beta} - \frac{2p_\alpha p_\beta}{p^2} \right), \\
 \int d^4x e^{ipx} \frac{x_\alpha x_\beta}{x^2} &= -\frac{8i\pi^2}{p^4} \left(g_{\alpha\beta} - \frac{4p_\alpha p_\beta}{p^2} \right) \\
 \int d^4x e^{ipx} \frac{x_\alpha}{x^6} &= \frac{-\pi^2}{4} p_\alpha \ln(-p^2), \\
 \int d^4x e^{ipx} \frac{1}{x^6} &= \frac{-i\pi^2}{8} p^2 \ln(-p^2) \\
 \int d^4x e^{ipx} \frac{x_\alpha x_\beta}{x^8} &= \frac{-i\pi^2}{48} \left(p^2 g_{\alpha\beta} + 2p_\alpha p_\beta \right) \ln(-p^2) \\
 \int d^4x e^{ipx} \frac{x_\alpha x_\beta x_\mu}{x^8} &= \frac{\pi^2}{24} \left(\frac{2p_\alpha p_\beta p_\mu}{p^2} - (p_\alpha g_{\beta\mu} + p_\beta g_{\alpha\mu} + p_\mu g_{\alpha\beta}) \ln(-p^2) \right)
 \end{aligned} \tag{D.8}$$

Here, the divergent terms which are proportional to p^2 are omitted as they goes to zero after Borel transformaion.

D.3 Borel Transformations

As listed in appendix-B and appendix-C, the correlation functions calculated in QCD involves,

$$P^2 = (p_p - uk)^2 = (p_e + uk)^2 = \bar{u}p_p^2 - uP_e^2 - u\bar{u}k^2 \tag{D.9}$$

with $P_e^2 = -p_e^2$ and $\bar{u} = 1 - u$ in case-1 and

$$(k - \alpha p_p)^2 = \alpha P'^2 - \bar{\alpha} K^2 - \alpha \bar{\alpha} m_p^2 \tag{D.10}$$

with $\alpha = \{\alpha_1, \alpha_3\}$, $K^2 = -k^2$ and $P'^2 = (p_p - k)^2$ in case-2. To calculate the final sum rules, one need to find the imaginary part of the correlation functions collected in appendix-B and appendix-C and substitute them in eq. (27) and eq. (44), which are obtained by performing the Borel transformations on the momentum trasferred square i.e. p_p^2 and $P'^2 = (p_p - k)^2$ for case-1 and case-2, respectively. To incorporate that, one need to make the following substitutions in the correlation functions of case-1,

$$\int_0^1 du \frac{F(u)}{P^2} G(u, s) \rightarrow - \int_0^{u_0} du \frac{F(u)}{\bar{u}} e^{\frac{-\bar{s}}{M^2}} G(u, \bar{s}) \tag{D.11}$$

$$\int_0^1 du \frac{F(u)}{P^4} G(u, s) \rightarrow \frac{e^{\frac{-s_0}{M^2}} F(u_0) G(s_0, u_0)}{P_e^2} + \int_0^{u_0} du \frac{F(u)}{\bar{u}^2} \frac{e^{\frac{-\bar{s}}{M^2}}}{M^2} \left(G(u, \bar{s}) - M^2 \frac{\partial}{\partial \bar{s}} G(u, \bar{s}) \right) \tag{D.12}$$

S.No.	Parameter	Value Used	Reference
1.	Proton mass (m_p)	0.938 GeV	[33]
2.	Fine Structure Constant ($\alpha = \frac{e^2}{4\pi}$)	$\frac{1}{137}$	[33]
3.	Quark condensate ($\langle \bar{q}q \rangle$)	$-((256 \pm 2)\text{MeV})^3$	[24]
4.	m_0^2	$(0.8 \pm 0.2)\text{GeV}^2$	[24]
5.	Magnetic Susceptibility (χ)	$(3.08 \pm 0.02)\text{GeV}^{-2}$	[49]
6.	$f_{3\gamma}$	$-(4 \pm 2) \cdot 10^{-3}\text{GeV}^2$	[49]
7.	ω_γ^v	3.8 ± 1.8	[49]
8.	ω_γ^a	-2.1 ± 1.0	[49]
9.	λ'_p	$(5.4 \pm 1.9) \cdot 10^{-2}\text{GeV}^2$	[47]
10.	λ_p	$-(2.7 \pm 0.9) \cdot 10^{-2}\text{GeV}^2$	[47]
11.	$\phi_3^0(\mu = 1\text{GeV})$	$(5.3 \pm 0.5) \cdot 10^{-3}\text{GeV}^2$	[51]
12.	$\tilde{\phi}_3^+(\mu = 1\text{GeV}) = \frac{\phi_3^+}{\phi_3^0}$	1.1 ± 0.3	[51]
13.	$\tilde{\phi}_3^-(\mu = 1\text{GeV}) = \frac{\phi_3^-}{\phi_3^0}$	4.0 ± 1.5	[51]

Table 1. Numerical Values for the parameters used for numerical analysis.

$$\begin{aligned}
 \int_0^1 du \frac{F(u)}{P^6} G(u, s) &\rightarrow - \int_0^1 du \frac{F(u)}{2\bar{u}^2} \left[e^{\frac{-s_0}{M^2}} G(u, s_0) \frac{\partial}{\partial s_0} \left(\delta(\bar{u}s_0 - uP_e^2) \right) \right] \\
 &+ \int_0^1 \frac{F(u)}{2\bar{u}^2} \left[\frac{\partial}{\partial s} \left(e^{\frac{-s}{M^2}} G(u, s) \right) \delta(\bar{u}s - uP_e^2) \right] \\
 &- \int_0^{u_0} du \frac{F(u)}{2\bar{u}^3} \frac{\partial^2}{\partial \bar{s}^2} \left(e^{\frac{-\bar{s}}{M^2}} G(u, \bar{s}) \right)
 \end{aligned} \tag{D.13}$$

with

$$\tilde{s} = \frac{uP_e^2}{\bar{u}} \quad \text{and} \quad u_0 = \frac{s_0}{s_0 + P_e^2}. \tag{D.14}$$

In these substitutions we put $s = p_p^2$ and $k^2 = 0$ as the photon is onshell. These substitutions are consistent with [47].

For case two, the substitution reads as,

$$\int \mathcal{D}\alpha_i \frac{F(\alpha_i)}{(k - \alpha p_p)^2} \rightarrow - \int_{\alpha_0}^1 \mathcal{D}\alpha_i \frac{F(\alpha_i)}{\alpha} e^{\frac{-s_1}{M^2}} \tag{D.15}$$

with $\alpha = \{\alpha_1, \alpha_3\}$, $\mathcal{D}\alpha_i = d\alpha_1 d\alpha_2 d\alpha_3 \delta(1 - \alpha_1 - \alpha_2 - \alpha_3)$,

$$s_1 = \frac{\bar{\alpha}K^2 + \alpha\bar{\alpha}m_p^2}{\alpha} \tag{D.16}$$

and

$$\alpha_0 = - \frac{K^2 - m_p^2 + s_0}{2m_p^2} + \frac{\sqrt{(K^2 + s_0)^2 + m_p^4 - 2m_p^2(s_0 - K^2)}}{2m_p^2}. \tag{D.17}$$

Here, $s = (p_p - k)^2$ and $K^2 = -k^2$.

E Values of parameters used

In this appendix, we collect all the numerical values of the parameters used for both case-1 and case-2 during numerical analysis. The numerical values are collected in table 1.

Open Access. This article is distributed under the terms of the Creative Commons Attribution License ([CC-BY 4.0](https://creativecommons.org/licenses/by/4.0/)), which permits any use, distribution and reproduction in any medium, provided the original author(s) and source are credited.

References

- [1] A.D. Sakharov, *Violation of CP Invariance, C asymmetry, and baryon asymmetry of the universe*, *Pisma Zh. Eksp. Teor. Fiz.* **5** (1967) 32 [[INSPIRE](#)].
- [2] J.C. Pati and A. Salam, *Unified Lepton-Hadron Symmetry and a Gauge Theory of the Basic Interactions*, *Phys. Rev. D* **8** (1973) 1240 [[INSPIRE](#)].
- [3] H. Georgi and S.L. Glashow, *Unity of All Elementary Particle Forces*, *Phys. Rev. Lett.* **32** (1974) 438 [[INSPIRE](#)].
- [4] H.P. Nilles, *Supersymmetry, Supergravity and Particle Physics*, *Phys. Rept.* **110** (1984) 1 [[INSPIRE](#)].
- [5] D.E. Morrissey and M.J. Ramsey-Musolf, *Electroweak baryogenesis*, *New J. Phys.* **14** (2012) 125003 [[arXiv:1206.2942](#)] [[INSPIRE](#)].
- [6] P. Fileviez Perez, *New Paradigm for Baryon and Lepton Number Violation*, *Phys. Rept.* **597** (2015) 1 [[arXiv:1501.01886](#)] [[INSPIRE](#)].
- [7] H.E. Haber and G.L. Kane, *The Search for Supersymmetry: Probing Physics Beyond the Standard Model*, *Phys. Rept.* **117** (1985) 75 [[INSPIRE](#)].
- [8] N. Chamoun, F. Domingo and H.K. Dreiner, *Nucleon decay in the R-parity violating MSSM*, *Phys. Rev. D* **104** (2021) 015020 [[arXiv:2012.11623](#)] [[INSPIRE](#)].
- [9] K.R. Dienes, E. Dudas and T. Gherghetta, *Extra space-time dimensions and unification*, *Phys. Lett. B* **436** (1998) 55 [[hep-ph/9803466](#)] [[INSPIRE](#)].
- [10] R.H. Brandenberger, A.-C. Davis and A.M. Matheson, *Cosmic Strings and Baryogenesis*, *Phys. Lett. B* **218** (1989) 304 [[INSPIRE](#)].
- [11] B. Fornal and B. Shams Es Haghi, *Baryon and Lepton Number Violation from Gravitational Waves*, *Phys. Rev. D* **102** (2020) 115037 [[arXiv:2008.05111](#)] [[INSPIRE](#)].
- [12] C. Murgui and M.B. Wise, *Scalar leptoquarks, baryon number violation, and Pati-Salam symmetry*, *Phys. Rev. D* **104** (2021) 035017 [[arXiv:2105.14029](#)] [[INSPIRE](#)].
- [13] P. Nath and P. Fileviez Perez, *Proton stability in grand unified theories, in strings and in branes*, *Phys. Rept.* **441** (2007) 191 [[hep-ph/0601023](#)] [[INSPIRE](#)].
- [14] P. Langacker, *Grand Unified Theories and Proton Decay*, *Phys. Rept.* **72** (1981) 185 [[INSPIRE](#)].
- [15] P.H. Frampton, *A novel viewpoint of proton decay*, *Mod. Phys. Lett. A* **37** (2022) 2250039 [[arXiv:2112.10720](#)] [[INSPIRE](#)].
- [16] J. Hisano, *Proton Decay in SUSY GUTs*, [arXiv:2202.01404](#) [[INSPIRE](#)].
- [17] Y. Aoki, C. Dawson, J. Noaki and A. Soni, *Proton decay matrix elements with domain-wall fermions*, *Phys. Rev. D* **75** (2007) 014507 [[hep-lat/0607002](#)] [[INSPIRE](#)].
- [18] Y. Aoki, T. Izubuchi, E. Shintani and A. Soni, *Improved lattice computation of proton decay matrix elements*, *Phys. Rev. D* **96** (2017) 014506 [[arXiv:1705.01338](#)] [[INSPIRE](#)].

- [19] V.S. Berezinsky, B.L. Ioffe and Y.I. Kogan, *The Calculation of Matrix Element for Proton Decay*, *Phys. Lett. B* **105** (1981) 33 [INSPIRE].
- [20] N. Isgur and M.B. Wise, *On the Consistency of Chiral Symmetry and the Quark Model in Proton Decay*, *Phys. Lett. B* **117** (1982) 179 [INSPIRE].
- [21] A.M. Din, G. Girardi and P. Sorba, *A Bag Model Calculation of the Nucleon Lifetime in Grand Unified Theories*, *Phys. Lett. B* **91** (1980) 77 [INSPIRE].
- [22] M.B. Gavela, A. Le Yaouanc, L. Oliver, O. Pene and J.C. Raynal, *Calculation of Proton Decay in the Nonrelativistic Quark Model*, *Phys. Rev. D* **23** (1981) 1580 [INSPIRE].
- [23] M. Machacek, *The Decay Modes of the Proton*, *Nucl. Phys. B* **159** (1979) 37 [INSPIRE].
- [24] U. Haisch and A. Hala, *Light-cone sum rules for proton decay*, *JHEP* **05** (2021) 258 [[arXiv:2103.13928](https://arxiv.org/abs/2103.13928)] [INSPIRE].
- [25] D. Silverman and A. Soni, *The Decay Proton $\rightarrow e^+\gamma$ in Grand Unified Gauge Theories*, *Phys. Lett. B* **100** (1981) 131 [INSPIRE].
- [26] J.O. Eeg and I. Picek, *Relevance of the 3_q -annihilation and the Radiative Proton Decay*, *Phys. Lett. B* **112** (1982) 59 [INSPIRE].
- [27] P.S.B. Dev et al., *Searches for Baryon Number Violation in Neutrino Experiments: A White Paper*, [arXiv:2203.08771](https://arxiv.org/abs/2203.08771) [INSPIRE].
- [28] M.R. Krishnaswamy, M.G.K. Menon, N.K. Mondal, V.S. Narasimham, B.V. Sreekantan, N. Ito et al., *Candidate Events for Nucleon Decay in the Kolar Gold Field Experiment*, *Phys. Lett. B* **106** (1981) 339 [INSPIRE].
- [29] G. Battistoni et al., *The Nusex Detector*, *Nucl. Instrum. Meth. A* **245** (1986) 277 [INSPIRE].
- [30] J.L. Thron, *The Soudan-II Proton Decay Experiment*, *Nucl. Instrum. Meth. A* **283** (1989) 642 [INSPIRE].
- [31] KAMIOKANDE-II collaboration, *Experimental Limits on Nucleon Lifetime for Lepton + Meson Decay Modes*, *Phys. Lett. B* **220** (1989) 308 [INSPIRE].
- [32] SUPER-KAMIOKANDE collaboration, *Search for proton decay via $p \rightarrow e^+\pi^0$ and $p \rightarrow \mu^+\pi^0$ in 0.31 megaton \cdot years exposure of the Super-Kamiokande water Cherenkov detector*, *Phys. Rev. D* **95** (2017) 012004 [[arXiv:1610.03597](https://arxiv.org/abs/1610.03597)] [INSPIRE].
- [33] PARTICLE DATA GROUP collaboration, *Review of Particle Physics*, *PTEP* **2020** (2020) 083C01 [INSPIRE].
- [34] SUPER-KAMIOKANDE collaboration, *Review of Nucleon Decay Searches at Super-Kamiokande*, in *51st Rencontres de Moriond on EW Interactions and Unified Theories*, Italy, March 12–19 2016, pp. 437–444 [[arXiv:1605.03235](https://arxiv.org/abs/1605.03235)] [INSPIRE].
- [35] P. Colangelo and A. Khodjamirian, *QCD sum rules, a modern perspective*, [hep-ph/0010175](https://arxiv.org/abs/hep-ph/0010175) [INSPIRE].
- [36] M.A. Shifman, A.I. Vainshtein and V.I. Zakharov, *QCD and Resonance Physics. Theoretical Foundations*, *Nucl. Phys. B* **147** (1979) 385 [INSPIRE].
- [37] M.A. Shifman, *Snapshots of hadrons or the story of how the vacuum medium determines the properties of the classical mesons which are produced, live and die in the QCD vacuum*, *Prog. Theor. Phys. Suppl.* **131** (1998) 1 [[hep-ph/9802214](https://arxiv.org/abs/hep-ph/9802214)] [INSPIRE].

- [38] V.M. Braun, *Light cone sum rules*, in *4th International Workshop on Progress in Heavy Quark Physics*, (1997), pp. 105–118 [[hep-ph/9801222](#)] [[INSPIRE](#)].
- [39] A. Khodjamirian, *Hadron Form Factors: From Basic Phenomenology to QCD Sum Rules*, CRC Press, Taylor & Francis Group, Boca Raton, U.S.A. (2020) [ISBN: 9781032173030].
- [40] S. Narison, *Qcd Spectral Sum Rules*, World Scientific Lecture Notes in Physics **26**, World Scientific Publishing Company, Singapore, Republic of Singapore (1990) [[DOI](#)].
- [41] S. Weinberg, *Baryon and Lepton Nonconserving Processes*, *Phys. Rev. Lett.* **43** (1979) 1566 [[INSPIRE](#)].
- [42] F. Wilczek and A. Zee, *Operator Analysis of Nucleon Decay*, *Phys. Rev. Lett.* **43** (1979) 1571 [[INSPIRE](#)].
- [43] M. Claudson, M.B. Wise and L.J. Hall, *Chiral Lagrangian for Deep Mine Physics*, *Nucl. Phys. B* **195** (1982) 297 [[INSPIRE](#)].
- [44] S. Chadha and M. Daniel, *Chiral Lagrangian Calculation of Nucleon Decay Modes Induced by $d = 5$ Supersymmetric Operators*, *Nucl. Phys. B* **229** (1983) 105 [[INSPIRE](#)].
- [45] N.G. Deshpande and G. Eilam, *Flavor-changing electromagnetic transitions*, *Phys. Rev. D* **26** (1982) 2463 [[INSPIRE](#)].
- [46] B.L. Ioffe, *On the choice of quark currents in the QCD sum rules for baryon masses*, *Z. Phys. C* **18** (1983) 67 [[INSPIRE](#)].
- [47] V.M. Braun, A. Lenz and M. Wittmann, *Nucleon Form Factors in QCD*, *Phys. Rev. D* **73** (2006) 094019 [[hep-ph/0604050](#)] [[INSPIRE](#)].
- [48] D.B. Leinweber, *Nucleon properties from unconventional interpolating fields*, *Phys. Rev. D* **51** (1995) 6383 [[nucl-th/9406001](#)] [[INSPIRE](#)].
- [49] P. Ball, V.M. Braun and N. Kivel, *Photon distribution amplitudes in QCD*, *Nucl. Phys. B* **649** (2003) 263 [[hep-ph/0207307](#)] [[INSPIRE](#)].
- [50] J.F. Nieves and P.B. Pal, *Generalized Fierz identities*, *Am. J. Phys.* **72** (2004) 1100 [[hep-ph/0306087](#)] [[INSPIRE](#)].
- [51] V. Braun, R.J. Fries, N. Mahnke and E. Stein, *Higher twist distribution amplitudes of the nucleon in QCD*, *Nucl. Phys. B* **589** (2000) 381 [*Erratum ibid.* **607** (2001) 433] [[hep-ph/0007279](#)] [[INSPIRE](#)].
- [52] K.M. Patel and S.K. Shukla, *Anatomy of scalar mediated proton decays in SO(10) models*, [arXiv:2203.07748](#) [[INSPIRE](#)].